THE UNIVERSITY OF OKLAHOMA

GRADUATE COLLEGE

RADIATIVE TRANSFER FROM LAMINAR DIFFUSION FLAMES

A DISSERTATION

SUBMITTED TO THE GRADUATE FACULTY

in partial fulfillment of the requirements for the

degree of

DOCTOR OF PHILOSOPHY

BY

DWIGHT B. PFENNING

Norman, Oklahoma

1970

RADIATIVE TRANSFER FROM LAMINAR DIFFUSION FLAMES

APPROVED BY

C. M. Sliepcevich

Fred Weber

F. M. Townsend

Gerald Thomas

K. E. Starling

DISSERTATION COMMITTEE

ABSTRACT

Radiation fields from conical laminar diffusion flames have been defined by analyzing data from natural gas and acetone flames burning in an unlimited air supply at atmospheric pressure. These results showed the radiation envelope extends approximately one radius horizontally and twice the height of the luminous portion of the flame for various wavelengths. Most radiation outside the luminous cone was emitted in two bands, CO_2 centered at 4.3 microns and H_2O and CO_2 centered at 2.7 microns. Tables of intensity as a function of wavelength, vertical flame coordinate, and horizontal distance are presented along with contours of band and total intensities.

Average monochromatic volumetric extinction and maximum emission coefficients were calculated along the axis of symmetry of the flame using the luminous portion of the flame as the path length. These results showed total emission from a cylindrical flame increased to a maximum at a point just above the inner luminous zone and decreased toward the top of the flame. Maximum intensities of 0.871 and 1.35 watts/cm^2-steradian were calculated for natural gas and acetone flames, respectively.

ACKNOWLEDGEMENTS

Sincere gratitude is extended the following people who contributed to completion of this dissertation:

Dr. C. M. Sliepcevich, George Lynn Cross Research Professor of Engineering, for providing guidance throughout the Ph.D. program.

Dr. J. R. Welker, Co-director of the Flame Dynamics Laboratory, for his assistance and direction of the project.

Dr. K. E. Starling, Associate Professor of Chemical Engineering; Dr. F. M. Townsend, Associate Professor of Chemical Engineering; and Mr. G. Tuma, David Ross Boyd Professor of Electrical Engineering, for their service on the graduate committee.

Dr. D. W. Johnson and V. H. Homer for their assistance with the equipment.

Dr. J. A. Havens, R. I. Loeffler, and H. M. Bradbury for their helpful suggestions and discussions.

Thanks go to Mr. T. J. Stone for providing a place of solitude for the preparation of the text.

Special thanks are due Academy Computing Corporation for their generous contribution of computer time through their Oklahoma City time sharing facility. Computer time was offered

to local area users as a debugging vehicle for Academy's new computer installation. In spite of its experimental nature, this service far exceeded other available sources.

I am thankful for the efforts of Mrs. Joyce Meyer, Mrs. Connie Kirk, Miss Ann Haynes, Miss Jan Trantham and Mrs. Nedra Eaton in the manuscript preparation.

Dwight B. Pfenning

TABLE OF CONTENTS

Page

APPENDICES

LIST OF TABLES

LIST OF ILLUSTRATIONS

CHAPTER I

INTRODUCTION

Use of fire has been one of man's most significant accomplishments. However, man's lack of ability to control fire, as witnessed by nearly $1.5 billion yearly fire loss, serves as a strong reminder of the task of understanding the basic nature and control of fire. In order to develop a fundamental understanding of the complexities of flames and the mechanisms by which objects are destroyed by flames, a many faceted flame study has been conducted by the Flame Dynamics Laboratory at the University of Oklahoma. The main areas of study are thermal decomposition and ignition of materials by flames, interaction of buoyant diffusion flames, wind effects on buoyant diffusion flames, and transport properties of flames. Radiative transfer is one important mechanism that is common to each of these studies. A few of the questions relating to radiative transfer from flames are: a) What is the spectral distribution of radiation from flames of different fuels? b) Can data from small laminar flames be used to predict the transfer from large turbulent uncontrolled flames? c) How much is the radiation attenuated within the flames?

and d) What is the distribution of radiation within the flame and its immediate surroundings?

The scope of this study was limited to radiative transfer from diffusion flames, which in themselves are of great industrial importance.

Background

The simplest gas-phase diffusion flame consists of a reaction zone separating oxidizer and fuel gases. The characteristics of a diffusion flame are markedly dependent on the aerodynamics of the particular flow situation, and any complete description of diffusion flame behavior must include the dynamics of the flow. An example of an aerodynamic consideration is the effect of buoyancy. Because of the complications due to the interaction of aerodynamic considerations, chemical reactions, and diffusion, diffusion flames have not been studied as intensively and quantitatively as other types of flames, even though diffusion flames are more widely used.

The most striking characteristics of ordinary diffusion flames are the predominantly yellow-white colors. In general there are at least two distinct luminous zones, an inner cone where the relatively pure fuel core becomes hot by thermal conduction and pyrolysis of the fuel occurs and an outer oxidation zone completely surrounding the inner cone. If the flame is overventilated, the outer zone will completely oxidize the hot carbon particles and prevent soot from forming.

If a cold object is placed in the outer cone, a lampblack deposit will form on the subject. In the burner system used in this experiment, a large flow rate of fuel gas would cause underventilation, the flame would "open" at the top and a stream of soot would leave the flame.

Due to the great influence of aerodynamic flow on the flame, two types of diffusion flame configurations are used experimentally. These are the impinging jet and the conical diffusion flames. Although the impinging jet is the simplest diffusion flame for study, the conical diffusion flame that occurs above a circular port was used because it was felt the information would apply better to larger buoyant diffusion flames. For the conical diffusion flame, the thicker regions of the flame are controlled by diffusion, while in the thin-flame region, chemical reaction rate becomes the controlling factor. A large hot gas cone surrounds the luminous cone and a significant amount of the total radiation is emitted in this cone.

In order to describe radiation from diffusion flames, emission, absorption, and scattering must be considered. Hot gases produced by the flame emit and absorb radiation through energy level transitions of atoms and molecules, while hot carbon particles emit and absorb radiation due solely to their temperature. Due to the wavelength emission band of flames, the hot carbon particles are the main contributors to attenuation of radiation due to scattering. Considerable variation

exists in the literature for nomenclature for radiative transfer. Therefore, to develop the notation used in this study and to achieve a firm understanding of the different radiation quantities, a few of the more important definitions are presented.

Definitions

Depending on the radiation phenomena being described, either electromagnetic wave theory or quantum theory is employed. In quantum theory energy is transported by photons which travel at the speed of light and in energy levels of $h\nu$, where h is Planck's constant and ν is frequency. In electromagnetic wave theory the group velocity of the waves is the speed of light. Since the photons or waves are traveling at the velocity of light, c, the characteristic length or wavelength, λ, is defined as

$$\lambda = \frac{c}{\nu} . \qquad \text{(I-1)}$$

For this study the wavelength unit will always be microns where

$$1 \text{ micron} = 10^{-6} \text{ meters} \qquad \text{(I-2)}$$

Radiant flux, dq, is defined as the total radiant energy, dE, leaving an area element dA, in a time interval dt so that

$$dq = \frac{dE}{dAdt} \cdot \qquad \text{(I-3)}$$

If one considers dq in a solid angle, $d\Omega$, and at an angle, θ, from the normal to dA, then intensity, I, is a proportionality constant relating dq to $d\Omega$ and θ by

$$dq = I d\Omega \cos \theta \qquad \text{(I-4)}$$

The radiant energy leaving the surface into a hemispherical space above the surface is obtained by the integration

$$q = \int_{\theta,\Omega} I \cos \theta \, d\Omega \qquad \text{(I-5)}$$

where the limits of integration are over the entire hemisphere. Letting

$$d\Omega = \frac{dA}{r^2} = \sin \theta \, d\theta \, d\Phi \qquad \text{(I-6)}$$

where Φ is the tangential spherical angle, then

$$q = \int_0^{2\pi} \int_0^{\pi/2} I \cos \theta \sin \theta \, d\theta \, d\Phi. \qquad \text{(I-7)}$$

If one assumes the radiation field is homogeneous then I is a constant and

$$q = \pi I. \qquad \text{(I-8)}$$

Although intensity has been defined over all wavelengths, the definitions apply on a monochromatic basis. Monochromatic quantities will be subscripted with λ used to denote the intensity in a wavelength band, $d\lambda$. Thus

$$I_\lambda = \frac{dE}{dA \cos\theta \, dt \, d\Omega d\lambda} \qquad \text{(I-9)}$$

$$I_\lambda = \frac{dq}{d\Omega d\lambda \cos\theta} \qquad \text{(I-10)}$$

giving units of $\frac{\text{energy}}{\text{area} \mid \text{time} \mid \text{solid angle} \mid \text{wavelength}}$. The total intensity is related to monochromatic intensity by

$$I = \int_0^\infty I_\lambda \, d\lambda. \qquad \text{(I-11)}$$

For a medium where temperature governs the emission, Planck (32) described the maximum amount of energy that can be radiated at a given equilibrium temperature and wavelength as

$$I_{\lambda,T} = \frac{C_1}{\lambda^5} \left(\frac{1}{e^{C_2/\lambda T} - 1}\right) \qquad \text{(I-12)}$$

where $I_{\lambda,T}$ is radiation emitted by a blackbody, per unit surface area per unit wavelength interval per

unit solid angle. The units are energy/area-time-solid angle-unit wavelength. $I_{\lambda T}$ is called the "spectral radiant emittance" of the blackbody at wavelength, λ, and temperature, T.

T is the absolute temperature of the blackbody.

λ is the wavelength of the emitted radiation.

C_1 and C_2 are constants depending on units of T and λ.

Integrating Planck's law over a hemisphere and over all wavelengths yields the Stefan-Boltzmann law

$$q = \sigma T^4 \qquad \text{(I-13)}$$

where σ is the Stefan-Boltzmann constant

T is the absolute temperature

Since no material is a perfect emitter of radiation, materials are described in terms of the amount of their emission in relation to Planck's law emission at the same absolute temperature. This radiating efficiency is called emissivity and is defined as

$$\epsilon_\lambda = \frac{\text{radiant intensity of the material}}{\text{Planck's law intensity at the same absolute temperature}} \qquad \text{(I-14)}$$

Thermal radiation is contained in the wavelength band from 0.3 to 50 microns and is usually subdivided into bands of

ultraviolet (0.3 to 0.4 microns), visible (0.4 to 0.7 microns), and infrared (0.7 to 50 microns). In the case of flames, the energy is emitted in the 1.0 to 6.0 microns range. Although some flames appear to be very bright to the eye, the visible energy is an insignificant portion of the total emitted energy.

Absorbing, Scattering, and Emitting Media

Since carbon dioxide (CO_2) and water (H_2O) are the main products of combustion of flames used in this study, the energy state transitions of these molecules account for a large part of the emission and absorption of the flame. Basic vibrational frequencies of these molecules account for the peaks in absorption and emission band of flames. Superimposed on these vibration frequencies are rotational transitions which result in a series of absorption-emission lines centered about the basic vibrational frequency. When this series of lines is viewed with a low resolution device, the discrete line structure appears as a broad band. Thus any measurement of the absorption and emission due to the vibration-rotation energy level transition is a function of the resolution of the measuring device.

Scattering of the radiant energy is mainly dependent on the size of hot carbon particles that are formed within the flame. Scattering and absorption are usually combined into one attenuation factor.

Absorption and Scattering: By taking an energy balance on a path length ds of a semitransparent medium and defining γ_λ as a monochromatic attenuation coefficient, the resulting differential equation is given by

$$dI_\lambda = \gamma_\lambda I_\lambda \, ds \qquad \text{(I-15)}$$

This law is known as Beer's law and is commonly used in the integrated form

$$\frac{I_\lambda}{I_\lambda} = e^{-\gamma_\lambda s} \qquad \text{(I-16)}$$

where $I_\lambda = I_{\lambda_0}$ at $s = 0$.

The combined total of absorption and scattering coefficients is the extinction coefficient. Thus, applying Beer's law for a given wavelength

$$I_\lambda = I_{\lambda_0} e^{-(k_{\lambda a} + k_{\lambda s})s} = I_{\lambda_0} e^{-\beta_\lambda s} \qquad \text{(I-17)}$$

where
- I_λ is intensity of emergent radiation
- I_{λ_0} is intensity of incident radiation
- $k_{\lambda a}$ is monochromatic absorption coefficient
- $k_{\lambda s}$ is monochromatic scattering coefficient
- β_λ is monochromatic extinction coefficient
- s is path length.

The function, $e^{-\beta_\lambda s}$, can be interperted as the probability that a photon will pass through the distance s without being absorbed or scattered.

Emission: The monochromatic volumetric emission coefficient, J_λ, is used to express the local emission of radiation in an absorbing, scattering and emitting medium. J_λ includes both spontaneous and induced emission and has units of emission per unit time, per unit volume, per unit solid angle.

Atmospheric Attenuation of Radiation

Atmospheric attenuation is the other important factor that must be considered in the measurement of radiation from flames.

Transmission of infrared radiation through the atmosphere is dependent on the concentration and distribution of gases and particles forming the atmosphere. For this study, the gases CO_2 and H_2O are of particular interest. Attenuation in the infrared spectrum results from molecular resonance absorption bands and scattering. Absorption may be much greater than scattering, or vice versa, depending on the nature of the atmosphere, particle size, and the wavelength. Attenuation of infrared radiation by absorption is strongly wavelength dependent, resulting from absorption bands within definite wavelength intervals which are separated by intervals of negligible absorption known as windows. Attenuation by

scattering, while strongly wavelength dependent for very small particle size as in Rayleigh scattering, becomes independent of wavelength when the particle sizes are large and Mie scattering occurs.

Absorption: The absorption spectrum of infrared radiation passing through the atmosphere is formed by the resonant vibration-rotation band of primarily CO_2 and H_2O. Other constituents of the atmosphere have a negligible attenuation of radiation from flames.

Water vapor is the principal attenuator of infrared radiation in the atmosphere. Its description is difficult in that the water content in a given parcel of air is subjected to severe fluctuations due to meteorological changes. To predict H_2O attenuation accurately, the precise amount of the H_2O vapor in the air must be known.

Carbon dioxide is the next most important attenuator of infrared radiation. The distribution of CO_2 in the atmosphere is practically constant and allows CO_2 absorption to be calculated virtually independent of meteorological conditions. According to Goody (13) the concentration of CO_2 in the atmosphere is constant at 0.029 percent by volume.

The CO_2 spectral lines of an absorption band are fairly equally spaced and the H_2O lines are randomly spaced. The intensity of the individual lines vary greatly. This varying intensity and spacing of the lines complicates the development of a model to describe the CO_2 and H_2O absorption.

In spite of these difficulties assumptions regarding the distribution and intensities of the spectral lines have been made in models which give results that accurately approximate the actual absorption.

Applying Beer's law the monochromatic absorption, A_λ, is defined as

$$A_\lambda = 1 - \frac{I_\lambda}{I_{\lambda_0}} \qquad \text{(I-18)}$$

or

$$A_\lambda = 1 - e^{-ks} \qquad \text{(I-19)}$$

Expressions for the monochromatic absorption coefficient can in principle be derived from quantum mechanics. However, the complexity of the calculations for the transition between energy levels of the triatomic molecules has made the quantum approach impractical. As a result, the information on absorption of infrared radiation is experimental or a combination of experimental and analytical.

Absorption by H_2O: Three principal H_2O absorption bands exist in the flame emission region and are centered at 1.38, 1.87 and 2.7 microns. Goldstein (12) has presented monochromatic absorption coefficient for these bands. Edwards and Menard (7) have demonstrated satisfactory correlations for absorption in these bands using an exponential band model. Ferriso and Ludwig (10) and Burch et al. (6) also present integrated band absorption for bands centered at 1.38, 1.87 and 2.7 microns. There are many models and

supporting data, but the most widely used model for absorption was presented by Elasser (9).

For a wavelength interval $\Delta\lambda = \lambda_2 - \lambda_1$, which is large compared to the individual line spacing, Elasser showed the absorption could be approximated with an error function by assuming the individual absorption lines are equally spaced and of equal intensity. He also expressed the path length s, in terms of precipitable water, W. Thus the absorption coefficient $k\lambda_s$ was changed to α with the units adjusted for the precipitable water units. The value of W is obtained from the absolute humidity which can be computed from observations of the relative humidity and temperature. Elsasser's model reduces to

$$A_\lambda \simeq \text{erf}\left(\frac{\beta_\lambda \sqrt{\pi w}}{2}\right) . \qquad \text{(I-20)}$$

Larmore (27) gives values at standard conditions of the error function-absorption coefficient, β, for water vapor as a function of wavelength from 0.3 to 7.0 microns.

Absorption by CO_2: The three principal absorption bands in the flame emission wavelength range are centered at 1.9, 2.7, and 4.3 microns. The 4.3 band encompasses several additional minor bands. Edwards and Menard (8) have presented monochromatic volumetric absorption coefficients for CO_2 over the 1.9, 2.7, and 4.3 micron bands. Breeze et al. (3) and Burch et al. (5) have presented integrated band absorption for the same three bands. The widely

used Elasser model applied to the CO_2 bands is given by

$$A_\lambda \simeq \text{erf}\ (K\sqrt{d}) \qquad \text{(I-21)}$$

where K is the error function absorption coefficient

d is the path length.

Larmore also gives the values of K versus wavelength.

Scattering: The scattering mechanisms are independent forms of attenuation and are not related to the molecular vibration-rotation absorption. Classification of scattering is determined by the size of the scattering particle in relation to the wavelength of the energy being scattered. Rayleigh scattering applies to particles smaller than the wavelength and Mie scattering applies to particles larger than the wavelength.

Rayleigh Scattering: The Rayleigh scattering law is

$$\frac{I_{\lambda s}}{I_{\lambda_0}} = kv^2 \lambda^{-4} \qquad \text{(I-22)}$$

where $I_{\lambda s}$ = intensity of scattered radiation

I_{λ_0} = intensity of incident radiation

v = volume of scattering particles

k = constant

λ = wavelength of incident radiation

From the equation it can be seen that the scattering is greatest for the shorter wavelengths and rapidly decreases for longer wavelengths. Since Rayleigh scattering applies

to particles considerably smaller than the incident infrared radiation, Rayleigh scattering applies to molecular particles.

Mie Scattering: Mie scattering applies to particle diameters in the range of 0.1 to 100 microns. Application of this complicated theory requires a knowledge of particle size and refractive index. Mie scattering is more important in artificial attenuation of radiation from flames than in ordinary atmospheric attenuation. An example of the application of Mie scattering is the use of powders to combat destructive flames from igniting adjacent materials by attenuating the radiation through scattering.

Previous Work

Many flame studies have been made. In this study the main emphasis will be focused on a portion of the literature relating to radiative transfer and methods of predicting radiative transfer from diffusion of flames or hot gases that are formed by diffusion flames. The two general methods of predicting radiative transfer are classified as effective emissivity and non-equilibrium techniques.

Emissivity Techniques

Radiative transfer from flames is characterized by using a flame temperature and an effective emissivity of gases and particles emitting the radiation. Separate methods are used for calculating the radiation from the luminous and

non-luminous portions of the flame. These techniques are based on data and correlations presented by Hottel and Egbert (19) and Hottel and Manglesdorf (20).

Non-Luminous Emissivities: The effective emissivity is defined as the ratio of the radiative energy emitted by the gas to the blackbody radiation at the same temperature. The effect of path length is introduced by applying the exponential absorption law which is a function of wavelength. The non-luminous effective emissivity is given as

$$\epsilon_n = \frac{\lambda_n (1-e^{-\beta_{\lambda n} x}) f(\lambda,T)\, d\lambda}{\sigma T^4} \qquad \text{(I-23)}$$

where β_n is absorption coefficient for the non-luminous radiation

x is radiation path length

σ is Stephan-Boltzman constant

T is absolute temperature of the emitting gas

λ is wavelength of emitted radiation

The function $f(\lambda,T)$ is Planck's law, Equation I-12, describing the distribution of energy emitted to a hemisphere at wavelength, λ, and equilibrium temperature, T. The integration is performed over the wavelength bands of the radiation for each gas. Since the different gases have different wavelength emission bands and the absorption coefficient varies with wavelength, separate effective emissivities are presented

for each gas in terms of volumetric concentration, path length, and temperature. Thus an exact knowledge of distribution and concentration of the emitting gases, the path length and temperature are required for prediction of the non-luminous radiation from flames. Hsu (23), McAdams (29) and Thring (38) all use this approach for prediction of the non-luminous radiation from flames even though the flame is by no means homogeneous in temperature and concentration of the hot emitting gases.

The only significant non-luminous emitting gases in hydrocarbon flames are carbon dioxide and water vapor. Total non-luminous radiation is obtained by adding the contributions from both gases. In the case where the emission bands overlap, a correction must be applied. This problem of overlapping emission bands is discussed by Hines and Edwards (15) in which they present a method to correct the absorption coefficient in the overlapping bands.

Luminous Emissivities: In flames where underventilation occurs, glowing soot particles are formed at or very near the local flame temperature. The thermal radiation from these particles has a Planck distribution. The soot particles further complicate the radiative mechanism by decreasing radiation from other sources through Mie type scattering. The luminous radiation is treated in an analogous manner to non-luminous by defining the effective emissivity as

$$\epsilon_L = \frac{\int_0^{\infty} (1-e^{-\eta sx}) f(\lambda,T)\, d}{\sigma T^4} \qquad \text{(I-24)}$$

where η is the absorption coefficient

s is the soot concentration

x is radiation path length

T is absolute temperature

$f(\lambda,T)$ is Planck's radiation law

The absorption coefficient η should have been named the scattering coefficient. Hottel and Broughton (21) simplified the absorption coefficient by setting

$$\eta = \frac{1}{\lambda^n}$$

where n is related to the type soot being produced. They present monograms for values of ϵ_L as functions of temperature, type of soot, soot concentrations, and path length. The temperature is stated in terms of intensity of the red (λ = 0.6651 microns) and green (λ = 0.5553 microns) lines of a blackbody radiator. Thus knowing the type of soot, concentration of soot, intensities of the red and green lines, and path length; an actual temperature and effective emissivity can be obtained to calculate the luminous radiative transfer.

Total Radiation: In the emissivity technique the non-luminous and luminous portion of the radiation are added to

obtain the total radiation from the flame. This approach can lead to radiation greater than the blackbody radiation at the flame temperature. This contradiction stems from the fact that the soot radiates over the entire spectrum. Thring (38) presents a technique that avoids this contradiction but requires a constant absorption (scattering) coefficient, η. Neill (30) shows the total radiation from a flame can be written as

$$q = \pi I = \epsilon_L \sigma T^4 + e^{-\eta s x} \epsilon_N \sigma T^4 . \qquad (I\text{-}25)$$

Hsu (23) presents other techniques which have been developed for determining effective emissivities. All of the emissivity type methods require a knowledge of the type of soot, flame temperature, path length and concentrations of soot, CO_2, and H_2O in the flame. By assuming chemical equilibrium of the fuel air mixture at the flame temperature, Gaydon and Wolfhard (11) present a method for computing these concentrations. This equilibrium constant method assumes a complete knowledge of the chemical reactions and a solution of the resulting simultaneous, non-linear equations. An alternate method by White, Johnson, and Dantzig (41) allows one to calculate concentrations by assuming the free energy of a gas mixture is a minimum. All of the radiative transfer methods that have been suggested so far require a knowledge of the flame temperature. This flame temperature is then

used as the equilibrium temperature even though there is little doubt that equilibrium does not exist over most of the flame.

Flame Temperature: The concept of temperature is inseparably bound up with the definition of equilibrium. The introduction on the article by Hollander (16) states the equilibrium temperature relation, "General thermodynamic equilibrium is defined as follows: a volume of gas is said to be in thermodynamic equilibrium at the temperature T, when this temperature sufficies to describe the radiation density in the volume, the distribution of energy in the internal and external degrees of freedom of the gas, and the degrees of ionization and dissociation. Only then does the temperature have a unique meaning." If a system is not in equilibrium, then one temperature cannot be used to describe the system, and the temperature must be named after the special processes to which they apply e.g. translational, rotational, excitation, radiation, etc.

The temperatures appear to coincide gradually in the following sequences--translational, rotational, electronic, vibrational, disassociation, and ionization temperature. One exception is the radiation temperature. The radiation temperature is based on the temperature derived by comparison of the emitted intensity of the gas to Planck's law intensity which relates intensity, wavelength and absolute temperature. As noted earlier, inspection of

the emission spectrum of a hot gas such as CO_2 with a high resolution spectrograph reveals emission occurs as discrete lines that are related to the structure of the emitting molecules and atoms. Thus it should be no surprise that the radiation temperature does not approach the magic equilibrium temperature.

In flames the translational temperature is most commonly used as the flame temperature. To define a translational temperature at any point in the flame, one must resort to the assumption of local thermodynamic equilibrium which says that in any volume of the gas with dimensions small compared to spatial resolution measurements, the particles have an energy distribution so that the gas in that volume may be assigned a translation temperature. Translational equilibrium is probably the first type of equilibrium to exist within a volume since translational equilibrium is a fast process requiring only a few collisions. It is this local translational equilibrium temperature that is commonly used in the equations of state and transport equations describing flames. Gaydon and Wolfhard (11), Thring (38), and Broida (4) present discussions of various methods for measuring this flame temperature.

The most widely accepted method for flame temperature measurements is spectral line reversal. Sodium metal is used extensively and when introduced into the flame it emits two yellow D lines at 0.5890 and 0.5896 microns. When a

background source of continuous thermal radiation is viewed through the sodium vapor, the yellow lines will appear in absorption as dark lines or in emission as bright lines against the continuum, according to whether the temperature of the background is higher or lower than the flame temperature. When the temperature of the background and the flame temperature are the same, the lines are not visible. The measurement is made by varying the temperature of the background radiation until the sodium line just disappears and then recording the temperature of the background. Hollander points out the existence of a concentration level of sodium atoms below which this measured effective electronic excitation temperature of sodium is lower than the translational temperature of the flame.

Lewis and von Elbe (28) made a valuable study of the sodium-line reversal temperature from laminar premixed flames with air. They used a rectangular burner, colored the central portion of the flame, and viewed the flame end-on. The temperatures presented are the mean temperatures along the viewing path. The maximum temperature occurred slightly above the inner flame cone. These results are in general agreement with other investigators who have studied the temperature as a function of position in premixed flames. These wide variations of measured temperatures from the flame place further doubt on the validity of using one equilibrium temperature to describe the radiation from an entire flame.

Non-Equilibrium Techniques

A prediction technique for flame radiation, that does not require the flame to be in equilibrium, was developed by Shahroki (37) and Hood (17). They applied the radiative transport equation to an element of flame and obtained the differential equation for radiative transfer in an absorbing, emitting, and scattering medium as

$$\frac{dI_\lambda}{dx} = -\beta_\lambda I_\lambda + J_\lambda \qquad \text{(I-26)}$$

where I_λ is intensity of radiation

x is path length

β_λ is monochromatic extinction coefficient

J_λ is monochromatic volumetric emission coefficient.

By using the boundary conditions,

$$I_\lambda = 0 \text{ at } x = 0$$

Equation I-26 can be integrated by use of an integrating factor to yield

$$I_\lambda = \frac{J_\lambda}{\beta_\lambda}\left(1-e^{-\beta_\lambda x}\right). \qquad \text{(I-27)}$$

To apply this method to predict the radiative flux from flames, average values of J_λ and β_λ must be known over the paths through the emitting volume, and integrations must be performed over the flame volume and all wavelengths. Data

to calculate the emission and extinction coefficients were first attempted by Hood for small, laminar diffusion flames. By making four measurements Hood was able to calculate the β_λ and J_λ at a particular wavelength. The four measurements were intensity of the continuum source, intensity of the flame, intensity of the source focused through the flame, and the path length. The measurements I_λ (source), I_λ (flame), and I_λ (attenuated source plus flame) are related by

$$e^{-\beta_\lambda x} = \frac{I_\lambda \text{ (attenuated source plus flame)} - I_\lambda \text{ (flame)}}{I_\lambda \text{ (source)}} \qquad \text{(I-28)}$$

Thus an average value of β_λ can be calculated if path length is known. If the absolute intensity of the flame is known, then the average volumetric emission coefficient can be calculated from Equation I-27. Although calculations, using the average emission and extinction coefficients from small laminar diffuision flames gave good agreement with measured flux from diffusion flames up to 10 centimeters in diameter, the calculated flux for larger flames gave lower values than those obtained by experimental measurements of large diffusion flames.

Because of the difficulties Hood encountered in maintaining sufficient accuracy in his measurements, Tsai (39) devised a two path method for obtaining data to calculate the emission and extinction coefficients. Penner (31) gives

a detailed account of the two path method which was first used by Hottel and Broughton (21) to obtain spectral absorption coefficients. Tsai used two different sized flames to obtain different path lengths. By measuring the intensity associated with each of two different path lengths and solving Equation I-27 by an iterative technique, he calculated values of β_λ and J_λ over the range of wavelengths of the flame emission. Tsai's coefficients were obtained for the section of the flame that gave the maximum emission. The two path results gave significantly higher extinction coefficients, and therefore lower calculated thicknesses for opaque flames, than the attenuated source method. Both techniques agree qualitatively in that emission and absorption peaks occur in the 2.7 and 4.3 micron bands. In this particular comparison the differences in the results cannot be attributed to differences in instrument resolution since the same instrument and same instrument settings were used in both experiments.

Object of Investigation

The objective of this study was to obtain information that would aid in the understanding and prediction of radiative transfer from diffusion flames. Two types of data were taken from laminar diffusion flames to accomplish this objective. First, intensity profile data were taken to show the spatial and spectral distribution of the radiation fields through the flame and the cone of hot gases surrounding the

flame. Second, data to calculate the emission and extinction coefficients were taken along the axis of symmetry of the flame.

Profile Information

Hartley (18) claims six sevenths of the radiated energy from a flame is radiated from the outer diffusion cone and the hot gases above and around this cone. Calculations to predict the flux from large diffusion flames have neglected the radiation from this hot gas envelope above the luminous portion of the flame. In large flames, the turbulence tends to decrease the radiation due to the hot gases by cooling them by conduction and convection rather than the gases losing their energy by radiation alone. Although turbulence would lessen the effect of radiation from the hot gases above the luminous zone, the hot gases could contribute significantly to the total radiation from the flame. In order to obtain some feel for the magnitude of the radiation outside the luminous flame zone, the spatial and spectral distributions of intensity were examined for small laminar diffusion flames of natural gas and acetone in air at atmospheric pressure.

Emission and Extinction Coefficients

The differences between the experimentally determined emission and extinction coefficients from the two path and attenuated source method need resolving. By

making a minor change in the equipment used to obtain the profile data, data were taken using a flame that had an elliptical cross section in the horizontal plane. Data were taken of the emission in the paths along the major and minor axes of the cross section. It was felt the use of a single flame would be a significant improvement over the use of two different sized flames for the two paths. The cross section would guarantee that the same flame regime was being considered in the two paths. It also permitted calculations of the coefficients at different positions of height in the flame.

Tsai (39) states that computed values of β_λ and J_λ were scattered throughout the entire emission region for every fuel and that the scatter is due to the small flicker of the flame. An error analysis (Appendix C) reveals it is necessary to have an extremely stable flame and measuring equipment in order to reproduce the results. The solution of the exponential transport of β_λ and J_λ equation is extremely sensitive for the short path lengths through the flame used in this experiment.

Since a much more stable flame was used in this experiment, it was felt the scatter of β_λ and J_λ would be reduced. An attempt was made to operate the monochromator at the same resolution that was used by earlier investigation.

CHAPTER II

EQUIPMENT

A fuel supply, a burner, a flame chimney, an external optical collection system, a monochrometer, and a blackbody radiation source were used in the experiment. The equipment was fastened to a 1.22 by 2.44 meter, vibration-free optical table. The table top was made from a 2.54 centimeter thick magnesium plate with quarter-twenty tapped holes on a 10.16 centimeter spacing. Most equipment was "dogged" to the table, which proved to be very useful for setting up and aligning the optical collection system. The fuel supply was not attached to the table. The assembled equipment is shown in Figure II-1.

Fuel Supply

Two separate fuel supplies were constructed, one for fuels that are normally gases at ambient conditions and one for fuels that are normally liquid at ambient conditions. The liquid fuel system was designed to vaporize the fuel and supply it to the burner in gaseous form. Thus, only one burner was required for both cases. Acetone was used for the liquid supply and natural gas was used for the gas supply.

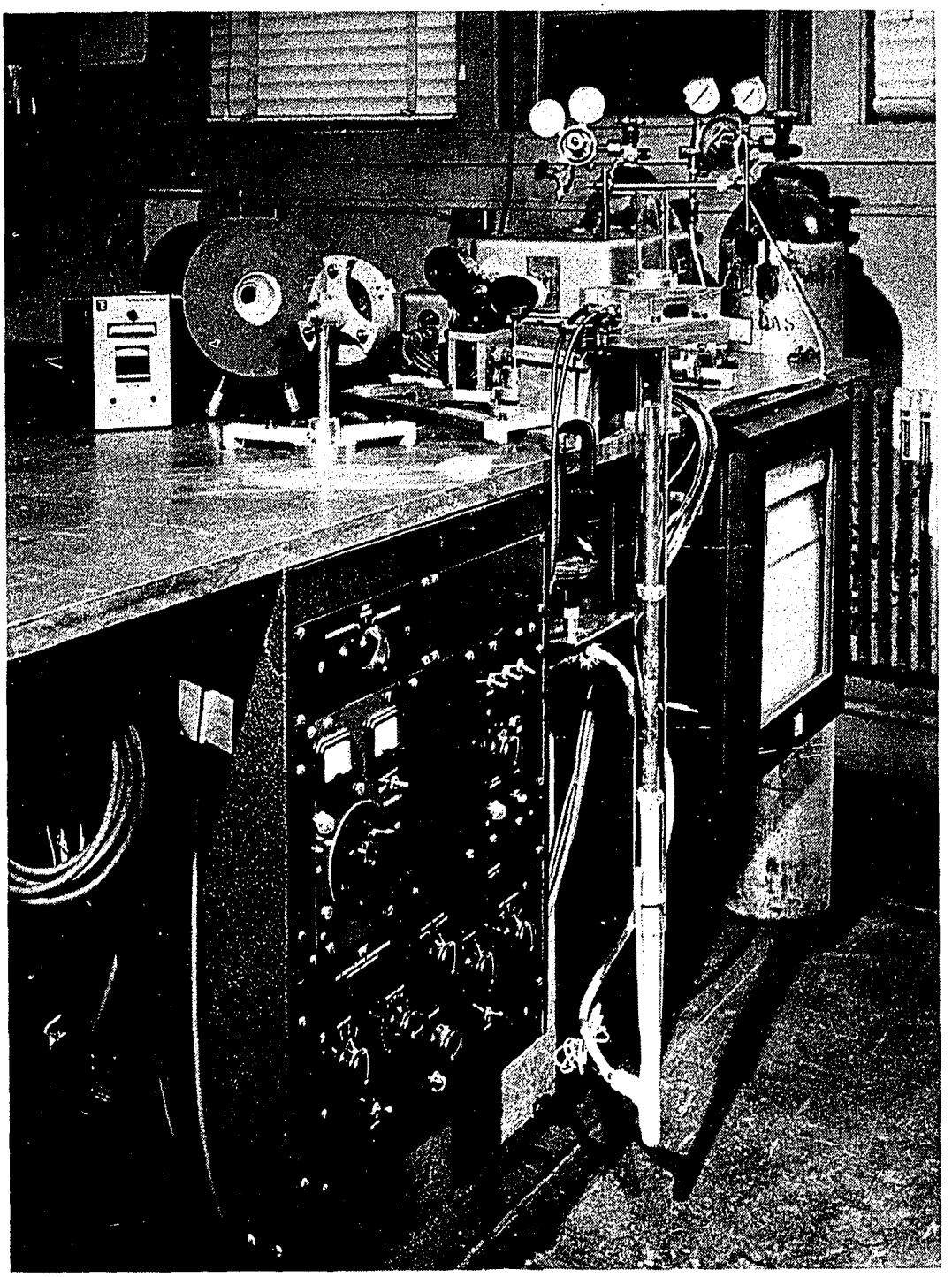

Figure II-1. Photograph of Experimental System.

Gas Supply

Approximately 3000 milliliters per minute of natural gas were required to produce a conical laminar flame 20 centimeters high with an 18 millimeter diameter base. Another requirement was to produce a steady flame for periods of 30 minutes. To meet these requirements, gas was supplied from a cylinder which contained 7000 liters of gas at standard conditions. The gas flowed through a two stage regulator, a 15 micron filter, and a low pressure regulator. The low pressure regulator maintained the gas pressure at 1.7 atmospheres. The gas flow to the burner was controlled by a metering valve. A schematic diagram of the supply is given in Figure II-2. The large cylinder of natural gas was purchased from Phillips Petroleum Company and had the approximate composition:

Component	Mol Percent
Nitrogen	0.2
Carbon Dioxide	0.8
Methane	91.4
Ethane	4.2
Propane	1.7
Butenes	0.3
Butanes	0.8
Pentenes	0.1
Pentanes	0.5

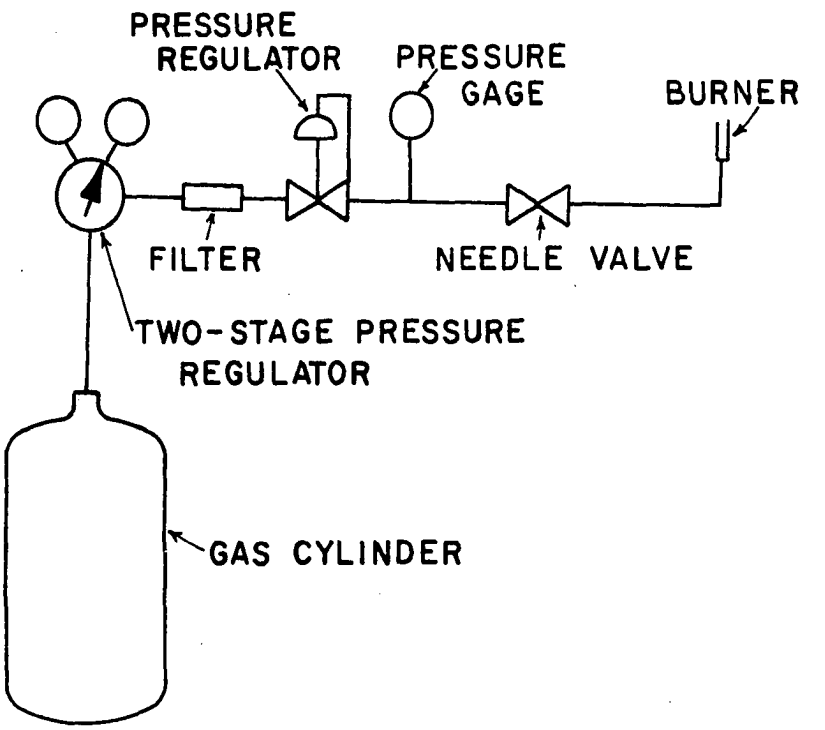

Figure II-2. Schematic Diagram of Gas Fuel Supply

Liquid Supply

Acetone expands approximately five hundred to one with the liquid to gas phase transition, thus about 3 to 5 milliliters per minute of liquid acetone are consumed by a steady conical laminar flame 20 centimeters in height and 1.8 centimeters in diameter at the base. The boiling point of acetone (56.5°C) forces the requirement of heating all parts of the supply system. A water bath, heating tape, and heater in the burner were used to prevent condensation. The bath consisted of an insulated tank, a temperature sensing element, a relay control box, heaters, and a stirrer.

Temperature control of plus or minus 0.1°C of the set point temperature was achieved with a sealed-glass, mercury sensing device. The sensing system consisted of a mercury filled glass bulb, a capillary, and reservoir. A tungsten wire electrode extended into the capillary. As heat was applied to the bulb, mercury rose in the capillary, made contact with the tungsten wire, and closed the circuit. Closing of the circuit actuated a relay for shutting off the supply power to the heaters.

Gas was generated by evaporation from a cylinder of liquid acetone and was regulated through a shut off valve, a filter, a low pressure regulator, and a metering valve. The cylinder, valves, filter, and regulator were submerged in the bath (Figure II-3). Operating the bath at 90°C provided

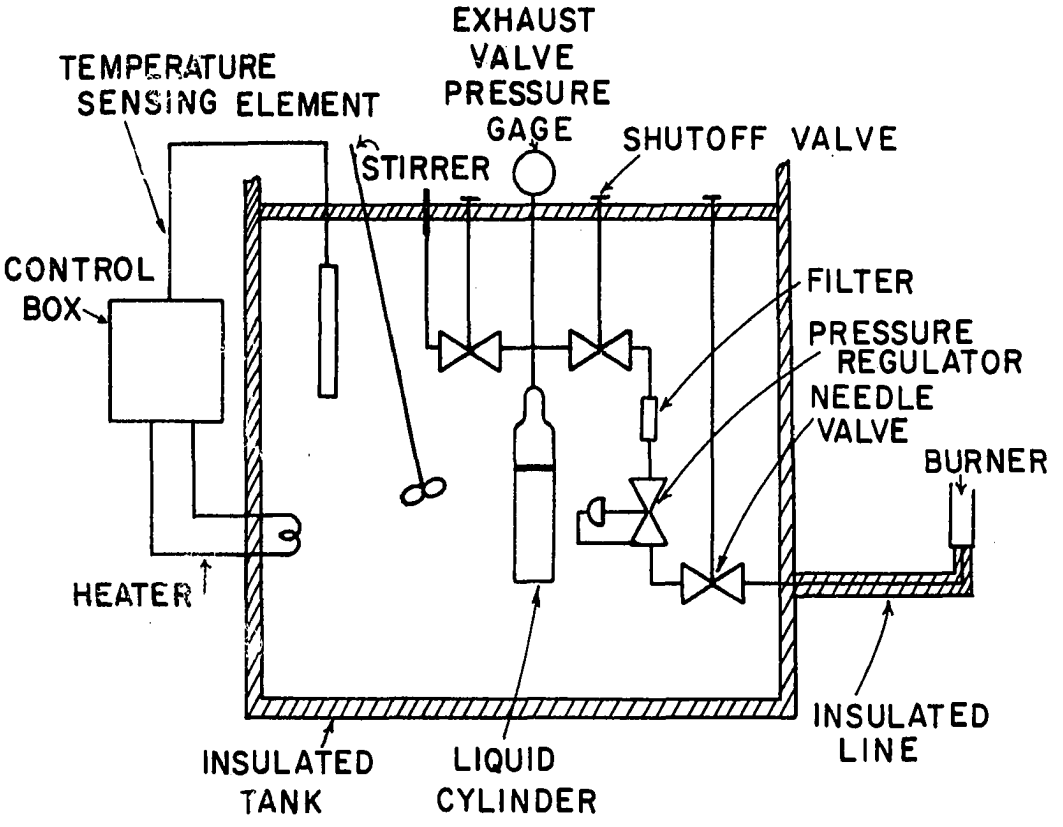

Figure II-3. Schematic Diagram of Liquid Fuel Supply and Bath

vapor to the pressure regulator at approximately 2 atmospheres for normal vapor withdrawal rates and 1.68 atmospheres pressure was maintained to the metering valve. Leaving the metering valve and the bath, gas flowed to the burner through a flexible tube wound with heating tape.

Due to the corrosive nature of acetone, the use of special seals, seats, and diaphrams was necessary. In the regulator, Teflon* faced butyl rubber was used for the diaphram and Teflon was used for the seat. Viton "A"* was used as seats in the metering valve.

Burner Assembly

From the literature it was apparent that there are as many burner designs as laboratories doing flame research. For this laminar diffusion flame study, the design for a burner assembly was taken from Barr (2). The requirements were to provide laminar flow and produce a steady flame for periods of at least thirty minutes. Two concentric cylinders were used in which the fuel gas flowed up the inner cylinder and oxidizer, air, flowed up the annulus. The air flow was not regulated and was a result of natural convection caused by the flame. Since calculations proved to be useless for selection of cylinder sizes, trial and error was used. Once satisfactory sizes of cylinders were determined the burner and special chimney were built.

---

*Trademark of E. I. du Pont de Nemours Co., Inc.

Burner

The burner barrel was made from 1.8 centimeter outside diameter, 0.090 centimeter thick wall stainless steel tubing. A 0.95 centimeter outside diameter cartridge heater was placed inside the barrel and extended from the base to the top of the barrel. The heater was supported by a heat exchanger type brass tee. Attached to the outside of the barrel were two 3-pronged standoffs. A friction fit was maintained between the chimney wall and the standoffs by nylon machine screws tapped into the standoffs. The centering of the barrel in the chimney was accomplished by adjusting the screws. A cross-section of the barrel is illustrated in Figure II-4.

Either a single tube or a double tube burner tip extended 20 centimeters above the top of the barrel. The single tube burner was made from the same size tubing as the barrel. The double tube burner tip was made from two 1.27 centimeters, outside diameter, stainless steel tubes. The two tubes were first welded together and then welded to a base that fit into the burner barrel. Figure II-5 shows a photograph of the barrel and the two burner tips.

Chimney

The chimney was made of three parts; a burner support, a viewing section, and a flue. The burner support and the various flues were made of 4.1 centimeters, inside diameter, Pyrex glass tubing. The burner support was 70 centimeters

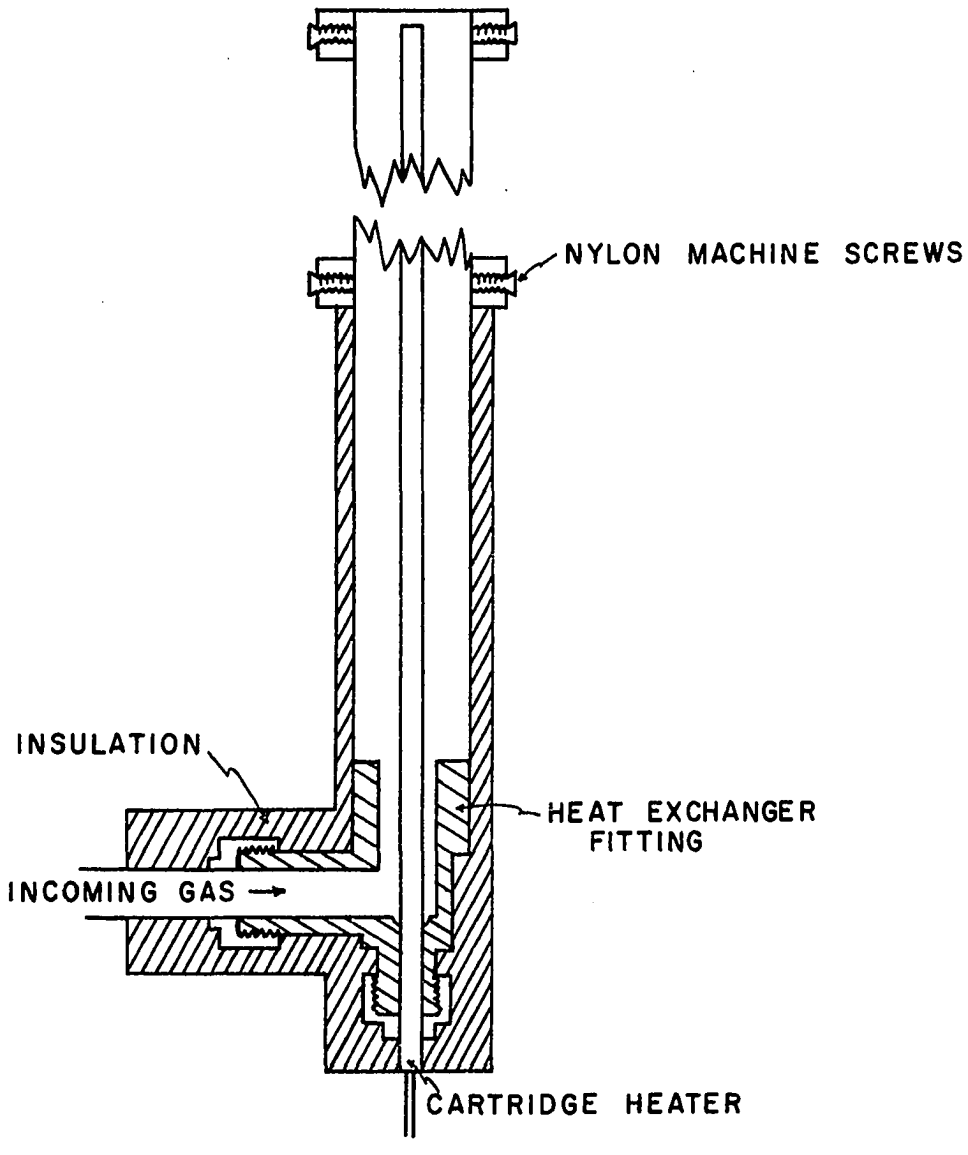

Figure II-4. Cross Section of Burner Barrel

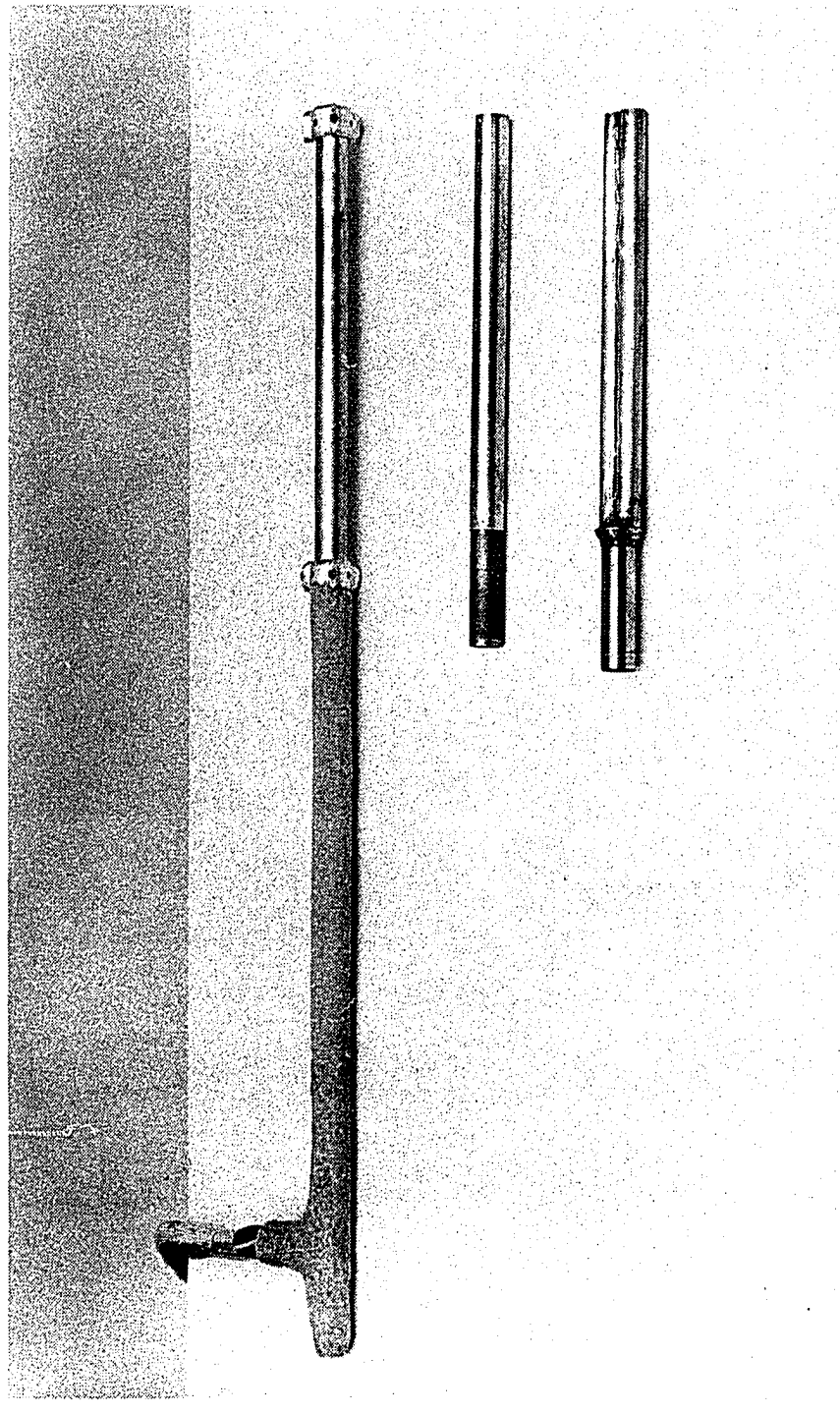

Figure II-5. Photograph of Burner Barrel and Tips.

high and the top of the tubing was cemented into an aluminum block. The aluminum block, which served as the viewing section, was 6.0 by 10.0 by 5.0 centimeters in dimensions of width, length, and height, respectively. A hole slightly larger than the outside diameter of the glass tubing was drilled in the center of the block along the vertical axis. Two oblong viewing ports were cut through the shorter horizontal dimension of the block, and one oblong port was cut in the end of the block. The block rested on a small aluminum table which had guides perpendicular to the viewing path. The guides also served as seals for the pair of viewing ports. Calcium fluoride windows for observing the flame were mounted on the guides. Since the block could slide perpendicular to the viewing path, different parts of the flame in the horizontal plane could be focused into the monochromator. Water was circulated through the block to keep the viewing section at a low enough temperature so that radiation added by the block was negligible compared to the radiation emitted by the flames. Flues of various heights (10.0 to 30.0 centimeters) were placed in the top of the block to provide some control of the air flow through the chimney. A distance of 1.0 centimeter separated the burner support and the flue. A photograph of the chimney and table are shown in Figure II-6. Figure II-7 is a photograph of the entire burner assembly.

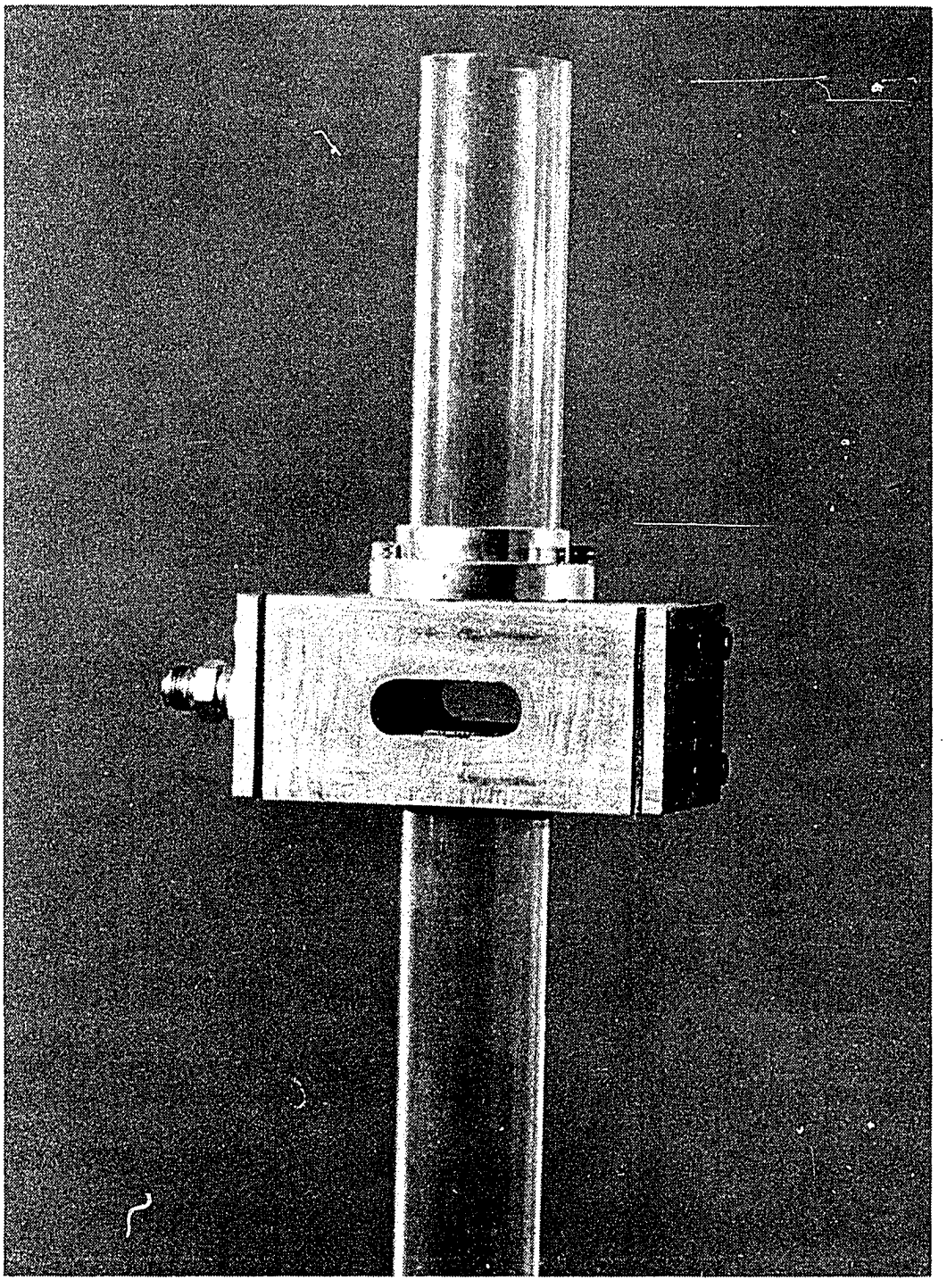

Figure II-6. Photograph of Flame Chimney.

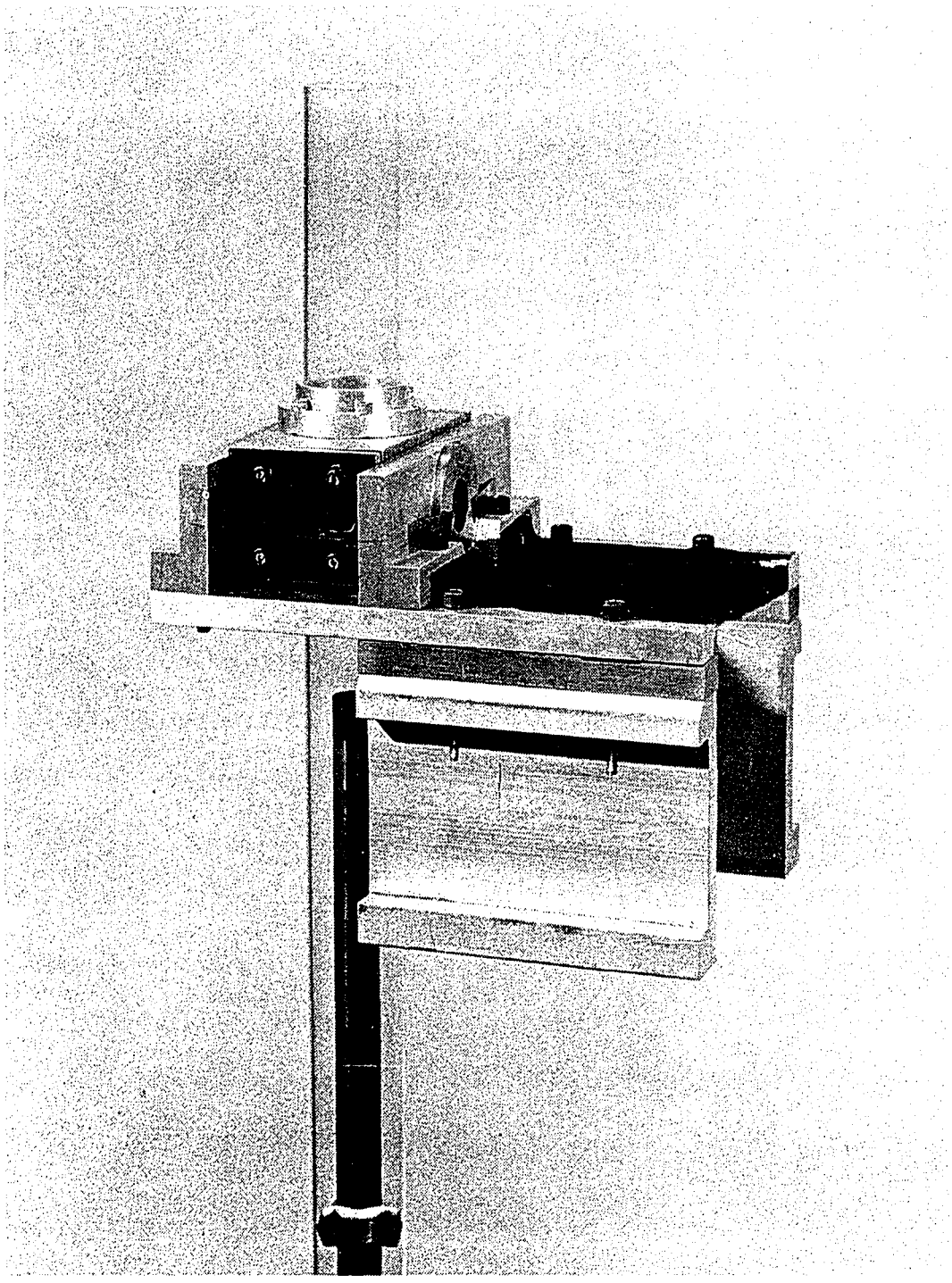

Figure II-7. Photograph of Complete Burner Assembly.

External Optics

The collection system was made of two high quality first surface mirrors as illustrated schematically in Figure II-8. Mirrors, M1, a flat elliptical diagonal, and M2, a concave spherical, were made of Pyrex brand glass and polished to 1/4 wavelength. The reflecting surface was an aluminum film with a protective coating of silicon monoxide. The main advantages of using mirrors in the collection system were to prevent selective absorption of infrared radiation and chromatic aberrations.

The experiment was run with the energy from the flames reflected from mirror, M1, onto spherical mirror, M2. Mirror, M2, then focused the energy onto the slits of the monochromator. The focal length of M2 was 28.9 centimeters and the diameter was 10.8 centimeters. Mirror M2 was placed 56.0 centimeters from the monochromator entrance, thereby forming an f-number (aperture ratio) of 5.18 and a viewing area with the same dimensions as the slit opening area. The f-number, 5.18, was slightly smaller than the f-number of the collimating optics of the monochromator. Thus, the maximum signal strength reaches the detector. Aberrations were minimized by placing mirror, M1, as close as possible to the beam emerging from M2.

A blackbody radiator replaced the flame source for calibration purposes. As long as each element of the collection system is flooded by its source of energy and the

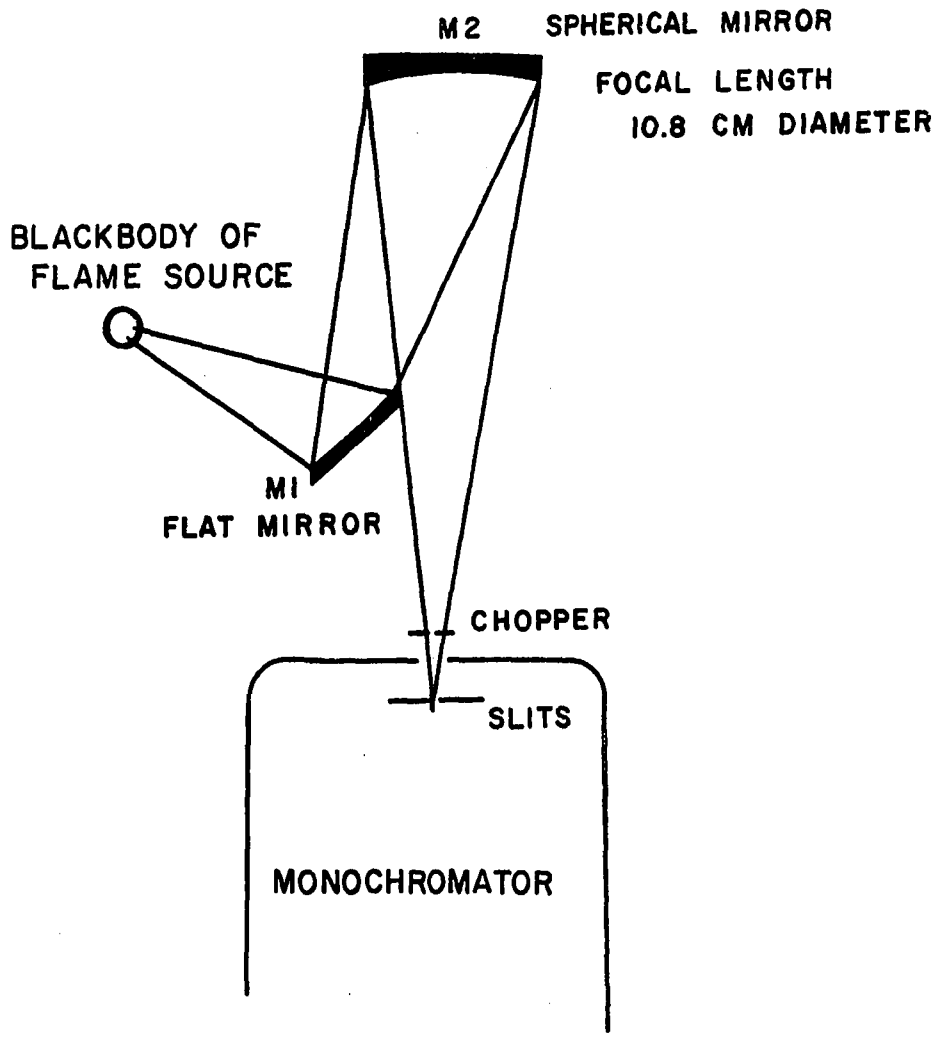

Figure II-8. Schematic Diagram of External Optics

monochromator optical system is flooded by the beam entering the monochromator, the solid angle and area of viewing do not have to be known. This technique eliminates a complicated analysis of the solid viewing angle versus wavelength.

Monochromator

A Perkin Elmer, Model 98, Single Pass Infrared Monochromator was used in this experiment. Calibration of the instrument was against a blackbody radiation source to obtain intensity versus wavelength. A NaCl prism and thermocouple detector were used to obtain the spectral distribution from 1.0-6.0 microns from the natural gas and acetone flames. A schematic diagram of the monochromator measurement system is illustrated in Figure II-8 and the internal optics are shown in Figure II-9. In order to interpret the calibration, an understanding of the system is necessary.

Radiation from the external optical collection system is focused on the variable width entrance slits, S1. The portion of the beam passing through the entrance slit is collimated by the off-axis paraboloid mirror, M3, and is refracted by the prism, P. The Littrow mirror, M4, returns the radiation which is again refracted by the prism. Energy is focused by the paraboloid onto mirror, M5, where it is reflected and brought to focus in a spectrum across the exit slits, S2. The exit slit passes radiation of a narrow wavelength range that depends on the slit width. The midband wavelength depends on the

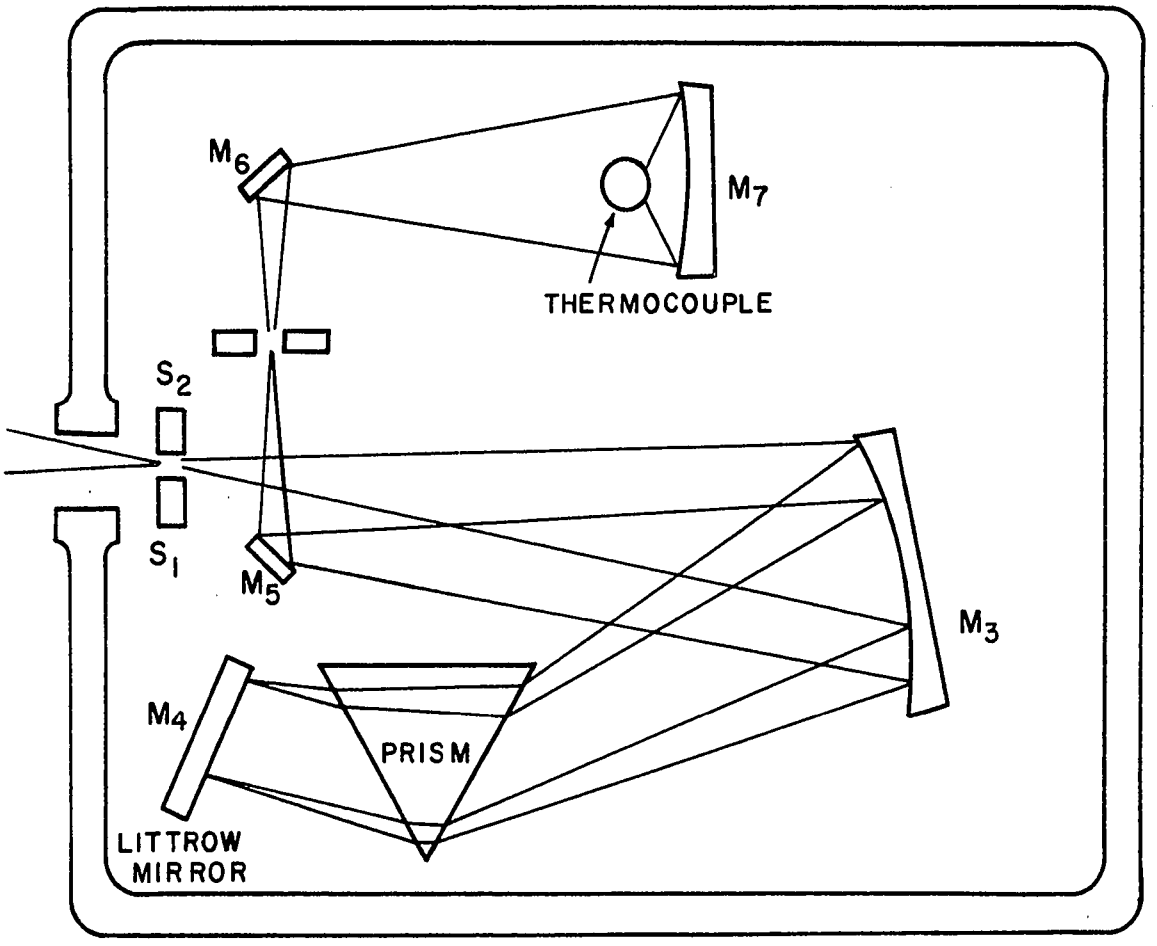

Figure II-9. Schematic Diagram of Monochromator Internal Optics

Littrow angle setting. This energy passing the exit slits is reflected by mirror, M6, and is focused on the thermocouple, T. Energy is modulated by the chopper, CH, as it enters the monochromator. After detection of this pulsating signal by the thermocouple, the signal is pre-amplified, amplified and rectified. The resulting direct-current signal is recorded on a strip-chart. Figure II-10 schematically shows the operation of the system.

A wavelength drive mechanism automatically rotates the Littrow mirror. This rotation is accomplished with a motor driven, threaded shaft and mechanical linkage. The wavelength micrometer drum is connected to the threaded shaft. It indicates the position of the Littrow mirror. The wavelength drive mechanism also sends a pulse signal to the amplifier at regular intervals of drum position. These pulses appear on the strip charts as narrow blips. These blips or wavelength marks are used for the identification of wavelength of the recorded spectra.

The only control available to alter the amount and spectral purity of energy striking the thermocouple is the slit size. In this monochromator the slits S1 and S2 are mechanically linked so they are each opened the same width. Thus the slit openings should be such that diffraction is minimized and spectral purity of the system is maximized.

In order to minimize diffraction effects of the monochromator, the aperture effect of the prism must be analyzed.

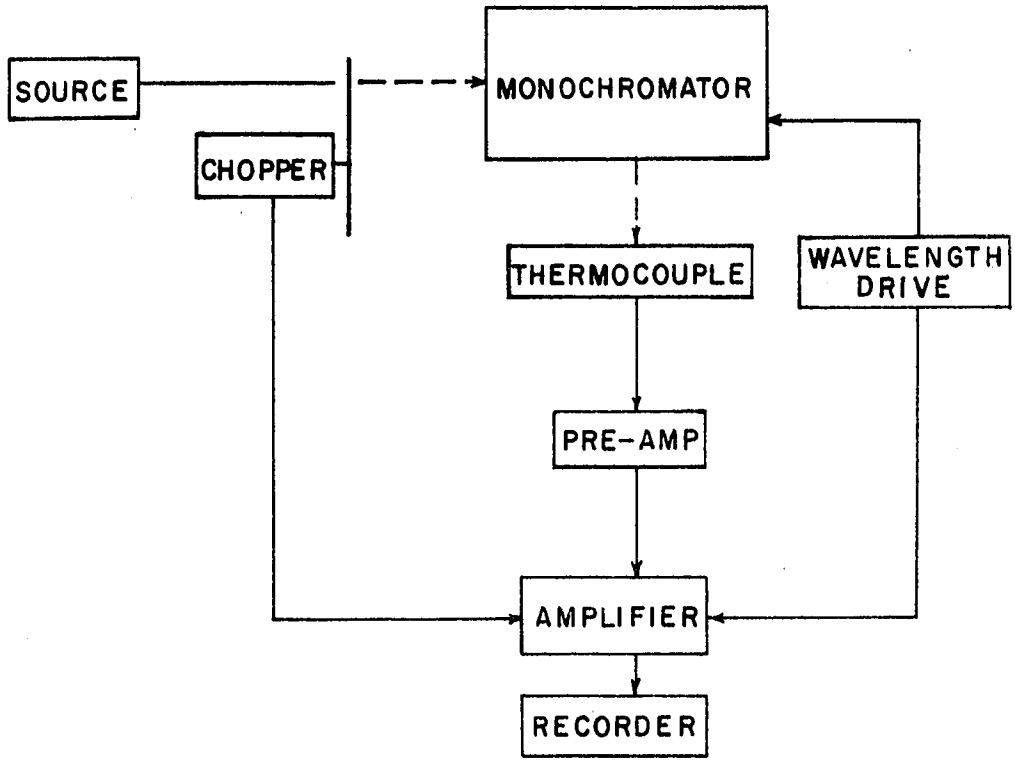

Figure II-10. Schematic Diagram of Monochromator Measurement System

The prism serves as the limiting aperture for the monochromator. Any energy passing through this rectangular aperture will have its intensity distribution altered. For this discussion a noncoherent monochromatic energy beam was used. The noncoherent beam assumption corresponds to actual conditions of the experiment since the source was either the flames or the blackbody. The validity of the assumption was given by Harrison, et al. (14). There would be no diffraction pattern caused by the slits because of the noncoherent beam. Rossi (36) gives a rigorous treatment of limiting aperture effect of a prism. The width of the entering beam is much narrower than the height because of the entrance slit shape. Thus, only the intensity pattern on the horizontal plane needs to be analyzed. Intensity along the horizontal axis is given by

$$I = \frac{I_0 \sin^2\alpha}{\alpha^2} \qquad \text{(II-1)}$$

where

$$\alpha = \frac{\pi\ a\ X}{f\lambda}$$

X is horizontal axis coordinate

I_0 is entering intensity

a is effective prism aperture

f is focal length of system

λ is wavelength.

The maxima of Equation II-1 occur at values of α that satisfy

$$\tan \alpha - \alpha = 0$$

and the minima occur at $\alpha = \pm\pi m$ ($m = 0,1,2,\ldots$). To compute the half interval of the central maximum

$$X = \frac{f\lambda}{a} .$$

For the prism used in this experiment f was 26.7 centimeters, a was 4.75 centimeters. Thus, for $\lambda = 5.0$ microns, $X = 28.2$ microns, and the width of the central maximum is 56.4 microns. Increasing the slit width to this value increased the intensity of the central maximum without much alteration of its width. As the slit is opened beyond this width, the width of the pattern is increased the same amount as the slit is opened while the intensity is not appreciably increased. After opening the slit past 56.4 microns, a square topped intensity pattern is formed, for which the width is the same as the slit opening. This result is due both to the magnification of the system being one and minimization of the diffraction effects.

Spectral purity is the remaining variable affected by the slit openings. When a source of energy composed of energy at different wavelengths is focused through a prism, a separation of the intensity pattern occurs for each wavelength of the source beam. The bending of the intensity pattern for each wavelength through a fixed angle is called the dispersion of the prism. The angle that the pattern is bent is a function of wavelength of the energy. The classic example is the separation

of light into color bands when it is passed through a prism. For a continuum energy source there will be an overlapping of the entrance slit intensity patterns at the exit slit. By making the slit opening smaller, there will be a smaller band of intensity patterns exiting the slit, thereby enhancing spectral purity.

The spectral slit width, $\Delta\lambda$, which is half of the total interval falling across the exit slit, was calculated as the sum of the dispersion and resolution effects of the prism. The diffraction was minimized by opening the slits to a width greater than the width of the central maximum of the intensity pattern. The remaining diffraction effects set the upper limit of the resolving power of the prism. The Rayleigh criterion was used to determine this resolution interval, $\Delta\lambda_R$. This criterion demands that two intensity patterns must have a wavelength separation of at least $\Delta\lambda_R$ before they can be resolved. Thus, the additional spectral width, $\Delta\lambda_R$, accounts for the fact that the wavelength can only be determined to within a wavelength interval.

The spectral slit width due to the resolution limit of the monochromator was calculated by determining the wavelength separation of two intensity patterns so that the central maximum of one wavelength was centered over the first minimum of the second wavelength. For a rectangular opening, Jenkins and

White (25) define resolving power to be

$$\frac{\lambda}{\Delta\lambda_R} = b \frac{dn}{d\lambda} \qquad \text{(II-3)}$$

where

λ is wavelength

n is refractive index of prism

b is width of base of the prism.

Thus,

$$\Delta\lambda_R = \frac{\lambda}{2b \frac{dn}{d\lambda}}, \qquad \text{(II-4)}$$

since the beam passes through the prism twice.

The equation for the spectral slit width due to dispersion was given by the monochromator manual (24) as

$$\Delta\lambda_D = \left[\frac{1 - n^2 \sin^2 (A/2)}{4 \frac{dn}{d\lambda} \sin (A/2)}\right]^{1/2} \frac{s}{d} \qquad \text{(II-5)}$$

where A is the apex angle of the prism

n is the refractive index of the prism

s is the width of the slit opening

d is the focal length of the paraboloid mirror M3.

The index of refraction versus wavelength for NaCl, as was used in these experiments, have been empirically fitted by Baly (1) to the equation

$$n^2 = a^2 + \frac{M_1}{\lambda^2 - \lambda_1^2} - \frac{M_2}{\lambda_2^2 - \lambda^2} \qquad \text{(II-6)}$$

where a^2 is 5.1790

M_1 is 0.018496

λ_1^2 is 0.01621

M_2 is 8977.0

λ_2^2 is 3149.3.

Thus, the derivative of index of refraction with respect to wavelength can be computed from Equation II-6. A slit width of 100 microns was used as the compromise to minimize diffraction effects and maximize spectral purity. The following Table II-1 gives spectral slit properties versus wavelength: total spectral slit width, $\Delta\lambda = \Delta\lambda_D + \Delta\lambda_R$; dispersion spectral slit width, $\Delta\lambda_D$; resolution spectral slit width, $\Delta\lambda_R$; index of refraction n; and derivative of index of refraction with respect to wavelength, $\frac{dn}{d\lambda}$. Table II-1 was computed using values of

s = 100 microns

d = 26.7 centimeters

A = 60°

d = 7.5 centimeters.

In the monochromator, the Littrow mirror, M4, is rotated about the vertical axis to scan the spectrum past the exit slit. The period of oscillation of the thermocouple signal is fixed by 13 Hertz rate of chopping of the radiation beam to the

TABLE II-1

SPECTRAL SLIT WIDTH VERSUS WAVELENGTH

Wavelength (Microns)	Total Spectral Slit Width (Microns)	Dispersion Slit Width (Microns)	Rayleigh Slit Width (Microns)	Refracture Index (Microns)	Dispersion (/Microns)
1.0	0.00972	0.00921	0.00051	1.53180	-.01307
1.2	0.01635	0.01533	0.00102	1.52978	-.00787
1.4	0.02448	0.02273	0.00176	1.52848	-.00531
1.6	0.03335	0.03065	0.00270	1.52757	-.00394
1.8	0.04197	0.03819	0.00379	1.52687	-.00317
2.0	0.04946	0.04455	0.00491	1.52628	-.00272
2.2	0.05528	0.04931	0.00597	1.52577	-.00246
2.4	0.05932	0.05240	0.00692	1.52529	-.00231
2.6	0.06174	0.05401	0.00773	1.52484	-.00224
2.8	0.06285	0.05446	0.00839	1.52439	-.00223
3.0	0.06298	0.05406	0.00892	1.52395	-.00224
3.2	0.06242	0.05309	0.00934	1.52349	-.00229
3.4	0.06141	0.05175	0.00966	1.52303	-.00235
3.6	0.06012	0.05020	0.00992	1.52256	-.00242
3.8	0.05866	0.04854	0.01012	1.52206	-.00250
4.0	0.05713	0.04685	0.01028	1.52155	-.00259
4.2	0.05557	0.04517	0.01040	1.52103	-.00269
4.4	0.05402	0.04353	0.01050	1.52048	-.00279
4.6	0.05251	0.04194	0.01057	1.51991	-.00290
4.8	0.05105	0.04043	0.01062	1.51932	-.00301
5.0	0.04965	0.03899	0.01067	1.51870	-.00313
5.2	0.04831	0.03761	0.01070	1.51807	-.00324
5.4	0.04703	0.03632	0.01072	1.51741	-.00336
5.6	0.04582	0.03508	0.01073	1.51672	-.00348
5.8	0.04466	0.03392	0.01074	1.51601	-.00360
6.0	0.04356	0.03282	0.01074	1.51528	-.00372

monochromator. The rotation of the Littrow mirror must be slow enough so that the change in wavelength per period of the chopped signal be small compared to the spectral slit width $\Delta\lambda$, being observed. The rotation of the drum of eight minutes per 100 drum numbers represents a scan of approximately 2.8 microns in the 1.0 to 6.0 micron range. At this scanning speed a shift of 0.00029 microns occurs for each cycle of the chopper. The minimum spectral slit width occurs at 1.0 micron and is 0.00972 microns. Since values of spectral slit width increase as the wavelength increases, the effect of the scanning rate is even less for the larger wavelengths and may be neglected.

Blackbody Radiator

In order to determine the absolute intensity of the flames, the output of the monochromator was calibrated using a blackbody radiator. A blackbody is an object that completely absorbs all radiant energy incident on it and the radiation emitted at any given temperature is the maximum possible. The maximum possible radiation that can be emitted is described by Planck's law given by Equation I-12. Since a blackbody radiator is a perfect absorber and radiator of radiation at all temperatures and wavelengths, a blackbody radiator has an emissivity, $\epsilon = 1$. Although no material has an $\epsilon = 1$, a cavity can be used to approximate the blackbody conditions. A cavity with a small opening has an emissivity

approximated by

$$\epsilon_c \cong \frac{\epsilon_m}{\epsilon_m + \frac{s}{S}(1 - \epsilon_m)} \qquad \text{(II-7)}$$

where ϵ_c is the emissivity of the cavity

ϵ_m is the emissivity of the materials of the cavity walls

s is the area of the aperture

S is the area of surface interior.

As can be seen from Equation II-7, a cavity with a small ratio of aperture area to interior surface area can closely approximate a blackbody radiator.

For this experiment the heated cavity was made of oxidized iron which according to Love (26) shows an emissivity greater than 0.8 in the temperature range 600 to 1000°K. The cavity was conical in shape with a circular aperture 1.0 centimeter in diameter. The cone was 20.0 centimeters long and 5.0 centimeters in diameter at the base. Using these dimensions in Equation II-7, yields an emissivity greater than 0.99. The cavity was made by cutting a 15° apex cone in a cylindrical iron bar and attaching the aperture face plate. A 30° aperture angle was cut in the face plate. Commercial cylindrical heating elements were placed around the bar. The end heaters were made of the same coiled resistance heating wire as contained in the commercial heating elements.

A jacket of insulation 4.0 centimeters thick was placed around the heating elements. Figures II-11 and II-12 show the construction of the cavity and the completed unit. The cavity, heaters, and insulation were placed in a cylindrical steel case. An air space of approximately 2.0 centimeters separated the case and the insulation. Mounted on the case were adjustable legs, a handle, and connections for the heaters and thermocouple.

A Chromel-Alumel thermocouple extending just inside the apex of the cone was used for the temperature sensing element of the cavity. A Thermo-Electric Indicating Thermocouple Proportional Controller, Model 400, was used for temperature control. The controller was able to hold the cavity to within ±1°C of the set point temperature. The indicated temperature of the controller was calibrated against the cavity temperature by placing a calibrated thermocouple in the cavity and recording the calibrated thermocouple temperature for several indicated controller temperatures. The calibrated thermocouple output was read using a Leeds and Northrup Millivolt Potentiometer, Catalog No. 8686, and using an ice bath for the reference junction.

In order to minimize temperature gradients in the cavity walls, the cavity was held at the controlling set point temperature for one hour before it was used as the radiation source. A maximum of 5°C variation of the cavity wall temperature over the interior of the cavity was determined by

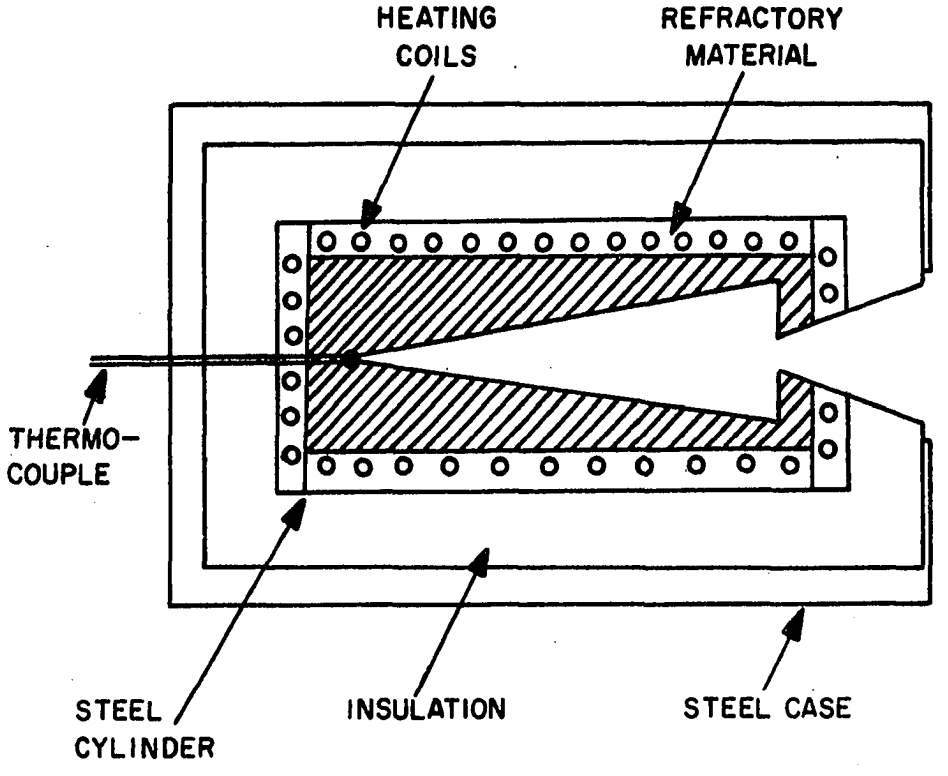

Figure II-11. Cross Section of Blackbody Radiator

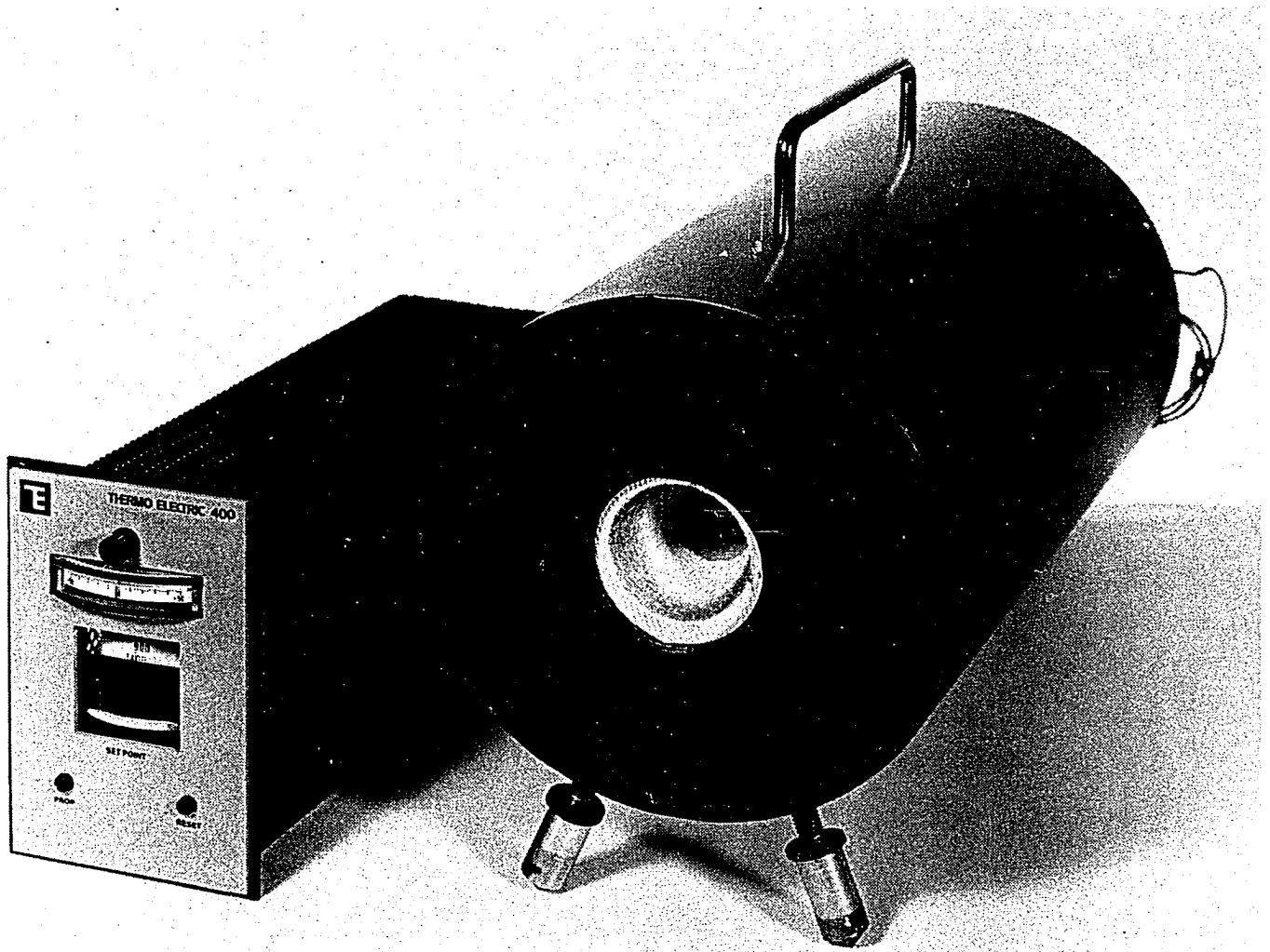

Figure II-12. Photograph of Blackbody Radiator.

thermocouple measurements. When the cavity was run at a temperature such that the cavity wall glowed a dull orange, no appreciable changes of intensity of the color could be distinguished over the interior of the cavity. An optical pyrometer temperature agreed to withing 5°C of the calibrated cavity temperature.

The blackbody radiator also permitted a check on the wavelength calibration of the monochromator by comparing the shift of peak intensity with temperature. The wavelength of peak intensity as given by Wiem's displacement law is

$$\lambda = \frac{2897.6}{T}$$

where λ is the wavelength in microns

T is absolute temperature in °K.

CHAPTER III

EXPERIMENTAL PROCEDURES

The calibration procedures were the same for both the emission and extinction coefficient data and the radiation profiles data. The emission coefficient and radiation profile data required absolute intensity measurements. On the other hand calculation of the extinction coefficient required relative intensities, only, for two different path lengths. Although the calibrations were the same for both types of data, the recording procedures and measurements were different.

Calibrations

Three types of calibration were necessary in order to translate the strip chart record into intensity measurements. First, the calibration was made to determine the relationship between the drum setting and the wavelength of energy being recorded. Second, since the detector views energy from a small bandwidth, a relationship between this total intensity and the intensity of the central wavelength of the band was derived. Third, the full scale pen deflection of the strip chart was calculated from the strip chart

recording of the intensity of radiation from the blackbody source.

Wavelength Versus Drum Setting

The monochromator and NaCl prism used in this experiment have been used by other investigators, Hood (17) and Tsai (39). Hood identified the drum settings corresponding to a number of absorption peaks of 1, 2, 4, trichlorobenzene; toluene; polystyrene; and didymium glass. The wavelengths of these absorption peaks were accurately determined by Plyler et al. (33, 34, and 35). For this experiment, the Littrow mirror was adjusted so that the absorption peaks of the polystyrene film agreed with drum settings recorded by Hood. His data in the 1.0 to 6.0 micron range were then fitted to the fourth order polynominal,

$$\lambda = A_0 + A_1 d + A_2 d^2 + A_3 d^3 + A_4 d^4 \qquad \text{(III-1)}$$

where λ is the wavelength in the range of 1.0 to 6.0 micron

d is the drum setting.

The constants of Equation III-1 were

$$A_0 = -6.4745574 \times 10^{3}$$
$$A_1 = 1.3675276 \times 10^{1}$$
$$A_2 = 1.0751986 \times 10^{-2}$$
$$A_3 = 3.7338540 \times 10^{-6}$$
$$A_4 = 4.8363304 \times 10^{-10}$$

A table of wavelength versus drum setting computed by using Equation III-1 is given in Table III-1. Other absorption peaks of known wavelengths agreed with the wavelength from the drum settings to within 0.5 percent. The absorption peaks of the polystyrene film were checked before each period of taking data. Over the period the data were taken, the drum settings for the absorption peaks did not vary any detectable amount. The intensity of the central wavelength can be accurately calculated knowing the wavelength and spectral slit width of the observed energy.

Bandwidth Intensity

Total intensity passing the exit slit of the monochromator can be expressed by the integral

$$I_{\lambda_0} = \int_{\lambda_0 - \Delta\lambda}^{\lambda_0 + \Delta\lambda} I_\lambda(\lambda) W(\lambda) d\lambda \qquad \text{(III-2)}$$

where $2\Delta\lambda$ is the wavelength interval of the intensity patterns leaving the exit slits

$W(\lambda)$ is a weighting function expressing the portion of an intensity pattern that is being observed

λ_0 is the wavelength of the intensity pattern that is centered in the slit.

The weighting function is given in Figure III-1. Upper and lower bounds of the integral can be computed by assuming

TABLE III-1

WAVELENGTH VERSUS DRUM SETTING

Drum Number	Wavelength (Microns)	Drum Number	Wavelength (Microns)
1650	5.614	1830	2.739
1655	5.609	1835	2.641
1660	5.596	1840	2.544
1665	5.575	1845	2.449
1670	5.547	1850	2.356
1675	5.512	1855	2.265
1680	5.470	1860	2.175
1685	5.422	1865	2.088
1690	5.369	1870	2.004
1695	5.310	1875	1.921
1700	5.245	1880	1.841
1705	5.177	1885	1.764
1710	5.103	1890	1.689
1715	5.026	1895	1.617
1720	4.944	1900	1.548
1725	4.860	1905	1.481
1730	4.772	1910	1.418
1735	4.681	1915	1.357
1740	4.587	1920	1.299
1745	4.491	1925	1.244
1750	4.393	1930	1.191
1755	4.294	1935	1.142
1760	4.192	1940	1.096
1765	4.090	1945	1.052
1770	3.986	1950	1.012
1775	3.882	1955	0.974
1780	3.777	1960	0.939
1785	3.671	1965	0.907
1790	3.566	1970	0.877
1795	3.460	1975	0.850
1800	3.355	1980	0.826
1805	3.250	1985	0.804
1810	3.146	1990	0.785
1815	3.043	1995	0.768
1820	2.941	2000	0.754
1825	2.839	2005	0.742

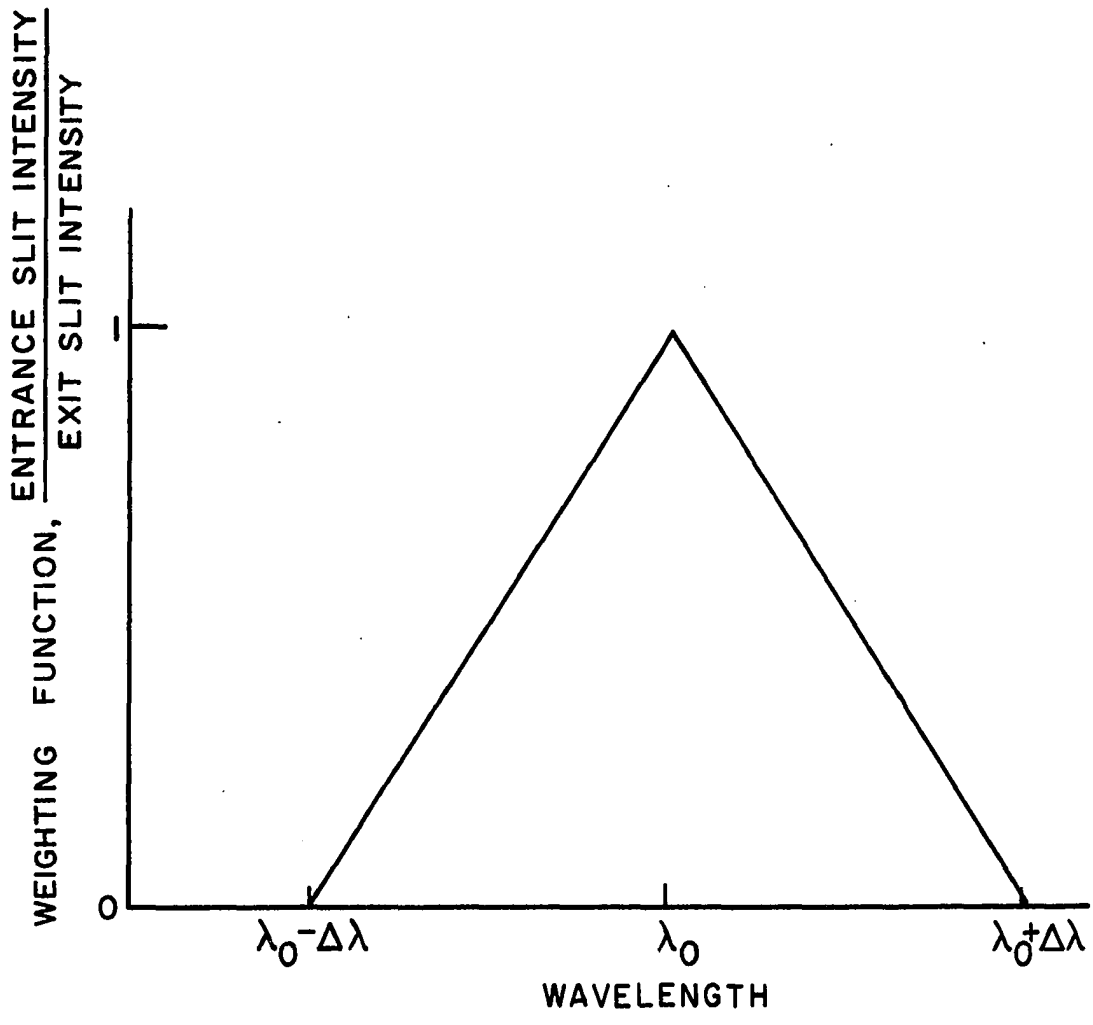

Figure III-1. Weighting Function for Exit Slit Intensity Patterns

$I_\lambda W(\lambda)$ is continuous and either monotonically increasing or decreasing over the interval. For a continuum of radiation, a small $\Delta\lambda$, and the given $W(\lambda)$ function, the assumptions are valid. Thus, the bounds are given by two approximation integrations; a mid-point formula, M, and the trapezoidal rule, T. Considering an interval b-a of a function f, T and M are defined as

$$T = (b - a)\left[\frac{f(a) + f(b)}{2}\right] \qquad \text{(III-3)}$$

and

$$M = (b - a)\left[f\left(\frac{a + b}{2}\right)\cdot\right] \qquad \text{(III-4)}$$

A negative second derivative yields

$$T < \int_a^b f(x)\,dx < M \qquad \text{(III-5)}$$

and a positive second derivative yields

$$T > \int_a^b f(x)\,dx > M \qquad \text{(III-6)}$$

Rewriting Equation III-2 as

$$I_{\lambda_0} = \int_{\lambda_0 - \Delta\lambda}^{\lambda_0} f(\lambda)\,d\lambda + \int_{\lambda_0}^{\lambda + \Delta\lambda} f(\lambda)\,d\lambda, \qquad \text{(III-7)}$$

where $f(\lambda) = I_\lambda(\lambda)\ W(\lambda)$,

conditions on T and M are met for each integral. Defining

$$T_1 = \Delta_\lambda\left[\frac{f(\lambda_0 - \Delta\lambda) + f(\lambda_0)}{2}\right] = \Delta\lambda \frac{I_\lambda(\lambda_0)}{2} \qquad \text{(III-8)}$$

$$T_2 = \Delta_\lambda\left[\frac{f(\lambda_0) + f(\lambda_0 + \Delta\lambda)}{2}\right] = \Delta\lambda \frac{I_\lambda(\lambda_0)}{2} \qquad \text{(III-9)}$$

$$M_1 = \Delta\lambda\left[f(\lambda_0 - \frac{\Delta\lambda}{2}\right] = \Delta\lambda \frac{I_\lambda(\lambda_0 - \frac{\Delta\lambda}{2})}{2} \qquad \text{(III-10)}$$

$$M_2 = \Delta\lambda\left[f(\lambda_0 + \frac{\Delta\lambda}{2}\right] = \Delta\lambda \frac{I_\lambda(\lambda_0 + \frac{\Delta\lambda}{2})}{2}, \qquad \text{(III-11)}$$

the maximum error was expressed by

$$\text{error} = \frac{2\left|M_1 - T_1\right|}{\left|M_1 + T_1\right|} + \frac{2\left|M_2 - T_2\right|}{\left|M_2 + T_2\right|} \cdot \qquad \text{(III-12)}$$

Errors were computed for a continuum source of a blackbody radiation at 933°K, over the 1.0 to 6.0 micron range. The 933°K temperature corresponds to a temperature used for calibration purposes.

Table III-2 shows that by using

$$I_{\lambda_0} = \Delta\lambda\ I_\lambda(\lambda_0). \qquad \text{(III-13)}$$

as the total band intensity, the maximum error of approximating the integral (III-2) is 1.07 percent. Using Equation III-13 and measuring the blackbody intensity, absolute intensity can be determined for the full scale pen deflection of the strip recorder for each gain setting of the amplifier.

Absolute Intensity

For the absolute intensity calibration, the blackbody radiator was placed at the same viewing location as the flames.

This procedure eliminated the need to know the solid angle and area of viewing since they were the same for both the flame and the calibration source. Using Equation I-12,

$$I_{\lambda b} = \frac{C_1}{\lambda^5} \left[e^{\left(\frac{1}{C_2/\lambda T - 1}\right)} \right],$$

and Equation III-13,

$$I_{\lambda_0} = \Delta\lambda \; I_{\lambda}(\lambda_0),$$

intensity related to the full scale pen deflection at any wavelength can be calculated from the blackbody intensity recording. The equation for the bandwidth intensity at λ_0 is given by

$$I_{\lambda_0} = \frac{\Delta\lambda \; C_1}{\lambda_0^5} \left[e^{\left(\frac{1}{C_2/\lambda_0 T - 1}\right)} \right] \qquad \text{(III-14)}$$

where I_{λ_0} is the intensity integrated over the bandwidth, $2\Delta\lambda$

λ_0 is the central wavelength.

The units of I_{λ_0} are watts/cm^2-steradian for

$\Delta\lambda$, the spectral slit width in microns

T, the absolute temperature in °K

C_1, a constant, 11,908.8 watts micron^{-4}/cm^2

C_2, a constant, 14,386.8 micron-°K.

In order to calculate the full scale bandwidth intensity, blackbody radiation was recorded on the strip chart over the

TABLE III-2

ERROR BOUNDS OF THE CENTRAL WAVELENGTH APPROXIMATION FOR THE MONOCHROMATOR EXIT SLIT INTENSITY

Wavelength Microns	Spectral Slit Width Microns	$\frac{2\lvert M_1 - T_1\rvert \times 100}{\lvert M_1 + T_1\rvert}$ Percent	$\frac{2\lvert M_2 - T_2\rvert \times 100}{\lvert M_2 + T_2\rvert}$ Percent	Error Percent
1.00	0.00972	0.50691	0.50630	1.01321
1.25	0.01826	0.53646	0.53541	1.07186
1.50	0.02889	0.50916	0.50772	1.01688
1.75	0.03990	0.43542	0.43373	0.86921
2.00	0.04946	0.33631	0.33472	0.67102
2.25	0.05646	0.23411	0.23274	0.46685
2.50	0.06071	0.14393	0.14286	0.28679
2.75	0.06267	0.07195	0.07115	0.14310
3.00	0.06298	0.01816	0.01759	0.03574
3.25	0.06220	0.02026	0.02066	0.04092
3.50	0.06079	0.04675	0.04702	0.09377
3.75	0.05904	0.06442	0.06461	0.12903
4.00	0.05713	0.07574	0.07587	0.15162
4.25	0.05513	0.08258	0.08267	0.16525
4.50	0.05326	0.08627	0.08633	0.17260
4.75	0.05141	0.08777	0.08781	0.17559
5.00	0.04965	0.08777	0.08780	0.17557
5.25	0.04799	0.08675	0.08677	0.17352
5.50	0.04642	0.08505	0.08505	0.17010
5.75	0.04494	0.08290	0.08290	0.16580
6.00	0.04356	0.08048	0.08048	0.16096

wavelength interval of 1.0 to 6.0 microns. Using the temperature of the blackbody radiation, the bandwidth intensity versus wavelength was calculated using Equation III-14. The full scale bandwidth intensity at a particular wavelength was then calculated by dividing the bandwidth intensity by the pen deflection from the strip chart. Since the full scale band intensity should be constant for all wavelengths, several full scale band intensities were compared to check the consistency of the entire monochromator system. Checks were made for several amplifier gain settings and blackbody temperatures. The full scale band intensities along each blackbody record agreed to within 2.0 percent. When selecting points for comparison, care was exercised to select points that did not fall into the strong CO_2 and H_2O and CO_2 absorption peaks centered at 2.7 and 4.3 microns, respectively. Calibrations were performed before each series of runs by comparing three points along the blackbody recording. Agreement to within 1.0 percent of the three points was achieved before the runs were made. The availability of a time-sharing computer terminal in the building was a tremendous help in speeding up the calibration calculations. The fact that the full scale band intensity for a particular blackbody recording can be calculated to within 2.0 percent over the wavelength range confirms the validity of the analysis of the monochromator system.

Once the full scale bandwidth intensity was known, the intensity was calculated by

$$I_\lambda = \frac{\text{(full scale bandwidth intensity)(pen deflection)}}{\Delta\lambda}$$

Using the full scale bandwidth intensity and the spectral slit width eliminated the need to compute the full scale intensity at each wavelength and greatly reduced the computation effort of the data analysis.

Flame Measurements

The radiation profiles data and the emission and extinction coefficient data required the same calibration calculations and prerun evaluations. A heating element and controlling mechanism holds the monochromator housing at a temperature to within ± 1°C. The room temperature was held at a temperature close to the controlled monochromator temperature in order to minimize the temperature gradient across the monochromator entrance. In preparation for a series of runs, the external optical collection system was checked for alignment. The alignment was very stable from one series of runs to another due to the method of fastening the collection system and monochromator to the large metal table. The black body radiator was brought up to controlling temperature. The amplifier and associated equipment were turned on and allowed to warm up for at least one hour. After the warm up period, several checks were made on the performance of the

amplifier for noise level, gain stability, optical stability, and gain setting sensitivities. Once satisfactory operation of the system was established, the wavelength versus drum setting was checked using the polystyrene film absorption peaks as the reference. Next the calibration against the blackbody radiator was performed. The blackbody was allowed to remain at the controlling temperature for one hour or more before use as the calibration source. The CaF_2 window that was ordinarily mounted on the viewing section of the chimney was placed at the monochromator entrance to account for the reduced transmission due to the window. Once the blackbody intensity was recorded, the CaF_2 window was placed back in the chimney, the burner assembly replaced the blackbody radiator, and the flame was ignited in the burner assembly. While the flame and the burner assembly were approaching steady state, full scale band intensities along the blackbody recording were calculated and checked for consistency. If the full scale band intensities were within a tolerance of 1.0 percent, the measurements of the flames were started.

Profile Data

For the radiation profile data it was necessary to know the exact position of the area of the flame being focused into the monochromator. Since the magnification of external optical collection system was one, the area of the

flame or around the flame that was observed was the same area as the entrance slits. The position of the viewing area of the flame was photographed for each recording position. A pin hole camera was mounted so that the pin hole was centered along the axis of viewing and the film plane was located perpendicular to the axis of viewing. With the camera in place, a photograph of a scale was taken and used as the reference scale. By making all measurements of the viewing position using the photograph of the scale, aberrations caused by the chimney window and the camera lens were eliminated.

Data were taken using the round burner tip on flames 125 mm in height and at heights of approximately 25 mm increments above the burner tip. For a particular height above the burner tip, the flame radiation was recorded beginning at the center of the flame and progressing along the horizontal at regular intervals until radiation could no longer be detected. In regions where the intensity recording ran off scale, the region was rescanned at a lower gain setting. Anytime a lower gain setting was used, it was compared with the calibrated gain setting and recorded. This comparison was made using special test signals built into the amplifier system. During a series of runs, the calibrated gain setting was checked for consistency of pen deflection for a given test signal. A series of profile data consisted of a blackbody calibration, a reference scale photograph, and a

photograph and strip chart recording of the spectral intensity for each position in and around the flame.

Emission and Extinction Data

For the emission and extinction coefficients, the length of viewing was an additional critical measurement parameter. The camera was placed perpendicular to the axis of viewing. A scale was photographed and used as the reference scale for the flame path measurements. The double-tubed burner tip was used to produce flames with an elliptical horizontal cross section. The viewing paths were through the major and minor axes of the elliptical cross section. The path through the major axis was approximately twice the path through the minor axis. Flames of 12.5 centimeters in height were used. Data were taken at 2.5 centimenters increments in height above the burner tips for the two paths. Each gain setting used in these runs was calibrated against the blackbody radiator.

CHAPTER IV

RESULTS

Measurements of intensity as a function of position and wavelength through the flame and the surrounding hot gas envelope reveal several problems with assumptions about laminar diffusion flames and with application of data from these flames. This chapter will discuss the analysis and presentation of the intensity profile measurements and will then show how this information applies to the calculation and application of the monochromatic extinction and maximum emission coefficients.

All intensity data from the flames are presented as radiation as it leaves the flame surface. This method of presentation made it necessary to correct the measurements for atmospheric attenuation that occurred in the path from the flame to the detector of the monochromator. The correction was made by using the blackbody radiation recording. A blackbody radiation curve would be a smooth curve if no attenuation occurred along the path from the blackbody radiator to the detector. By drawing a smooth curve on the blackbody recording to span the regions of atmospheric attenuation,

the fractional amount of attenuation was determined. Denoting the strip-chart recording of the actual blackbody radiation as $R_{a,\lambda}$ and the smoothed blackbody radiation (corresponding to no attenuation) as $R_{b,\lambda}$, then the fractional attenuation, τ_λ, can be written as

$$\tau_\lambda = \frac{R_{a,\lambda}}{R_{b,\lambda}} \qquad \text{(IV-1)}$$

where the subscript denotes the attenuation at a specific wavelength. Values of τ_λ were calculated at wavelengths in the two principal absorption bands, CO_2 and H_2O centered at 2.7 microns and CO_2 centered at 4.3 microns. Maximum attenuation occurred in the CO_2 band, where at the central wavelength of 4.3 microns the emitted energy was diminished by 75 percent ($\tau_{4.3} = 0.25$). Separate atmospheric attenuation corrections were applied to each series of experimental runs since there were day-to-day variations in the attenuation. While attenuation was constant for the CO_2 absorption band, variations as large as 10 percent occurred in the combined CO_2 and H_2O absorption band. The 10 percent figure does not represent a maximum variation of atmospheric attenuation that can occur in the 2.7 micron absorption band, but it does represent the maximum variation of attenuation on the days these experiments were run.

Values of intensity at the flame surface were computed from the strip charts using Equation III-15. Pen

deflections used in Equation III-15 were corrected for atmospheric attenuation in the path from the flame to the monochromator detector. Denoting the corrected pen deflection as CPD_λ and the actual pen deflection as APD_λ the correction at each wavelength was made using the equation,

$$CPD_\lambda = \frac{APD_\lambda}{\tau_\lambda} \qquad \text{(IV-2)}$$

where τ_λ is the fractional attenuation defined by Equation IV-1.

For flames from natural gas and acetone, emission occurred in the wavelength interval from 0.71 to 5.60 microns. In this interval specific wavelengths were selected for presenting the spectrum. Wavelengths were selected at each valley and peak of the emission band. Selection of intermediate wavelengths was based on the gradients between the valleys and peaks. A higher concentration of points was used in regions where steeper gradients occurred. The emission spectra of natural gas and acetone were similar although the intensity of the acetone spectrum was greater in magnitude. Therefore, many of the selected wavelengths for the two fuels are the same.

Intensity Profile Data

Cross sections of the flame at different heights are shown in Figure IV-1. For the luminous portion of the

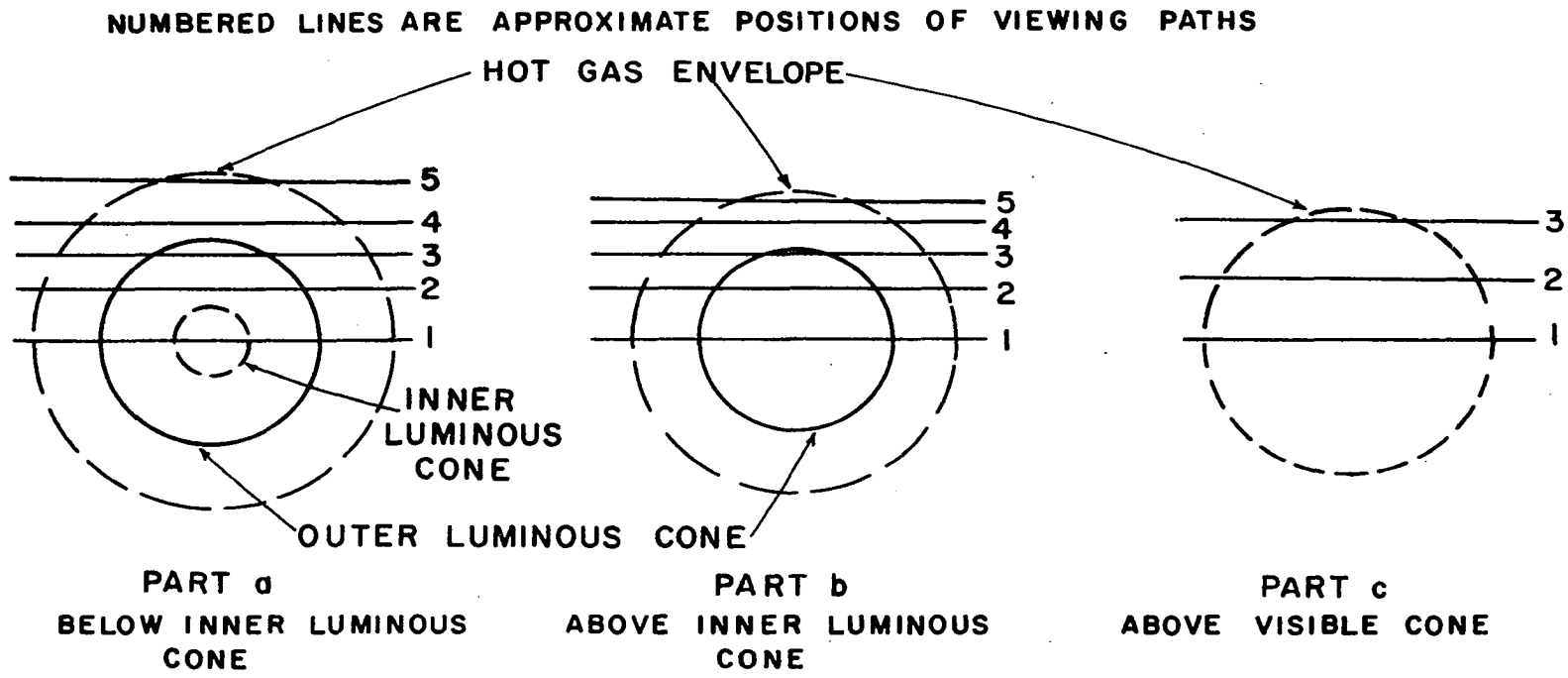

Figure IV-1. Flame Cross Sections.

flame at selected heights above the burner, intensities were analyzed for five paths. The approximate positions of these paths are indicated by the numbered horizontal lines (1 through 5) in parts a) and b) of Figure IV-1. The three paths through the luminous portion of the flame were spaced with one through the axis of symmetry, one equidistant from the center and the edge, and one near the edge. The two paths outside the luminous flame cone were taken with the first just outside the luminous cone and the second a distance from the center such that the intensity at 4.3 microns was approximately 10 percent of the intensity at 4.3 microns of the path just outside the luminous cone. In the region of emission above the luminous flame cone three paths were used. The three positions are indicated in part c) of Figure IV-1. The emission at 4.3 microns was used as the basis for deciding the positions of the paths. The first path was always through the center or axis of symmetry. The second and third paths were at a distance from the center so that the emission at 4.3 microns was approximately 50 and 10 percent of the first path.

It is important to note the change in path length as paths away from the center of the flame are considered. The length of the viewing path, a chord through the flame cross section, is a maximum at the center of the flame and decreases to zero for a path right at the edge of the hot gas envelope surrounding the luminous flame cone. The

emission path, x, can be expressed as a function of the distance from the center of the flame as

$$x = 2\sqrt{\left(\frac{D}{2}\right)^2 - y^2} \qquad \text{(IV-3)}$$

for $0 \leq y \leq D$

where D is the diameter of the hot gas emission envelope

y is the distance of path from the center of the flame.

The function described by Equation IV-3 shows the path length decreases at a faster rate as paths are considered near the edge of the emitting volume.

To aid in understanding the reduction and presentation of the data, consider the intensity along one position of height above the burner and one of the selected wavelengths. Depending on whether the vertical position was above or below the height of the luminous portion of the flame, there were either three or five data points, respectively. The measurements of distance from the viewing path to the center of the flame were taken from photographs of the flame for each viewing position. The intensity at the flame surface versus distance of viewing path from the center of the flame was plotted and a smooth curve was drawn through the points. Values of intensity were then read from the graph at even horizontal spacings. This process was repeated at each of the selected heights and the data were converted to computer

input. For each of the evenly spaced horizontal positions, values of intensity were computed by linear interpolation in an evenly spaced vertical direction. The above procedure was used to produce values of intensity on an evenly spaced path from the center of the flame at each of the selected wavelengths and for both natural gas and acetone flames.

Vertical position above the burner was converted to a dimensionless variable, $\bar{y}$, by the transformation

$$\bar{y} = \frac{\text{vertical distance above the burner}}{\text{visible flame height}} \quad \text{(IV-4)}$$

Using the vertical position variable, $\bar{y}$, the intensity fields for flames of 30 to 200 millimeters in height agreed to within 10 percent. This agreement occurred only when the same burner was used to produce the flame. To emphasize that the burner effects the radiation field through control of the passage of air to the flame, the horizontal component was not presented in dimensionless form.

Spatial distribution of intensity at each of the selected wavelengths for natural gas and acetone flames are presented in Tables A-1 and A-2. The vertical grid is presented as a dimensionless variable and covers the range 0.0 to 2.0 visible flame heights in 0.1 increments. The horizontal coordinate, which is the distance of the viewing path to the axis of symmetry of the flame, covers the range 0.0 to 10.0 millimeters in 1.0 millimeter increments. To compute the actual intensity at a particular position, the

value in the table must be multiplied by the units factor given at the head of each table. The outline of the visible flame cone is shown at the beginning of each table.

The luminous inner reaction cone extends 0.6 of the height of the visible flame for both natural gas and acetone. It was not possible to tell the exact height of the inner cone by direct visual observations or by photographs of the flame. However, the extent of the inner cone is well defined in the data by its lower volumetric emission. The outer visible cone of higher volumetric emission completely envelopes the inner cone and gives rise to a horizontal cross section as seen in part a) of Figure IV-1. As paths are considered from the center to edge of the luminous cone, intensity increases since the path length through the outer visible cone increases. The magnitude of the difference in volumetric emission between the inner and outer visible flame cones is actually greater than the intensity values presented in the tables since the path length decreases as paths are considered away from the center of the flame.

The strongest emission from the outer luminous cone occurs along two paths. The positions of the paths are just above the inner reaction zone at 0.6 of the visible height and near the edge of the flame at 0.4 of the visible height. These two strong emission paths are accounted for by a single consideration of path length. The longest paths through the high volumetric emission zone of the flames occurred at 0.4

and 0.6 of the visible flame height. Since the flame was conical, the path off the centerline through the outer visible cone at 0.4 was approximately the same length as the path through the center of the flame at 0.6. A similar result of maximum temperature occurring off the axis of symmetry and below the top of the inner reaction zone has been demonstrated by Lewis and von Elbe (28) for premixed flames.

With the exception of wavelength intervals centered about 2.7 and 4.3 microns, almost all emission was produced in the luminous flame cone. For the wavelength bands centered about 2.7 microns (the strong CO_2 and H_2O emission) and the wavelength band centered about 4.3 microns (the strong CO_2 emission) there was no discontinuity of emission at the luminous interface. The general shape of the intensity versus radius plots for wavelengths where emission extends beyond the luminous cone is shown in Figure IV-2. For horizontal sections below the inner luminous cone, intensity at the center of the flame is lower than at the edge of the luminous cone sections. Above the inner zone, the maximum intensity occurs at the center of the flame and gradually decreases toward the edge of the luminous flame. Outside the luminous cone, the plots were the same general shape. Intensity decreased rapidly through the region of one and one-half to two visible flame radii. Gradual decreases in intensity occurred for larger distances from the center of the flame.

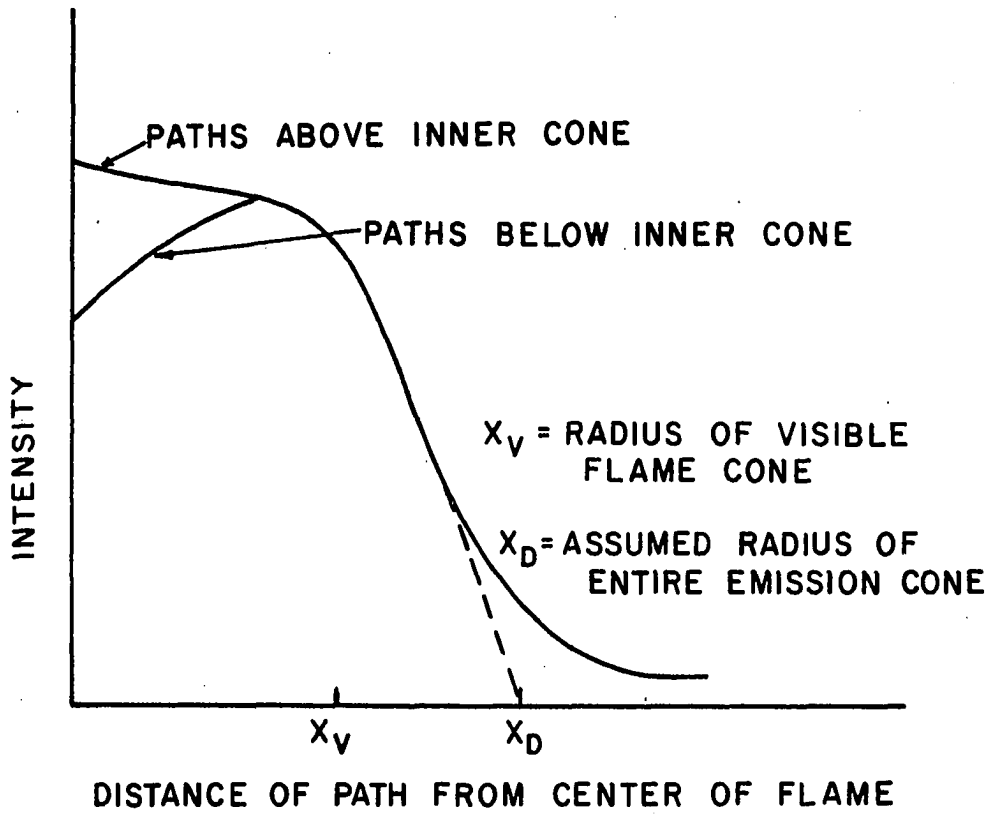

Figure IV-2. General Shape of Intensity Versus Radius for Emission Beyond the Visible Flame Cone

Radii of the emission cones, x_D, are presented for 0.2, 0.4, 0.6 and 0.8 visible flame heights in Figures IV-3 and IV-4 for natural gas and acetone flames. The radii were obtained by drawing a straight line through the inflection point of the curve and tangent to the curve as shown by the dotted line in Figure IV-2. The value along the intersection of the dotted line with the abscissa was used as the radius of the emission envelope. Assuming a bell shaped curve, radii selected in this manner include 92.5 percent of the total emission. The distance of the extension of the emission envelope beyond the visible cone is well defined for the main combustion products, CO_2 and H_2O at 2.7 microns and CO_2 at 4.3 microns. As seen from the Figures IV-3 and IV-4, one extension distance--difference between actual emission radius and visible radius--does not suffice for the entire range of flame heights. Extension beyond the visible flame of 4.3 emission was approximately one flame radius just above the burner to mid-height of the flame and gradually closed at a height over twice the height of the flame. Extention of 2.7 emission was approximately half the size of the 4.3 emission band. Although emission is weak in the wavelength interval above 5.0 microns, the data shows a slight extension beyond the visible flame.

To demonstrate the extent and strength of emission beyond the visible flame cone, average intensity was computed for wavelength intervals centered at 2.7 microns and at 4.3

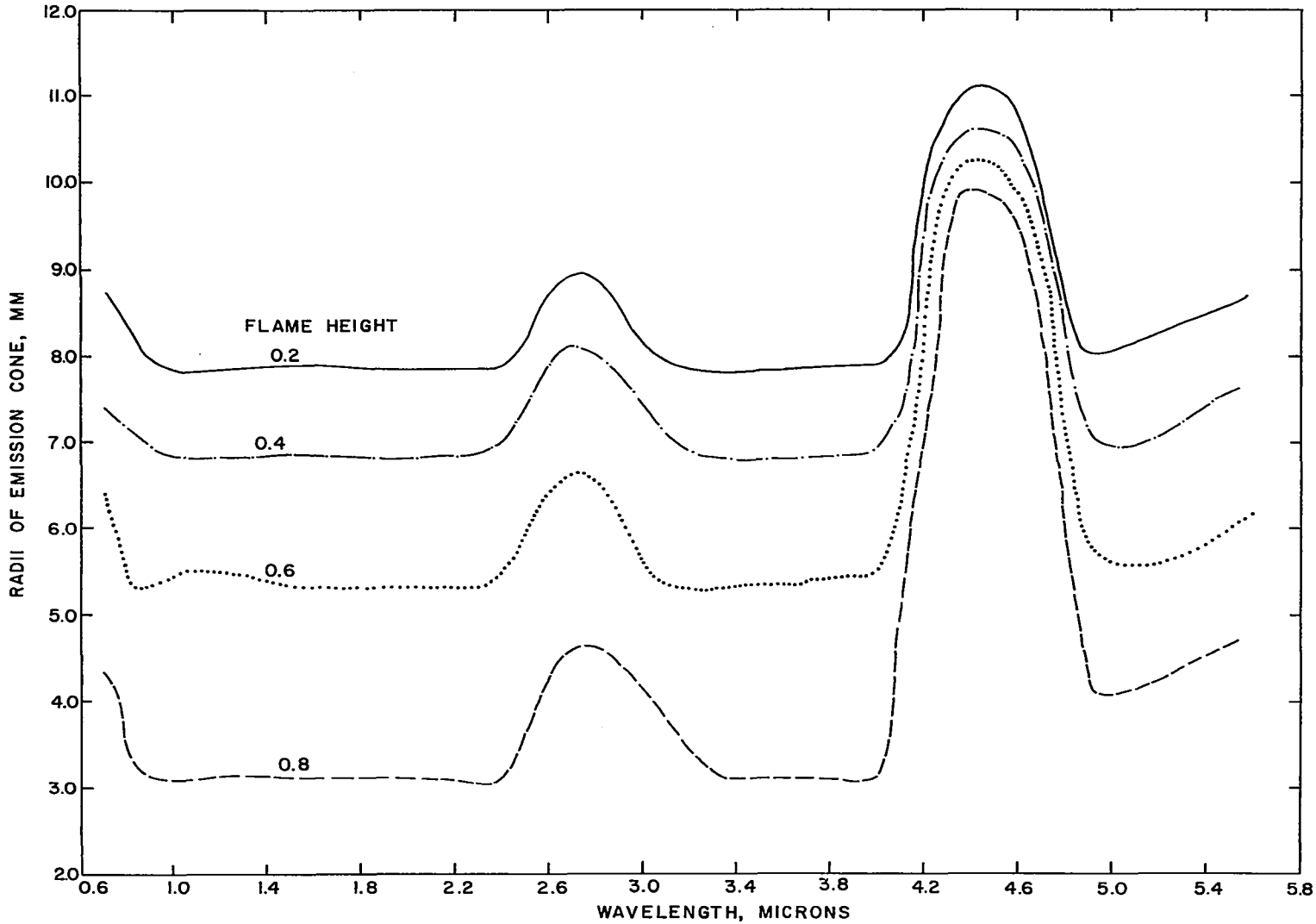

Figure IV-3. Radii of Emission Cone Versus Wavelength for 0.2, 0.4, 0.6, 0.8 Visible Flame Heights for a Laminar Natural Gas Flame.

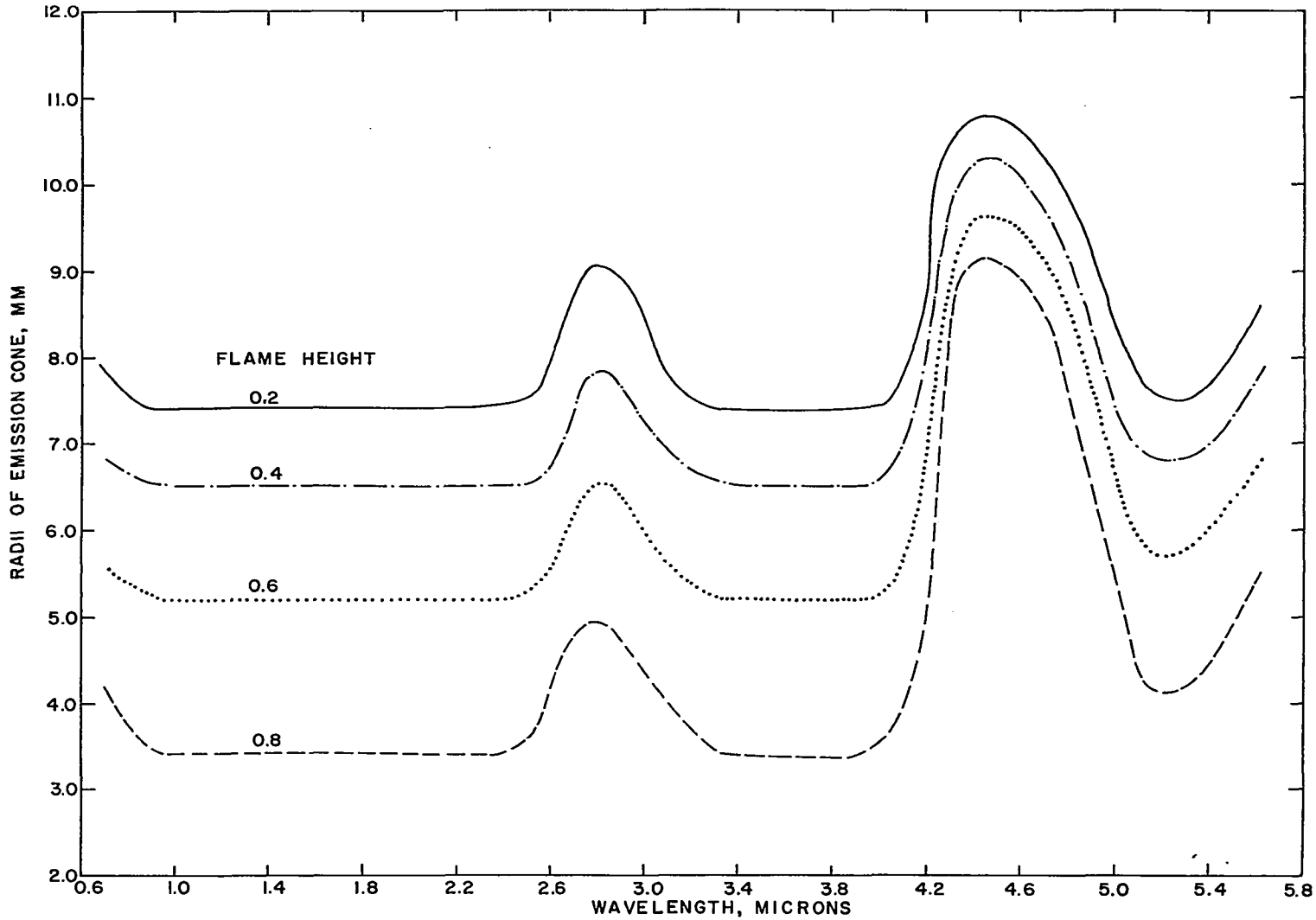

Figure IV-4. Radii of Emission Cone Versus Wavelength for 0.2, 0.4, 0.6, 0.8, Visible Flame Heights for a Laminar Acetone Flame.

microns. Average intensity was also computed for the total flame emission band and for the total band minus the 2.7 and 4.3 micron bands. The total flame emission band minus the 2.7 and 4.3 micron bands was labeled the weak emission band.

The average intensity for a particular band was computed at each spatial position by numerically integrating the intensiy over the wavelength interval of the band. Since the lengths of the wavelength intervals were different for each of the bands, the integrated value of intensity was divided by the length of the interval to obtain the average intensity over the interval. This average intensity provided an easier means for comparing the relative strength and distribution of radiation from the different emission bands. Denoting the spatial position by (x,y), the numerical integration and averaging was obtained by an approximation of the function,

$$I_{(x,y)} = \frac{\int_{\lambda_1}^{\lambda_2} I_{\lambda,(x,y)}\, d\lambda}{\lambda_2 - \lambda_1} \qquad \text{(IV-5)}$$

where λ_1 is the beginning of the interval

λ_2 is the end of the interval

$I_{\lambda,(x,y)}$ is intensity as a function wavelength at the spatial position (x,y)

$I_{(x,y)}$ is the average intensity at spatial position (x,y)

Placing the selected wavelengths in ascending order and denoting the wavelengths with the subscript i, the integral of Equation IV-5 was approximated by

$$I_{(x,y)} = \frac{\frac{1}{2} \sum_{i=j}^{k-1} \left(I_{\lambda_i,(x,y)} + I_{\lambda_{i+1},(x,y)}\right)\left(\lambda_{i+1} - \lambda_i\right)}{\lambda_k - \lambda_j} \qquad \text{(IV-6)}$$

where j is the subscript for the beginning of the wavelength interval

k is the subscript for the wavelength of the end of the interval

$I_{\lambda_i,(x,y)}$ is the intensity at the selected wavelength λ_i and at the spatial position (x,y).

The wavelength intervals were:

Emission Band	Wavelength Interval in Microns
Total	0.71 to 5.60
2.7 Micron	2.54 to 3.15
4.3 Micron	4.19 to 4.77
Weak	0.71 to 2.54
	3.51 to 4.19
	4.77 to 5.60

For each of the four wavelength intervals, the average intensities were computed on the same spatial grid and format as Tables A-1 and A-2. Arrays for each of the four wavelength intervals are presented as Table A-3 (natural gas) and Table A-4 (acetone).

To aid further in the comparison between emission bands, the four arrays for each of the fuels were plotted as contours of constant intensity and are presented as Figures IV-5 through IV-8 for natural gas and Figures IV-9 through IV-12 for acetone. Inspection of the intensity profiles shows that below the mid-height of the flame and any horizontal path away from the center of the flame the intensity of radiation increases to a maximum near the edge of the flame and then steadily decreases outside the luminous flame cone. This feature prevails in each of the wavelength intervals and, as previously pointed out, is accounted for by the lower volumetric emission of the inner flame cone. Since the path length of viewing decreases near the edge of the luminous portion of the flame, the increases in intensity near the edge of the flame illustrate the magnitude of the differences in volumetric emission that occur between the inner and outer luminous cones of the flame.

Comparisons of the graphs of intensity contours for the natural gas and acetone flames show very little difference in shape for any given wavelength band. The magnitude of the intensity profiles for acetone is approximately 1.6 times as great as the magnitude of the intensity profiles for natural gas. The main variations in the shape of the intensity fields occur among the different wavelength bands. All bands show a maximum emission at a point along the centerline

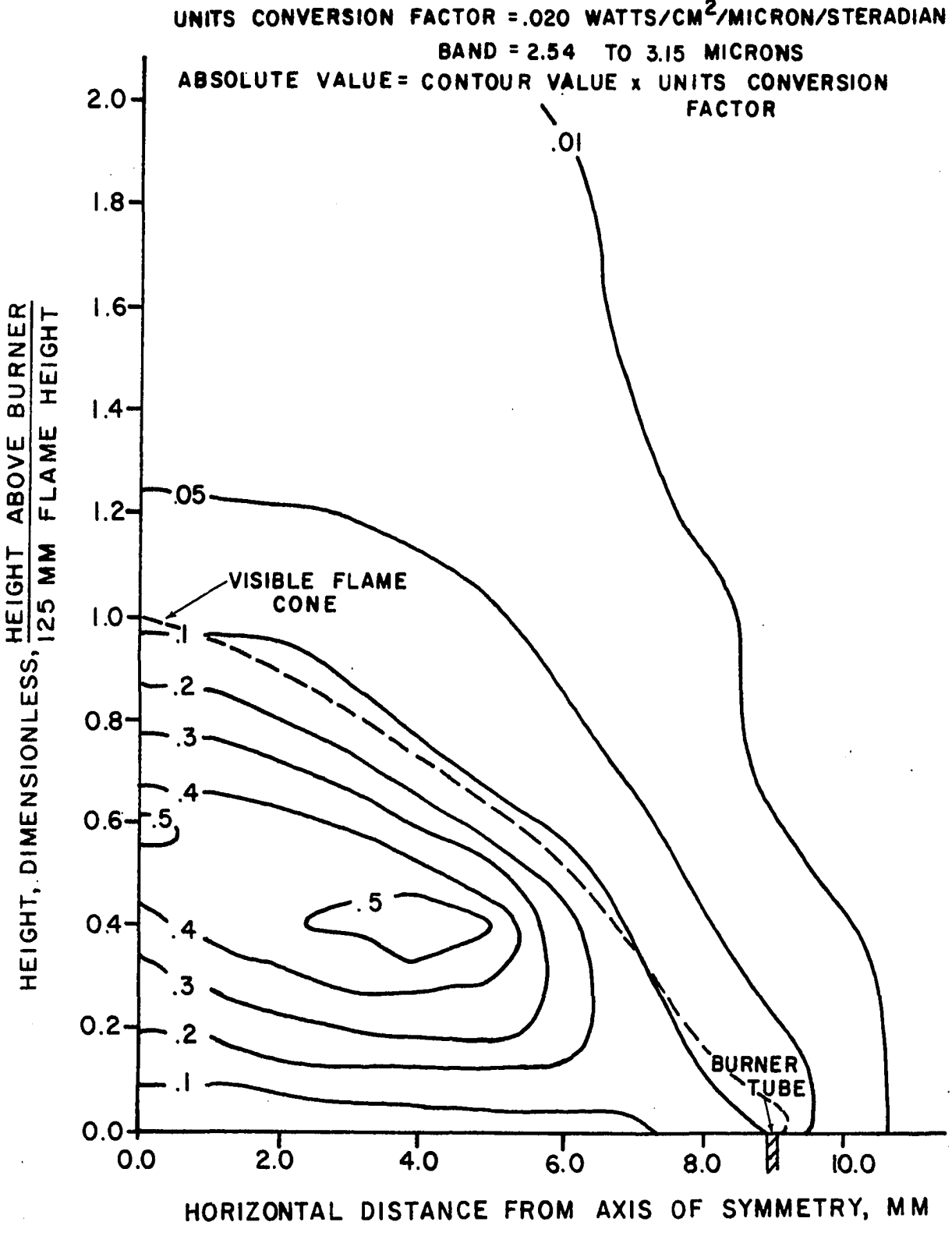

Figure IV-5. Average Intensity Profiles of the 2.7 Micron CO_2 and H_2O Emission Band for a Laminar Natural Gas Diffusion Flame.

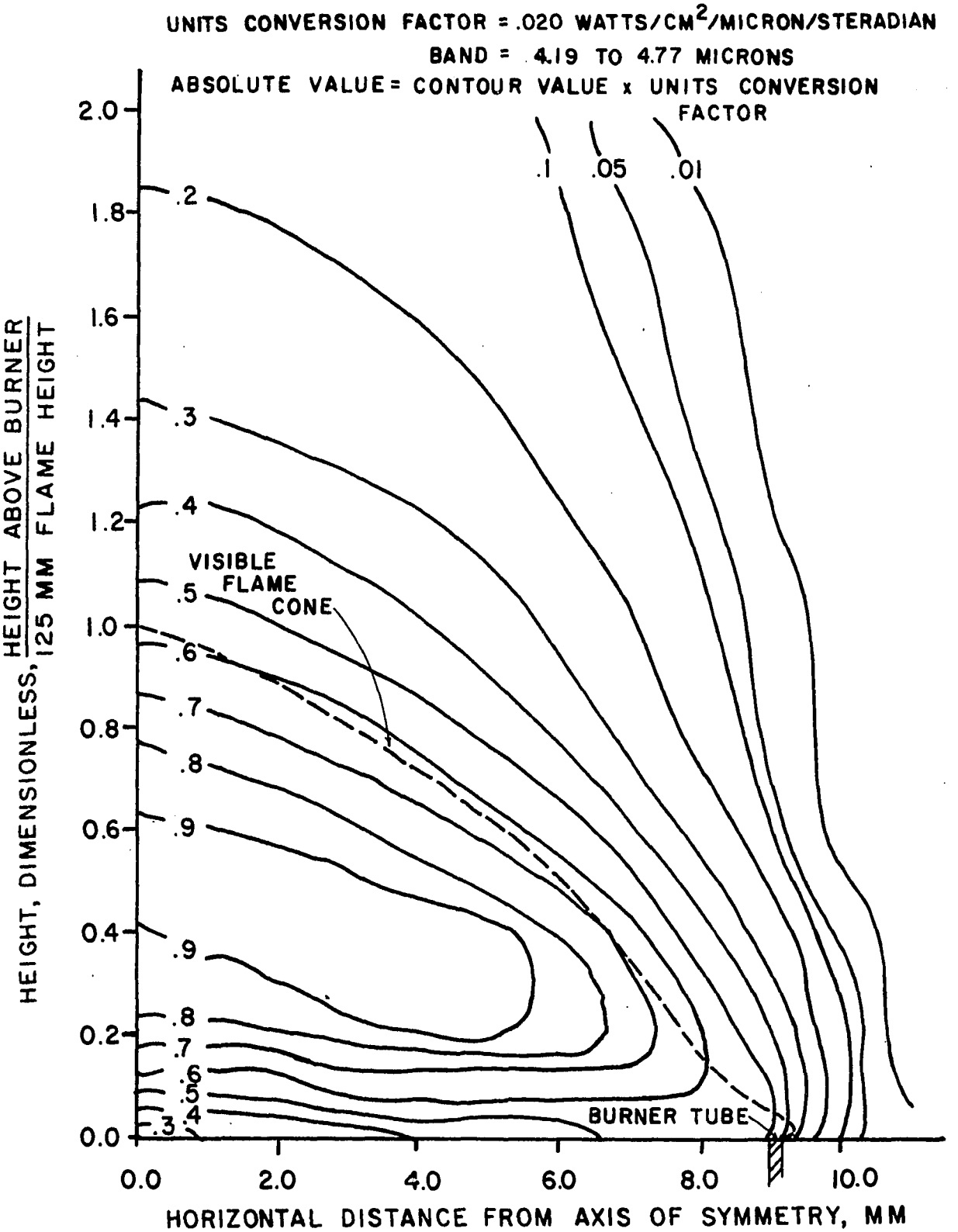

Figure IV-6. Average Intensity Profiles of the 4.3 Micron CO_2 Emission Band for a Laminar Natural Gas Diffusion Flame.

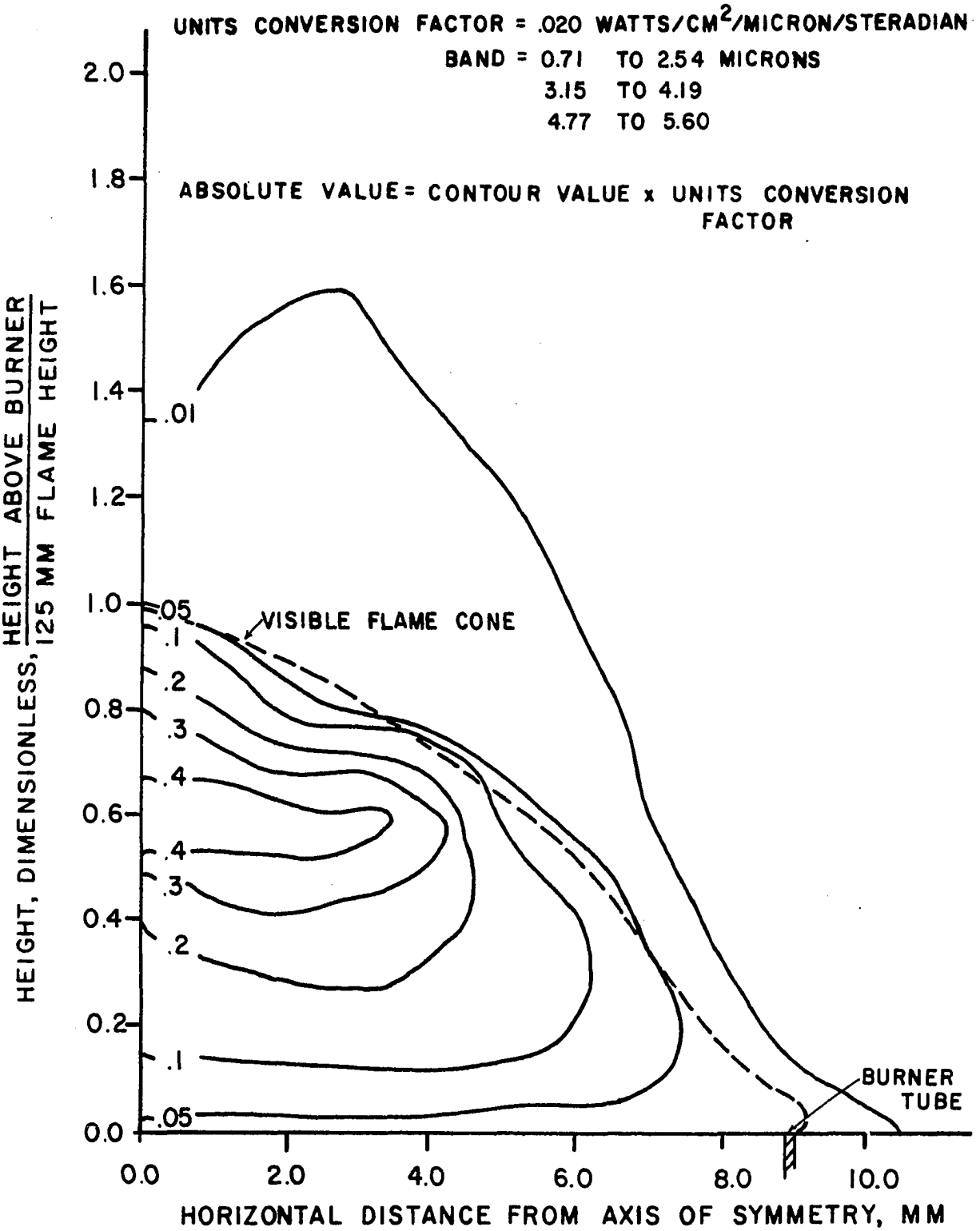

Figure IV-7. Average Intensity Profiles of the Weak Emission Bands for a Laminar Natural Gas Diffusion Flame.

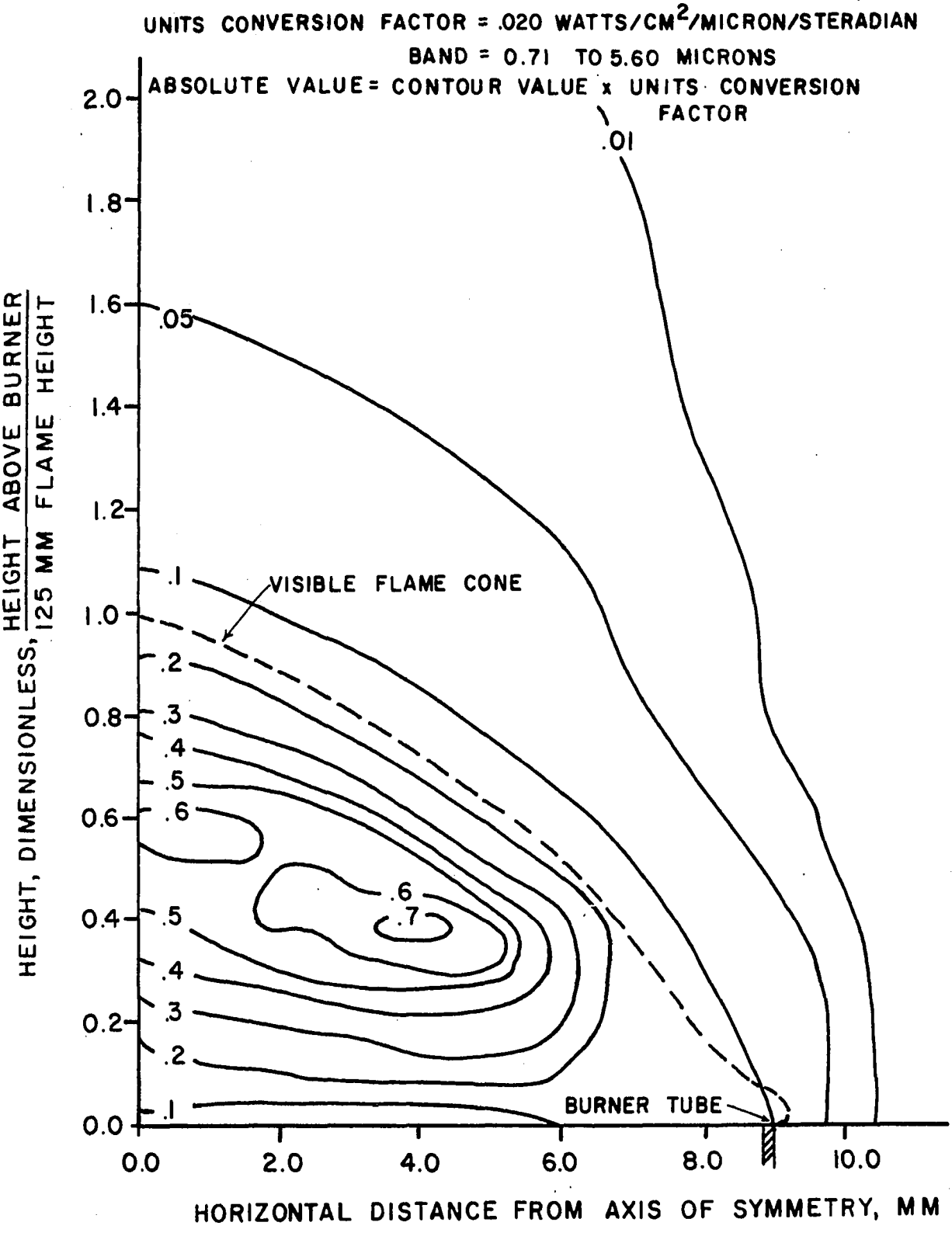

Figure IV-8. Average Intensity Profiles of the Total Emission Band for a Laminar Natural Gas Diffusion Flame.

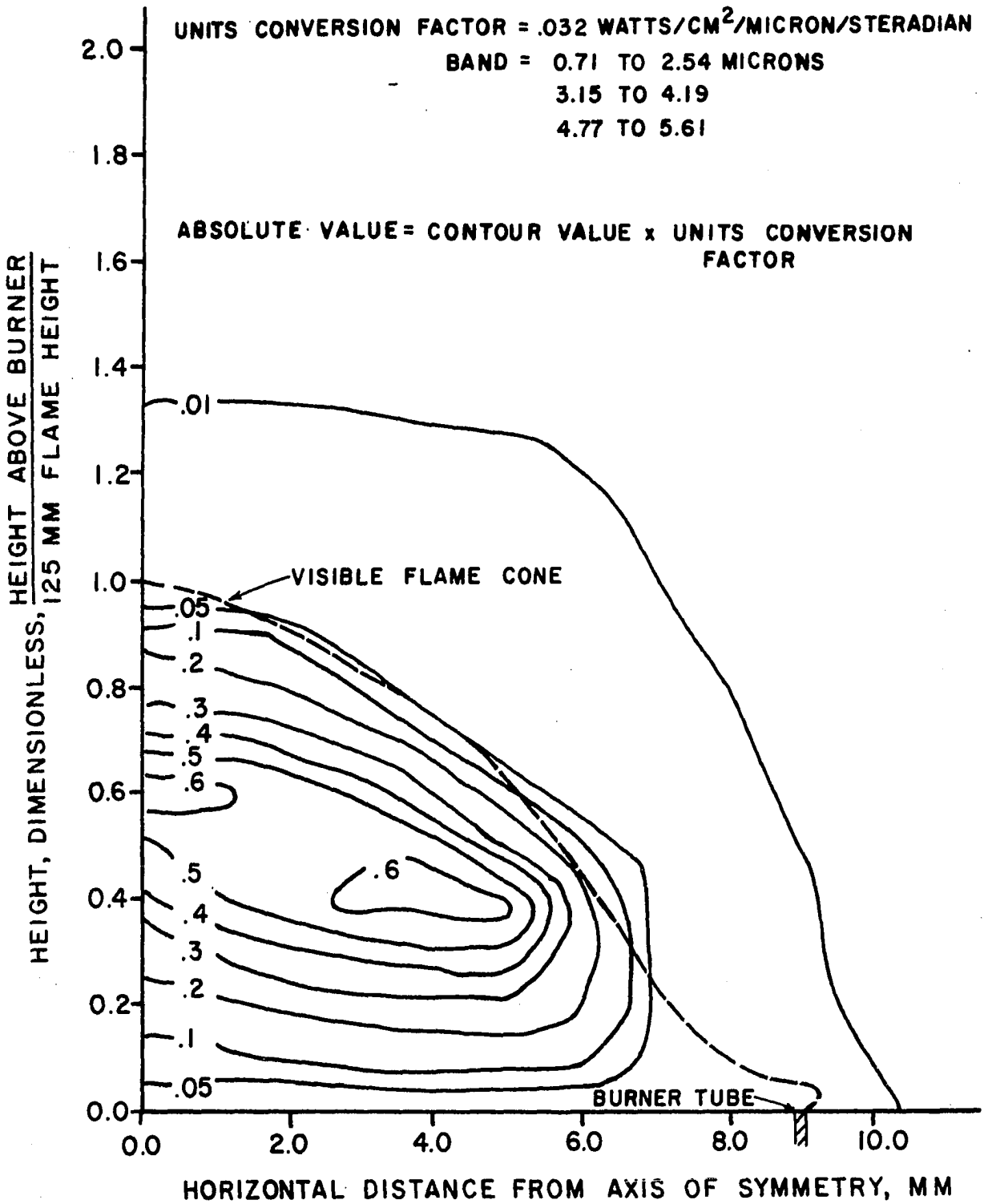

Figure IV-9. Average Intensity Profiles of the 2.7 Micron CO_2 and H_2O Emission Band for a Laminar Acetone Diffusion Flame.

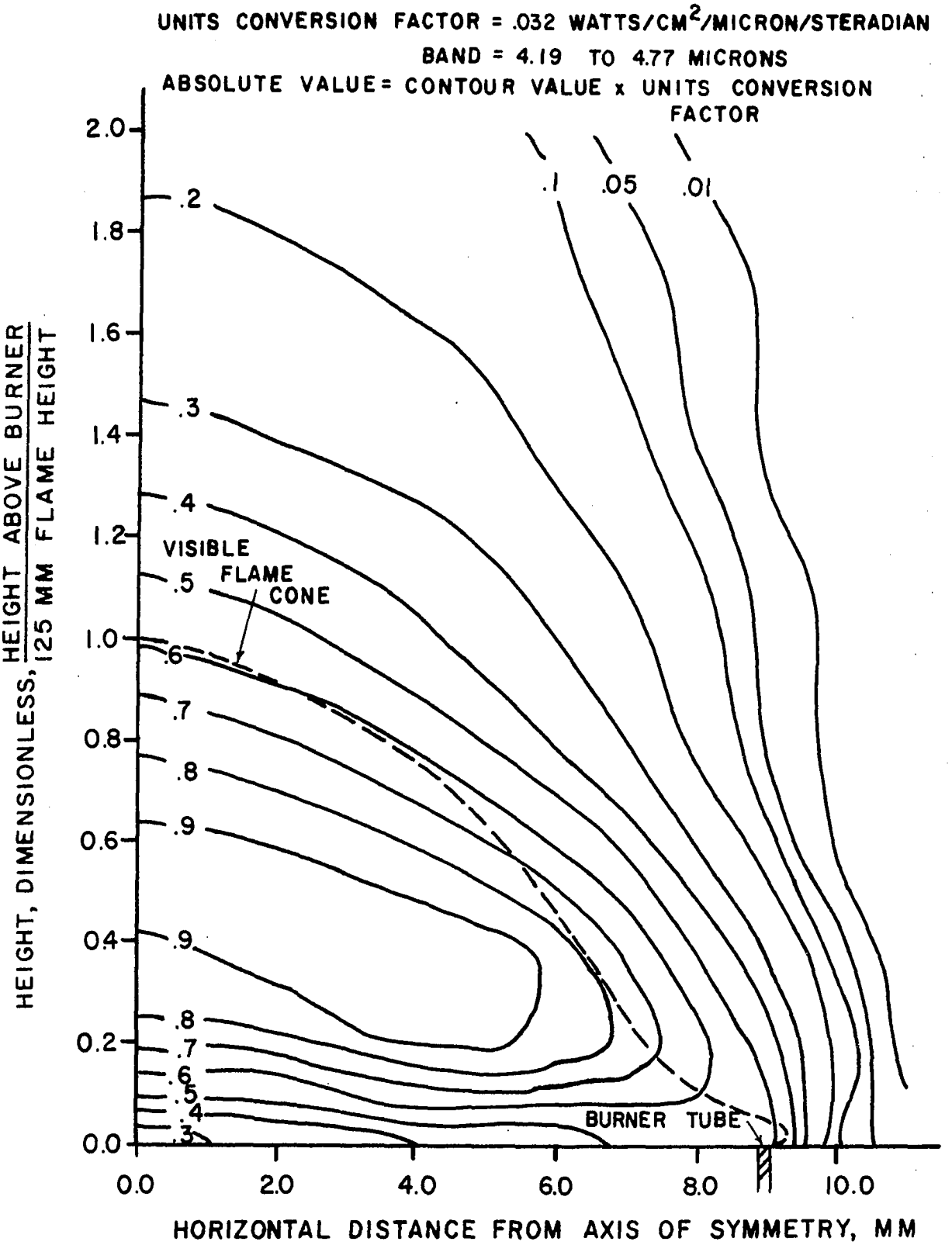

Figure IV-10. Average Intensity Profiles of the 4.3 Micron CO_2 Emission Band for a Laminar Acetone Diffusion Flame.

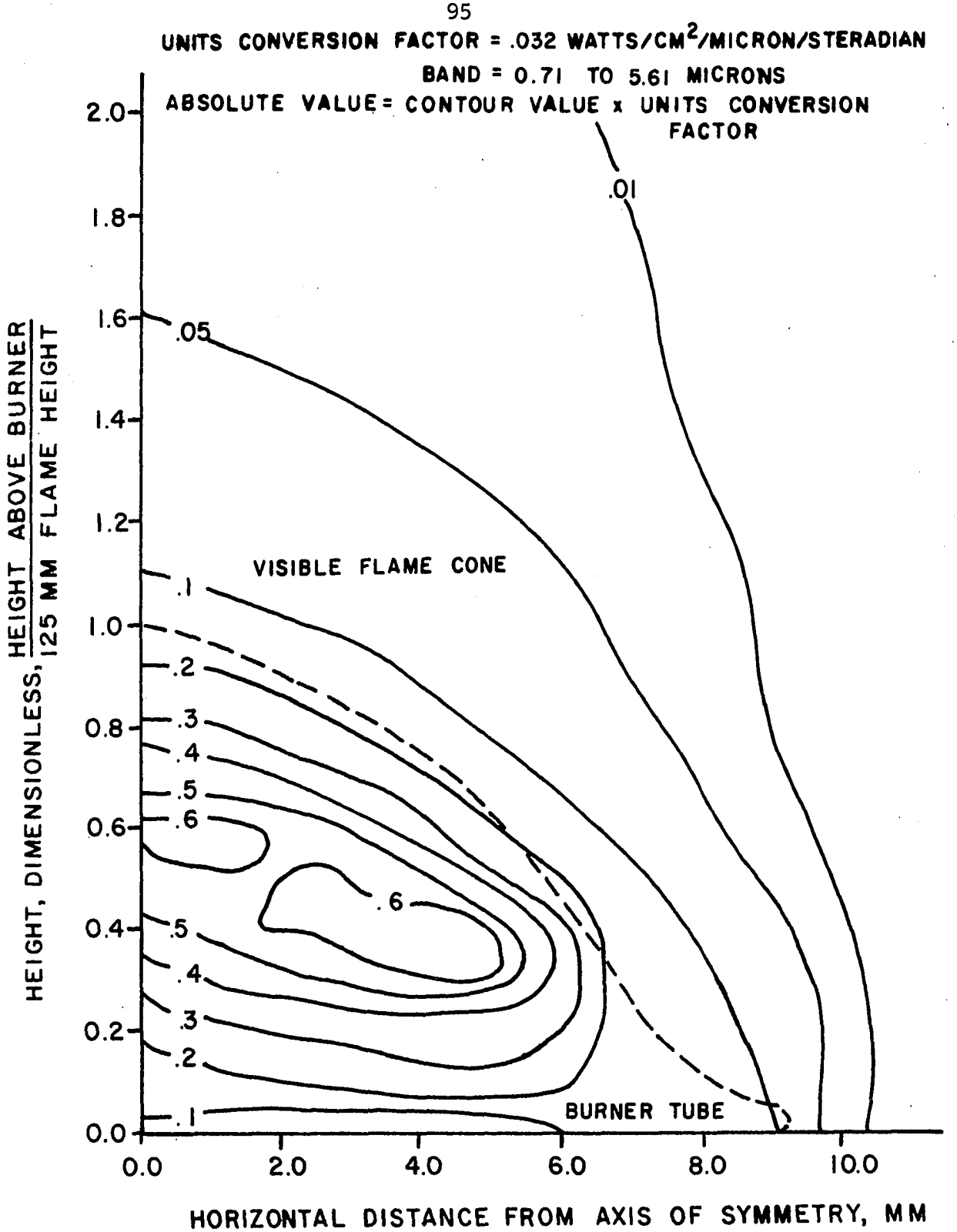

Figure IV-11. Average Intensity Profiles of the Weak Emission Bands for a Laminar Acetone Diffusion Flame.

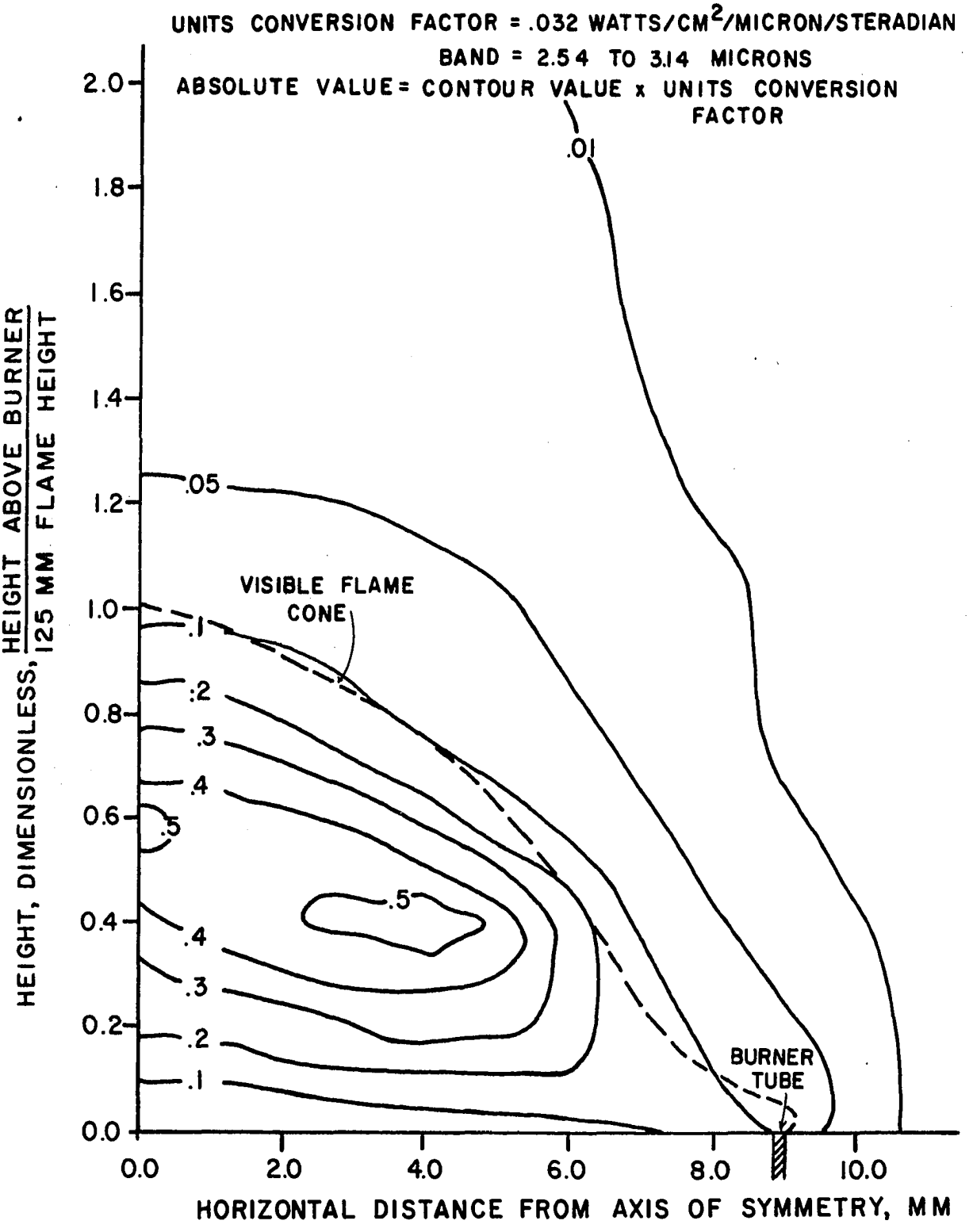

Figure IV-12. Average Intensity Profiles of the Total Emission Band for a Laminar Acetone Diffusion Flame.

and at 0.6 of the flame height. The 2.7 band and the weak emission bands also show the equally intense emission region at 0.4 of the flame height and at a horizontal position near the edge of luminous portion of the flame.

The 2.7 and 4.3 micron bands show the emission extending beyond the luminous flame cones. The emission from the 2.7 band just outside the luminous cone is only one-fifth of the magnitude of the maximum emission of the band. The 4.3 band emission just outside the luminous cone is approximately one-half of the value the maximum emission in the band. Only small gradients of emission occur at the luminous flame boundary for both the 2.7 and 4.3 bands. The 4.3 micron band extends approximately one flame radius and more than twice the height of the flame while the 2.7 micron band extends about one-half a flame radius horizontally and more than twice the flame height vertically.

The bands composed of wavelength intervals excluding the 2.7 and 4.3 bands clearly define the luminous flame zone since the emission in these bands is mainly from hot carbon particles. Because the total band emission is an average of three bands, many of the outstanding features of the indivdual bands show less definition in the total band emission profiles. The strong emission region off the centerline below the top of the inner flame cone retains its definition while the strong CO_2 emission of the 4.3 band outside the luminous flame cone appears much weaker when averaged over the entire emission band.

The most significant information of the profile data is the definition of the size of the emission volume for various wavelengths. The increased emission paths at 2.7 microns and at 4.3 microns beyond the luminous flame cone, with no abrupt changes in emission at the luminous interface, have an important influence on the calculation of the maximum emission and extinction coefficients from small flame data.

Coefficient Data

Monochromatic extinction (β_λ), maximum emission ($\frac{J_\lambda}{\beta_\lambda}$), and volumetric emission (J_λ) coefficients were computed at fifty selected wavelengths and four vertical positions for small laminar natural gas and acetone flames. Flames with eliptical horizontal cross sections were used to obtain the intensity and path length data for computation of the coefficients. Intensities versus wavelength were recorded along the major and minor axes of the cross sections at each height. The lengths of the major and minor axes of the luminous portion of the flame were used as the path lengths. Since the transport equation cannot be solved explicitly, an iteration technique was used to solve for the maximum emission coefficient. Once the maximum emission was computed the extinction and volumetric emission coefficients were computed by rearranging the transport equation. The maximum emission coefficient was selected as the iteration

parameter since the error analysis, Appendix C, showed the solution of the transport equation for the maximum emission coefficient to be slightly less sensitive to measurement errors.

Two data points are necessary to solve the transport equation, Equation I-25,

$$I_\lambda = \frac{J_\lambda}{\beta_\lambda} (1 - e^{-\beta_\lambda x}),$$

for $\frac{J_\lambda}{\beta_\lambda}$ (maximum emission coefficient) and β_λ (extinction coefficient). Defining a data point as $\left[I_\lambda(x_i);\ x_i\right]$ and denoting two data points with subscripts 1 and 2, necessary conditions for solution of the transport equation require if $x_1 < x_2$ then $I_\lambda(x_1) < I_\lambda(x_2)$ and $\frac{I_\lambda(x_1)}{I_\lambda(x_2)} > \frac{x_1}{x_2}$. The pair of equations,

$$I_\lambda(x_1) = \frac{J_\lambda}{\beta_\lambda} (1 - e^{-\beta_\lambda x_1}) \qquad \text{(IV-7)}$$

and

$$I_\lambda(x_2) = \frac{J_\lambda}{\beta_\lambda} (1 - e^{-\beta_\lambda x_2}), \qquad \text{(IV-8)}$$

were solved for $\frac{J_\lambda}{\beta_\lambda}$ by rearranging the equations to produce a function of $\frac{J_\lambda}{\beta_\lambda}$ and contained the path lengths as a ratio. Substituting C_λ for $\frac{J_\lambda}{\beta_\lambda}$ the function can be written as

$$f(C_\lambda) = \left[1 - \frac{I_\lambda(x_2)}{C_\lambda}\right] \frac{x_1}{x_2} - \left[1 - \frac{I_\lambda(x_1)}{C_\lambda}\right] \quad \text{(IV-9)}$$

If the data pair meet the stated necessary conditions, then Equation IV-9 has three roots, one at C_λ equal to infinity, one at C_λ equal to a positive value and one at C_λ equal to a negative value. The positive value was the root of interest. The root was calculated from the Newton-Raphson iteration technique by using the equation

$$C_\lambda^{m+1} = C_\lambda^m - \frac{f(C_\lambda^m)}{f(C_\lambda^m)} \quad \text{(IV-10)}$$

where C_λ^m and C_λ^{m+1} were sucessive values of C_λ and $f(C_\lambda^m)$ was the first derivative of Equation IV-4 evaluated at C^m. The iteration was allowed to proceed until the separation between sucessive guesses was less than 0.0001 where the separation, S, was defined as

$$S = 2 \frac{|C_\lambda^{m+1} - C_\lambda^m|}{|C_\lambda^{m+1} + C_\lambda^m|} \quad \text{(IV-11)}$$

The starting value, C_λ^0, for the iteration was set equal to twice the value of $I_\lambda(x_2)$, where $I_\lambda(x_2)$ was the value of intensity defined in the statement of necessary conditions for solution. Once C_λ was computed, β_λ was calculated from the equation,

$$\beta_\lambda = - \frac{\ln \left(1 - \frac{I_\lambda(x_2)}{C_\lambda}\right)}{x_2} \qquad \text{(IV-12)}$$

to complete the solution of Equations IV-7 and IV-8.

As seen in Figures IV-3 and IV-4 the emission volume extends beyond the visible flame cone. An attempt was made in the coefficient calculation to account for the increased path lengths. The path lengths were corrected by adding the extension lengths taken from Figures IV-3 and IV-4 to the visible paths lengths. Since the cross section of the eliptical flame had nearly the same area as the cross section of the circular, it was felt the extension distance beyond the flame could be accurately approximated. However, in all cases where the extension distance made a change in the path lengths, the necessary conditions for solution of the transport equation were contradicted. Recalling the necessary conditions of $\frac{I_\lambda(x_1)}{I_\lambda(x_2)} > \frac{x_1}{x_2}$ for $x_2 > x_1$ and letting the extension distance be x_d, it can be shown

$$\frac{x_1 + x_d}{x_2 + x_d} > \frac{x_1}{x_2} .$$

In this experiment x_1 and x_2 were in the neighborhood of 1.0 and 2.0 centimeters and when x_d was added to both path lengths

$$\frac{x_1 + x_d}{x_2 + x_d} > \frac{I_\lambda(x_1)}{I_\lambda(x_2)}$$

and the equations do not have meaningful solutions. When path lengths are extended to include the regions of greatly different volumetric non-isotropic emission, the measured intensity apparently does not represent the correct average intensity over the emission path and is a possible reason for the lack of success in the attempt to correct the path lengths. Further attempts to correct the path lengths were abandoned and the coefficients were calculated using only the visible flame paths. Graphs of maximum emission, extinction, and volumetric emission coefficients versus wavelengths are presented as Figures IV-13 through IV-15 (natural gas) and Figure IV-16 through IV-18 (acetone). The general shapes of the maximum emission and volumetric emission are similar for the two fuels. Acetone has a higher volumetric emission in the outer luminous cone. Peaks in the maximum emission curves occur at 2.0 microns for the thermal emission due to the hot carbon particles, at 2.7 microns for the combined CO_2 and H_2O emission, and at 4.3 microns for the CO_2 emission. The maximum emission curve has the general shape of a 2.0 micron peak blackbody emission curve with two superimposed peaks at 2.7 and 4.3 microns. The 2.0-micron hot carbon particle emission peak and the 2.7-micron combined CO_2 and H_2O emission peak were nearly the same magnitude. The 4.3 micron CO_2 emission peak was twice the magnitude of the 2.0 and 2.7 micron band emission. Assuming a blackbody intensity with a peak emission at 2.0 microns and using the maximum

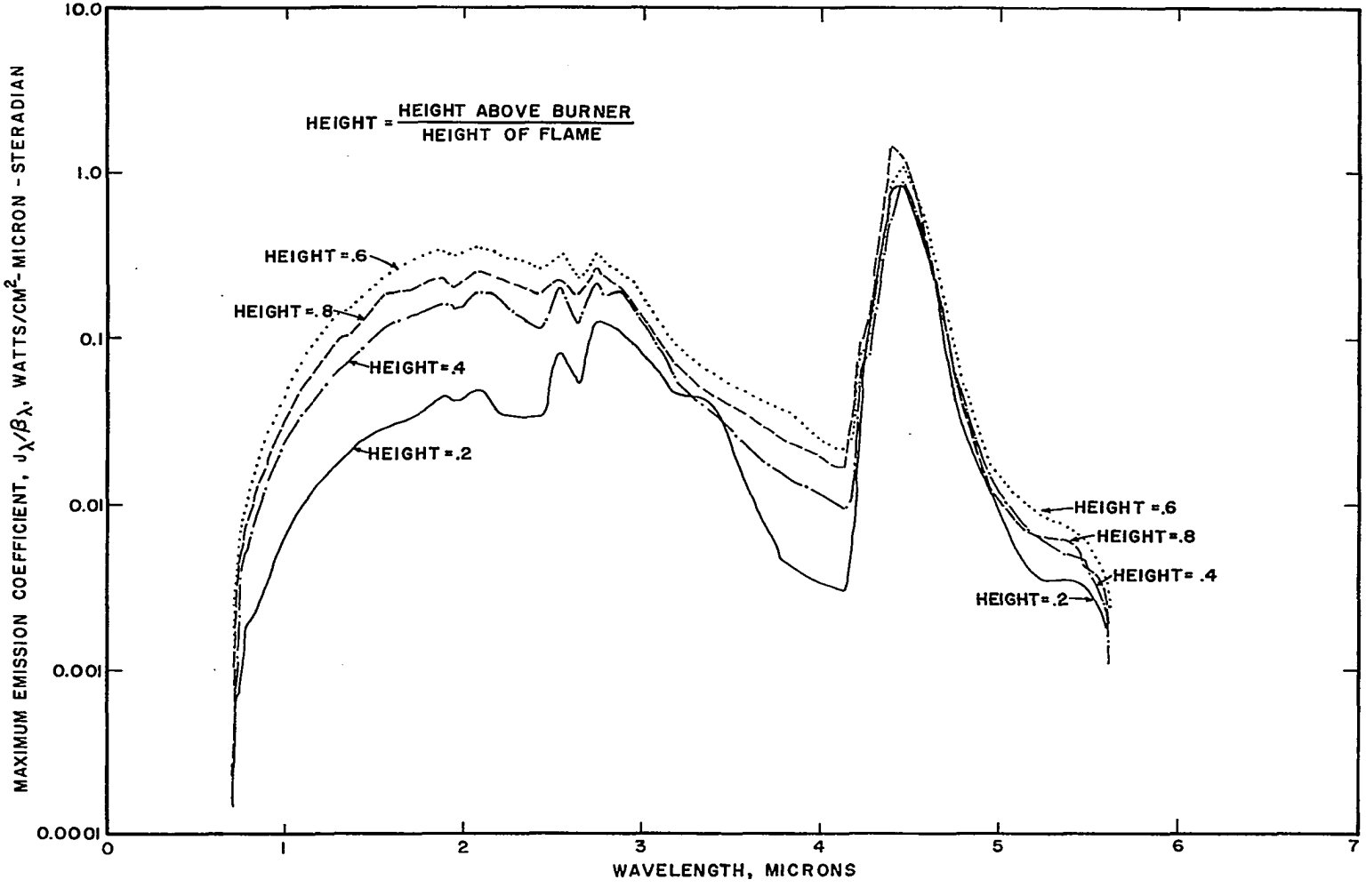

Figure IV-13. Monochromatic Maximum Emission Coefficients Versus Height for a Laminar Natural Gas Diffusion Flame.

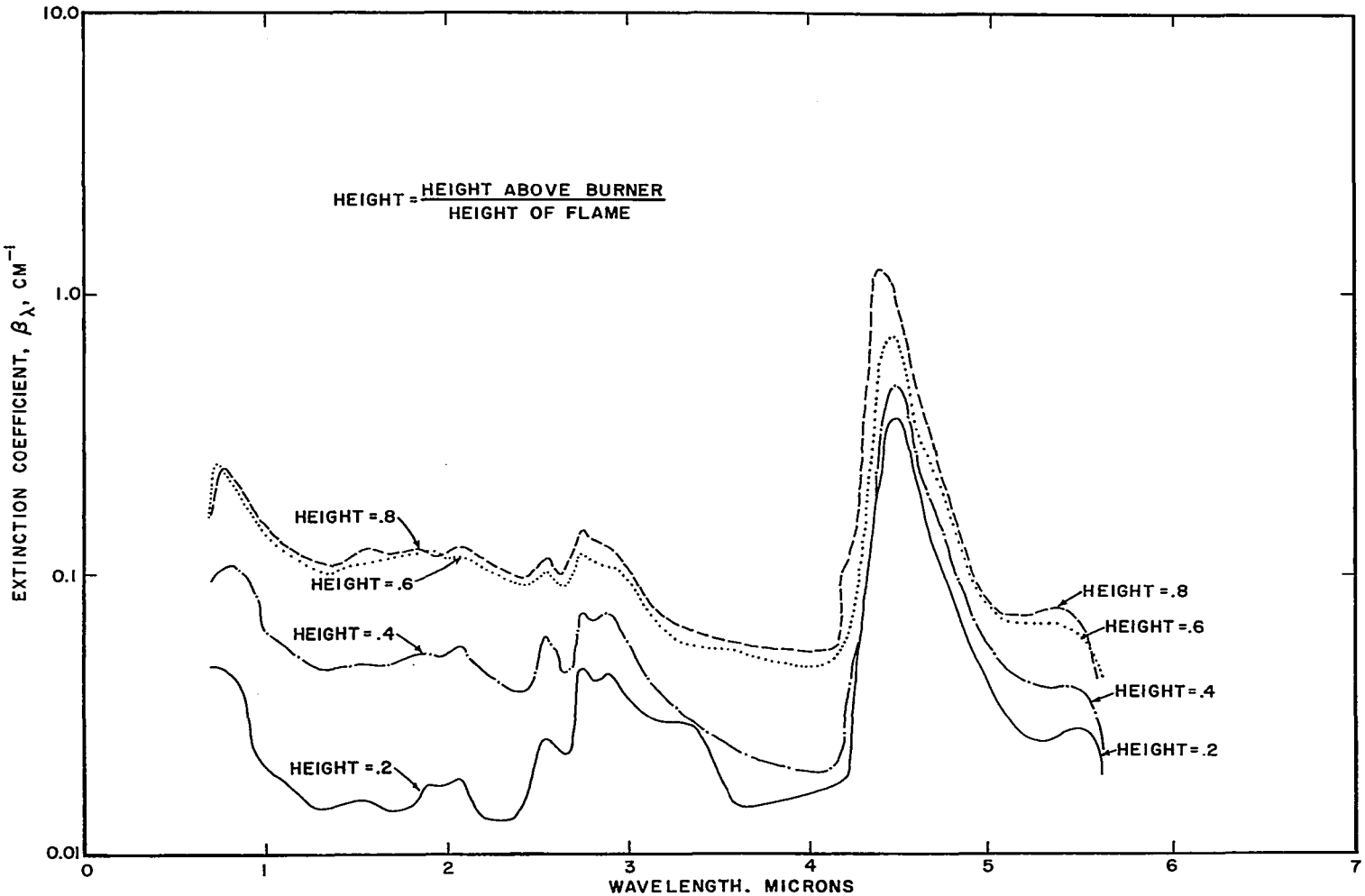

Figure IV-14. Monochromatic Extinction Coefficient Versus Height for a Laminar Natural Gas Diffusion Flame.

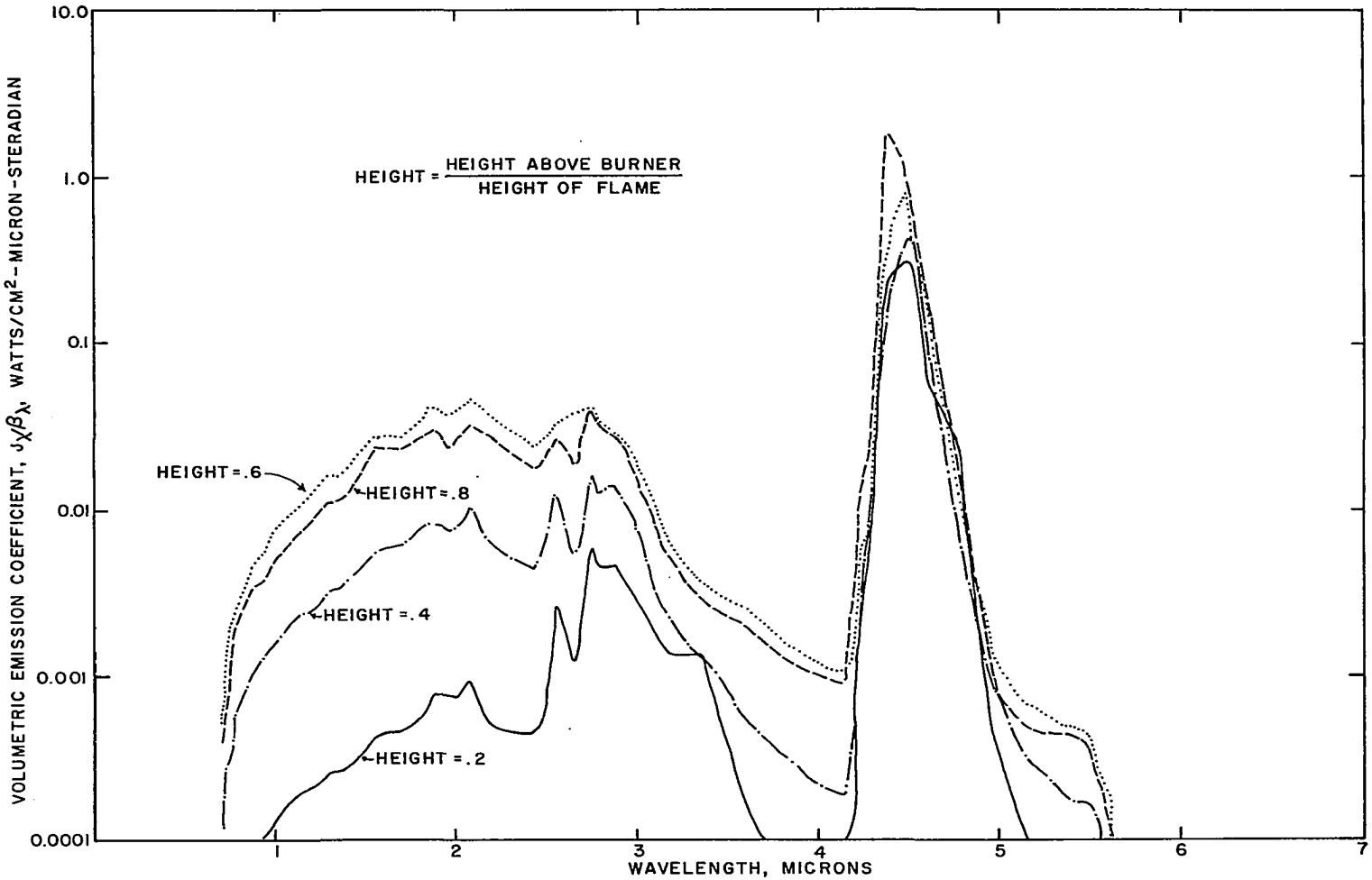

Figure IV-15. Monochromatic Volumetric Emission Coefficient Versus Height for a Laminar Natural Gas Diffusion Flame.

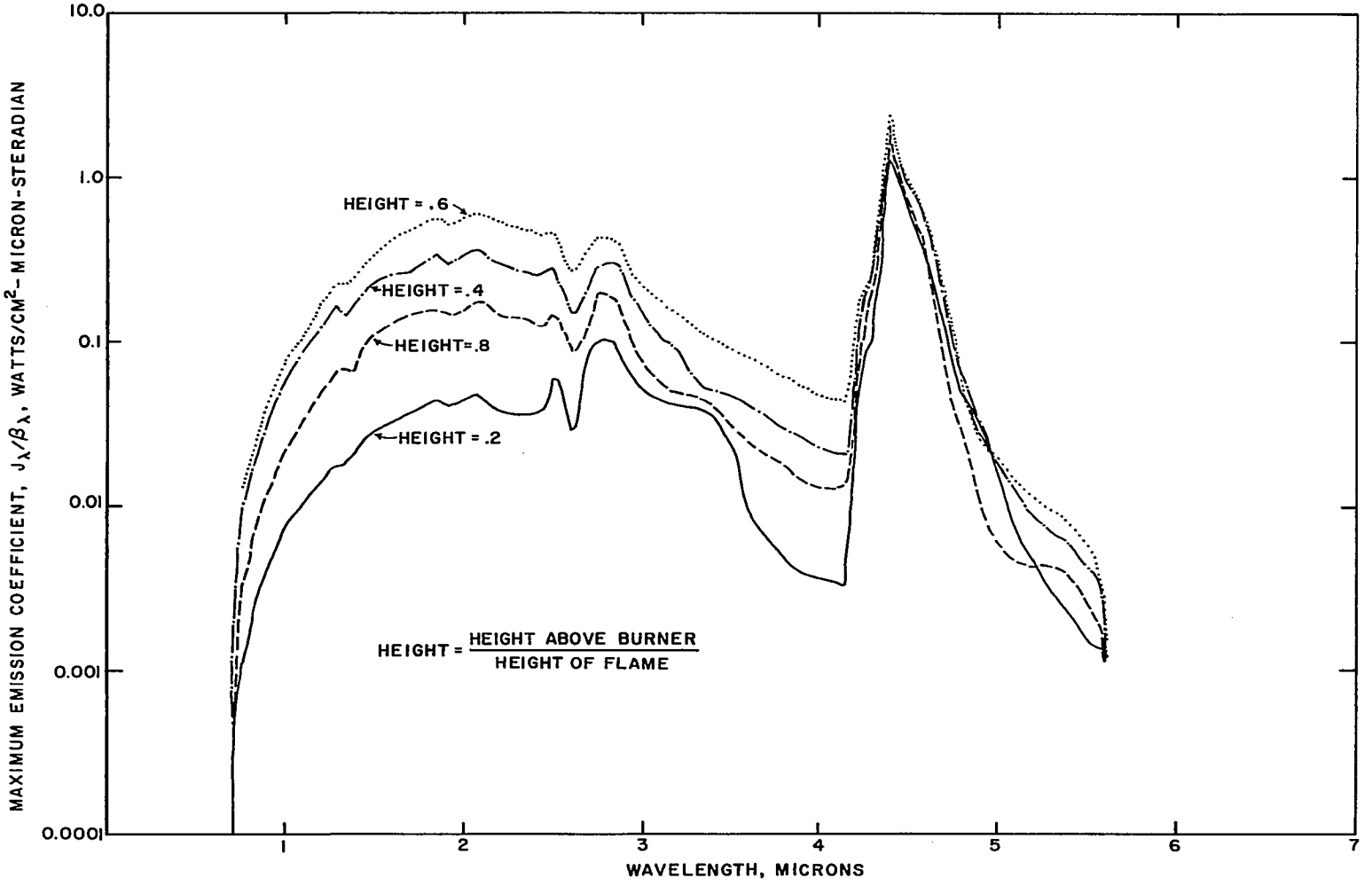

Figure IV-16. Monochromatic Maximum Emission Coefficients Versus Height for a Laminar Acetone Diffusion Flame.

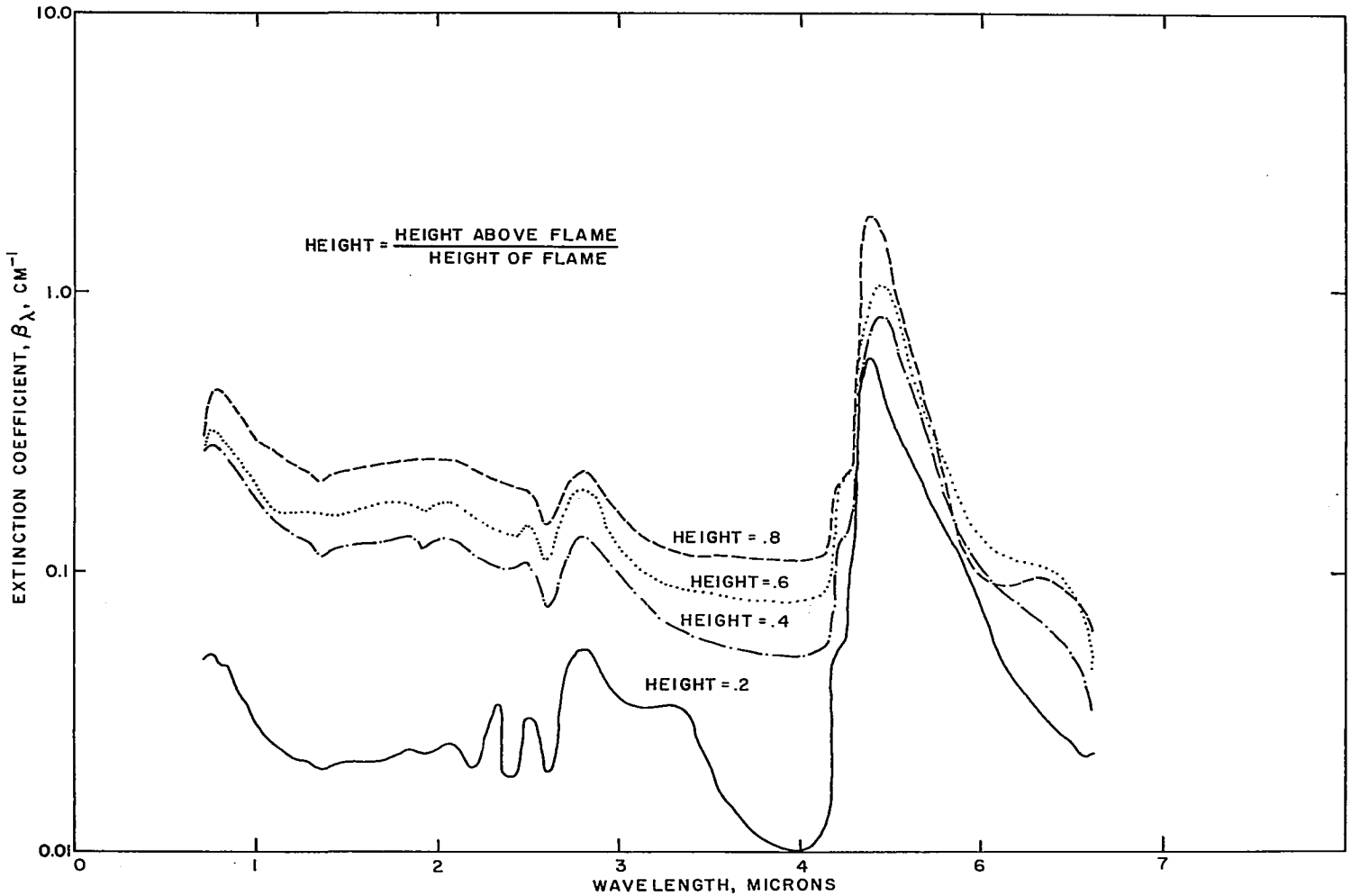

Figure IV-17. Monochromatic Extinction Coefficient Versus Height for a Laminar Acetone Diffusion Flame.

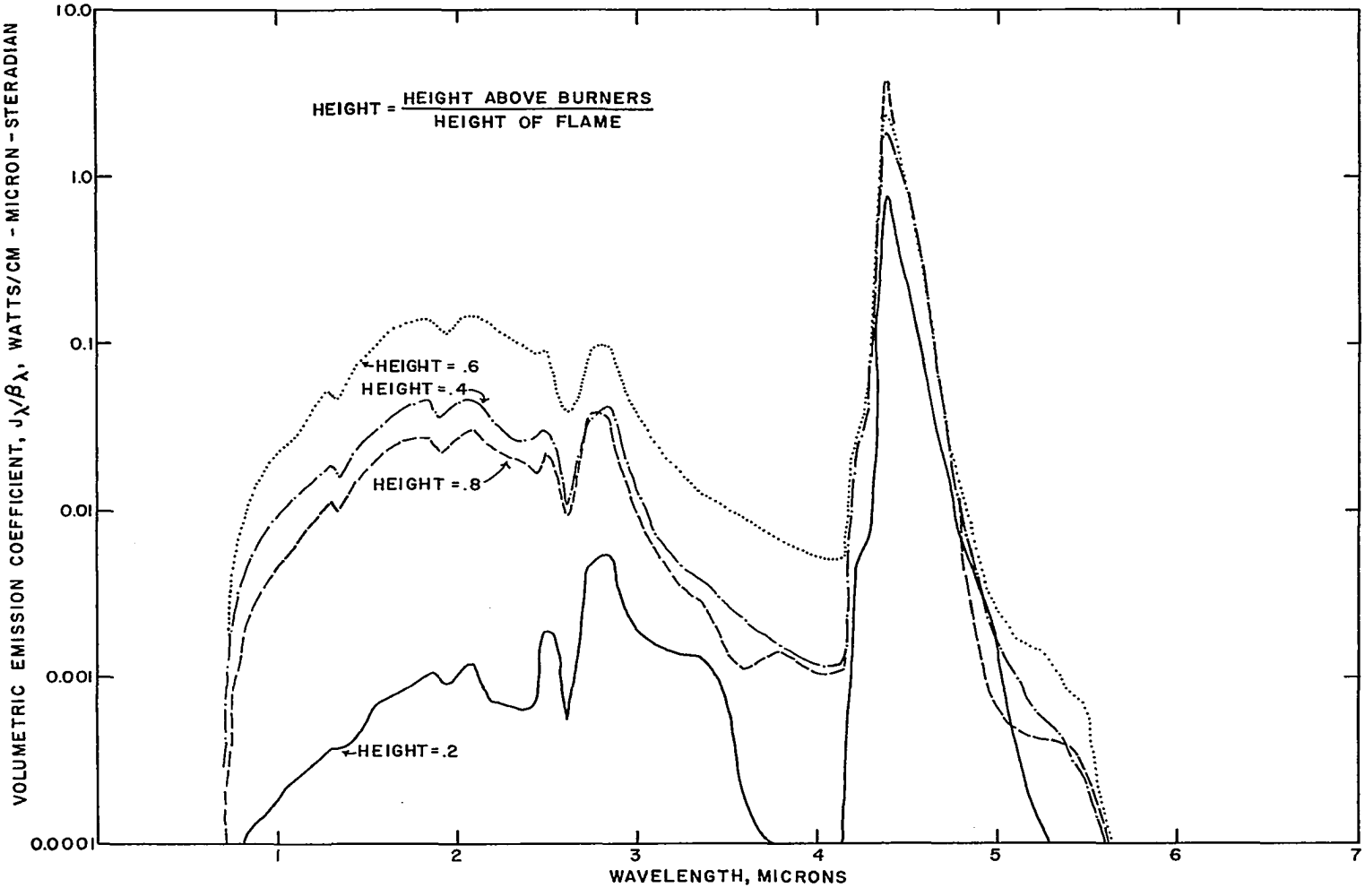

Figure IV-18. Monochromatic Volumetric Emission Coefficient Versus Height for a Laminar Acetone Diffusion Flame.

flame emission, the emissivity of the hot carbon particles at 2.0 microns is 0.1 for natural gas and 0.2 for acetone. Comparisons with literature values are difficult due to the many variables that must be estimated in order to use available correlations. However, Hottel and Sarofim (22) state, "If interest is in the prediction of total radiative transfer from furnace gases to wall sink, the addition of 0.1 to the nonluminous gas emissivity to allow for soot luminosity is often sufficient when calculations are based on a mean flame temperature."

The extinction coefficients for both natural gas and acetone have peak values at 2.7 and 4.3 microns. The larger values in the 4.3 micron band mean flames from both fuels achieve their maximum emission in a smaller flame thickness than in other wavelength intervals. By the same argument, the larger values of the extinction coefficients for acetone imply that laminar acetone diffusion flames reach maximum emission in a smaller thickness than similar flames from natural gas.

In order to demonstrate variations in the sets of coefficients, radiative flux was computed as a function of flame thickness for the four vertical positions and for both natural gas and acetone flames. An isotropic hemispherical flame was used as the flame model for the computation. The target was assumed to be oriented normal to the axis of symmetry, at the base of the hemisphere. In the

flame model, thickness of the flame to the target was the radius, r, of the hemisphere. This particular flame model with the target in contact with the flame was used because it eliminates the need for an atmospheric attenuation correction factor. The radiative flux at the center of a hemispherical flame can be written as a combination of Equation I-8 and I-11 to give

$$q = \pi \int_{\text{wavelength interval.}} I_\lambda \, d\lambda \qquad \text{(IV-13)}$$

Substituting in Equation I-25

$$q = \pi \int_{\text{wavelength interval.}} \frac{J_\lambda}{\beta_\lambda} (1 - e^{-\beta_\lambda r}) \, d\lambda \qquad \text{(IV-14)}$$

Using the trapezoidal rule approximation of the integral, values of q/π versus flame thickness are presented in Figures IV-19 and IV-21 for natural gas and Figure IV-20 and IV-22 for acetone. Figures IV-19 and IV-20 show total intensity versus flame path length for various positions of height in the flame. These graphs show a laminar layer of natural gas flame reaches a maximum intensity of 0.871 watts/cm^2-steradian at a thickness of approximately 100 centimeters and an acetone flame reaches its maximum intensity of 1.35 watts cm^2-steradian at a thickness of approximately 50 centimeters. Figures IV-21 and IV-22 are plots

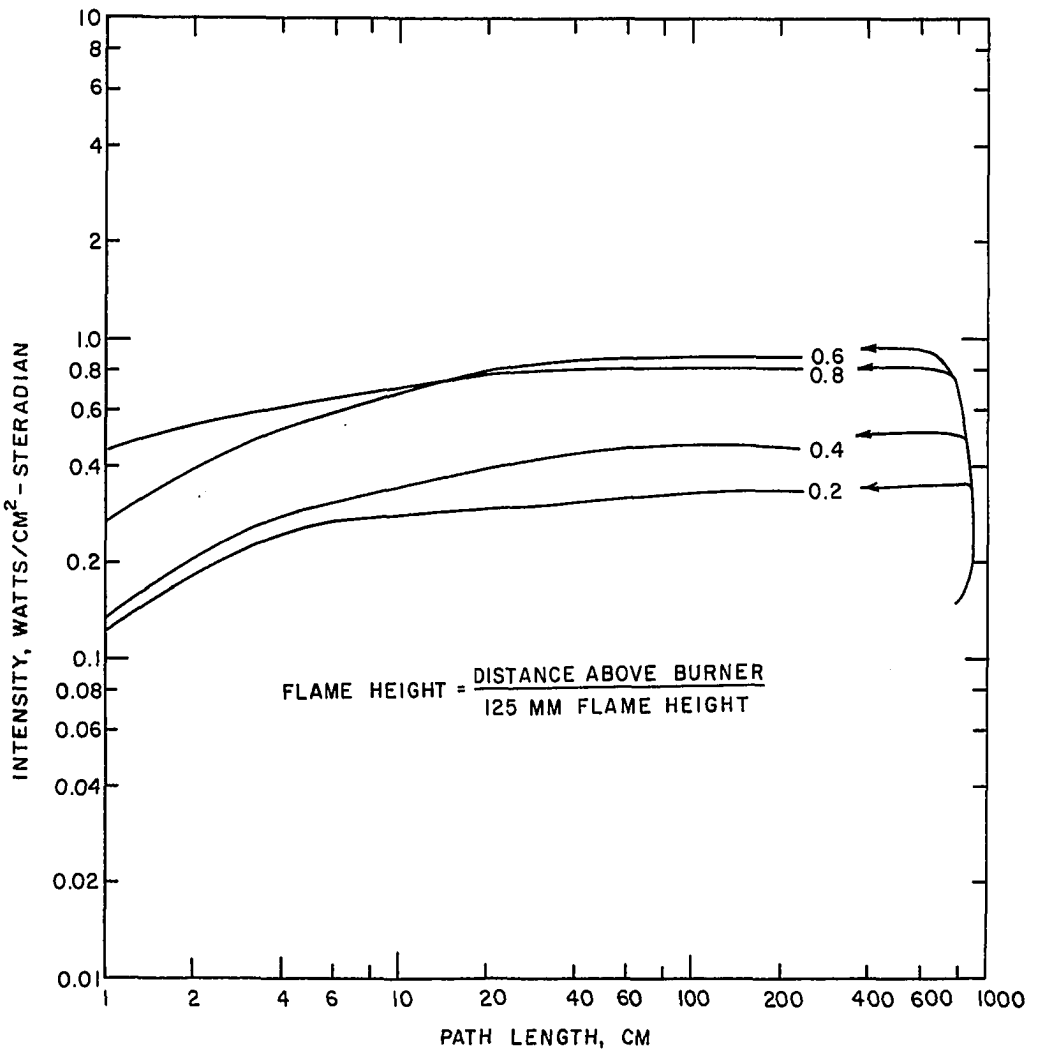

Figure IV-19. Calculated Intensity Versus Path Length for Various Heights for a Laminar Natural Gas Diffusion Flame.

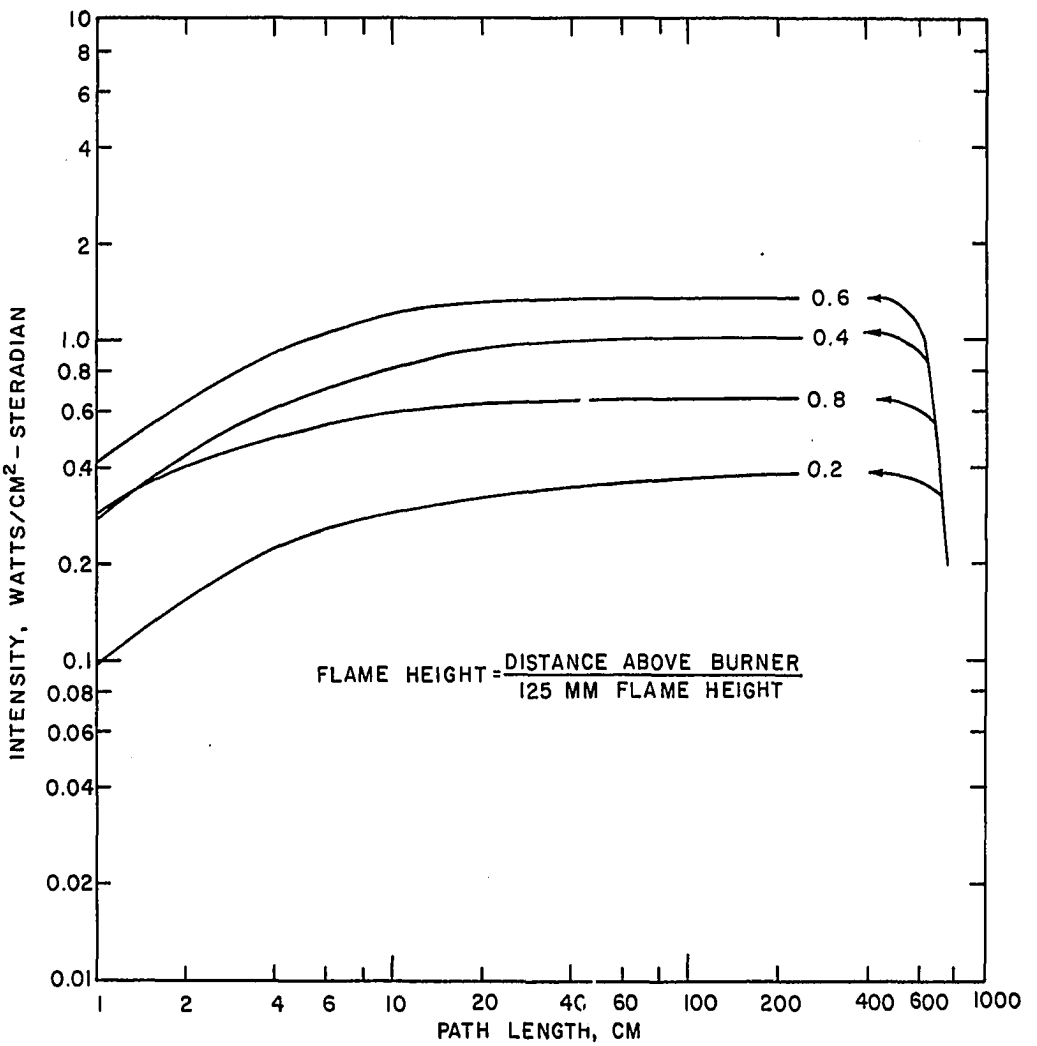

Figure IV-20. Calculated Intensity Versus Path Length for Various Heights for a Laminar Acetone Diffusion Flame.

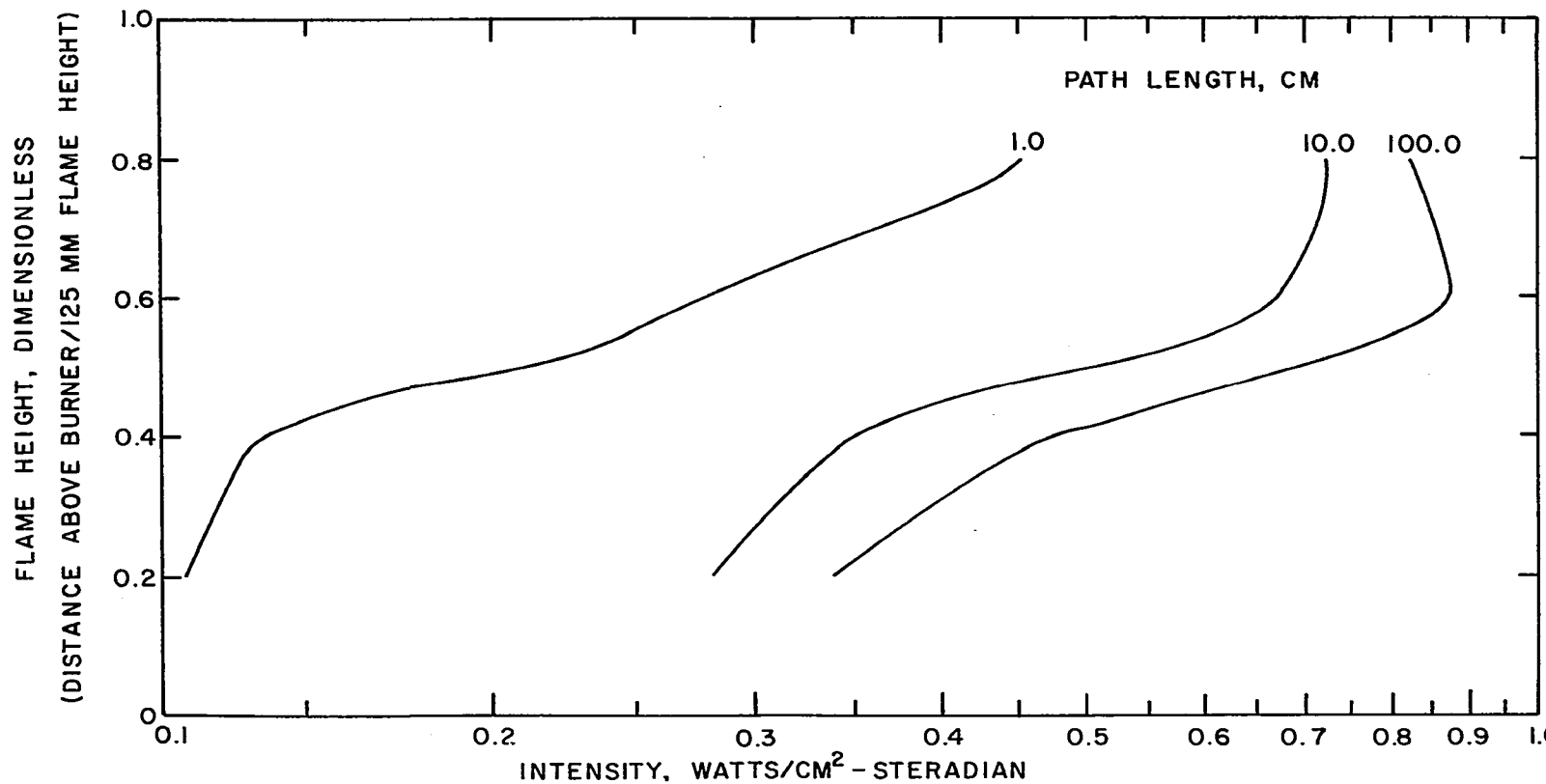

Figure IV-21. Calculated Intensity Versus Flame Height for Various Path Lengths for a Laminar Natural Gas Diffusion Flame.

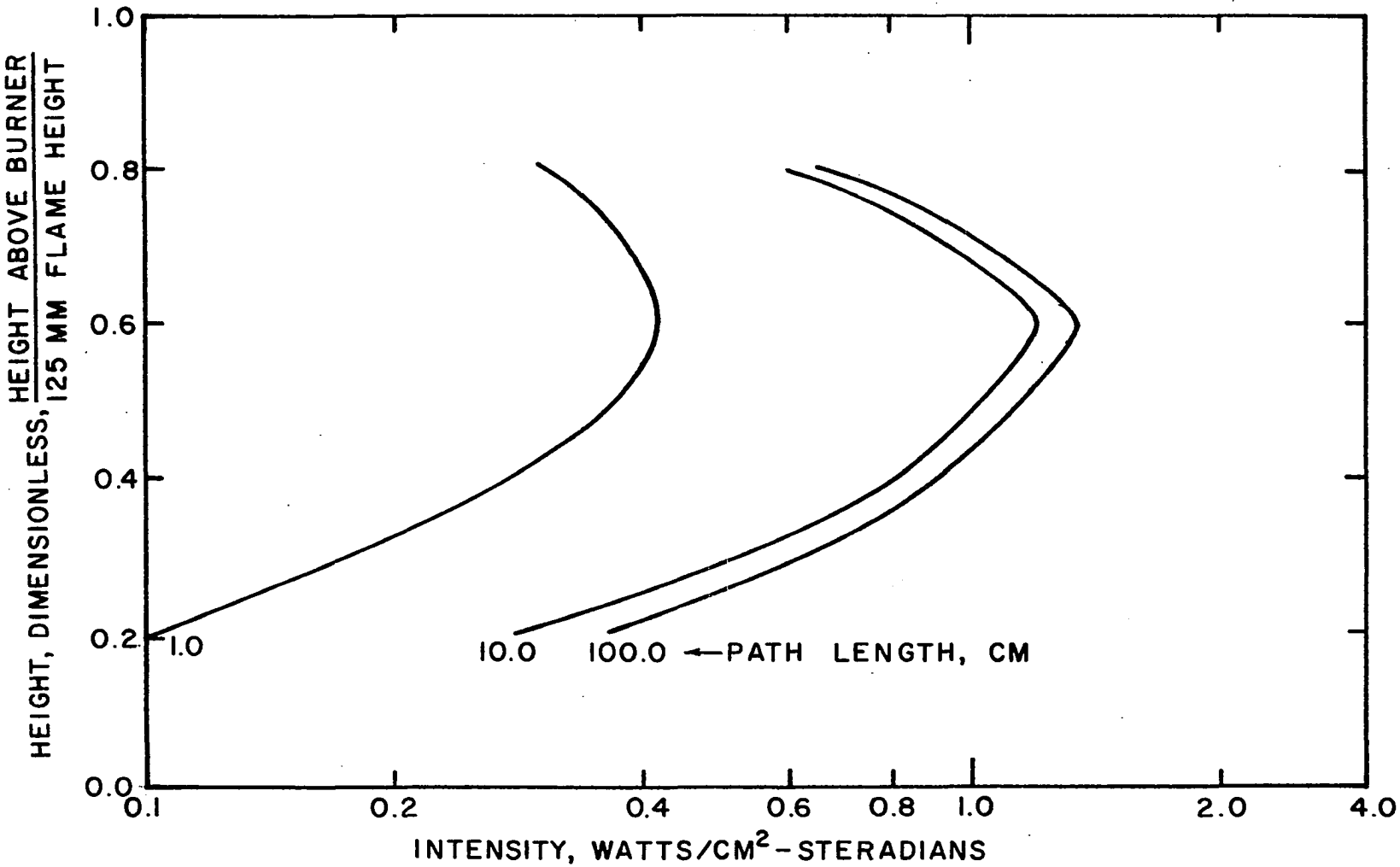

Figure IV-22. Calculated Intensity Versus Flame Height for Various Path Lengths for a Laminar Acetone Diffusion Flame.

of total intensity versus position of height in the flame for path lengths of 1, 10 and 100 centimeters. For path lengths of 100 centimeters or greater, the values of the flux increase to a point above the mid-point of the flame height and decrease towards the top of the flame.

Wesson (40) of this laboratory has shown that piloted ignition time for various woods when exposed to various radiation fluxes can be correlated as a function of density and average absorptance of the wood. Piloted ignition data for ash and mahogany exposed to acetone flames were available for comparing the average absorptances from Wesson's correlation with the average absorptance calculated from maximum emission and the coefficient data. Values of average absorptance were calculated from the correlation for the given values of incident radiative flux, piloted ignition time, sample thickness, thermal diffusivity, and density. Average absorptances were calculated from the 0.8 flame height acetone coefficients assuming a flame thickness necessary to reach maximum emission and defining average absorptance as

$$\bar{\alpha} = \frac{\int_{\lambda_1}^{\lambda_2} \alpha_\lambda \, I_\lambda \, d\lambda}{\int_{\lambda_1}^{\lambda_2} I_\lambda \, d\lambda}$$

where α_λ is the monochromatic absorption taken normal to the surface of the sample

I_λ is the monochromatic intensity

λ_1 and λ_2 are the bounds of the wavelength interval.

The 0.8 flame height coefficients were used since the calculated maximum radiative flux from the 0.8 flame height coefficients was near the average radiative flux measured for the piloted ignition data. The integrations of Equation IV-15 were performed by trapezoidal rule approximations. Average absorptances from the correlation and coefficients are given in Table IV-1.

TABLE IV-1

CALCULATED VALUES OF AVERAGE ABSORPTANCE OF WOOD FOR ACETONE FLAME RADIATION

Wood	from Wesson's Correlation	from Maximum Emission Coefficient Data
Ash	.77	.71
	.75	
	.73	
	.69	
Mahogany	.76	
	.71	
	.80	
	.77	.71
	.72	

The agreement between the average absorptance from the coefficient data and from the correlation implies that the coefficient data closely describes the shape of the emission versus wavelength curve of the actual flame.

The magnitude of maximum radiative flux (1.35 watts/cm^2-steradian) calculated from 0.6 flame height coefficients

compares favorably with the estimates of Neill (30) for maximum radiative flux (1.20 watts/cm^2-steradian) from an acetone diffusion flame.

The goal of describing the small laminar diffusion flames is to apply the information to predict the spectral distribution and intensity of radiation from buoyant diffusion flames. Calculations for total flux from buoyant diffusion flames have previously been obtained by the following method:

1. A time exposure photograph of the large flame was taken to determine the size and shape.
2. Using the size and shape of flame, the radiative flux was computed for several positions around the flame.
3. Comparisons were then made with actual flux measurements for the various positions and the flame size was then corrected to minimize the differences in calculated and measured values.

Values of the average maximum emssion and extinction coefficients used in the predictions were computed from data from small laminar diffusion flames. The data were taken from small flames at a point just above the inner reaction zone and the coefficients were calculated using the path length of the visible portion of the flames. Variations in the shape of a medium size turbulent buoyant diffusion flame of acetone burning from a 30 centimeter diameter pool are presented in Figure IV-23 (a through e) as a series of one millisecond exposure photographs.

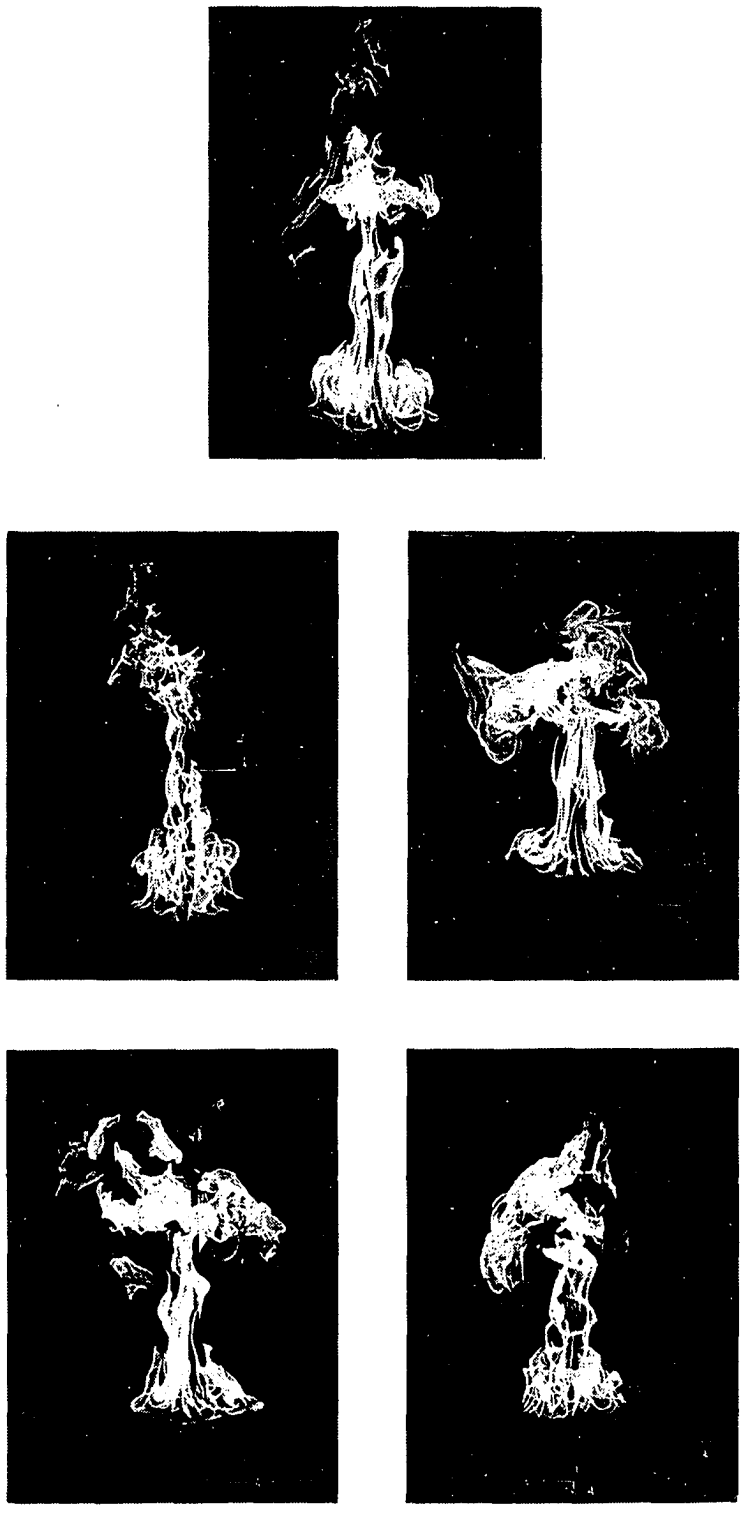

Figure IV-23. Series of One Thousandth Second Exposure Time Photographs of an Acetone Pool Flame.

Although the correction method has given good agreement between measured and calculated radiant fluxes for a few cases of fires of nearly equal size, it can be seen from the turbulent nature of the flame shown in Figure IV-23 that the time of exposure of the photograph determines the estimated flame size.

CHAPTER V

CONCLUSIONS

A specially designed burner system that produces a steady flame for long periods of time has permitted the study of radiation fields from conical laminar diffusion flames burning in an unlimited air supply at atmospheric pressure. Insight to problems with applications of information derived from data on small flames has been provided by spectral variations of intensity, size, and shape of the radiation fields for small laminar diffusion flames of natural gas and acetone. Profiles of the average intensity for the principal emission bands of these flames have shown the following:

1. Radiation fields extend outside the visible flame cone as much as the visible flame diameter horizontally and twice the height of the visible cone vertically.
2. The size of the emission envelope varies with wavelength. The maximum size occurs at 4.3 microns (peak of the CO_2 emission band). Another extension about half the size of the 4.3 micron envelope occurs at 2.7 microns (peak of the combined CO_2 and

H_2O emission band). All other emission from the flame is confined to the luminous flame cone.

3. Maximum intensity was emitted from the CO_2 emission band at 4.3 microns and the next strongest emission band, which is about half the strength, occurred from the combined CO_2 and H_2O emission at 2.7 microns.
4. Two positions of maximum intensity occurred: along the path through the center of the flame at the height just above the inner reaction zone (at approximately 0.6 of visible flame height) and along a path through the edge of the visible cone and adjacent to the inner reaction zone at a height of approximately 0.4 of the visible flame height.
5. Using the same burner and chimney assembly, a non-dimensionalized height parameter can be used to describe the vertical position adequately in radiation fields from laminar diffusion flames.

Intensity profile data revealed the path lengths used to calculate values of maximum emission and extinction coefficients were incorrect in the primary emission bands. However, the visible path lengths were used to calculate the coefficients after attempts to adjust the path lengths were unsuccessful. When emission extended beyond the visible flame cone and the extension distance was added to the visible flame paths, solutions for the extinction coefficient from the transport

equation were negative. Negative extinction coefficients are meaningless. The extension of the emission region beyong the luminous cone should decrease the values of maximum emission and extinction coefficients. As seen from the transport equation, the decrease in the extinction coefficient implies that a greater flame thickness is required to obtain maximum emission. While the increased path lengths are important in the calculation of the radiative flux from small flames, (1.0 to 10.0 centimeters visible thickness), the additional path length has very little effect on prediction calculations for medium flames (10.0 to 100.0 centimeter visible thickness) and large flames (over 100 centimeter visible thickness). Probably for the medium flames and certainly for the large flames the additional emission path is well within the errors involved in measuring the visible path length. Average maximum emission and extinction coefficients obtained by the single flame two-path technique have shown:

1. Reproducibility of the coefficients requires accurate measurements of intensity and path length, plus excellent stability of the flame and monochromator detection and recording system.
2. For the primary emission bands, path lengths greater than the visible paths need to be considered in coefficient calculation from small flames. Paths through the inner reaction zone

have order of magnitude lower emission and thereby cause large variations of the coefficients along vertical extent of the flame.

3. Calculations with the set of coefficients for the section of the flame just above the inner reaction zone (0.6 of the visible flame height) yield the maximum total intensity for both fuels. The thickness of the flame required to obtain the maximum emission was calculated to be approximately 100 centimeters for a natural gas flame and 50 centimeters for an acetone flame. The values represent the limits for "optically-thick" flames.

Maximum intensity for acetone flames estimated by Niell (30) and calculated from the coefficient are in good agreement considering differences in flame size and turbulence. Once turbulence effects can be included in the prediction calculations, the transport equation method has several advantages over conventional methods. Two of these advantages are input requirements of any size and shape of the flame and prediction of the spectral properties.

REFERENCES

1. Baly, E. C. C., Spectroscopy, Vol. 1, Longmans, Green and Co. Ltd., London (1927) p. 86.

2. Barr, J., "Length of Cylindrical Laminar Diffusion Flames", Fuel, Vol. 33 (1954), p. 51.

3. Breeze, J. C., Ferriso, C. C., Ludwig, C. B., and Malkums, W., "Temperature Dependence of the Total Integrated Intensity of Vibrational-Rotational Band Systems," Journal of Chemical Physics, Vol. 42 (1965) pp. 402-406.

4. Broida, H. P., "Experimental Temperature Measurements in Flames and Hot Gases," Temperature; Its Measurement and Control in Science and Industry, Vol. II, Reinhold Publishing Corp., New York, 1955.

5. Burch, D. E., Gryvnak, D. A., and Williams, D., "Total Absorption of Carbon Dioxide in the Infrared," Applied Optics, Vol. 2, No. 6, 1962.

6. Burch, D. E., France, W. L., and Williams, D., "Total Absorption of Water Vapor in the Near Infrared," Applied Optics, Vol. 2, No. 6, 1963.

7. Edwards, D. K. and Menard, W. A., "Comparison of Models for Correlation of Total Band Absorption," Applied Optics, Vol. 3 (1964), p. 621-625.

8. Edwards, D. K. and Menard, W. A., "Correlation for Absorption by Methane and Carbon Dioxide Gases," Applied Optics, Vol. 3 (1964), pp. 847-852.

9. Elsasser, W. M., "Heat Transfer by Infrared Radiation in the Atmosphere," Howard Meterotogical Series 6 (1942), Harvard University Press, Cambridge, Mass.

10. Ferriso, C. C., and Ludwig, C. B., "Spectral Emissivities and Integrated Intensities of the 1.87-1.38-, and 1.14 μ H_2O Bands between 1000° and 2200°K," Journal of Chemical Physics, Vol. 41 (1964) pp. 1668-1674.

11. Gaydon, A. G. and Wolfhard, H. G., Flames, Their Structure, Radiation and Temperature, Chapman and Hall, Ltd., London, (1960).

12. Goldstein, R., "Measurements of Infrared Absorption by Water Vapor at Temperatures to 1000°K," Journal of Quantum Spectrum Radiative Transfer, Vol. 4 (1964), pp. 343-352.

13. Goody, R. M., Physics of the Stratosphere, Cambridge University Press, New York, 1954.

14. Harrison, G. R., Lord, R. C., and Loofbourow, J. R., Practical Spectroscopy, Prentice Hall, Inc., New York, (1948), pp. 118-119.

15. Hines, W. S. and Edwards, D. K., "Infrared Absorptivities of Mixtures of Carbon Dioxide and Water Vapor," Ninth National Heat Transfer Conference, AIChE-ASME, Seattle, Washington, August 6 to 9, 1967.

16. Hollander, Tj., "Photometric Measurements on the Deviations from the Equilibrium State in Flames," AIAA Journal, Vol. 6 (1968) pp. 385-393.

17. Hood, J. D., "A Method for the Determination of the Radiative Properties of Flames," Ph.D. Thesis, University of Oklahoma (1966).

18. Hartley, H., "Report on Conversion of Potential Energy of Coal Gas into Radiant Energy," Institute of Gas Engineering Transaction, (1932), p. 51.

19. Hottel, H. C., and Egbert, R. B., "Radiation from Furnace Gases," Trans. ASME, Vol. 63 (1941), p. 297.

20. Hottel, H. C. and Manglesdorf, H. G., "Heat Transmission by Radiation from Non-luminous Gases II. Experimental Study of CO_2 and H_2O," Trans. AIChE, Vol. 31 (1935). p. 517.

21. Hottel, H. C., and Broughton, F. P., "Determination of True Temperature and Total Radiation from Luminous Gas Flames," Industrial Engineering Chemistry, Anal. Ed. 4 (1932), p. 517.

22. Hottel, H. C. and Sarofim, A. F, Radiative Transfer, McGraw-Hill Book Co., Inc., New York (1967), pp. 240-247.

23. Hsu, S. T., Engineering Heat Transfer, D. Van Nostrand Co., New York, (1963).

24. Instruction Manual for Model 12-C Single Pass Infrared Spectrometer. Perkin-Elmer Corporation, Norwalk, Connecticut, (1956) p. 33.

25. Jenkins, F. A. and White, H. E., Fundamentals of Optics, McGraw-Hill Book Co., Inc., New York, (1957).

26. Love, T. J., Jr., Radiative Heat Transfer, Charles E. Merrill Books, Inc., Columbus, Ohio, (1968) p. 210.

27. Larmore, Lewis, "Transmission of Infrared Radiation Through the Atmosphere," Office of Naval Research Proceeding Infrared Information Symposia, Vol. 1, No. 1, June, 1956.

28. Lewis, B. and von Elbe, G., "Stability and Structure of Burner Flames," Journal of Chemical Physics, Vol. 11 (1943) p. 75.

29. McAdams, W. H., Heat Transmission, McGraw-Hill, New York, (1954).

30. Neill, D. T., "Heat Transfer from Uncontrolled Buoyant Diffusion Flames," Ph.D. Thesis, University of Oklahoma, (1966).

31. Penner, S. S., "A Two-Path Method for Measuring Flame Temperatures and Concentrations in Low Pressure Combustion Chambers," Journal of Chemical Physics, Vol. 19 (1951) pp. 272-280.

32. Planck, M., Theory of Heat Radiation, Dover Publications, Inc., New York, (1959).

33. Pyler, E. K., Allen, H. C., and Tidwell, E. D., "Infrared Spectra of Polycholorbenzenes," Journal of Research of the National Bureau of Standards, Vol. 58 (1957) pp. 255-263.

34. Pyler, E. K., Blaine, L. R., and Nowak, N., "Reference Wavelengths of Calibrating Prism Spectrometers," Journal of Research of the National Bureau of Standards, Vol. 58 (1957) pp. 195-200.

35. Pyler, E. K., and Peters, C. W., "Wavelengths for Calibration of Prism Spectrometers," Journal of Research of the National Bureau of Standards, Vol. 45 (1950) pp. 462-467.

36. Rossi, B., Optics, Addison-Wesley Publishing Co., Inc. Reading, Massachusetts, (1959) pp. 202-208.

37. Shahroki, F., "Numerical Technique for Calculation of Radiant Energy Flux to Targets from Flames," Ph.D. Thesis, University of Oklahoma, (1965).

38. Thring, M. W., The Science of Furnaces and Flames, Chapman and Hall, Ltd., London, (1962).

39. Tsai, W., "Radiative Transport Properties of Flames," Ph.D. Thesis, University of Oklahoma, (1968).

40. Wesson, H. S., "Piloted Ignition of Wood by Radiant Heat," Dr. of Engr., University of Oklahoma, (1970).

41. White, W. G., Johnson, S. M. and Dantzig, A. B., "Chemical Equilibrium in Complex Mixtures," Journal of Chemical Physics, Vol. 28 (1958) pp. 751-755.

APPENDIX A

TABULAR SUMMARY OF INTENSITY PROFILE DATA

Values of intensity are presented on a spatial grid for fifty wavelengths in Tables A-1 (natural gas) and Table A-2 (acetone) for laminar flames. Average intensity for four wavelength intervals are presented on the same spatial grid as Table A-3 (natural gas) and Table A-4 (acetone).

The vertical grid is presented as a dimensionless variable and covers the range 0.0 to 2.0 visible flame heights in 0.1 increments. The horizontal coordinate, which is the distance of the viewing path to the axis of symmetry of the flame, covers the range 0.0 to 10.0 millimeters in 1.0 millimeter increments. To compute the actual intensity at a particular position, the value in the table must be multiplied by the units conversion factor given at the head of each table. The outline of the visible flame cone is shown at the beginning of each table.

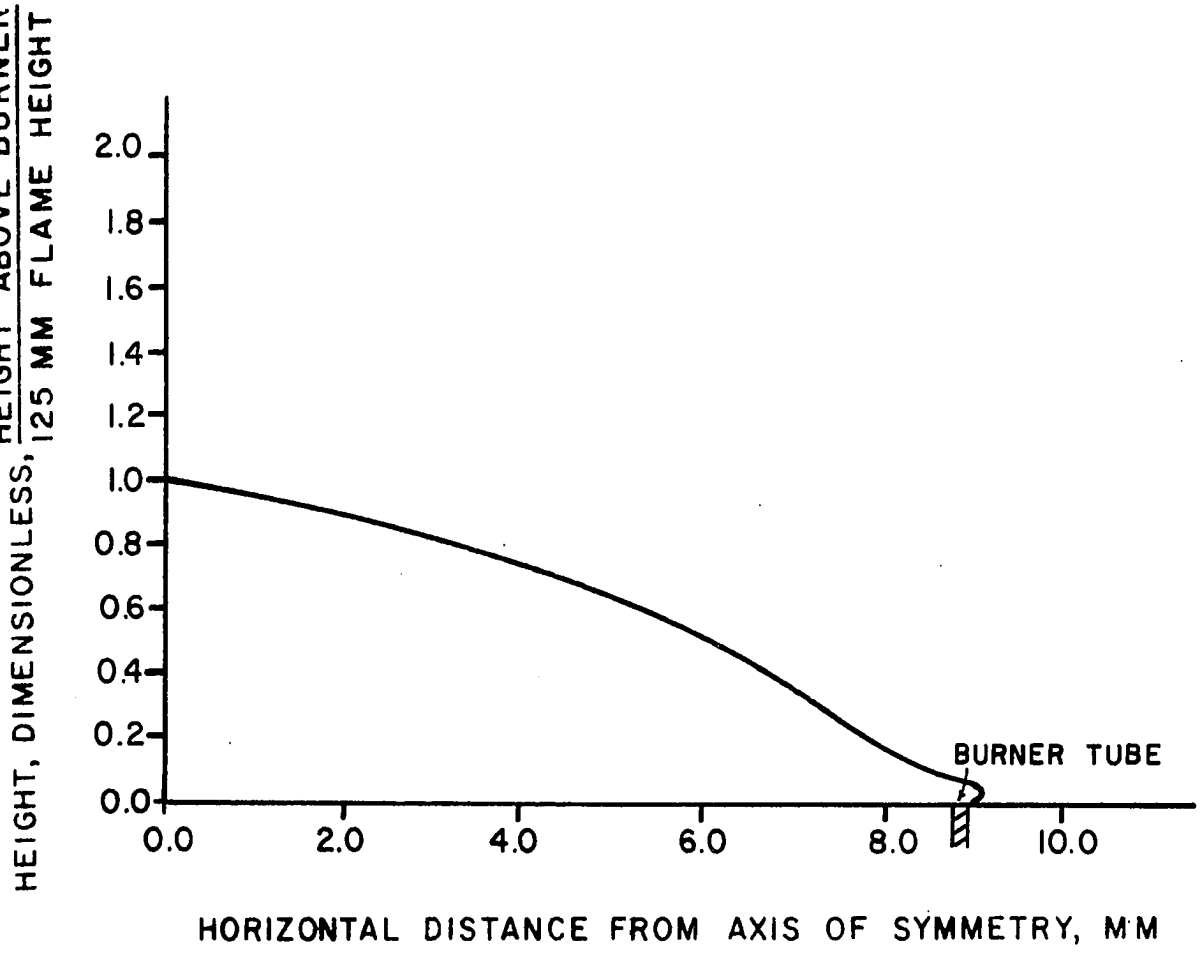

Figure A-1. Outline of Visible Cone for a Laminar Natural Gas Flame.

TABLE A-1

INTENSITY PROFILES FOR A LAMINAR NATURAL GAS DIFFUSION FLAME

HT = (DISTANCE ABOVE BURNER)/(125 MM FLAME HEIGHT)
WAVELENGTH = 0.71 MICRONS
UNITS = .00050 WATTS/SQCM/MICRON/STERADIAN

	HORIZONTAL DISTANCE FROM AXIS OF SYMMETRY - MM										
HT	0.0	1.0	2.0	3.0	4.0	5.0	6.0	7.0	8.0	9.0	10.0
2.0	.000	.000	.000	.000	.000	.000	.000	.000	.000	.000	.000
1.9	.000	.000	.000	.000	.000	.000	.000	.000	.000	.000	.000
1.8	.000	.000	.000	.000	.000	.000	.000	.000	.000	.000	.000
1.7	.000	.000	.000	.000	.000	.000	.000	.000	.000	.000	.000
1.6	.000	.000	.000	.000	.000	.000	.000	.000	.000	.000	.000
1.5	.000	.000	.000	.000	.000	.000	.000	.000	.000	.000	.000
1.4	.000	.000	.000	.000	.000	.000	.000	.000	.000	.000	.000
1.3	.000	.000	.000	.000	.000	.000	.000	.000	.000	.000	.000
1.2	.000	.000	.000	.000	.000	.000	.000	.000	.000	.000	.000
1.1	.000	.000	.000	.000	.000	.000	.000	.000	.000	.000	.000
1.0	.000	.000	.000	.000	.000	.000	.000	.000	.000	.000	.000
0.9	.330	.165	.165	.165	.000	.000	.000	.000	.000	.000	.000
0.8	.660	.330	.330	.330	.000	.000	.000	.000	.000	.000	.000
0.7	.825	.495	.495	.330	.165	.165	.000	.000	.000	.000	.000
0.6	.990	.660	.660	.330	.330	.330	.000	.000	.000	.000	.000
0.5	.825	.660	.660	.495	.495	.495	.165	.165	.000	.000	.000
0.4	.660	.660	.660	.660	.660	.660	.330	.330	.000	.000	.000
0.3	.495	.495	.495	.495	.495	.495	.330	.330	.000	.000	.000
0.2	.330	.330	.330	.330	.330	.330	.330	.330	.000	.000	.000
0.1	.142	.142	.142	.142	.142	.142	.142	.142	.000	.000	.000
0.0	.000	.000	.000	.000	.000	.000	.000	.000	.000	.000	.000

TABLE A-1(CONTINUED)

WAVELENGTH OF UPPER ARRAY = 0.72 MICRONS

WAVELENGTH OF LOWER ARRAY = 0.73 MICRONS

UNITS = .00090 WATTS/SQCM/MICRON/STERADIAN

HORIZONTAL DISTANCE FROM AXIS OF SYMMETRY - MM

HT	0.0	1.0	2.0	3.0	4.0	5.0	6.0	7.0	8.0	9.0	10.0
2.0	.000	.000	.000	.000	.000	.000	.000	.000	.000	.000	.000
1.9	.000	.000	.000	.000	.000	.000	.000	.000	.000	.000	.000
1.8	.000	.000	.000	.000	.000	.000	.000	.000	.000	.000	.000
1.7	.000	.000	.000	.000	.000	.000	.000	.000	.000	.000	.000
1.6	.000	.000	.000	.000	.000	.000	.000	.000	.000	.000	.000
1.5	.000	.000	.000	.000	.000	.000	.000	.000	.000	.000	.000
1.4	.000	.000	.000	.000	.000	.000	.000	.000	.000	.000	.000
1.3	.000	.000	.000	.000	.000	.000	.000	.000	.000	.000	.000
1.2	.000	.000	.000	.000	.000	.000	.000	.000	.000	.000	.000
1.1	.000	.000	.000	.000	.000	.000	.000	.000	.000	.000	.000
1.0	.000	.000	.000	.000	.000	.000	.000	.000	.000	.000	.000
0.9	.183	.183	.092	.092	.092	.000	.000	.000	.000	.000	.000
0.8	.367	.367	.183	.183	.183	.000	.000	.000	.000	.000	.000
0.7	.458	.458	.367	.367	.275	.000	.000	.000	.000	.000	.000
0.6	.550	.550	.550	.550	.367	.000	.000	.000	.000	.000	.000
0.5	.458	.458	.458	.458	.367	.183	.092	.000	.000	.000	.000
0.4	.367	.367	.367	.367	.367	.367	.183	.000	.000	.000	.000
0.3	.275	.275	.275	.275	.275	.367	.275	.092	.000	.000	.000
0.2	.183	.183	.183	.183	.183	.367	.367	.183	.000	.000	.000
0.1	.079	.079	.079	.079	.079	.158	.158	.079	.000	.000	.000
0.0	.000	.000	.000	.000	.000	.000	.000	.000	.000	.000	.000
2.0	.000	.000	.000	.000	.000	.000	.000	.000	.000	.000	.000
1.9	.000	.000	.000	.000	.000	.000	.000	.000	.000	.000	.000
1.8	.000	.000	.000	.000	.000	.000	.000	.000	.000	.000	.000
1.7	.000	.000	.000	.000	.000	.000	.000	.000	.000	.000	.000
1.6	.000	.000	.000	.000	.000	.000	.000	.000	.000	.000	.000
1.5	.000	.000	.000	.000	.000	.000	.000	.000	.000	.000	.000
1.4	.000	.000	.000	.000	.000	.000	.000	.000	.000	.000	.000
1.3	.000	.000	.000	.000	.000	.000	.000	.000	.000	.000	.000
1.2	.000	.000	.000	.000	.000	.000	.000	.000	.000	.000	.000
1.1	.000	.000	.000	.000	.000	.000	.000	.000	.000	.000	.000
1.0	.000	.000	.000	.000	.000	.000	.000	.000	.000	.000	.000
0.9	.275	.183	.092	.092	.000	.000	.000	.000	.000	.000	.000
0.8	.550	.367	.183	.183	.000	.000	.000	.000	.000	.000	.000
0.7	.733	.642	.550	.550	.367	.000	.000	.000	.000	.000	.000
0.6	.917	.917	.917	.917	.733	.000	.000	.000	.000	.000	.000
0.5	.733	.733	.733	.733	.550	.183	.092	.000	.000	.000	.000
0.4	.550	.550	.550	.550	.367	.367	.183	.000	.000	.000	.000
0.3	.367	.367	.367	.367	.275	.275	.183	.092	.000	.000	.000
0.2	.183	.183	.183	.183	.183	.183	.183	.183	.000	.000	.000
0.1	.079	.079	.079	.079	.079	.079	.079	.079	.000	.000	.000
0.0	.000	.000	.000	.000	.000	.000	.000	.000	.000	.000	.000

TABLE A-1(CONTINUED)

WAVELENGTH OF UPPER ARRAY = 0.75 MICRONS
WAVELENGTH OF LOWER ARRAY = 0.79 MICRONS
UNITS = .00150 WATTS/SQCM/MICRON/STERADIAN
HORIZONTAL DISTANCE FROM AXIS OF SYMMETRY - MM

HT	0.0	1.0	2.0	3.0	4.0	5.0	6.0	7.0	8.0	9.0	10.0
2.0	.000	.000	.000	.000	.000	.000	.000	.000	.000	.000	.000
1.9	.000	.000	.000	.000	.000	.000	.000	.000	.000	.000	.000
1.8	.000	.000	.000	.000	.000	.000	.000	.000	.000	.000	.000
1.7	.000	.000	.000	.000	.000	.000	.000	.000	.000	.000	.000
1.6	.000	.000	.000	.000	.000	.000	.000	.000	.000	.000	.000
1.5	.000	.000	.000	.000	.000	.000	.000	.000	.000	.000	.000
1.4	.000	.000	.000	.000	.000	.000	.000	.000	.000	.000	.000
1.3	.027	.027	.027	.027	.000	.000	.000	.000	.000	.000	.000
1.2	.055	.055	.055	.055	.000	.000	.000	.000	.000	.000	.000
1.1	.082	.082	.082	.082	.000	.000	.000	.000	.000	.000	.000
1.0	.110	.110	.110	.110	.000	.000	.000	.000	.000	.000	.000
0.9	.275	.220	.165	.165	.110	.055	.000	.000	.000	.000	.000
0.8	.440	.330	.220	.220	.220	.110	.000	.000	.000	.000	.000
0.7	.605	.550	.495	.440	.385	.220	.055	.000	.000	.000	.000
0.6	.770	.770	.770	.660	.550	.330	.110	.000	.000	.000	.000
0.5	.495	.550	.605	.550	.495	.330	.165	.055	.000	.000	.000
0.4	.220	.330	.440	.440	.440	.330	.220	.110	.000	.000	.000
0.3	.165	.220	.275	.330	.330	.330	.275	.165	.055	.000	.000
0.2	.110	.110	.110	.220	.220	.330	.330	.220	.110	.000	.000
0.1	.110	.110	.110	.157	.157	.205	.205	.157	.110	.062	.062
0.0	.110	.110	.110	.095	.095	.080	.080	.095	.110	.125	.125
2.0	.000	.000	.000	.000	.000	.000	.000	.000	.000	.000	.000
1.9	.000	.000	.000	.000	.000	.000	.000	.000	.000	.000	.000
1.8	.000	.000	.000	.000	.000	.000	.000	.000	.000	.000	.000
1.7	.000	.000	.000	.000	.000	.000	.000	.000	.000	.000	.000
1.6	.000	.000	.000	.000	.000	.000	.000	.000	.000	.000	.000
1.5	.000	.000	.000	.000	.000	.000	.000	.000	.000	.000	.000
1.4	.000	.000	.000	.000	.000	.000	.000	.000	.000	.000	.000
1.3	.027	.027	.027	.027	.000	.000	.000	.000	.000	.000	.000
1.2	.055	.055	.055	.055	.000	.000	.000	.000	.000	.000	.000
1.1	.082	.082	.082	.082	.000	.000	.000	.000	.000	.000	.000
1.0	.110	.110	.110	.110	.000	.000	.000	.000	.000	.000	.000
0.9	.330	.220	.165	.165	.055	.000	.000	.000	.000	.000	.000
0.8	.550	.330	.220	.220	.110	.000	.000	.000	.000	.000	.000
0.7	.770	.660	.605	.605	.495	.165	.055	.000	.000	.000	.000
0.6	.990	.990	.990	.990	.880	.330	.110	.000	.000	.000	.000
0.5	.715	.715	.770	.770	.715	.440	.275	.110	.055	.000	.000
0.4	.440	.440	.550	.550	.550	.550	.440	.220	.110	.000	.000
0.3	.275	.330	.385	.385	.385	.385	.330	.220	.110	.000	.000
0.2	.110	.220	.220	.220	.220	.220	.220	.220	.110	.000	.000
0.1	.110	.157	.157	.157	.157	.157	.157	.157	.110	.062	.062
0.0	.110	.095	.095	.095	.095	.095	.095	.095	.110	.125	.125

TABLE A-1(CONTINUED)

WAVELENGTH OF UPPER ARRAY = 0.83 MICRONS

WAVELENGTH OF LOWER ARRAY = 0.88 MICRONS

UNITS = .00350 WATTS/SQCM/MICRON/STERADIAN

HORIZONTAL DISTANCE FROM AXIS OF SYMMETRY - MM

HT	0.0	1.0	2.0	3.0	4.0	5.0	6.0	7.0	8.0	9.0	10.0
2.0	.000	.000	.000	.000	.000	.000	.000	.000	.000	.000	.000
1.9	.000	.000	.000	.000	.000	.000	.000	.000	.000	.000	.000
1.8	.000	.000	.000	.000	.000	.000	.000	.000	.000	.000	.000
1.7	.000	.000	.000	.000	.000	.000	.000	.000	.000	.000	.000
1.6	.000	.000	.000	.000	.000	.000	.000	.000	.000	.000	.000
1.5	.000	.000	.000	.000	.000	.000	.000	.000	.000	.000	.000
1.4	.000	.000	.000	.000	.000	.000	.000	.000	.000	.000	.000
1.3	.000	.000	.000	.000	.000	.000	.000	.000	.000	.000	.000
1.2	.000	.000	.000	.000	.000	.000	.000	.000	.000	.000	.000
1.1	.000	.000	.000	.000	.000	.000	.000	.000	.000	.000	.000
1.0	.000	.000	.000	.000	.000	.000	.000	.000	.000	.000	.000
0.9	.165	.071	.024	.024	.024	.024	.024	.000	.000	.000	.000
0.8	.330	.141	.047	.047	.047	.047	.047	.000	.000	.000	.000
0.7	.448	.354	.306	.283	.236	.141	.094	.024	.000	.000	.000
0.6	.566	.566	.566	.518	.424	.236	.141	.047	.000	.000	.000
0.5	.424	.424	.424	.401	.330	.212	.118	.047	.000	.000	.000
0.4	.283	.283	.283	.283	.236	.189	.094	.047	.000	.000	.000
0.3	.165	.189	.189	.189	.165	.141	.094	.047	.024	.000	.000
0.2	.047	.094	.094	.094	.094	.094	.094	.047	.047	.000	.000
0.1	.047	.067	.067	.067	.067	.067	.067	.047	.047	.027	.027
0.0	.047	.041	.041	.041	.041	.041	.041	.047	.047	.054	.054
2.0	.000	.000	.000	.000	.000	.000	.000	.000	.000	.000	.000
1.9	.000	.000	.000	.000	.000	.000	.000	.000	.000	.000	.000
1.8	.000	.000	.000	.000	.000	.000	.000	.000	.000	.000	.000
1.7	.000	.000	.000	.000	.000	.000	.000	.000	.000	.000	.000
1.6	.000	.000	.000	.000	.000	.000	.000	.000	.000	.000	.000
1.5	.000	.000	.000	.000	.000	.000	.000	.000	.000	.000	.000
1.4	.000	.000	.000	.000	.000	.000	.000	.000	.000	.000	.000
1.3	.035	.035	.024	.012	.000	.000	.000	.000	.000	.000	.000
1.2	.071	.071	.047	.024	.000	.000	.000	.000	.000	.000	.000
1.1	.106	.106	.071	.035	.000	.000	.000	.000	.000	.000	.000
1.0	.141	.141	.094	.047	.000	.000	.000	.000	.000	.000	.000
0.9	.306	.212	.118	.047	.000	.000	.000	.000	.000	.000	.000
0.8	.471	.283	.141	.047	.000	.000	.000	.000	.000	.000	.000
0.7	.613	.566	.495	.401	.236	.094	.024	.000	.000	.000	.000
0.6	.754	.848	.848	.754	.471	.189	.047	.000	.000	.000	.000
0.5	.518	.613	.613	.566	.401	.236	.094	.024	.000	.000	.000
0.4	.283	.377	.377	.377	.330	.283	.141	.047	.000	.000	.000
0.3	.636	.683	.660	.613	.471	.212	.118	.047	.000	.000	.000
0.2	.990	.990	.943	.848	.613	.141	.094	.047	.000	.000	.000
0.1	.454	.454	.434	.393	.291	.088	.067	.047	.027	.027	.027
0.0	.000	.000	.000	.000	.000	.034	.041	.047	.054	.054	.054

TABLE A-1(CONTINUED)

WAVELENGTH OF UPPER ARRAY = 0.94 MICRONS

WAVELENGTH OF LOWER ARRAY = 1.01 MICRONS

UNITS = .00530 WATTS/SQCM/MICRON/STERADIAN

HORIZONTAL DISTANCE FROM AXIS OF SYMMETRY - MM

HT	0.0	1.0	2.0	3.0	4.0	5.0	6.0	7.0	8.0	9.0	10.0
2.0	.000	.000	.000	.000	.000	.000	.000	.000	.000	.000	.000
1.9	.000	.000	.000	.000	.000	.000	.000	.000	.000	.000	.000
1.8	.000	.000	.000	.000	.000	.000	.000	.000	.000	.000	.000
1.7	.000	.000	.000	.000	.000	.000	.000	.000	.000	.000	.000
1.6	.000	.000	.000	.000	.000	.000	.000	.000	.000	.000	.000
1.5	.000	.000	.000	.000	.000	.000	.000	.000	.000	.000	.000
1.4	.000	.000	.000	.000	.000	.000	.000	.000	.000	.000	.000
1.3	.016	.016	.016	.008	.008	.000	.000	.000	.000	.000	.000
1.2	.031	.031	.031	.016	.016	.000	.000	.000	.000	.000	.000
1.1	.047	.047	.047	.023	.023	.000	.000	.000	.000	.000	.000
1.0	.062	.062	.062	.031	.031	.000	.000	.000	.000	.000	.000
0.9	.218	.140	.062	.031	.031	.000	.000	.000	.000	.000	.000
0.8	.374	.218	.062	.031	.031	.000	.000	.000	.000	.000	.000
0.7	.498	.436	.358	.296	.187	.031	.016	.000	.000	.000	.000
0.6	.623	.654	.654	.560	.342	.062	.031	.000	.000	.000	.000
0.5	.436	.467	.482	.436	.311	.140	.078	.016	.000	.000	.000
0.4	.249	.280	.311	.311	.280	.218	.125	.031	.000	.000	.000
0.3	.467	.560	.654	.623	.482	.140	.078	.031	.000	.000	.000
0.2	.685	.840	.996	.934	.685	.062	.031	.031	.000	.000	.000
0.1	.331	.398	.465	.439	.331	.062	.031	.031	.018	.018	.000
0.0	.000	.000	.000	.000	.000	.062	.031	.031	.035	.035	.000
2.0	.000	.000	.000	.000	.000	.000	.000	.000	.000	.000	.000
1.9	.000	.000	.000	.000	.000	.000	.000	.000	.000	.000	.000
1.8	.000	.000	.000	.000	.000	.000	.000	.000	.000	.000	.000
1.7	.000	.000	.000	.000	.000	.000	.000	.000	.000	.000	.000
1.6	.000	.000	.000	.000	.000	.000	.000	.000	.000	.000	.000
1.5	.000	.000	.000	.000	.000	.000	.000	.000	.000	.000	.000
1.4	.000	.000	.000	.000	.000	.000	.000	.000	.000	.000	.000
1.3	.008	.008	.008	.008	.000	.000	.000	.000	.000	.000	.000
1.2	.016	.016	.016	.016	.000	.000	.000	.000	.000	.000	.000
1.1	.023	.023	.023	.023	.000	.000	.000	.000	.000	.000	.000
1.0	.031	.031	.031	.031	.000	.000	.000	.000	.000	.000	.000
0.9	.280	.202	.047	.031	.016	.000	.000	.000	.000	.000	.000
0.8	.529	.374	.062	.031	.031	.000	.000	.000	.000	.000	.000
0.7	.685	.638	.467	.405	.280	.140	.016	.000	.000	.000	.000
0.6	.840	.903	.872	.778	.529	.280	.031	.000	.000	.000	.000
0.5	.638	.669	.654	.591	.467	.265	.093	.016	.000	.000	.000
0.4	.436	.436	.436	.405	.405	.249	.156	.031	.000	.000	.000
0.3	.249	.265	.265	.265	.280	.218	.156	.062	.016	.000	.000
0.2	.062	.093	.093	.125	.156	.187	.156	.093	.031	.000	.000
0.1	.045	.058	.058	.071	.085	.098	.085	.058	.031	.018	.018
0.0	.027	.023	.023	.018	.014	.010	.014	.023	.031	.035	.035

TABLE A-1(CONTINUED)

WAVELENGTH OF UPPER ARRAY = 1.10 MICRONS
WAVELENGTH OF LOWER ARRAY = 1.19 MICRONS
UNITS = .00760 WATTS/SQCM/MICRON/STERADIAN
HORIZONTAL DISTANCE FROM AXIS OF SYMMETRY - MM

HT	0.0	1.0	2.0	3.0	4.0	5.0	6.0	7.0	8.0	9.0	10.0
2.0	.000	.000	.000	.000	.000	.000	.000	.000	.000	.000	.000
1.9	.000	.000	.000	.000	.000	.000	.000	.000	.000	.000	.000
1.8	.000	.000	.000	.000	.000	.000	.000	.000	.000	.000	.000
1.7	.000	.000	.000	.000	.000	.000	.000	.000	.000	.000	.000
1.6	.000	.000	.000	.000	.000	.000	.000	.000	.000	.000	.000
1.5	.000	.000	.000	.000	.000	.000	.000	.000	.000	.000	.000
1.4	.000	.000	.000	.000	.000	.000	.000	.000	.000	.000	.000
1.3	.005	.005	.005	.005	.000	.000	.000	.000	.000	.000	.000
1.2	.011	.011	.011	.011	.000	.000	.000	.000	.000	.000	.000
1.1	.016	.016	.016	.016	.000	.000	.000	.000	.000	.000	.000
1.0	.022	.022	.022	.022	.000	.000	.000	.000	.000	.000	.000
0.9	.228	.141	.033	.033	.011	.000	.000	.000	.000	.000	.000
0.8	.434	.260	.043	.043	.022	.000	.000	.000	.000	.000	.000
0.7	.575	.521	.423	.402	.326	.206	.098	.011	.000	.000	.000
0.6	.716	.781	.803	.760	.630	.412	.195	.022	.000	.000	.000
0.5	.510	.554	.575	.554	.478	.336	.174	.033	.000	.000	.000
0.4	.304	.326	.347	.347	.326	.260	.152	.043	.000	.000	.000
0.3	.195	.217	.228	.228	.195	.152	.087	.033	.000	.000	.000
0.2	.087	.109	.109	.109	.065	.043	.022	.022	.000	.000	.000
0.1	.050	.059	.059	.059	.040	.031	.022	.022	.000	.000	.000
0.0	.013	.010	.010	.010	.016	.019	.022	.022	.000	.000	.000
2.0	.000	.000	.000	.000	.000	.000	.000	.000	.000	.000	.000
1.9	.000	.000	.000	.000	.000	.000	.000	.000	.000	.000	.000
1.8	.000	.000	.000	.000	.000	.000	.000	.000	.000	.000	.000
1.7	.000	.000	.000	.000	.000	.000	.000	.000	.000	.000	.000
1.6	.000	.000	.000	.000	.000	.000	.000	.000	.000	.000	.000
1.5	.000	.000	.000	.000	.000	.000	.000	.000	.000	.000	.000
1.4	.000	.000	.000	.000	.000	.000	.000	.000	.000	.000	.000
1.3	.033	.033	.033	.005	.000	.000	.000	.000	.000	.000	.000
1.2	.065	.065	.065	.011	.000	.000	.000	.000	.000	.000	.000
1.1	.098	.098	.098	.016	.000	.000	.000	.000	.000	.000	.000
1.0	.130	.130	.130	.022	.000	.000	.000	.000	.000	.000	.000
0.9	.336	.293	.152	.033	.011	.000	.000	.000	.000	.000	.000
0.8	.543	.456	.174	.043	.022	.000	.000	.000	.000	.000	.000
0.7	.760	.727	.586	.488	.402	.282	.174	.065	.011	.000	.000
0.6	.977	.999	.999	.933	.781	.564	.347	.130	.022	.000	.000
0.5	.662	.695	.705	.684	.597	.456	.304	.152	.033	.000	.000
0.4	.347	.391	.412	.434	.412	.347	.260	.174	.043	.000	.000
0.3	.217	.271	.293	.304	.250	.206	.152	.098	.033	.000	.000
0.2	.087	.152	.174	.174	.087	.065	.043	.022	.022	.000	.000
0.1	.050	.078	.087	.087	.050	.040	.031	.022	.022	.012	.012
0.0	.013	.004	.001	.001	.013	.016	.019	.022	.022	.025	.025

TABLE A-1(CONTINUED)

WAVELENGTH OF UPPER ARRAY = 1.30 MICRONS

WAVELENGTH OF LOWER ARRAY = 1.42 MICRONS

UNITS = .01040 WATTS/SQCM/MICRON/STERADIAN

HORIZONTAL DISTANCE FROM AXIS OF SYMMETRY - MM

HT	0.0	1.0	2.0	3.0	4.0	5.0	6.0	7.0	8.0	9.0	10.0
2.0	.000	.000	.000	.000	.000	.000	.000	.000	.000	.000	.000
1.9	.000	.000	.000	.000	.000	.000	.000	.000	.000	.000	.000
1.8	.000	.000	.000	.000	.000	.000	.000	.000	.000	.000	.000
1.7	.000	.000	.000	.000	.000	.000	.000	.000	.000	.000	.000
1.6	.000	.000	.000	.000	.000	.000	.000	.000	.000	.000	.000
1.5	.000	.000	.000	.000	.000	.000	.000	.000	.000	.000	.000
1.4	.000	.000	.000	.000	.000	.000	.000	.000	.000	.000	.000
1.3	.008	.008	.008	.004	.000	.000	.000	.000	.000	.000	.000
1.2	.016	.016	.016	.008	.000	.000	.000	.000	.000	.000	.000
1.1	.024	.024	.024	.012	.000	.000	.000	.000	.000	.000	.000
1.0	.032	.032	.032	.016	.000	.000	.000	.000	.000	.000	.000
0.9	.254	.174	.040	.016	.000	.000	.000	.000	.000	.000	.000
0.8	.476	.317	.048	.016	.000	.000	.000	.000	.000	.000	.000
0.7	.658	.587	.428	.349	.214	.151	.048	.008	.000	.000	.000
0.6	.841	.857	.809	.682	.428	.301	.095	.016	.000	.000	.000
0.5	.579	.611	.611	.563	.428	.333	.174	.056	.016	.000	.000
0.4	.317	.365	.412	.444	.428	.365	.254	.095	.032	.000	.000
0.3	.182	.206	.230	.254	.254	.238	.174	.079	.032	.000	.000
0.2	.048	.048	.048	.063	.079	.111	.095	.063	.032	.000	.000
0.1	.030	.030	.030	.036	.043	.057	.050	.036	.023	.009	.000
0.0	.012	.012	.012	.009	.007	.003	.005	.009	.014	.018	.000
2.0	.000	.000	.000	.000	.000	.000	.000	.000	.000	.000	.000
1.9	.000	.000	.000	.000	.000	.000	.000	.000	.000	.000	.000
1.8	.000	.000	.000	.000	.000	.000	.000	.000	.000	.000	.000
1.7	.000	.000	.000	.000	.000	.000	.000	.000	.000	.000	.000
1.6	.000	.000	.000	.000	.000	.000	.000	.000	.000	.000	.000
1.5	.000	.000	.000	.000	.000	.000	.000	.000	.000	.000	.000
1.4	.000	.000	.000	.000	.000	.000	.000	.000	.000	.000	.000
1.3	.004	.004	.004	.004	.004	.000	.000	.000	.000	.000	.000
1.2	.008	.008	.008	.008	.008	.000	.000	.000	.000	.000	.000
1.1	.012	.012	.012	.012	.012	.000	.000	.000	.000	.000	.000
1.0	.016	.016	.016	.016	.016	.000	.000	.000	.000	.000	.000
0.9	.286	.230	.048	.032	.024	.008	.000	.000	.000	.000	.000
0.8	.555	.444	.079	.048	.032	.016	.000	.000	.000	.000	.000
0.7	.761	.722	.539	.492	.412	.254	.174	.056	.008	.000	.000
0.6	.968	.999	.999	.936	.793	.492	.349	.111	.016	.000	.000
0.5	.674	.722	.761	.746	.666	.484	.333	.095	.024	.008	.000
0.4	.381	.444	.523	.555	.539	.476	.317	.079	.032	.016	.000
0.3	.254	.301	.357	.389	.397	.365	.262	.056	.024	.008	.000
0.2	.127	.159	.190	.222	.254	.254	.206	.032	.016	.000	.000
0.1	.064	.078	.091	.105	.119	.119	.098	.023	.007	.000	.000
0.0	.001	.000	.000	.000	.000	.000	.000	.014	.000	.000	.000

TABLE A-1(CONTINUED)

WAVELENGTH OF UPPER ARRAY = 1.55 MICRONS

WAVELENGTH OF LOWER ARRAY = 1.69 MICRONS

UNITS = .01440 WATTS/SQCM/MICRON/STERADIAN

HORIZONTAL DISTANCE FROM AXIS OF SYMMETRY - MM

HT	0.0	1.0	2.0	3.0	4.0	5.0	6.0	7.0	8.0	9.0	10.0
2.0	.011	.011	.011	.011	.011	.002	.000	.000	.000	.000	.000
1.9	.011	.011	.011	.011	.011	.004	.000	.000	.000	.000	.000
1.8	.011	.011	.011	.011	.011	.005	.000	.000	.000	.000	.000
1.7	.011	.011	.011	.011	.011	.007	.000	.000	.000	.000	.000
1.6	.011	.011	.011	.011	.011	.008	.000	.000	.000	.000	.000
1.5	.011	.011	.011	.011	.011	.010	.000	.000	.000	.000	.000
1.4	.011	.011	.011	.011	.011	.011	.000	.000	.000	.000	.000
1.3	.014	.014	.014	.011	.011	.011	.003	.000	.000	.000	.000
1.2	.017	.017	.017	.011	.011	.011	.006	.000	.000	.000	.000
1.1	.020	.020	.020	.011	.011	.011	.009	.000	.000	.000	.000
1.0	.023	.023	.023	.011	.011	.011	.011	.000	.000	.000	.000
0.9	.258	.109	.069	.023	.017	.017	.017	.000	.000	.000	.000
0.8	.493	.195	.115	.034	.023	.023	.023	.000	.000	.000	.000
0.7	.670	.544	.510	.447	.384	.034	.023	.006	.000	.000	.000
0.6	.848	.894	.905	.859	.745	.046	.023	.011	.000	.000	.000
0.5	.584	.624	.647	.630	.556	.172	.097	.023	.006	.000	.000
0.4	.321	.355	.390	.401	.367	.298	.172	.034	.011	.000	.000
0.3	.206	.229	.252	.269	.264	.246	.166	.023	.006	.000	.000
0.2	.092	.103	.115	.137	.160	.195	.160	.011	.000	.000	.000
0.1	.046	.051	.056	.066	.076	.091	.076	.011	.000	.000	.000
0.0	.001	.000	.000	.000	.000	.000	.000	.011	.000	.000	.000
2.0	.011	.011	.011	.011	.002	.000	.000	.000	.000	.000	.000
1.9	.011	.011	.011	.011	.004	.000	.000	.000	.000	.000	.000
1.8	.011	.011	.011	.011	.005	.000	.000	.000	.000	.000	.000
1.7	.011	.011	.011	.011	.007	.000	.000	.000	.000	.000	.000
1.6	.011	.011	.011	.011	.008	.000	.000	.000	.000	.000	.000
1.5	.011	.011	.011	.011	.010	.000	.000	.000	.000	.000	.000
1.4	.011	.011	.011	.011	.011	.000	.000	.000	.000	.000	.000
1.3	.011	.011	.011	.011	.011	.003	.000	.000	.000	.000	.000
1.2	.011	.011	.011	.011	.011	.006	.000	.000	.000	.000	.000
1.1	.011	.011	.011	.011	.011	.009	.000	.000	.000	.000	.000
1.0	.011	.011	.011	.011	.011	.011	.000	.000	.000	.000	.000
0.9	.292	.149	.046	.029	.017	.011	.000	.000	.000	.000	.000
0.8	.573	.286	.080	.046	.023	.011	.000	.000	.000	.000	.000
0.7	.756	.642	.527	.481	.401	.292	.011	.000	.000	.000	.000
0.6	.939	.997	.974	.917	.779	.573	.023	.000	.000	.000	.000
0.5	.802	.802	.756	.687	.561	.401	.069	.011	.000	.000	.000
0.4	.664	.607	.538	.458	.344	.229	.115	.023	.000	.000	.000
0.3	.372	.355	.332	.298	.258	.212	.149	.017	.000	.000	.000
0.2	.080	.103	.126	.137	.172	.195	.183	.011	.000	.000	.000
0.1	.041	.051	.061	.066	.081	.091	.086	.011	.000	.000	.000
0.0	.002	.000	.000	.000	.000	.000	.000	.011	.000	.000	.000

TABLE A-1(CONTINUED)

WAVELENGTH OF UPPER ARRAY = 1.84 MICRONS

WAVELENGTH OF LOWER ARRAY = 2.00 MICRONS

UNITS = .01610 WATTS/SQCM/MICRON/STERADIAN

HORIZONTAL DISTANCE FROM AXIS OF SYMMETRY - MM

HT	0.0	1.0	2.0	3.0	4.0	5.0	6.0	7.0	8.0	9.0	10.0
2.0	.010	.010	.010	.010	.002	.000	.000	.000	.000	.000	.000
1.9	.010	.010	.010	.010	.003	.000	.000	.000	.000	.000	.000
1.8	.010	.010	.010	.010	.005	.000	.000	.000	.000	.000	.000
1.7	.010	.010	.010	.010	.006	.000	.000	.000	.000	.000	.000
1.6	.010	.010	.010	.010	.007	.000	.000	.000	.000	.000	.000
1.5	.010	.010	.010	.010	.009	.000	.000	.000	.000	.000	.000
1.4	.010	.010	.010	.010	.010	.000	.000	.000	.000	.000	.000
1.3	.013	.010	.010	.010	.010	.003	.000	.000	.000	.000	.000
1.2	.015	.010	.010	.010	.010	.005	.000	.000	.000	.000	.000
1.1	.018	.010	.010	.010	.010	.008	.000	.000	.000	.000	.000
1.0	.020	.010	.010	.010	.010	.010	.000	.000	.000	.000	.000
0.9	.297	.159	.046	.031	.026	.020	.010	.000	.000	.000	.000
0.8	.574	.307	.082	.051	.041	.031	.020	.000	.000	.000	.000
0.7	.753	.651	.528	.482	.405	.056	.031	.005	.000	.000	.000
0.6	.932	.994	.973	.912	.769	.082	.041	.010	.000	.000	.000
0.5	.651	.702	.712	.687	.615	.256	.174	.015	.000	.000	.000
0.4	.369	.410	.451	.461	.461	.430	.307	.020	.000	.000	.000
0.3	.241	.277	.307	.323	.338	.338	.272	.087	.010	.000	.000
0.2	.113	.143	.164	.184	.215	.246	.236	.154	.020	.000	.000
0.1	.054	.068	.077	.085	.099	.112	.108	.072	.015	.006	.000
0.0	.000	.000	.000	.000	.000	.000	.000	.000	.009	.012	.000
2.0	.012	.015	.019	.020	.020	.020	.019	.003	.000	.000	.000
1.9	.013	.020	.026	.029	.029	.029	.026	.006	.000	.000	.000
1.8	.015	.024	.033	.037	.037	.037	.033	.009	.000	.000	.000
1.7	.016	.028	.040	.046	.046	.046	.040	.012	.000	.000	.000
1.6	.018	.032	.047	.055	.055	.055	.047	.015	.000	.000	.000
1.5	.019	.037	.054	.063	.063	.063	.054	.018	.000	.000	.000
1.4	.020	.041	.061	.072	.072	.072	.061	.020	.000	.000	.000
1.3	.026	.041	.056	.064	.064	.059	.051	.018	.000	.000	.000
1.2	.031	.041	.051	.056	.056	.046	.041	.015	.000	.000	.000
1.1	.036	.041	.046	.049	.049	.033	.031	.013	.000	.000	.000
1.0	.041	.041	.041	.041	.041	.020	.020	.010	.000	.000	.000
0.9	.307	.199	.066	.046	.041	.026	.020	.010	.000	.000	.000
0.8	.572	.358	.092	.051	.041	.031	.020	.010	.000	.000	.000
0.7	.756	.664	.532	.486	.429	.118	.061	.026	.005	.000	.000
0.6	.940	.971	.971	.920	.818	.204	.102	.041	.010	.000	.000
0.5	.664	.705	.726	.705	.654	.322	.204	.051	.020	.005	.000
0.4	.388	.440	.480	.491	.491	.440	.307	.061	.031	.010	.000
0.3	.256	.296	.332	.353	.363	.353	.291	.133	.041	.010	.000
0.2	.123	.153	.184	.215	.235	.266	.276	.204	.051	.010	.000
0.1	.070	.084	.097	.110	.119	.132	.137	.106	.039	.016	.006
0.0	.018	.014	.010	.006	.003	.000	.000	.007	.028	.022	.012

TABLE A-1(CONTINUED)

WAVELENGTH OF UPPER ARRAY = 2.05 MICRONS

WAVELENGTH OF LOWER ARRAY = 2.18 MICRONS

UNITS = .01600 WATTS/SQCM/MICRON/STERADIAN

HORIZONTAL DISTANCE FROM AXIS OF SYMMETRY - MM

HT	0.0	1.0	2.0	3.0	4.0	5.0	6.0	7.0	8.0	9.0	10.0
2.0	.012	.012	.012	.012	.012	.010	.002	.000	.000	.000	.000
1.9	.013	.013	.013	.013	.013	.010	.003	.000	.000	.000	.000
1.8	.014	.014	.014	.014	.014	.010	.004	.000	.000	.000	.000
1.7	.016	.016	.016	.016	.016	.010	.006	.000	.000	.000	.000
1.6	.017	.017	.017	.017	.017	.010	.007	.000	.000	.000	.000
1.5	.019	.019	.019	.019	.019	.010	.009	.000	.000	.000	.000
1.4	.020	.020	.020	.020	.020	.010	.010	.000	.000	.000	.000
1.3	.025	.025	.025	.025	.025	.017	.015	.005	.000	.000	.000
1.2	.030	.030	.030	.030	.030	.025	.020	.010	.000	.000	.000
1.1	.035	.035	.035	.035	.035	.032	.025	.015	.000	.000	.000
1.0	.040	.040	.040	.040	.040	.040	.030	.020	.000	.000	.000
0.9	.319	.169	.065	.050	.045	.045	.035	.020	.000	.000	.000
0.8	.597	.299	.090	.060	.050	.050	.040	.020	.000	.000	.000
0.7	.772	.647	.543	.498	.418	.124	.050	.025	.010	.000	.000
0.6	.946	.996	.996	.936	.787	.199	.060	.030	.020	.000	.000
0.5	.667	.712	.732	.707	.607	.269	.144	.050	.025	.005	.000
0.4	.388	.428	.468	.478	.428	.339	.229	.070	.030	.010	.000
0.3	.264	.294	.329	.354	.344	.309	.244	.124	.045	.015	.005
0.2	.139	.159	.189	.229	.259	.279	.259	.179	.060	.020	.010
0.1	.077	.086	.110	.127	.146	.154	.146	.106	.048	.031	.021
0.0	.015	.012	.031	.025	.033	.030	.033	.032	.037	.043	.033
2.0	.009	.009	.009	.009	.009	.002	.000	.000	.000	.000	.000
1.9	.009	.009	.009	.009	.009	.003	.000	.000	.000	.000	.000
1.8	.009	.009	.009	.009	.009	.004	.000	.000	.000	.000	.000
1.7	.009	.009	.009	.009	.009	.005	.000	.000	.000	.000	.000
1.6	.009	.009	.009	.009	.009	.007	.000	.000	.000	.000	.000
1.5	.009	.009	.009	.009	.009	.008	.000	.000	.000	.000	.000
1.4	.009	.009	.009	.009	.009	.009	.000	.000	.000	.000	.000
1.3	.014	.014	.014	.014	.012	.009	.002	.000	.000	.000	.000
1.2	.019	.019	.019	.019	.014	.009	.005	.000	.000	.000	.000
1.1	.023	.023	.023	.023	.016	.009	.007	.000	.000	.000	.000
1.0	.028	.028	.028	.028	.019	.009	.009	.000	.000	.000	.000
0.9	.275	.201	.047	.028	.019	.014	.009	.005	.005	.000	.000
0.8	.522	.373	.065	.028	.019	.019	.009	.009	.009	.000	.000
0.7	.681	.616	.457	.415	.322	.061	.028	.019	.014	.005	.000
0.6	.840	.858	.849	.802	.625	.103	.047	.028	.019	.009	.000
0.5	.574	.602	.611	.597	.504	.229	.140	.084	.051	.014	.000
0.4	.308	.345	.373	.392	.383	.355	.233	.140	.084	.019	.000
0.3	.201	.229	.257	.275	.285	.280	.210	.126	.070	.014	.000
0.2	.093	.112	.140	.159	.187	.205	.187	.112	.056	.009	.000
0.1	.051	.059	.071	.079	.091	.105	.096	.064	.035	.015	.005
0.0	.008	.006	.002	.000	.000	.004	.006	.017	.014	.020	.011

TABLE A-1(CONTINUED)

WAVELENGTH OF UPPER ARRAY = 2.36 MICRONS

WAVELENGTH OF LOWER ARRAY = 2.54 MICRONS

UNITS = .01220 WATTS/SQCM/MICRON/STERADIAN

HORIZONTAL DISTANCE FROM AXIS OF SYMMETRY - MM

HT	0.0	1.0	2.0	3.0	4.0	5.0	6.0	7.0	8.0	9.0	10.0
2.0	.011	.011	.011	.011	.002	.000	.000	.000	.000	.000	.000
1.9	.011	.011	.011	.011	.003	.000	.000	.000	.000	.000	.000
1.8	.011	.011	.011	.011	.005	.000	.000	.000	.000	.000	.000
1.7	.011	.011	.011	.011	.007	.000	.000	.000	.000	.000	.000
1.6	.011	.011	.011	.011	.008	.000	.000	.000	.000	.000	.000
1.5	.011	.011	.011	.011	.010	.000	.000	.000	.000	.000	.000
1.4	.011	.011	.011	.011	.011	.000	.000	.000	.000	.000	.000
1.3	.014	.014	.014	.014	.014	.000	.000	.000	.000	.000	.000
1.2	.017	.017	.017	.017	.017	.000	.000	.000	.000	.000	.000
1.1	.020	.020	.020	.020	.020	.000	.000	.000	.000	.000	.000
1.0	.023	.023	.023	.023	.023	.000	.000	.000	.000	.000	.000
0.9	.303	.183	.046	.034	.023	.006	.000	.000	.000	.000	.000
0.8	.582	.343	.069	.046	.023	.011	.000	.000	.000	.000	.000
0.7	.742	.639	.497	.434	.297	.034	.006	.000	.000	.000	.000
0.6	.902	.936	.925	.822	.571	.057	.011	.000	.000	.000	.000
0.5	.622	.662	.674	.628	.502	.211	.120	.011	.006	.000	.000
0.4	.343	.388	.422	.434	.434	.365	.228	.023	.011	.000	.000
0.3	.223	.280	.325	.337	.331	.291	.200	.069	.034	.006	.000
0.2	.103	.171	.228	.240	.228	.217	.171	.114	.057	.011	.000
0.1	.064	.093	.118	.123	.118	.113	.093	.069	.038	.011	.000
0.0	.025	.016	.008	.006	.008	.009	.016	.023	.018	.011	.000
2.0	.048	.049	.049	.049	.038	.034	.013	.013	.002	.000	.000
1.9	.049	.053	.053	.053	.041	.034	.015	.015	.003	.000	.000
1.8	.051	.056	.056	.056	.044	.034	.016	.016	.005	.000	.000
1.7	.052	.059	.059	.059	.048	.034	.018	.018	.007	.000	.000
1.6	.054	.062	.062	.062	.051	.034	.020	.020	.008	.000	.000
1.5	.055	.065	.065	.065	.054	.034	.021	.021	.010	.000	.000
1.4	.057	.068	.068	.068	.057	.034	.023	.023	.011	.000	.000
1.3	.080	.091	.091	.088	.077	.057	.043	.037	.014	.000	.000
1.2	.103	.114	.114	.108	.097	.080	.063	.051	.017	.000	.000
1.1	.125	.137	.137	.128	.117	.103	.083	.066	.020	.000	.000
1.0	.148	.160	.160	.148	.137	.125	.103	.080	.023	.000	.000
0.9	.411	.388	.222	.205	.188	.165	.137	.108	.034	.011	.000
0.8	.673	.616	.285	.262	.240	.205	.171	.137	.046	.023	.000
0.7	.827	.804	.627	.576	.445	.217	.188	.143	.051	.029	.006
0.6	.981	.992	.970	.890	.650	.228	.205	.148	.057	.034	.011
0.5	.764	.781	.787	.759	.633	.382	.302	.205	.063	.040	.011
0.4	.547	.570	.605	.627	.616	.536	.399	.262	.068	.046	.011
0.3	.445	.485	.530	.553	.553	.508	.416	.319	.148	.114	.051
0.2	.342	.399	.456	.479	.490	.479	.433	.376	.228	.182	.091
0.1	.226	.263	.307	.324	.328	.330	.310	.279	.209	.176	.124
0.0	.109	.127	.158	.168	.166	.181	.187	.182	.189	.170	.156

TABLE A-1(CONTINUED)

WAVELENGTH OF UPPER ARRAY = 2.64 MICRONS

WAVELENGTH OF LOWER ARRAY = 2.74 MICRONS

UNITS = .01270 WATTS/SQCM/MICRON/STERADIAN

HORIZONTAL DISTANCE FROM AXIS OF SYMMETRY - MM

HT	0.0	1.0	2.0	3.0	4.0	5.0	6.0	7.0	8.0	9.0	10.0
2.0	.033	.033	.033	.033	.031	.028	.016	.002	.000	.000	.000
1.9	.037	.037	.037	.037	.033	.028	.018	.004	.000	.000	.000
1.8	.041	.041	.041	.041	.034	.028	.020	.006	.000	.000	.000
1.7	.045	.045	.045	.045	.036	.028	.022	.008	.000	.000	.000
1.6	.049	.049	.049	.049	.038	.028	.024	.010	.000	.000	.000
1.5	.053	.053	.053	.053	.040	.028	.026	.012	.000	.000	.000
1.4	.056	.056	.056	.056	.042	.028	.028	.014	.000	.000	.000
1.3	.067	.067	.067	.067	.053	.039	.035	.021	.007	.000	.000
1.2	.078	.078	.078	.078	.063	.049	.042	.028	.014	.000	.000
1.1	.088	.088	.088	.088	.074	.060	.049	.035	.021	.000	.000
1.0	.099	.099	.099	.099	.085	.071	.056	.042	.028	.000	.000
0.9	.289	.261	.134	.120	.113	.106	.092	.049	.035	.014	.000
0.8	.480	.423	.169	.141	.141	.141	.127	.056	.042	.028	.000
0.7	.606	.578	.451	.423	.367	.176	.134	.063	.042	.028	.000
0.6	.733	.733	.733	.705	.592	.212	.141	.071	.042	.028	.000
0.5	.571	.585	.592	.585	.529	.331	.282	.212	.092	.035	.000
0.4	.409	.437	.451	.465	.465	.451	.423	.353	.141	.042	.000
0.3	.310	.346	.367	.388	.402	.395	.388	.317	.155	.035	.000
0.2	.212	.254	.282	.310	.339	.339	.353	.282	.169	.028	.000
0.1	.139	.166	.186	.214	.234	.242	.256	.234	.185	.108	.056
0.0	.067	.078	.090	.118	.130	.146	.160	.186	.201	.188	.112
2.0	.084	.084	.084	.082	.077	.060	.019	.005	.002	.000	.000
1.9	.094	.094	.094	.090	.081	.062	.023	.009	.004	.000	.000
1.8	.104	.104	.104	.098	.085	.064	.027	.013	.006	.000	.000
1.7	.114	.114	.114	.106	.089	.066	.031	.017	.008	.000	.000
1.6	.124	.124	.124	.114	.093	.068	.035	.021	.010	.000	.000
1.5	.134	.134	.134	.122	.097	.070	.039	.025	.012	.000	.000
1.4	.144	.144	.144	.130	.101	.072	.043	.029	.014	.000	.000
1.3	.184	.184	.184	.173	.152	.123	.090	.058	.022	.007	.004
1.2	.224	.224	.224	.217	.202	.173	.137	.087	.029	.014	.007
1.1	.264	.264	.264	.260	.253	.224	.184	.116	.036	.022	.011
1.0	.303	.303	.303	.303	.303	.275	.231	.144	.043	.029	.014
0.9	.520	.520	.368	.354	.325	.289	.246	.159	.058	.043	.022
0.8	.737	.737	.433	.405	.347	.303	.260	.173	.072	.058	.029
0.7	.852	.867	.708	.665	.549	.332	.231	.195	.094	.072	.036
0.6	.968	.997	.983	.925	.751	.361	.202	.217	.116	.087	.043
0.5	.838	.867	.867	.831	.730	.506	.390	.253	.130	.101	.051
0.4	.708	.737	.751	.737	.708	.650	.578	.289	.144	.116	.058
0.3	.592	.636	.657	.672	.672	.643	.592	.426	.253	.188	.116
0.2	.477	.535	.564	.607	.636	.636	.607	.564	.361	.260	.173
0.1	.329	.370	.391	.418	.439	.439	.434	.408	.304	.235	.157
0.0	.181	.206	.219	.229	.242	.242	.262	.252	.246	.211	.141

TABLE A-1(CONTINUED)

WAVELENGTH OF UPPER ARRAY = 2.78 MICRONS

WAVELENGTH OF LOWER ARRAY = 2.88 MICRONS

UNITS = .01180 WATTS/SQCM/MICRON/STERADIAN

HORIZONTAL DISTANCE FROM AXIS OF SYMMETRY - MM

HT	0.0	1.0	2.0	3.0	4.0	5.0	6.0	7.0	8.0	9.0	10.0
2.0	.086	.086	.071	.069	.051	.034	.002	.000	.000	.000	.000
1.9	.096	.096	.081	.077	.058	.038	.004	.000	.000	.000	.000
1.8	.106	.106	.091	.085	.064	.042	.007	.000	.000	.000	.000
1.7	.116	.116	.102	.093	.070	.047	.009	.000	.000	.000	.000
1.6	.126	.126	.112	.101	.076	.051	.011	.000	.000	.000	.000
1.5	.137	.137	.122	.109	.082	.055	.013	.000	.000	.000	.000
1.4	.147	.147	.132	.117	.088	.059	.015	.000	.000	.000	.000
1.3	.184	.184	.173	.162	.140	.110	.066	.040	.015	.011	.004
1.2	.220	.220	.213	.206	.191	.162	.117	.081	.029	.022	.007
1.1	.257	.257	.253	.250	.242	.213	.169	.121	.044	.033	.011
1.0	.294	.294	.294	.294	.294	.264	.220	.162	.059	.044	.015
0.9	.514	.448	.360	.352	.338	.308	.242	.176	.073	.051	.015
0.8	.734	.602	.426	.411	.382	.352	.264	.191	.088	.059	.015
0.7	.852	.800	.698	.646	.551	.360	.279	.206	.103	.059	.022
0.6	.969	.999	.969	.881	.720	.367	.294	.220	.117	.059	.029
0.5	.837	.866	.852	.800	.712	.514	.441	.330	.110	.066	.037
0.4	.705	.734	.734	.720	.705	.661	.587	.441	.103	.073	.044
0.3	.595	.624	.646	.654	.661	.646	.602	.507	.235	.169	.110
0.2	.485	.514	.558	.587	.617	.631	.617	.573	.367	.264	.176
0.1	.334	.364	.391	.412	.425	.440	.442	.414	.309	.239	.160
0.0	.184	.214	.224	.237	.233	.248	.266	.256	.250	.214	.143
2.0	.071	.071	.068	.066	.062	.057	.046	.024	.002	.000	.000
1.9	.085	.085	.078	.075	.068	.058	.047	.025	.003	.000	.000
1.8	.099	.099	.089	.084	.074	.060	.049	.027	.005	.000	.000
1.7	.113	.113	.100	.093	.080	.061	.050	.028	.006	.000	.000
1.6	.126	.126	.110	.102	.087	.063	.052	.030	.008	.000	.000
1.5	.140	.140	.121	.112	.093	.064	.053	.031	.009	.000	.000
1.4	.154	.154	.132	.121	.099	.066	.055	.033	.011	.000	.000
1.3	.187	.187	.170	.162	.143	.110	.093	.060	.019	.003	.000
1.2	.220	.220	.209	.203	.187	.154	.132	.088	.027	.005	.000
1.1	.252	.252	.247	.244	.231	.198	.170	.115	.036	.008	.000
1.0	.285	.285	.285	.285	.274	.241	.209	.143	.044	.011	.000
0.9	.494	.439	.351	.346	.329	.291	.247	.176	.077	.038	.011
0.8	.702	.593	.417	.406	.384	.340	.285	.209	.110	.066	.022
0.7	.823	.774	.681	.653	.576	.362	.307	.241	.137	.071	.033
0.6	.944	.955	.944	.900	.768	.384	.329	.274	.165	.077	.044
0.5	.807	.823	.834	.818	.746	.527	.461	.357	.192	.093	.055
0.4	.670	.692	.724	.735	.724	.670	.593	.439	.220	.110	.066
0.3	.576	.604	.631	.653	.659	.637	.593	.505	.302	.165	.115
0.2	.483	.516	.538	.571	.593	.604	.593	.571	.384	.220	.165
0.1	.327	.354	.376	.402	.418	.429	.431	.409	.309	.207	.152
0.0	.171	.192	.214	.234	.243	.254	.268	.246	.234	.195	.140

TABLE A-1(CONTINUED)

WAVELENGTH OF UPPER ARRAY = 2.94 MICRONS

WAVELENGTH OF LOWER ARRAY = 3.15 MICRONS

UNITS = .01000 WATTS/SQCM/MICRON/STERADIAN

HORIZONTAL DISTANCE FROM AXIS OF SYMMETRY - MM

HT	0.0	1.0	2.0	3.0	4.0	5.0	6.0	7.0	8.0	9.0	10.0
2.0	.078	.076	.076	.073	.069	.065	.037	.002	.000	.000	.000
1.9	.088	.085	.085	.081	.073	.065	.035	.004	.000	.000	.000
1.8	.099	.094	.094	.088	.076	.065	.033	.006	.000	.000	.000
1.7	.110	.102	.102	.095	.080	.065	.031	.008	.000	.000	.000
1.6	.121	.111	.111	.102	.083	.065	.029	.009	.000	.000	.000
1.5	.132	.120	.120	.109	.087	.065	.028	.011	.000	.000	.000
1.4	.142	.129	.129	.117	.091	.065	.026	.013	.000	.000	.000
1.3	.172	.162	.162	.152	.126	.100	.061	.039	.006	.000	.000
1.2	.201	.194	.194	.188	.162	.136	.097	.065	.013	.000	.000
1.1	.230	.227	.227	.223	.197	.172	.133	.091	.019	.000	.000
1.0	.259	.259	.259	.259	.233	.207	.168	.117	.026	.000	.000
0.9	.492	.479	.324	.311	.285	.246	.201	.142	.071	.019	.000
0.8	.725	.699	.388	.363	.337	.285	.233	.168	.117	.039	.000
0.7	.842	.848	.693	.660	.602	.304	.246	.181	.123	.052	.013
0.6	.958	.997	.997	.958	.867	.324	.259	.194	.129	.065	.026
0.5	.803	.842	.855	.835	.770	.479	.408	.291	.142	.091	.052
0.4	.647	.686	.712	.712	.673	.634	.557	.388	.155	.117	.078
0.3	.550	.589	.621	.634	.628	.615	.570	.473	.272	.188	.117
0.2	.453	.492	.531	.557	.583	.596	.583	.557	.388	.259	.155
0.1	.313	.338	.369	.388	.406	.426	.428	.410	.315	.222	.141
0.0	.174	.183	.207	.218	.230	.257	.274	.262	.241	.185	.126
2.0	.013	.013	.013	.013	.013	.013	.013	.000	.000	.000	.000
1.9	.013	.013	.013	.013	.013	.013	.013	.000	.000	.000	.000
1.8	.013	.013	.013	.013	.013	.013	.013	.000	.000	.000	.000
1.7	.013	.013	.013	.013	.013	.013	.013	.000	.000	.000	.000
1.6	.013	.013	.013	.013	.013	.013	.013	.000	.000	.000	.000
1.5	.013	.013	.013	.013	.013	.013	.013	.000	.000	.000	.000
1.4	.013	.013	.013	.013	.013	.013	.013	.000	.000	.000	.000
1.3	.023	.023	.023	.023	.023	.023	.020	.003	.000	.000	.000
1.2	.033	.033	.033	.033	.033	.033	.026	.007	.000	.000	.000
1.1	.042	.042	.042	.042	.042	.042	.033	.010	.000	.000	.000
1.0	.052	.052	.052	.052	.052	.052	.039	.013	.000	.000	.000
0.9	.182	.156	.078	.072	.065	.059	.052	.026	.007	.000	.000
0.8	.313	.261	.104	.091	.078	.065	.065	.039	.013	.000	.000
0.7	.430	.410	.326	.306	.267	.085	.072	.052	.026	.007	.000
0.6	.547	.560	.547	.521	.456	.104	.078	.065	.039	.013	.000
0.5	.443	.456	.450	.436	.397	.215	.182	.124	.072	.013	.000
0.4	.339	.352	.352	.352	.339	.326	.287	.182	.104	.013	.000
0.3	.358	.365	.358	.345	.326	.306	.261	.182	.104	.020	.000
0.2	.378	.378	.365	.339	.313	.287	.235	.182	.104	.026	.000
0.1	.319	.326	.335	.331	.320	.316	.294	.256	.178	.100	.022
0.0	.259	.274	.306	.324	.328	.346	.353	.330	.252	.174	.044

TABLE A-1(CONTINUED)

WAVELENGTH OF UPPER ARRAY = 3.25 MICRONS
WAVELENGTH OF LOWER ARRAY = 3.31 MICRONS
UNITS = .00630 WATTS/SQCM/MICRON/STERADIAN
HORIZONTAL DISTANCE FROM AXIS OF SYMMETRY - MM

HT	0.0	1.0	2.0	3.0	4.0	5.0	6.0	7.0	8.0	9.0	10.0
2.0	.042	.042	.042	.042	.021	.000	.000	.000	.000	.000	.000
1.9	.042	.042	.042	.042	.021	.000	.000	.000	.000	.000	.000
1.8	.042	.042	.042	.042	.021	.000	.000	.000	.000	.000	.000
1.7	.042	.042	.042	.042	.021	.000	.000	.000	.000	.000	.000
1.6	.042	.042	.042	.042	.021	.000	.000	.000	.000	.000	.000
1.5	.042	.042	.042	.042	.021	.000	.000	.000	.000	.000	.000
1.4	.042	.042	.042	.042	.021	.000	.000	.000	.000	.000	.000
1.3	.042	.042	.042	.042	.026	.005	.005	.000	.000	.000	.000
1.2	.042	.042	.042	.042	.031	.010	.010	.000	.000	.000	.000
1.1	.042	.042	.042	.042	.036	.016	.016	.000	.000	.000	.000
1.0	.042	.042	.042	.042	.042	.021	.021	.000	.000	.000	.000
0.9	.260	.208	.083	.062	.052	.042	.031	.010	.000	.000	.000
0.8	.479	.375	.125	.083	.062	.062	.042	.021	.000	.000	.000
0.7	.604	.552	.427	.385	.323	.083	.042	.021	.000	.000	.000
0.6	.729	.729	.729	.687	.583	.104	.042	.021	.000	.000	.000
0.5	.583	.583	.583	.541	.448	.156	.052	.031	.000	.000	.000
0.4	.437	.437	.437	.396	.312	.208	.062	.042	.000	.000	.000
0.3	.448	.448	.437	.396	.333	.260	.156	.125	.042	.010	.000
0.2	.458	.458	.437	.396	.354	.312	.250	.208	.083	.021	.000
0.1	.434	.446	.449	.443	.425	.407	.380	.338	.225	.127	.024
0.0	.411	.434	.461	.490	.496	.502	.510	.468	.367	.234	.047
2.0	.021	.021	.021	.021	.021	.003	.000	.000	.000	.000	.000
1.9	.021	.021	.021	.021	.021	.006	.000	.000	.000	.000	.000
1.8	.021	.021	.021	.021	.021	.009	.000	.000	.000	.000	.000
1.7	.021	.021	.021	.021	.021	.012	.000	.000	.000	.000	.000
1.6	.021	.021	.021	.021	.021	.015	.000	.000	.000	.000	.000
1.5	.021	.021	.021	.021	.021	.018	.000	.000	.000	.000	.000
1.4	.021	.021	.021	.021	.021	.021	.000	.000	.000	.000	.000
1.3	.026	.026	.026	.026	.026	.026	.005	.000	.000	.000	.000
1.2	.031	.031	.031	.031	.031	.031	.010	.000	.000	.000	.000
1.1	.037	.037	.037	.037	.037	.037	.016	.000	.000	.000	.000
1.0	.042	.042	.042	.042	.042	.042	.021	.000	.000	.000	.000
0.9	.230	.188	.063	.052	.052	.052	.042	.010	.000	.000	.000
0.8	.419	.335	.084	.063	.063	.063	.063	.021	.000	.000	.000
0.7	.534	.502	.377	.335	.241	.136	.073	.031	.000	.000	.000
0.6	.649	.670	.670	.607	.419	.209	.084	.042	.000	.000	.000
0.5	.544	.555	.555	.523	.419	.293	.178	.073	.031	.000	.000
0.4	.439	.439	.439	.439	.419	.377	.272	.105	.063	.000	.000
0.3	.565	.555	.513	.481	.408	.335	.241	.115	.052	.000	.000
0.2	.691	.670	.586	.523	.398	.293	.209	.126	.042	.000	.000
0.1	.750	.765	.740	.725	.671	.638	.602	.554	.470	.380	.024
0.0	.809	.860	.895	.927	.944	.983	.994	.982	.898	.761	.048

TABLE A-1(CONTINUED)

WAVELENGTH OF UPPER ARRAY = 3.36 MICRONS

WAVELENGTH OF LOWER ARRAY = 3.57 MICRONS

UNITS = .00550 WATTS/SQCM/MICRON/STERADIAN

HORIZONTAL DISTANCE FROM AXIS OF SYMMETRY - MM

HT	0.0	1.0	2.0	3.0	4.0	5.0	6.0	7.0	8.0	9.0	10.0
2.0	.024	.024	.024	.024	.024	.004	.000	.000	.000	.000	.000
1.9	.024	.024	.024	.024	.024	.007	.000	.000	.000	.000	.000
1.8	.024	.024	.024	.024	.024	.011	.000	.000	.000	.000	.000
1.7	.024	.024	.024	.024	.024	.014	.000	.000	.000	.000	.000
1.6	.024	.024	.024	.024	.024	.017	.000	.000	.000	.000	.000
1.5	.024	.024	.024	.024	.024	.021	.000	.000	.000	.000	.000
1.4	.024	.024	.024	.024	.024	.024	.000	.000	.000	.000	.000
1.3	.030	.030	.030	.030	.030	.024	.000	.000	.000	.000	.000
1.2	.036	.036	.036	.036	.036	.024	.000	.000	.000	.000	.000
1.1	.042	.042	.042	.042	.042	.024	.000	.000	.000	.000	.000
1.0	.048	.048	.048	.048	.048	.024	.000	.000	.000	.000	.000
0.9	.265	.253	.060	.060	.048	.036	.012	.000	.000	.000	.000
0.8	.481	.457	.072	.072	.048	.048	.024	.000	.000	.000	.000
0.7	.601	.601	.409	.373	.325	.144	.072	.024	.000	.000	.000
0.6	.722	.746	.746	.674	.601	.241	.120	.048	.000	.000	.000
0.5	.565	.577	.577	.553	.505	.289	.168	.060	.012	.000	.000
0.4	.409	.409	.409	.433	.409	.337	.217	.072	.024	.000	.000
0.3	.529	.505	.469	.433	.385	.325	.241	.120	.072	.024	.000
0.2	.650	.601	.529	.433	.361	.313	.265	.168	.120	.048	.000
0.1	.759	.752	.721	.679	.662	.641	.620	.578	.530	.417	.027
0.0	.868	.902	.912	.925	.962	.969	.975	.989	.940	.786	.055
2.0	.025	.025	.025	.025	.004	.000	.000	.000	.000	.000	.000
1.9	.025	.025	.025	.025	.008	.000	.000	.000	.000	.000	.000
1.8	.025	.025	.025	.025	.011	.000	.000	.000	.000	.000	.000
1.7	.025	.025	.025	.025	.014	.000	.000	.000	.000	.000	.000
1.6	.025	.025	.025	.025	.018	.000	.000	.000	.000	.000	.000
1.5	.025	.025	.025	.025	.021	.000	.000	.000	.000	.000	.000
1.4	.025	.025	.025	.025	.025	.000	.000	.000	.000	.000	.000
1.3	.025	.025	.025	.025	.025	.006	.000	.000	.000	.000	.000
1.2	.025	.025	.025	.025	.025	.012	.000	.000	.000	.000	.000
1.1	.025	.025	.025	.025	.025	.018	.000	.000	.000	.000	.000
1.0	.025	.025	.025	.025	.025	.025	.000	.000	.000	.000	.000
0.9	.197	.197	.049	.037	.025	.025	.012	.000	.000	.000	.000
0.8	.369	.369	.074	.049	.025	.025	.025	.000	.000	.000	.000
0.7	.467	.479	.332	.307	.246	.049	.025	.000	.000	.000	.000
0.6	.565	.590	.590	.565	.467	.074	.025	.000	.000	.000	.000
0.5	.430	.455	.455	.442	.369	.160	.098	.025	.000	.000	.000
0.4	.295	.320	.320	.320	.270	.246	.172	.049	.000	.000	.000
0.3	.270	.307	.320	.307	.258	.209	.160	.074	.012	.000	.000
0.2	.246	.295	.320	.295	.246	.172	.147	.098	.025	.000	.000
0.1	.260	.281	.292	.281	.260	.228	.217	.196	.150	.112	.014
0.0	.274	.267	.264	.267	.274	.284	.287	.294	.276	.223	.028

TABLE A-1(CONTINUED)

WAVELENGTH OF UPPER ARRAY = 3.78 MICRONS
WAVELENGTH OF LOWER ARRAY = 3.99 MICRONS
UNITS = .00270 WATTS/SQCM/MICRON/STERADIAN
HORIZONTAL DISTANCE FROM AXIS OF SYMMETRY - MM

HT	0.0	1.0	2.0	3.0	4.0	5.0	6.0	7.0	8.0	9.0	10.0
2.0	.051	.051	.051	.051	.051	.051	.000	.000	.000	.000	.000
1.9	.051	.051	.051	.051	.051	.051	.000	.000	.000	.000	.000
1.8	.051	.051	.051	.051	.051	.051	.000	.000	.000	.000	.000
1.7	.051	.051	.051	.051	.051	.051	.000	.000	.000	.000	.000
1.6	.051	.051	.051	.051	.051	.051	.000	.000	.000	.000	.000
1.5	.051	.051	.051	.051	.051	.051	.000	.000	.000	.000	.000
1.4	.051	.051	.051	.051	.051	.051	.000	.000	.000	.000	.000
1.3	.090	.128	.154	.154	.141	.116	.039	.000	.000	.000	.000
1.2	.128	.205	.257	.257	.231	.180	.077	.000	.000	.000	.000
1.1	.167	.282	.360	.360	.321	.244	.116	.000	.000	.000	.000
1.0	.205	.360	.462	.462	.411	.308	.154	.000	.000	.000	.000
0.9	.437	.514	.282	.257	.231	.180	.103	.026	.000	.000	.000
0.8	.668	.668	.103	.051	.051	.051	.051	.051	.000	.000	.000
0.7	.822	.822	.539	.462	.360	.154	.051	.051	.000	.000	.000
0.6	.976	.976	.976	.873	.668	.257	.051	.051	.000	.000	.000
0.5	.950	.899	.847	.719	.539	.282	.103	.077	.026	.000	.000
0.4	.925	.822	.719	.565	.411	.308	.154	.103	.051	.000	.000
0.3	.565	.591	.591	.514	.411	.308	.180	.128	.077	.026	.000
0.2	.205	.360	.462	.462	.411	.308	.205	.154	.103	.051	.000
0.1	.147	.243	.287	.287	.265	.221	.176	.154	.132	.081	.029
0.0	.089	.126	.112	.112	.119	.133	.147	.154	.161	.110	.058
2.0	.053	.053	.053	.053	.053	.009	.000	.000	.000	.000	.000
1.9	.053	.053	.053	.053	.053	.016	.000	.000	.000	.000	.000
1.8	.053	.053	.053	.053	.053	.023	.000	.000	.000	.000	.000
1.7	.053	.053	.053	.053	.053	.031	.000	.000	.000	.000	.000
1.6	.053	.053	.053	.053	.053	.038	.000	.000	.000	.000	.000
1.5	.053	.053	.053	.053	.053	.045	.000	.000	.000	.000	.000
1.4	.053	.053	.053	.053	.053	.053	.000	.000	.000	.000	.000
1.3	.066	.053	.053	.053	.053	.053	.000	.000	.000	.000	.000
1.2	.079	.053	.053	.053	.053	.053	.000	.000	.000	.000	.000
1.1	.092	.053	.053	.053	.053	.053	.000	.000	.000	.000	.000
1.0	.106	.053	.053	.053	.053	.053	.000	.000	.000	.000	.000
0.9	.343	.290	.079	.079	.079	.079	.026	.000	.000	.000	.000
0.8	.581	.528	.106	.106	.106	.106	.053	.000	.000	.000	.000
0.7	.713	.686	.475	.449	.290	.158	.079	.000	.000	.000	.000
0.6	.845	.845	.845	.792	.475	.211	.106	.000	.000	.000	.000
0.5	.607	.634	.634	.607	.449	.290	.158	.026	.000	.000	.000
0.4	.370	.422	.422	.422	.422	.370	.211	.053	.000	.000	.000
0.3	.264	.317	.343	.343	.343	.290	.185	.079	.026	.000	.000
0.2	.158	.211	.264	.264	.264	.211	.158	.106	.053	.000	.000
0.1	.098	.121	.144	.144	.174	.151	.128	.106	.083	.030	.000
0.0	.038	.031	.024	.024	.084	.091	.098	.106	.113	.060	.000

TABLE A-1(CONTINUED)

WAVELENGTH OF UPPER ARRAY = 4.19 MICRONS
WAVELENGTH OF LOWER ARRAY = 4.23 MICRONS
UNITS = .00730 WATTS/SQCM/MICRON/STERADIAN
HORIZONTAL DISTANCE FROM AXIS OF SYMMETRY - MM

HT	0.0	1.0	2.0	3.0	4.0	5.0	6.0	7.0	8.0	9.0	10.0
2.0	.030	.030	.030	.027	.027	.027	.020	.003	.000	.000	.000
1.9	.039	.039	.039	.032	.032	.032	.020	.006	.000	.000	.000
1.8	.047	.047	.047	.038	.038	.038	.020	.009	.000	.000	.000
1.7	.055	.055	.055	.044	.044	.044	.020	.012	.000	.000	.000
1.6	.064	.064	.064	.049	.049	.049	.020	.015	.000	.000	.000
1.5	.072	.072	.072	.055	.055	.055	.020	.017	.000	.000	.000
1.4	.080	.080	.080	.060	.060	.060	.020	.020	.000	.000	.000
1.3	.095	.095	.095	.080	.080	.080	.050	.045	.025	.010	.000
1.2	.111	.111	.111	.100	.100	.100	.080	.070	.050	.020	.000
1.1	.126	.126	.126	.121	.121	.121	.111	.095	.075	.030	.000
1.0	.141	.141	.141	.141	.141	.141	.141	.121	.100	.040	.000
0.9	.251	.241	.241	.231	.221	.201	.181	.151	.121	.050	.000
0.8	.362	.342	.342	.321	.301	.261	.221	.181	.141	.060	.000
0.7	.462	.432	.412	.372	.321	.281	.231	.191	.131	.050	.000
0.6	.563	.522	.482	.422	.342	.301	.241	.201	.121	.040	.000
0.5	.472	.472	.462	.432	.392	.352	.291	.231	.111	.040	.000
0.4	.382	.422	.442	.442	.442	.402	.342	.261	.100	.040	.000
0.3	.301	.321	.342	.352	.372	.362	.332	.281	.161	.050	.020
0.2	.221	.221	.241	.261	.301	.321	.321	.301	.221	.060	.040
0.1	.130	.130	.150	.170	.187	.207	.207	.187	.153	.083	.063
0.0	.038	.038	.058	.079	.073	.093	.093	.073	.084	.106	.086
2.0	.263	.263	.245	.226	.199	.132	.079	.030	.004	.000	.000
1.9	.276	.276	.260	.245	.215	.147	.088	.036	.007	.000	.000
1.8	.289	.289	.276	.263	.231	.163	.098	.043	.010	.000	.000
1.7	.301	.301	.292	.282	.246	.179	.107	.049	.013	.000	.000
1.6	.314	.314	.307	.301	.262	.194	.117	.055	.016	.000	.000
1.5	.326	.326	.323	.320	.278	.210	.126	.061	.019	.000	.000
1.4	.339	.339	.339	.339	.294	.226	.135	.068	.023	.000	.000
1.3	.423	.423	.412	.406	.361	.294	.215	.141	.085	.034	.011
1.2	.508	.508	.485	.474	.429	.361	.294	.215	.147	.068	.023
1.1	.593	.593	.559	.542	.497	.429	.373	.288	.209	.102	.034
1.0	.677	.677	.632	.610	.564	.497	.452	.361	.271	.135	.045
0.9	.824	.824	.790	.756	.711	.632	.553	.452	.339	.124	.045
0.8	.971	.971	.948	.903	.858	.768	.655	.542	.406	.113	.045
0.7	.982	.982	.971	.937	.881	.711	.655	.553	.429	.124	.056
0.6	.993	.993	.993	.971	.903	.655	.655	.564	.452	.135	.068
0.5	.869	.881	.881	.881	.847	.723	.723	.666	.531	.260	.102
0.4	.745	.768	.768	.790	.790	.790	.790	.768	.610	.384	.135
0.3	.745	.768	.768	.790	.790	.790	.790	.768	.610	.429	.203
0.2	.745	.768	.768	.790	.790	.790	.790	.768	.610	.474	.271
0.1	.553	.575	.601	.623	.636	.662	.675	.652	.558	.449	.258
0.0	.360	.383	.434	.457	.482	.534	.559	.537	.507	.423	.245

TABLE A-1(CONTINUED)

WAVELENGTH OF UPPER ARRAY = 4.27 MICRONS
WAVELENGTH OF LOWER ARRAY = 4.39 MICRONS
UNITS = .05400 WATTS/SQCM/MICRON/STERADIAN
HORIZONTAL DISTANCE FROM AXIS OF SYMMETRY - MM

HT	0.0	1.0	2.0	3.0	4.0	5.0	6.0	7.0	8.0	9.0	10.0
2.0	.059	.058	.057	.050	.043	.035	.021	.006	.000	.000	.000
1.9	.068	.067	.065	.057	.049	.039	.024	.006	.000	.000	.000
1.8	.078	.075	.072	.064	.055	.044	.026	.006	.000	.000	.000
1.7	.087	.083	.080	.070	.061	.048	.029	.006	.000	.000	.000
1.6	.096	.092	.087	.077	.067	.052	.031	.006	.000	.000	.000
1.5	.105	.100	.095	.084	.072	.056	.034	.006	.000	.000	.000
1.4	.114	.108	.102	.090	.078	.060	.036	.006	.000	.000	.000
1.3	.124	.119	.114	.104	.092	.074	.051	.023	.011	.002	.000
1.2	.133	.130	.127	.117	.105	.087	.066	.039	.021	.003	.000
1.1	.142	.140	.139	.131	.119	.101	.081	.056	.032	.005	.000
1.0	.151	.151	.151	.145	.133	.114	.096	.072	.042	.006	.000
0.9	.172	.169	.166	.160	.148	.133	.114	.090	.057	.018	.003
0.8	.193	.187	.181	.175	.163	.151	.133	.108	.072	.030	.006
0.7	.190	.187	.181	.175	.163	.148	.130	.105	.072	.036	.009
0.6	.187	.187	.181	.175	.163	.145	.127	.102	.072	.042	.012
0.5	.157	.166	.172	.175	.169	.157	.142	.117	.081	.036	.012
0.4	.127	.145	.163	.175	.175	.169	.157	.133	.090	.030	.012
0.3	.148	.163	.172	.181	.181	.175	.169	.151	.108	.045	.027
0.2	.169	.181	.181	.187	.187	.181	.181	.169	.127	.060	.042
0.1	.128	.140	.147	.156	.163	.164	.167	.158	.133	.091	.056
0.0	.087	.099	.112	.125	.139	.147	.153	.148	.140	.122	.070
2.0	.198	.188	.183	.166	.148	.106	.062	.026	.003	.000	.000
1.9	.224	.212	.203	.182	.161	.117	.069	.032	.006	.000	.000
1.8	.251	.235	.224	.199	.174	.128	.077	.038	.009	.000	.000
1.7	.278	.259	.244	.215	.187	.139	.084	.043	.012	.000	.000
1.6	.304	.283	.264	.232	.199	.150	.091	.049	.014	.000	.000
1.5	.331	.307	.284	.248	.212	.161	.099	.054	.017	.000	.000
1.4	.358	.331	.305	.265	.225	.172	.106	.060	.020	.000	.000
1.3	.411	.394	.377	.351	.321	.276	.212	.151	.061	.007	.000
1.2	.464	.457	.450	.437	.417	.381	.318	.242	.103	.013	.000
1.1	.517	.520	.523	.523	.513	.485	.424	.333	.144	.020	.000
1.0	.569	.583	.596	.609	.609	.589	.530	.424	.185	.026	.000
0.9	.771	.738	.699	.669	.642	.599	.526	.424	.278	.106	.026
0.8	.973	.894	.801	.728	.675	.609	.523	.424	.371	.185	.053
0.7	.987	.844	.725	.646	.579	.513	.434	.344	.278	.146	.040
0.6	.*00	.795	.649	.563	.483	.417	.344	.265	.185	.106	.026
0.5	.765	.662	.596	.563	.530	.500	.454	.328	.192	.109	.033
0.4	.530	.530	.543	.563	.576	.583	.563	.391	.199	.113	.040
0.3	.629	.646	.669	.692	.705	.718	.718	.639	.510	.384	.189
0.2	.728	.762	.795	.821	.834	.854	.874	.887	.821	.656	.338
0.1	.480	.517	.550	.577	.601	.625	.648	.654	.607	.486	.266
0.0	.232	.272	.306	.332	.368	.395	.423	.421	.392	.317	.195

TABLE A-1(CONTINUED)

WAVELENGTH OF UPPER ARRAY = 4.47 MICRONS

WAVELENGTH OF LOWER ARRAY = 4.59 MICRONS

UNITS = .03520 WATTS/SQCM/MICRON/STERADIAN

HORIZONTAL DISTANCE FROM AXIS OF SYMMETRY - MM

HT	0.0	1.0	2.0	3.0	4.0	5.0	6.0	7.0	8.0	9.0	10.0
2.0	.281	.276	.265	.239	.200	.151	.089	.024	.012	.001	.000
1.9	.314	.309	.293	.261	.215	.160	.088	.026	.013	.002	.000
1.8	.347	.342	.321	.283	.231	.168	.086	.029	.015	.002	.000
1.7	.380	.375	.349	.306	.246	.176	.085	.032	.016	.003	.000
1.6	.413	.408	.377	.328	.262	.185	.083	.035	.017	.004	.000
1.5	.446	.441	.405	.351	.277	.193	.082	.038	.019	.004	.000
1.4	.479	.474	.433	.373	.292	.202	.081	.040	.020	.005	.000
1.3	.586	.575	.533	.473	.394	.302	.187	.127	.079	.029	.006
1.2	.693	.675	.633	.572	.496	.403	.292	.214	.139	.053	.013
1.1	.800	.776	.732	.672	.599	.504	.398	.301	.198	.077	.019
1.0	.907	.877	.832	.771	.701	.605	.504	.388	.257	.101	.025
0.9	.953	.930	.905	.875	.839	.761	.655	.496	.300	.126	.025
0.8	.998	.983	.978	.978	.978	.917	.806	.605	.343	.151	.025
0.7	.963	.975	.980	.978	.968	.907	.791	.615	.398	.202	.023
0.6	.927	.968	.983	.978	.958	.897	.776	.625	.454	.252	.020
0.5	.922	.958	.975	.978	.970	.938	.872	.771	.605	.277	.060
0.4	.917	.948	.968	.978	.983	.978	.968	.917	.756	.302	.101
0.3	.912	.912	.900	.877	.842	.791	.736	.653	.507	.197	.076
0.2	.907	.877	.832	.776	.701	.605	.504	.388	.257	.091	.050
0.1	.632	.648	.657	.659	.646	.622	.596	.551	.460	.320	.171
0.0	.357	.419	.482	.541	.592	.639	.687	.715	.664	.549	.291
2.0	.131	.140	.140	.137	.131	.117	.089	.068	.047	.023	.015
1.9	.188	.203	.209	.205	.200	.185	.149	.114	.079	.039	.028
1.8	.245	.267	.277	.274	.268	.252	.208	.160	.111	.055	.040
1.7	.302	.331	.345	.343	.336	.320	.268	.205	.143	.070	.053
1.6	.359	.395	.413	.412	.404	.387	.327	.251	.175	.086	.065
1.5	.416	.459	.481	.481	.472	.455	.387	.297	.207	.101	.078
1.4	.473	.523	.550	.550	.541	.523	.446	.342	.239	.117	.090
1.3	.455	.487	.499	.488	.470	.444	.374	.282	.188	.091	.069
1.2	.437	.451	.448	.426	.399	.365	.302	.221	.137	.065	.047
1.1	.419	.414	.398	.364	.328	.286	.230	.160	.087	.039	.026
1.0	.401	.378	.347	.302	.257	.207	.158	.099	.036	.014	.005
0.9	.482	.460	.424	.399	.374	.329	.268	.187	.099	.020	.011
0.8	.563	.541	.500	.496	.491	.451	.378	.275	.162	.027	.018
0.7	.518	.532	.525	.523	.516	.487	.412	.311	.198	.072	.054
0.6	.473	.523	.550	.550	.541	.523	.446	.347	.234	.117	.090
0.5	.527	.554	.572	.577	.570	.554	.507	.412	.239	.115	.090
0.4	.581	.586	.595	.604	.599	.586	.568	.478	.243	.113	.090
0.3	.509	.563	.608	.624	.608	.579	.534	.433	.241	.115	.090
0.2	.437	.541	.622	.644	.617	.572	.500	.387	.239	.117	.090
0.1	.319	.361	.386	.386	.361	.332	.288	.234	.170	.117	.103
0.0	.202	.182	.151	.127	.105	.091	.075	.080	.101	.117	.116

TABLE A-1(CONTINUED)

WAVELENGTH OF UPPER ARRAY = 4.77 MICRONS

WAVELENGTH OF LOWER ARRAY = 4.94 MICRONS

UNITS = .00530 WATTS/SQCM/MICRON/STERADIAN

HORIZONTAL DISTANCE FROM AXIS OF SYMMETRY - MM

HT	0.0	1.0	2.0	3.0	4.0	5.0	6.0	7.0	8.0	9.0	10.0
2.0	.075	.075	.070	.065	.040	.005	.000	.000	.000	.000	.000
1.9	.088	.088	.078	.069	.048	.009	.000	.000	.000	.000	.000
1.8	.100	.100	.087	.073	.057	.013	.000	.000	.000	.000	.000
1.7	.113	.113	.095	.078	.065	.018	.000	.000	.000	.000	.000
1.6	.125	.125	.103	.082	.073	.022	.000	.000	.000	.000	.000
1.5	.138	.138	.112	.086	.082	.026	.000	.000	.000	.000	.000
1.4	.150	.150	.120	.090	.090	.030	.000	.000	.000	.000	.000
1.3	.210	.203	.173	.143	.135	.083	.045	.030	.008	.000	.000
1.2	.270	.255	.225	.195	.180	.135	.090	.060	.015	.000	.000
1.1	.330	.308	.278	.248	.225	.188	.135	.090	.023	.000	.000
1.0	.390	.360	.330	.300	.270	.240	.180	.120	.030	.000	.000
0.9	.601	.526	.481	.436	.390	.345	.270	.195	.090	.045	.015
0.8	.811	.691	.631	.571	.511	.451	.360	.270	.150	.090	.030
0.7	.871	.841	.811	.766	.691	.541	.330	.360	.135	.090	.030
0.6	.931	.991	.991	.961	.871	.631	.300	.451	.120	.090	.030
0.5	.841	.886	.901	.886	.841	.706	.526	.526	.180	.135	.045
0.4	.751	.781	.811	.811	.811	.781	.751	.601	.240	.180	.060
0.3	.706	.751	.811	.811	.826	.811	.781	.646	.270	.195	.075
0.2	.661	.721	.811	.811	.841	.841	.811	.691	.300	.210	.090
0.1	.456	.499	.572	.589	.619	.636	.623	.571	.369	.279	.124
0.0	.251	.277	.333	.367	.397	.431	.436	.452	.437	.347	.158
2.0	.031	.031	.031	.031	.005	.000	.000	.000	.000	.000	.000
1.9	.031	.031	.031	.031	.009	.000	.000	.000	.000	.000	.000
1.8	.031	.031	.031	.031	.014	.000	.000	.000	.000	.000	.000
1.7	.031	.031	.031	.031	.018	.000	.000	.000	.000	.000	.000
1.6	.031	.031	.031	.031	.022	.000	.000	.000	.000	.000	.000
1.5	.031	.031	.031	.031	.026	.000	.000	.000	.000	.000	.000
1.4	.031	.031	.031	.031	.031	.000	.000	.000	.000	.000	.000
1.3	.054	.054	.054	.054	.038	.000	.000	.000	.000	.000	.000
1.2	.077	.077	.077	.077	.046	.000	.000	.000	.000	.000	.000
1.1	.100	.100	.100	.100	.054	.000	.000	.000	.000	.000	.000
1.0	.123	.123	.123	.123	.062	.000	.000	.000	.000	.000	.000
0.9	.200	.169	.138	.138	.092	.046	.015	.000	.000	.000	.000
0.8	.277	.215	.154	.154	.123	.092	.031	.000	.000	.000	.000
0.7	.354	.338	.292	.277	.200	.138	.046	.015	.000	.000	.000
0.6	.431	.462	.431	.400	.277	.185	.062	.031	.000	.000	.000
0.5	.400	.415	.400	.385	.308	.246	.154	.077	.015	.000	.000
0.4	.369	.369	.369	.369	.338	.308	.246	.123	.031	.000	.000
0.3	.323	.338	.338	.354	.354	.338	.292	.200	.092	.046	.000
0.2	.277	.308	.308	.338	.369	.369	.338	.277	.154	.092	.000
0.1	.207	.238	.255	.269	.282	.282	.269	.242	.171	.127	.052
0.0	.137	.168	.203	.199	.194	.194	.199	.207	.189	.162	.105

TABLE A-1(CONTINUED)

WAVELENGTH OF UPPER ARRAY = 5.10 MICRONS
WAVELENGTH OF LOWER ARRAY = 5.25 MICRONS
UNITS = .00170 WATTS/SQCM/MICRON/STERADIAN
HORIZONTAL DISTANCE FROM AXIS OF SYMMETRY - MM

HT	0.0	1.0	2.0	3.0	4.0	5.0	6.0	7.0	8.0	9.0	10.0
2.0	.114	.114	.114	.114	.114	.033	.000	.000	.000	.000	.000
1.9	.128	.128	.128	.128	.128	.060	.000	.000	.000	.000	.000
1.8	.142	.142	.142	.142	.142	.087	.000	.000	.000	.000	.000
1.7	.155	.155	.155	.155	.155	.114	.000	.000	.000	.000	.000
1.6	.169	.169	.169	.169	.169	.142	.000	.000	.000	.000	.000
1.5	.182	.182	.182	.182	.182	.169	.000	.000	.000	.000	.000
1.4	.196	.196	.196	.196	.196	.196	.000	.000	.000	.000	.000
1.3	.196	.196	.196	.196	.196	.196	.049	.000	.000	.000	.000
1.2	.196	.196	.196	.196	.196	.196	.098	.000	.000	.000	.000
1.1	.196	.196	.196	.196	.196	.196	.147	.000	.000	.000	.000
1.0	.196	.196	.196	.196	.196	.196	.196	.000	.000	.000	.000
0.9	.392	.343	.245	.196	.196	.196	.196	.000	.000	.000	.000
0.8	.588	.490	.294	.196	.196	.196	.196	.000	.000	.000	.000
0.7	.735	.735	.637	.539	.490	.392	.196	.000	.000	.000	.000
0.6	.882	.981	.981	.882	.784	.588	.196	.000	.000	.000	.000
0.5	.833	.882	.931	.833	.735	.539	.245	.098	.000	.000	.000
0.4	.784	.784	.882	.784	.686	.490	.294	.196	.000	.000	.000
0.3	.686	.784	.931	.833	.784	.637	.441	.343	.147	.000	.000
0.2	.588	.784	.981	.882	.882	.784	.588	.490	.294	.000	.000
0.1	.421	.562	.646	.604	.604	.617	.533	.435	.294	.167	.056
0.0	.254	.339	.312	.325	.325	.450	.477	.379	.294	.334	.111
2.0	.100	.100	.100	.100	.100	.100	.017	.000	.000	.000	.000
1.9	.100	.100	.100	.100	.100	.100	.031	.000	.000	.000	.000
1.8	.100	.100	.100	.100	.100	.100	.044	.000	.000	.000	.000
1.7	.100	.100	.100	.100	.100	.100	.058	.000	.000	.000	.000
1.6	.100	.100	.100	.100	.100	.100	.072	.000	.000	.000	.000
1.5	.100	.100	.100	.100	.100	.100	.086	.000	.000	.000	.000
1.4	.100	.100	.100	.100	.100	.100	.100	.000	.000	.000	.000
1.3	.125	.125	.125	.125	.125	.125	.125	.025	.000	.000	.000
1.2	.150	.150	.150	.150	.150	.150	.150	.050	.000	.000	.000
1.1	.175	.175	.175	.175	.175	.175	.175	.075	.000	.000	.000
1.0	.200	.200	.200	.200	.200	.200	.200	.100	.000	.000	.000
0.9	.450	.350	.250	.250	.250	.250	.200	.150	.050	.000	.000
0.8	.700	.500	.300	.300	.300	.300	.200	.200	.100	.000	.000
0.7	.750	.650	.550	.500	.450	.350	.250	.250	.100	.000	.000
0.6	.800	.800	.800	.700	.600	.400	.300	.300	.100	.000	.000
0.5	.700	.700	.750	.700	.650	.500	.400	.350	.150	.000	.000
0.4	.600	.600	.700	.700	.700	.600	.500	.400	.200	.000	.000
0.3	.500	.550	.600	.650	.650	.600	.550	.450	.300	.050	.000
0.2	.400	.500	.500	.600	.600	.600	.600	.500	.400	.100	.000
0.1	.286	.386	.386	.429	.429	.429	.486	.386	.343	.214	.057
0.0	.173	.273	.273	.259	.259	.259	.373	.273	.286	.327	.114

TABLE A-1(CONTINUED)

WAVELENGTH OF UPPER ARRAY = 5.37 MICRONS

WAVELENGTH OF LOWER ARRAY = 5.47 MICRONS

UNITS = .00140 WATTS/SQCM/MICRON/STERADIAN

HORIZONTAL DISTANCE FROM AXIS OF SYMMETRY - MM

HT	0.0	1.0	2.0	3.0	4.0	5.0	6.0	7.0	8.0	9.0	10.0
2.0	.144	.144	.144	.144	.144	.041	.000	.000	.000	.000	.000
1.9	.161	.161	.161	.161	.161	.075	.000	.000	.000	.000	.000
1.8	.178	.178	.178	.178	.178	.110	.000	.000	.000	.000	.000
1.7	.195	.195	.195	.195	.195	.144	.000	.000	.000	.000	.000
1.6	.213	.213	.213	.213	.213	.178	.000	.000	.000	.000	.000
1.5	.230	.230	.230	.230	.230	.213	.000	.000	.000	.000	.000
1.4	.247	.247	.247	.247	.247	.247	.000	.000	.000	.000	.000
1.3	.247	.247	.247	.247	.247	.247	.000	.000	.000	.000	.000
1.2	.247	.247	.247	.247	.247	.247	.000	.000	.000	.000	.000
1.1	.247	.247	.247	.247	.247	.247	.000	.000	.000	.000	.000
1.0	.247	.247	.247	.247	.247	.247	.000	.000	.000	.000	.000
0.9	.494	.432	.309	.309	.309	.247	.123	.000	.000	.000	.000
0.8	.740	.617	.370	.370	.370	.247	.247	.000	.000	.000	.000
0.7	.802	.802	.617	.617	.555	.309	.247	.000	.000	.000	.000
0.6	.864	.987	.864	.864	.740	.370	.247	.000	.000	.000	.000
0.5	.802	.864	.802	.802	.740	.494	.432	.247	.000	.000	.000
0.4	.740	.740	.740	.740	.740	.617	.617	.494	.000	.000	.000
0.3	.679	.679	.740	.740	.740	.679	.617	.555	.247	.000	.000
0.2	.617	.617	.740	.740	.740	.740	.617	.617	.494	.000	.000
0.1	.477	.477	.530	.530	.600	.600	.547	.547	.494	.210	.140
0.0	.337	.337	.320	.320	.460	.460	.477	.477	.494	.421	.280
2.0	.146	.146	.146	.146	.146	.146	.042	.021	.000	.000	.000
1.9	.163	.163	.163	.163	.163	.163	.076	.038	.000	.000	.000
1.8	.181	.181	.181	.181	.181	.181	.111	.056	.000	.000	.000
1.7	.198	.198	.198	.198	.198	.198	.146	.073	.000	.000	.000
1.6	.215	.215	.215	.215	.215	.215	.181	.090	.000	.000	.000
1.5	.233	.233	.233	.233	.233	.233	.215	.108	.000	.000	.000
1.4	.250	.250	.250	.250	.250	.250	.250	.125	.000	.000	.000
1.3	.281	.281	.281	.281	.281	.281	.250	.156	.000	.000	.000
1.2	.313	.313	.313	.313	.313	.313	.250	.188	.000	.000	.000
1.1	.344	.344	.344	.344	.344	.344	.250	.219	.000	.000	.000
1.0	.375	.375	.375	.375	.375	.375	.250	.250	.000	.000	.000
0.9	.563	.500	.438	.375	.375	.375	.250	.250	.063	.000	.000
0.8	.750	.625	.500	.375	.375	.375	.250	.250	.125	.000	.000
0.7	.813	.750	.688	.625	.563	.500	.313	.250	.125	.000	.000
0.6	.875	.875	.875	.875	.750	.625	.375	.250	.125	.000	.000
0.5	.813	.813	.813	.813	.750	.625	.500	.375	.188	.000	.000
0.4	.750	.750	.750	.750	.750	.625	.625	.500	.250	.000	.000
0.3	.625	.688	.688	.688	.688	.625	.625	.500	.313	.125	.000
0.2	.500	.625	.625	.625	.625	.625	.625	.500	.375	.250	.000
0.1	.429	.483	.483	.554	.554	.554	.554	.500	.446	.321	.142
0.0	.358	.341	.341	.483	.483	.483	.483	.500	.517	.392	.284

TABLE A-1(CONTINUED)

WAVELENGTH OF UPPER ARRAY = 5.55 MICRONS
WAVELENGTH OF LOWER ARRAY = 5.60 MICRONS
UNITS = .00090 WATTS/SQCM/MICRON/STERADIAN
HORIZONTAL DISTANCE FROM AXIS OF SYMMETRY - MM

HT	0.0	1.0	2.0	3.0	4.0	5.0	6.0	7.0	8.0	9.0	10.0
2.0	.229	.229	.229	.229	.229	.197	.197	.033	.000	.000	.000
1.9	.257	.257	.257	.257	.257	.197	.197	.060	.000	.000	.000
1.8	.284	.284	.284	.284	.284	.197	.197	.087	.000	.000	.000
1.7	.311	.311	.311	.311	.311	.197	.197	.115	.000	.000	.000
1.6	.338	.338	.338	.338	.338	.197	.197	.142	.000	.000	.000
1.5	.366	.366	.366	.366	.366	.197	.197	.169	.000	.000	.000
1.4	.393	.393	.393	.393	.393	.197	.197	.197	.000	.000	.000
1.3	.393	.393	.393	.393	.393	.246	.246	.246	.049	.000	.000
1.2	.393	.393	.393	.393	.393	.295	.295	.295	.098	.000	.000
1.1	.393	.393	.393	.393	.393	.344	.344	.344	.147	.000	.000
1.0	.393	.393	.393	.393	.393	.393	.393	.393	.197	.000	.000
0.9	.590	.590	.491	.491	.491	.491	.491	.393	.197	.000	.000
0.8	.786	.786	.590	.590	.590	.590	.590	.393	.197	.000	.000
0.7	.884	.884	.786	.786	.688	.590	.590	.393	.197	.000	.000
0.6	.983	.983	.983	.983	.786	.590	.590	.393	.197	.000	.000
0.5	.983	.983	.983	.983	.884	.688	.688	.491	.197	.000	.000
0.4	.983	.983	.983	.983	.983	.786	.786	.590	.197	.000	.000
0.3	.884	.884	.884	.884	.983	.786	.786	.688	.393	.197	.000
0.2	.786	.786	.786	.786	.983	.786	.786	.786	.590	.393	.000
0.1	.674	.674	.674	.674	.759	.674	.674	.674	.590	.393	.223
0.0	.563	.563	.563	.563	.536	.563	.563	.563	.590	.393	.447
2.0	.396	.396	.396	.396	.396	.198	.033	.000	.000	.000	.000
1.9	.396	.396	.396	.396	.396	.198	.060	.000	.000	.000	.000
1.8	.396	.396	.396	.396	.396	.198	.088	.000	.000	.000	.000
1.7	.396	.396	.396	.396	.396	.198	.115	.000	.000	.000	.000
1.6	.396	.396	.396	.396	.396	.198	.143	.000	.000	.000	.000
1.5	.396	.396	.396	.396	.396	.198	.170	.000	.000	.000	.000
1.4	.396	.396	.396	.396	.396	.198	.198	.000	.000	.000	.000
1.3	.396	.396	.396	.396	.396	.247	.247	.099	.000	.000	.000
1.2	.396	.396	.396	.396	.396	.297	.297	.198	.000	.000	.000
1.1	.396	.396	.396	.396	.396	.346	.346	.297	.000	.000	.000
1.0	.396	.396	.396	.396	.396	.396	.396	.396	.000	.000	.000
0.9	.593	.494	.494	.494	.494	.494	.494	.396	.198	.000	.000
0.8	.791	.593	.593	.593	.593	.593	.593	.396	.396	.000	.000
0.7	.791	.692	.692	.692	.593	.593	.593	.396	.396	.000	.000
0.6	.791	.791	.791	.791	.593	.593	.593	.396	.396	.000	.000
0.5	.791	.791	.791	.791	.692	.692	.593	.494	.396	.000	.000
0.4	.791	.791	.791	.791	.791	.791	.593	.593	.396	.000	.000
0.3	.692	.692	.791	.791	.791	.791	.593	.593	.396	.099	.000
0.2	.593	.593	.791	.791	.791	.791	.593	.593	.396	.198	.000
0.1	.481	.481	.566	.679	.679	.679	.593	.593	.508	.310	.112
0.0	.369	.369	.342	.566	.566	.566	.593	.593	.620	.423	.225

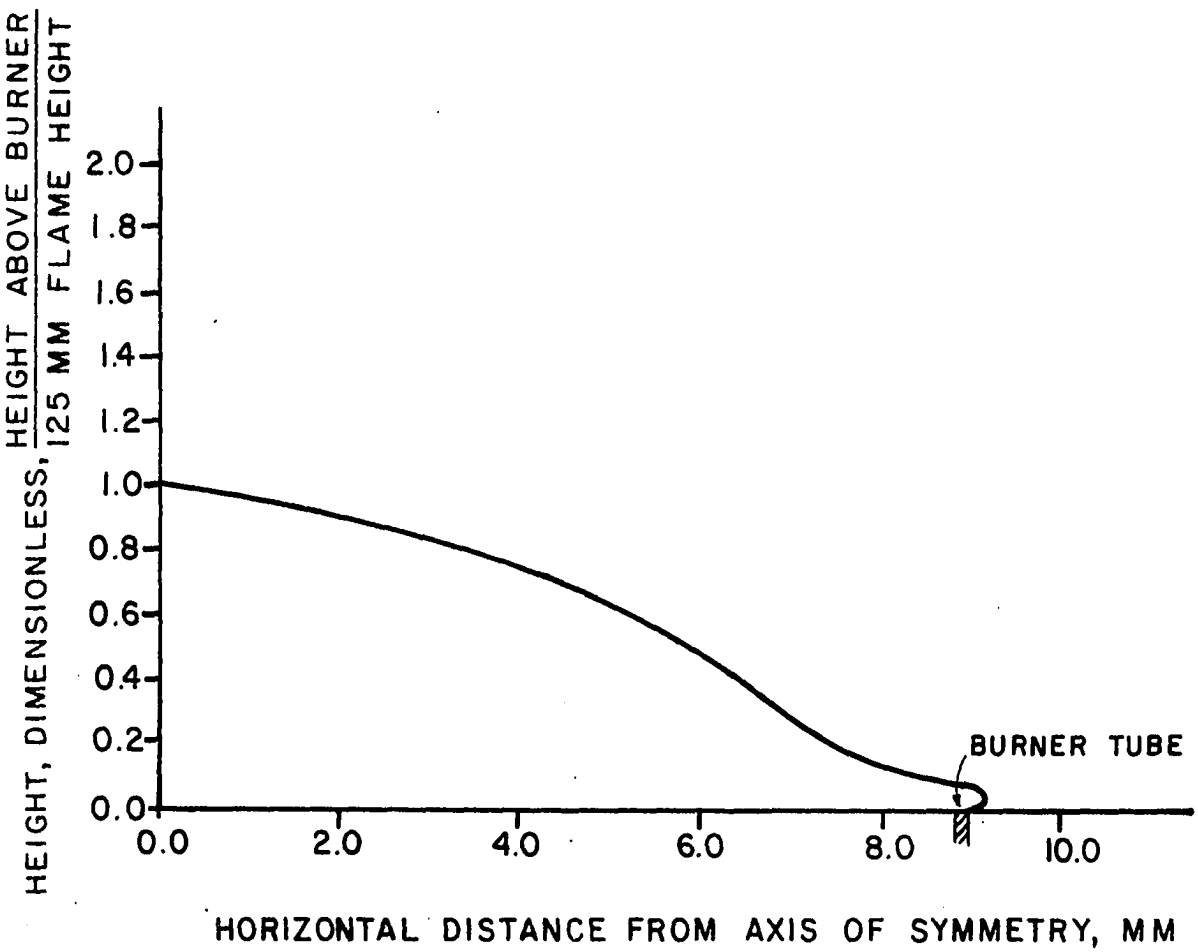

Figure A-2. Outline of Visible Cone for a Laminar Acetone Flame.

TABLE A-2

INTENSITY PROFILES FOR A LAMINAR ACETONE DIFFUSION FLAME

HT = (DISTANCE ABOVE BURNER)/(125 MM FLAME HEIGHT)
WAVELENGTH = 0,71 MICRONS
UNITS = ,00090 WATTS/SQCM/MICRON/STERADIAN

	HORIZONTAL DISTANCE FROM AXIS OF SYMMETRY - MM										
HT	0,0	1,0	2,0	3,0	4,0	5,0	6,0	7,0	8,0	9,0	10,0
2,0	,000	,000	,000	,000	,000	,000	,000	,000	,000	,000	,000
1,9	,000	,000	,000	,000	,000	,000	,000	,000	,000	,000	,000
1,8	,000	,000	,000	,000	,000	,000	,000	,000	,000	,000	,000
1,7	,000	,000	,000	,000	,000	,000	,000	,000	,000	,000	,000
1,6	,000	,000	,000	,000	,000	,000	,000	,000	,000	,000	,000
1,5	,000	,000	,000	,000	,000	,000	,000	,000	,000	,000	,000
1,4	,000	,000	,000	,000	,000	,000	,000	,000	,000	,000	,000
1,3	,046	,046	,046	,046	,046	,046	,046	,046	,000	,000	,000
1,2	,092	,092	,092	,092	,092	,092	,092	,092	,000	,000	,000
1,1	,137	,137	,137	,137	,137	,137	,137	,137	,000	,000	,000
1,0	,183	,183	,183	,183	,183	,183	,183	,183	,000	,000	,000
0,9	,275	,275	,275	,183	,183	,183	,183	,183	,092	,000	,000
0,8	,367	,367	,367	,183	,183	,183	,183	,183	,183	,000	,000
0,7	,550	,550	,550	,367	,367	,183	,183	,183	,183	,092	,000
0,6	,733	,733	,733	,550	,550	,183	,183	,183	,183	,183	,000
0,5	,642	,733	,825	,733	,733	,550	,367	,183	,183	,183	,092
0,4	,550	,733	,917	,917	,917	,917	,550	,183	,183	,183	,183
0,3	,458	,550	,642	,733	,733	,733	,550	,183	,183	,183	,183
0,2	,367	,367	,367	,550	,550	,550	,550	,183	,183	,183	,183
0,1	,262	,262	,262	,342	,342	,342	,342	,183	,183	,183	,183
0,0	,158	,158	,158	,133	,133	,133	,133	,183	,183	,183	,183

TABLE A-2(CONTINUED)

WAVELENGTH OF UPPER ARRAY = 0,72 MICRONS
WAVELENGTH OF LOWER ARRAY = 0,73 MICRONS
UNITS = ,00140 WATTS/SQCM/MICRON/STERADIAN
HORIZONTAL DISTANCE FROM AXIS OF SYMMETRY - MM

HT	0,0	1,0	2,0	3,0	4,0	5,0	6,0	7,0	8,0	9,0	10,0
2,0	,000	,000	,000	,000	,000	,000	,000	,000	,000	,000	,000
1,9	,000	,000	,000	,000	,000	,000	,000	,000	,000	,000	,000
1,8	,000	,000	,000	,000	,000	,000	,000	,000	,000	,000	,000
1,7	,000	,000	,000	,000	,000	,000	,000	,000	,000	,000	,000
1,6	,000	,000	,000	,000	,000	,000	,000	,000	,000	,000	,000
1,5	,000	,000	,000	,000	,000	,000	,000	,000	,000	,000	,000
1,4	,000	,000	,000	,000	,000	,000	,000	,000	,000	,000	,000
1,3	,029	,029	,029	,029	,029	,029	,029	,029	,000	,000	,000
1,2	,059	,059	,059	,059	,059	,059	,059	,059	,000	,000	,000
1,1	,088	,088	,088	,088	,088	,088	,088	,088	,000	,000	,000
1,0	,118	,118	,118	,118	,118	,118	,118	,118	,000	,000	,000
0,9	,177	,177	,177	,118	,118	,118	,118	,118	,059	,000	,000
0,8	,236	,236	,236	,118	,118	,118	,118	,118	,118	,000	,000
0,7	,471	,471	,471	,354	,295	,177	,118	,118	,118	,059	,000
0,6	,707	,707	,707	,589	,471	,236	,118	,118	,118	,118	,000
0,5	,589	,648	,707	,707	,648	,530	,295	,118	,118	,118	,000
0,4	,471	,589	,707	,825	,825	,825	,471	,118	,118	,118	,000
0,3	,354	,412	,471	,589	,589	,589	,354	,118	,118	,118	,059
0,2	,236	,236	,236	,354	,354	,354	,236	,118	,118	,118	,118
0,1	,169	,169	,169	,220	,220	,220	,169	,118	,118	,118	,118
0,0	,102	,102	,102	,086	,086	,086	,102	,118	,118	,118	,118
2,0	,000	,000	,000	,000	,000	,000	,000	,000	,000	,000	,000
1,9	,000	,000	,000	,000	,000	,000	,000	,000	,000	,000	,000
1,8	,000	,000	,000	,000	,000	,000	,000	,000	,000	,000	,000
1,7	,000	,000	,000	,000	,000	,000	,000	,000	,000	,000	,000
1,6	,000	,000	,000	,000	,000	,000	,000	,000	,000	,000	,000
1,5	,000	,000	,000	,000	,000	,000	,000	,000	,000	,000	,000
1,4	,000	,000	,000	,000	,000	,000	,000	,000	,000	,000	,000
1,3	,088	,088	,088	,059	,029	,029	,029	,029	,000	,000	,000
1,2	,177	,177	,177	,118	,059	,059	,059	,059	,000	,000	,000
1,1	,265	,265	,265	,177	,088	,088	,088	,088	,000	,000	,000
1,0	,354	,354	,354	,236	,118	,118	,118	,118	,000	,000	,000
0,9	,354	,354	,295	,177	,118	,118	,118	,118	,059	,000	,000
0,8	,354	,354	,236	,118	,118	,118	,118	,118	,118	,000	,000
0,7	,648	,648	,589	,471	,412	,236	,118	,118	,118	,059	,000
0,6	,943	,943	,943	,825	,707	,354	,118	,118	,118	,118	,000
0,5	,825	,825	,825	,707	,471	,236	,118	,118	,118	,118	,059
0,4	,707	,707	,707	,589	,236	,118	,118	,118	,118	,118	,118
0,3	,530	,530	,589	,530	,412	,354	,295	,177	,118	,118	,118
0,2	,354	,354	,471	,471	,589	,589	,471	,236	,118	,118	,118
0,1	,220	,220	,270	,270	,321	,321	,270	,169	,118	,118	,118
0,0	,086	,086	,070	,070	,054	,054	,070	,102	,118	,118	,118

TABLE A-2(CONTINUED)

WAVELENGTH OF UPPER ARRAY = 0.75 MICRONS
WAVELENGTH OF LOWER ARRAY = 0.79 MICRONS
UNITS = .00330 WATTS/SQCM/MICRON/STERADIAN
HORIZONTAL DISTANCE FROM AXIS OF SYMMETRY - MM

HT	0.0	1.0	2.0	3.0	4.0	5.0	6.0	7.0	8.0	9.0	10.0
2.0	.000	.000	.000	.000	.000	.000	.000	.000	.000	.000	.000
1.9	.000	.000	.000	.000	.000	.000	.000	.000	.000	.000	.000
1.8	.000	.000	.000	.000	.000	.000	.000	.000	.000	.000	.000
1.7	.000	.000	.000	.000	.000	.000	.000	.000	.000	.000	.000
1.6	.000	.000	.000	.000	.000	.000	.000	.000	.000	.000	.000
1.5	.000	.000	.000	.000	.000	.000	.000	.000	.000	.000	.000
1.4	.000	.000	.000	.000	.000	.000	.000	.000	.000	.000	.000
1.3	.012	.012	.012	.012	.012	.012	.000	.000	.000	.000	.000
1.2	.025	.025	.025	.025	.025	.025	.000	.000	.000	.000	.000
1.1	.037	.037	.037	.037	.037	.037	.000	.000	.000	.000	.000
1.0	.050	.050	.050	.050	.050	.050	.000	.000	.000	.000	.000
0.9	.175	.150	.100	.075	.050	.050	.025	.025	.025	.000	.000
0.8	.300	.250	.150	.100	.050	.050	.050	.050	.050	.000	.000
0.7	.450	.425	.350	.300	.175	.075	.050	.050	.050	.000	.000
0.6	.600	.600	.550	.500	.300	.100	.050	.050	.050	.000	.000
0.5	.500	.575	.575	.600	.500	.375	.150	.100	.050	.000	.000
0.4	.400	.550	.600	.700	.700	.650	.250	.150	.050	.000	.000
0.3	.250	.375	.425	.500	.525	.500	.225	.125	.050	.025	.000
0.2	.100	.200	.250	.300	.350	.350	.200	.100	.050	.050	.000
0.1	.072	.115	.136	.158	.180	.180	.115	.072	.050	.050	.028
0.0	.043	.030	.023	.016	.009	.009	.030	.043	.050	.050	.057
2.0	.000	.000	.000	.000	.000	.000	.000	.000	.000	.000	.000
1.9	.000	.000	.000	.000	.000	.000	.000	.000	.000	.000	.000
1.8	.000	.000	.000	.000	.000	.000	.000	.000	.000	.000	.000
1.7	.000	.000	.000	.000	.000	.000	.000	.000	.000	.000	.000
1.6	.000	.000	.000	.000	.000	.000	.000	.000	.000	.000	.000
1.5	.000	.000	.000	.000	.000	.000	.000	.000	.000	.000	.000
1.4	.000	.000	.000	.000	.000	.000	.000	.000	.000	.000	.000
1.3	.012	.012	.012	.012	.012	.012	.012	.012	.000	.000	.000
1.2	.025	.025	.025	.025	.025	.025	.025	.025	.000	.000	.000
1.1	.037	.037	.037	.037	.037	.037	.037	.037	.000	.000	.000
1.0	.050	.050	.050	.050	.050	.050	.050	.050	.000	.000	.000
0.9	.200	.175	.150	.075	.050	.050	.050	.050	.025	.000	.000
0.8	.350	.300	.250	.100	.050	.050	.050	.050	.050	.000	.000
0.7	.575	.550	.525	.400	.275	.100	.050	.050	.050	.025	.000
0.6	.800	.800	.800	.700	.500	.150	.050	.050	.050	.050	.000
0.5	.675	.750	.800	.800	.750	.525	.275	.175	.050	.050	.000
0.4	.550	.700	.800	.900	.*00	.900	.500	.300	.050	.050	.000
0.3	.350	.450	.550	.625	.700	.675	.450	.275	.075	.050	.025
0.2	.150	.200	.300	.350	.400	.450	.400	.250	.100	.050	.050
0.1	.122	.143	.215	.236	.258	.280	.286	.222	.157	.107	.050
0.0	.093	.086	.130	.123	.116	.109	.173	.193	.214	.164	.050

TABLE A-2(CONTINUED)

WAVELENGTH OF UPPER ARRAY = 0.83 MICRONS
WAVELENGTH OF LOWER ARRAY = 0.88 MICRONS
UNITS = .00620 WATTS/SQCM/MICRON/STERADIAN
HORIZONTAL DISTANCE FROM AXIS OF SYMMETRY - MM

HT	0.0	1.0	2.0	3.0	4.0	5.0	6.0	7.0	8.0	9.0	10.0
2.0	.000	.000	.000	.000	.000	.000	.000	.000	.000	.000	.000
1.9	.000	.000	.000	.000	.000	.000	.000	.000	.000	.000	.000
1.8	.000	.000	.000	.000	.000	.000	.000	.000	.000	.000	.000
1.7	.000	.000	.000	.000	.000	.000	.000	.000	.000	.000	.000
1.6	.000	.000	.000	.000	.000	.000	.000	.000	.000	.000	.000
1.5	.000	.000	.000	.000	.000	.000	.000	.000	.000	.000	.000
1.4	.000	.000	.000	.000	.000	.000	.000	.000	.000	.000	.000
1.3	.007	.007	.007	.007	.007	.007	.007	.007	.000	.000	.000
1.2	.013	.013	.013	.013	.013	.013	.013	.013	.000	.000	.000
1.1	.020	.020	.020	.020	.020	.020	.020	.020	.000	.000	.000
1.0	.027	.027	.027	.027	.027	.027	.027	.027	.000	.000	.000
0.9	.146	.133	.093	.053	.027	.027	.027	.027	.013	.000	.000
0.8	.266	.239	.160	.080	.027	.027	.027	.027	.027	.000	.000
0.7	.426	.412	.359	.306	.213	.080	.027	.027	.027	.013	.000
0.6	.585	.585	.559	.532	.399	.133	.027	.027	.027	.027	.000
0.5	.492	.532	.559	.599	.545	.412	.213	.027	.027	.027	.000
0.4	.399	.479	.559	.665	.692	.692	.399	.027	.027	.027	.000
0.3	.253	.319	.386	.452	.492	.506	.253	.027	.027	.027	.000
0.2	.106	.160	.213	.239	.293	.319	.106	.027	.027	.027	.000
0.1	.076	.099	.137	.149	.172	.198	.106	.072	.072	.057	.030
0.0	.046	.039	.062	.058	.051	.077	.106	.117	.117	.087	.060
2.0	.000	.000	.000	.000	.000	.000	.000	.000	.000	.000	.000
1.9	.000	.000	.000	.000	.000	.000	.000	.000	.000	.000	.000
1.8	.000	.000	.000	.000	.000	.000	.000	.000	.000	.000	.000
1.7	.000	.000	.000	.000	.000	.000	.000	.000	.000	.000	.000
1.6	.000	.000	.000	.000	.000	.000	.000	.000	.000	.000	.000
1.5	.000	.000	.000	.000	.000	.000	.000	.000	.000	.000	.000
1.4	.000	.000	.000	.000	.000	.000	.000	.000	.000	.000	.000
1.3	.007	.007	.007	.007	.007	.007	.007	.007	.000	.000	.000
1.2	.013	.013	.013	.013	.013	.013	.013	.013	.000	.000	.000
1.1	.020	.020	.020	.020	.020	.020	.020	.020	.000	.000	.000
1.0	.027	.027	.027	.027	.027	.027	.027	.027	.000	.000	.000
0.9	.186	.160	.120	.053	.027	.027	.027	.027	.000	.000	.000
0.8	.346	.293	.213	.080	.027	.027	.027	.027	.000	.000	.000
0.7	.559	.532	.479	.386	.279	.080	.027	.027	.013	.013	.000
0.6	.772	.772	.745	.692	.532	.133	.027	.027	.027	.027	.000
0.5	.652	.718	.772	.785	.758	.532	.186	.027	.027	.027	.000
0.4	.532	.665	.798	.878	.985	.931	.346	.027	.027	.027	.000
0.3	.333	.439	.532	.599	.679	.665	.346	.027	.027	.027	.000
0.2	.133	.213	.266	.319	.373	.399	.346	.027	.027	.027	.000
0.1	.073	.107	.130	.153	.191	.203	.180	.042	.042	.042	.015
0.0	.012	.001	.000	.000	.010	.006	.013	.057	.057	.057	.030

TABLE A-2(CONTINUED)

WAVELENGTH OF UPPER ARRAY = 0.94 MICRONS — WAVELENGTH OF LOWER ARRAY = 1.01 MICRONS

UNITS = .00990 WATTS/SQCM/MICRON/STERADIAN

HORIZONTAL DISTANCE FROM AXIS OF SYMMETRY - MM

HT	0.0	1.0	2.0	3.0	4.0	5.0	6.0	7.0	8.0	9.0	10.0
2.0	.000	.000	.000	.000	.000	.000	.000	.000	.000	.000	.000
1.9	.000	.000	.000	.000	.000	.000	.000	.000	.000	.000	.000
1.8	.000	.000	.000	.000	.000	.000	.000	.000	.000	.000	.000
1.7	.000	.000	.000	.000	.000	.000	.000	.000	.000	.000	.000
1.6	.000	.000	.000	.000	.000	.000	.000	.000	.000	.000	.000
1.5	.000	.000	.000	.000	.000	.000	.000	.000	.000	.000	.000
1.4	.000	.000	.000	.000	.000	.000	.000	.000	.000	.000	.000
1.3	.004	.004	.004	.004	.004	.004	.004	.004	.000	.000	.000
1.2	.008	.008	.008	.008	.008	.008	.008	.008	.000	.000	.000
1.1	.012	.012	.012	.012	.012	.012	.012	.012	.000	.000	.000
1.0	.017	.017	.017	.017	.017	.017	.017	.017	.000	.000	.000
0.9	.150	.133	.100	.042	.017	.017	.017	.017	.008	.000	.000
0.8	.283	.250	.183	.067	.017	.017	.017	.017	.017	.000	.000
0.7	.467	.433	.392	.317	.217	.042	.017	.017	.017	.008	.000
0.6	.650	.617	.600	.567	.417	.067	.017	.017	.017	.017	.000
0.5	.542	.600	.617	.642	.600	.408	.075	.017	.017	.017	.000
0.4	.433	.583	.633	.717	.783	.750	.133	.017	.017	.017	.000
0.3	.225	.300	.325	.367	.400	.383	.075	.017	.017	.017	.000
0.2	.017	.017	.017	.017	.017	.017	.017	.017	.017	.017	.000
0.1	.017	.017	.017	.017	.017	.017	.017	.017	.017	.017	.009
0.0	.017	.017	.017	.017	.017	.017	.017	.017	.017	.017	.019
2.0	.017	.017	.017	.017	.017	.017	.017	.002	.000	.000	.000
1.9	.017	.017	.017	.017	.017	.017	.017	.004	.000	.000	.000
1.8	.017	.017	.017	.017	.017	.017	.017	.007	.000	.000	.000
1.7	.017	.017	.017	.017	.017	.017	.017	.009	.000	.000	.000
1.6	.017	.017	.017	.017	.017	.017	.017	.012	.000	.000	.000
1.5	.017	.017	.017	.017	.017	.017	.017	.014	.000	.000	.000
1.4	.017	.017	.017	.017	.017	.017	.017	.017	.000	.000	.000
1.3	.017	.017	.017	.017	.017	.017	.017	.017	.004	.000	.000
1.2	.017	.017	.017	.017	.017	.017	.017	.017	.008	.000	.000
1.1	.017	.017	.017	.017	.017	.017	.017	.017	.012	.000	.000
1.0	.017	.017	.017	.017	.017	.017	.017	.017	.017	.000	.000
0.9	.192	.175	.133	.058	.017	.017	.017	.017	.017	.000	.000
0.8	.367	.333	.250	.100	.017	.017	.017	.017	.017	.000	.000
0.7	.600	.567	.508	.400	.258	.050	.017	.017	.017	.008	.000
0.6	.833	.800	.767	.700	.500	.083	.017	.017	.017	.017	.000
0.5	.692	.742	.783	.808	.750	.475	.158	.017	.017	.017	.000
0.4	.550	.683	.800	.917	.900	.867	.300	.017	.017	.017	.000
0.3	.350	.458	.550	.658	.708	.650	.275	.017	.017	.017	.008
0.2	.150	.233	.300	.400	.417	.433	.250	.017	.017	.017	.017
0.1	.074	.110	.139	.182	.189	.197	.117	.017	.017	.017	.017
0.0	.000	.000	.000	.000	.000	.000	.000	.017	.017	.017	.017

TABLE A-2(CONTINUED)

WAVELENGTH OF UPPER ARRAY = 1.10 MICRONS
WAVELENGTH OF LOWER ARRAY = 1.19 MICRONS
UNITS = .01570 WATTS/SQCM/MICRON/STERADIAN
HORIZONTAL DISTANCE FROM AXIS OF SYMMETRY - MM

HT	0.0	1.0	2.0	3.0	4.0	5.0	6.0	7.0	8.0	9.0	10.0
2.0	.011	.011	.011	.011	.011	.011	.011	.001	.000	.000	.000
1.9	.011	.011	.011	.011	.011	.011	.011	.003	.000	.000	.000
1.8	.011	.011	.011	.011	.011	.011	.011	.004	.000	.000	.000
1.7	.011	.011	.011	.011	.011	.011	.011	.006	.000	.000	.000
1.6	.011	.011	.011	.011	.011	.011	.011	.007	.000	.000	.000
1.5	.011	.011	.011	.011	.011	.011	.011	.009	.000	.000	.000
1.4	.011	.011	.011	.011	.011	.011	.011	.011	.000	.000	.000
1.3	.011	.011	.011	.011	.011	.011	.011	.011	.000	.000	.000
1.2	.011	.011	.011	.011	.011	.011	.011	.011	.000	.000	.000
1.1	.011	.011	.011	.011	.011	.011	.011	.011	.000	.000	.000
1.0	.011	.011	.011	.011	.011	.011	.011	.011	.000	.000	.000
0.9	.158	.137	.152	.037	.011	.011	.011	.011	.000	.000	.000
0.8	.305	.263	.294	.063	.011	.011	.011	.011	.000	.000	.000
0.7	.494	.457	.447	.305	.215	.058	.011	.011	.005	.005	.000
0.6	.683	.651	.599	.546	.420	.105	.011	.011	.011	.011	.000
0.5	.562	.599	.620	.641	.609	.426	.163	.011	.011	.011	.005
0.4	.441	.546	.641	.736	.799	.746	.315	.011	.011	.011	.011
0.3	.284	.363	.436	.510	.562	.546	.289	.011	.011	.011	.011
0.2	.126	.179	.231	.284	.326	.347	.263	.011	.011	.011	.011
0.1	.060	.083	.106	.128	.147	.156	.119	.011	.011	.011	.011
0.0	.000	.000	.000	.000	.000	.000	.000	.011	.011	.011	.011
2.0	.011	.011	.011	.011	.011	.011	.011	.001	.000	.000	.000
1.9	.011	.011	.011	.011	.011	.011	.011	.003	.000	.000	.000
1.8	.011	.011	.011	.011	.011	.011	.011	.004	.000	.000	.000
1.7	.011	.011	.011	.011	.011	.011	.011	.006	.000	.000	.000
1.6	.011	.011	.011	.011	.011	.011	.011	.007	.000	.000	.000
1.5	.011	.011	.011	.011	.011	.011	.011	.009	.000	.000	.000
1.4	.011	.011	.011	.011	.011	.011	.011	.011	.000	.000	.000
1.3	.013	.013	.013	.013	.013	.011	.011	.011	.000	.000	.000
1.2	.016	.016	.016	.016	.016	.011	.011	.011	.000	.000	.000
1.1	.018	.018	.018	.018	.018	.011	.011	.011	.000	.000	.000
1.0	.021	.021	.021	.021	.021	.011	.011	.011	.000	.000	.000
0.9	.147	.137	.121	.047	.021	.011	.011	.011	.005	.000	.000
0.8	.273	.252	.221	.074	.021	.011	.011	.011	.011	.000	.000
0.7	.567	.546	.499	.389	.226	.047	.011	.011	.011	.000	.000
0.6	.862	.841	.778	.704	.431	.084	.011	.011	.011	.000	.000
0.5	.704	.762	.788	.804	.715	.541	.242	.016	.011	.005	.000
0.4	.546	.683	.799	.904	.998	.998	.473	.021	.011	.011	.000
0.3	.347	.452	.536	.620	.694	.715	.399	.021	.011	.011	.000
0.2	.147	.221	.273	.336	.389	.431	.326	.021	.011	.011	.000
0.1	.075	.107	.130	.157	.180	.198	.153	.015	.011	.011	.000
0.0	.004	.000	.000	.000	.000	.000	.000	.009	.011	.011	.000

TABLE A-2(CONTINUED)

WAVELENGTH OF UPPER ARRAY = 1.30 MICRONS

WAVELENGTH OF LOWER ARRAY = 1.42 MICRONS

UNITS = .03140 WATTS/SQCM/MICRON/STERADIAN

HORIZONTAL DISTANCE FROM AXIS OF SYMMETRY - MM

HT	0.0	1.0	2.0	3.0	4.0	5.0	6.0	7.0	8.0	9.0	10.0
2.0	.005	.005	.005	.005	.005	.005	.001	.000	.000	.000	.000
1.9	.005	.005	.005	.005	.005	.005	.001	.000	.000	.000	.000
1.8	.005	.005	.005	.005	.005	.005	.002	.000	.000	.000	.000
1.7	.005	.005	.005	.005	.005	.005	.003	.000	.000	.000	.000
1.6	.005	.005	.005	.005	.005	.005	.004	.000	.000	.000	.000
1.5	.005	.005	.005	.005	.005	.005	.004	.000	.000	.000	.000
1.4	.005	.005	.005	.005	.005	.005	.005	.000	.000	.000	.000
1.3	.007	.007	.007	.007	.005	.005	.005	.000	.000	.000	.000
1.2	.008	.008	.008	.008	.005	.005	.005	.000	.000	.000	.000
1.1	.009	.009	.009	.009	.005	.005	.005	.000	.000	.000	.000
1.0	.011	.011	.011	.011	.005	.005	.005	.000	.000	.000	.000
0.9	.097	.092	.074	.034	.005	.005	.005	.003	.003	.000	.000
0.8	.184	.173	.137	.058	.005	.005	.005	.005	.005	.000	.000
0.7	.347	.328	.292	.231	.152	.037	.005	.005	.005	.000	.000
0.6	.510	.483	.447	.405	.299	.068	.005	.005	.005	.000	.000
0.5	.428	.457	.475	.486	.460	.326	.144	.008	.005	.003	.000
0.4	.347	.431	.504	.567	.620	.583	.284	.011	.005	.005	.000
0.3	.221	.284	.339	.389	.428	.420	.257	.032	.005	.005	.000
0.2	.095	.137	.173	.210	.236	.257	.231	.053	.005	.005	.000
0.1	.044	.062	.078	.094	.105	.114	.103	.026	.005	.005	.000
0.0	.000	.000	.000	.000	.000	.000	.000	.000	.005	.005	.000
2.0	.005	.005	.005	.005	.005	.005	.005	.000	.000	.000	.000
1.9	.005	.005	.005	.005	.005	.005	.005	.000	.000	.000	.000
1.8	.005	.005	.005	.005	.005	.005	.005	.000	.000	.000	.000
1.7	.005	.005	.005	.005	.005	.005	.005	.000	.000	.000	.000
1.6	.005	.005	.005	.005	.005	.005	.005	.000	.000	.000	.000
1.5	.005	.005	.005	.005	.005	.005	.005	.000	.000	.000	.000
1.4	.005	.005	.005	.005	.005	.005	.005	.000	.000	.000	.000
1.3	.007	.007	.007	.007	.007	.007	.007	.001	.001	.000	.000
1.2	.008	.008	.008	.008	.008	.008	.008	.003	.003	.000	.000
1.1	.009	.009	.009	.009	.009	.009	.009	.004	.004	.000	.000
1.0	.011	.011	.011	.011	.011	.011	.011	.005	.005	.000	.000
0.9	.144	.131	.100	.047	.011	.011	.011	.008	.005	.000	.000
0.8	.278	.252	.189	.084	.011	.011	.011	.011	.005	.000	.000
0.7	.436	.625	.357	.260	.137	.021	.011	.011	.005	.003	.000
0.6	.594	.998	.525	.436	.263	.032	.011	.011	.005	.005	.000
0.5	.491	.757	.567	.560	.504	.368	.110	.013	.008	.008	.003
0.4	.389	.515	.609	.683	.746	.704	.210	.016	.011	.011	.005
0.3	.252	.347	.420	.478	.525	.510	.231	.034	.016	.016	.005
0.2	.116	.179	.231	.273	.305	.315	.252	.053	.021	.021	.005
0.1	.053	.080	.103	.121	.135	.139	.112	.026	.012	.012	.005
0.0	.000	.000	.000	.000	.000	.000	.000	.000	.003	.003	.005

TABLE A-2(CONTINUED)

WAVELENGTH OF UPPER ARRAY = 1.55 MICRONS — WAVELENGTH OF LOWER ARRAY = 1.69 MICRONS

UNITS = .03110 WATTS/SQCM/MICRON/STERADIAN

HORIZONTAL DISTANCE FROM AXIS OF SYMMETRY - MM

HT	0.0	1.0	2.0	3.0	4.0	5.0	6.0	7.0	8.0	9.0	10.0
2.0	.005	.005	.005	.005	.005	.005	.005	.001	.000	.000	.000
1.9	.005	.005	.005	.005	.005	.005	.005	.001	.000	.000	.000
1.8	.005	.005	.005	.005	.005	.005	.005	.002	.000	.000	.000
1.7	.005	.005	.005	.005	.005	.005	.005	.003	.000	.000	.000
1.6	.005	.005	.005	.005	.005	.005	.005	.004	.000	.000	.000
1.5	.005	.005	.005	.005	.005	.005	.005	.005	.000	.000	.000
1.4	.005	.005	.005	.005	.005	.005	.005	.005	.000	.000	.000
1.3	.007	.007	.007	.007	.005	.005	.005	.005	.001	.000	.000
1.2	.008	.008	.008	.008	.005	.005	.005	.005	.003	.000	.000
1.1	.009	.009	.009	.009	.005	.005	.005	.005	.004	.000	.000
1.0	.011	.011	.011	.011	.005	.005	.005	.005	.005	.000	.000
0.9	.183	.162	.125	.048	.008	.008	.008	.008	.005	.000	.000
0.8	.355	.313	.239	.085	.011	.011	.011	.011	.005	.000	.000
0.7	.546	.515	.454	.350	.223	.042	.011	.011	.008	.003	.000
0.6	.737	.716	.668	.615	.435	.074	.011	.011	.011	.005	.000
0.5	.613	.671	.706	.727	.668	.464	.239	.011	.011	.005	.000
0.4	.488	.626	.743	.838	.902	.854	.467	.011	.011	.005	.000
0.3	.313	.419	.515	.589	.639	.618	.358	.016	.011	.005	.000
0.2	.138	.212	.286	.340	.377	.382	.249	.021	.011	.005	.000
0.1	.063	.095	.127	.150	.166	.168	.111	.012	.008	.005	.003
0.0	.000	.000	.000	.000	.000	.000	.000	.003	.005	.005	.006
2.0	.005	.005	.005	.005	.005	.005	.005	.001	.000	.000	.000
1.9	.005	.005	.005	.005	.005	.005	.005	.001	.000	.000	.000
1.8	.005	.005	.005	.005	.005	.005	.005	.002	.000	.000	.000
1.7	.005	.005	.005	.005	.005	.005	.005	.003	.000	.000	.000
1.6	.005	.005	.005	.005	.005	.005	.005	.004	.000	.000	.000
1.5	.005	.005	.005	.005	.005	.005	.005	.005	.000	.000	.000
1.4	.005	.005	.005	.005	.005	.005	.005	.005	.000	.000	.000
1.3	.007	.007	.007	.007	.005	.005	.005	.005	.001	.000	.000
1.2	.008	.008	.008	.008	.005	.005	.005	.005	.003	.000	.000
1.1	.009	.009	.009	.009	.005	.005	.005	.005	.004	.000	.000
1.0	.011	.011	.011	.011	.005	.005	.005	.005	.005	.000	.000
0.9	.210	.170	.111	.032	.008	.008	.005	.005	.005	.000	.000
0.8	.408	.329	.212	.053	.011	.011	.005	.005	.005	.000	.000
0.7	.631	.586	.493	.371	.239	.069	.008	.005	.005	.003	.000
0.6	.854	.843	.774	.690	.467	.127	.011	.005	.005	.005	.000
0.5	.692	.761	.790	.804	.732	.541	.138	.008	.008	.005	.000
0.4	.530	.679	.806	.918	.997	.955	.265	.011	.011	.005	.000
0.3	.342	.456	.552	.634	.695	.690	.292	.021	.011	.005	.000
0.2	.154	.233	.297	.350	.393	.424	.318	.032	.011	.005	.000
0.1	.069	.104	.131	.154	.173	.186	.140	.017	.008	.005	.003
0.0	.000	.000	.000	.000	.000	.000	.000	.002	.005	.005	.006

TABLE A-2(CONTINUED)

WAVELENGTH OF UPPER ARRAY = 1.84 MICRONS

WAVELENGTH OF LOWER ARRAY = 1.95 MICRONS

UNITS = .03390 WATTS/SQCM/MICRON/STERADIAN

HORIZONTAL DISTANCE FROM AXIS OF SYMMETRY - MM

HT	0.0	1.0	2.0	3.0	4.0	5.0	6.0	7.0	8.0	9.0	10.0
2.0	.005	.005	.005	.005	.005	.005	.005	.001	.000	.000	.000
1.9	.005	.005	.005	.005	.005	.005	.005	.001	.000	.000	.000
1.8	.005	.005	.005	.005	.005	.005	.005	.002	.000	.000	.000
1.7	.005	.005	.005	.005	.005	.005	.005	.003	.000	.000	.000
1.6	.005	.005	.005	.005	.005	.005	.005	.003	.000	.000	.000
1.5	.005	.005	.005	.005	.005	.005	.005	.004	.000	.000	.000
1.4	.005	.005	.005	.005	.005	.005	.005	.005	.000	.000	.000
1.3	.007	.007	.007	.007	.006	.006	.006	.005	.001	.000	.000
1.2	.010	.010	.010	.010	.007	.007	.007	.005	.002	.000	.000
1.1	.012	.012	.012	.012	.009	.009	.009	.005	.004	.000	.000
1.0	.015	.015	.015	.015	.010	.010	.010	.005	.005	.000	.000
0.9	.219	.190	.139	.046	.010	.010	.007	.005	.005	.000	.000
0.8	.423	.365	.263	.078	.010	.010	.005	.005	.005	.000	.000
0.7	.650	.601	.523	.392	.243	.029	.012	.010	.007	.002	.000
0.6	.876	.837	.784	.706	.477	.049	.019	.015	.010	.005	.000
0.5	.708	.759	.796	.810	.737	.511	.204	.012	.010	.005	.000
0.4	.540	.681	.808	.915	.998	.973	.389	.010	.010	.005	.000
0.3	.355	.465	.560	.635	.696	.703	.348	.029	.010	.005	.002
0.2	.170	.248	.311	.355	.394	.433	.307	.049	.010	.005	.005
0.1	.079	.113	.140	.159	.173	.190	.135	.024	.007	.005	.005
0.0	.000	.000	.000	.000	.000	.000	.000	.000	.004	.005	.005
2.0	.005	.005	.005	.005	.005	.005	.005	.001	.000	.000	.000
1.9	.005	.005	.005	.005	.005	.005	.005	.001	.000	.000	.000
1.8	.005	.005	.005	.005	.005	.005	.005	.002	.000	.000	.000
1.7	.005	.005	.005	.005	.005	.005	.005	.003	.000	.000	.000
1.6	.005	.005	.005	.005	.005	.005	.005	.003	.000	.000	.000
1.5	.005	.005	.005	.005	.005	.005	.005	.004	.000	.000	.000
1.4	.005	.005	.005	.005	.005	.005	.005	.005	.000	.000	.000
1.3	.009	.009	.007	.007	.007	.006	.005	.005	.001	.000	.000
1.2	.012	.012	.010	.010	.010	.007	.005	.005	.002	.000	.000
1.1	.016	.016	.012	.012	.012	.009	.005	.005	.004	.000	.000
1.0	.019	.019	.015	.015	.015	.010	.005	.005	.005	.000	.000
0.9	.200	.178	.146	.071	.015	.012	.007	.005	.005	.000	.000
0.8	.380	.336	.277	.127	.015	.015	.010	.005	.005	.000	.000
0.7	.591	.540	.450	.474	.134	.032	.010	.007	.005	.002	.000
0.6	.803	.745	.623	.822	.253	.049	.010	.010	.005	.005	.000
0.5	.655	.689	.684	.798	.569	.448	.202	.019	.010	.005	.000
0.4	.506	.633	.745	.774	.886	.847	.394	.029	.015	.005	.000
0.3	.336	.440	.526	.565	.638	.625	.367	.039	.012	.005	.000
0.2	.165	.248	.307	.355	.389	.404	.341	.049	.010	.005	.000
0.1	.077	.113	.138	.159	.171	.177	.150	.024	.007	.005	.003
0.0	.000	.000	.000	.000	.000	.000	.000	.000	.004	.005	.006

TABLE A-2(CONTINUED)

WAVELENGTH OF UPPER ARRAY = 2.00 MICRONS
WAVELENGTH OF LOWER ARRAY = 2.09 MICRONS
UNITS = .03210 WATTS/SQCM/MICRON/STERADIAN
HORIZONTAL DISTANCE FROM AXIS OF SYMMETRY - MM

HT	0.0	1.0	2.0	3.0	4.0	5.0	6.0	7.0	8.0	9.0	10.0
2.0	.005	.005	.005	.005	.005	.005	.005	.001	.000	.000	.000
1.9	.005	.005	.005	.005	.005	.005	.005	.001	.000	.000	.000
1.8	.005	.005	.005	.005	.005	.005	.005	.002	.000	.000	.000
1.7	.005	.005	.005	.005	.005	.005	.005	.003	.000	.000	.000
1.6	.005	.005	.005	.005	.005	.005	.005	.004	.000	.000	.000
1.5	.005	.005	.005	.005	.005	.005	.005	.004	.000	.000	.000
1.4	.005	.005	.005	.005	.005	.005	.005	.005	.000	.000	.000
1.3	.010	.010	.009	.009	.009	.008	.006	.005	.001	.000	.000
1.2	.015	.015	.013	.013	.013	.010	.008	.005	.003	.000	.000
1.1	.021	.021	.017	.017	.017	.013	.009	.005	.004	.000	.000
1.0	.026	.026	.021	.021	.021	.015	.010	.005	.005	.000	.000
0.9	.236	.210	.161	.067	.018	.015	.010	.008	.005	.000	.000
0.8	.446	.395	.302	.113	.015	.015	.010	.010	.005	.000	.000
0.7	.664	.620	.546	.418	.238	.028	.015	.013	.008	.003	.000
0.6	.882	.846	.790	.723	.461	.041	.021	.015	.010	.005	.000
0.5	.725	.769	.800	.818	.731	.513	.190	.026	.018	.005	.000
0.4	.569	.692	.810	.913	.*00	.984	.359	.036	.026	.005	.000
0.3	.377	.469	.533	.610	.679	.715	.333	.044	.026	.008	.000
0.2	.185	.246	.256	.308	.359	.446	.308	.051	.026	.010	.000
0.1	.086	.112	.114	.136	.158	.196	.136	.025	.014	.007	.003
0.0	.000	.000	.000	.000	.000	.000	.000	.000	.002	.004	.006
2.0	.005	.005	.005	.005	.005	.005	.001	.000	.000	.000	.000
1.9	.005	.005	.005	.005	.005	.005	.001	.000	.000	.000	.000
1.8	.005	.005	.005	.005	.005	.005	.002	.000	.000	.000	.000
1.7	.005	.005	.005	.005	.005	.005	.003	.000	.000	.000	.000
1.6	.005	.005	.005	.005	.005	.005	.003	.000	.000	.000	.000
1.5	.005	.005	.005	.005	.005	.005	.004	.000	.000	.000	.000
1.4	.005	.005	.005	.005	.005	.005	.005	.000	.000	.000	.000
1.3	.011	.010	.009	.009	.006	.006	.006	.001	.000	.000	.000
1.2	.017	.015	.012	.012	.007	.007	.007	.002	.000	.000	.000
1.1	.023	.019	.016	.016	.009	.009	.009	.004	.000	.000	.000
1.0	.029	.024	.019	.019	.010	.010	.010	.005	.000	.000	.000
0.9	.238	.199	.141	.056	.010	.010	.010	.005	.002	.000	.000
0.8	.448	.375	.263	.092	.010	.010	.010	.005	.005	.000	.000
0.7	.679	.625	.540	.404	.248	.063	.015	.010	.007	.002	.000
0.6	.910	.876	.817	.715	.486	.117	.019	.015	.010	.005	.000
0.5	.739	.795	.837	.820	.739	.550	.448	.022	.015	.007	.000
0.4	.569	.715	.856	.924	.992	.983	.876	.029	.019	.010	.000
0.3	.377	.474	.576	.640	.701	.720	.608	.041	.022	.010	.002
0.2	.185	.234	.297	.355	.409	.457	.341	.054	.024	.010	.005
0.1	.088	.109	.134	.159	.179	.200	.150	.026	.013	.007	.005
0.0	.000	.000	.000	.000	.000	.000	.000	.000	.002	.004	.005

TABLE A-2(CONTINUED)

WAVELENGTH OF UPPER ARRAY = 2.18 MICRONS
WAVELENGTH OF LOWER ARRAY = 2.36 MICRONS
UNITS = .03020 WATTS/SQCM/MICRON/STERADIAN
HORIZONTAL DISTANCE FROM AXIS OF SYMMETRY - MM

HT	0.0	1.0	2.0	3.0	4.0	5.0	6.0	7.0	8.0	9.0	10.0
2.0	.005	.005	.005	.005	.005	.005	.005	.001	.000	.000	.000
1.9	.005	.005	.005	.005	.005	.005	.005	.001	.000	.000	.000
1.8	.005	.005	.005	.005	.005	.005	.005	.002	.000	.000	.000
1.7	.005	.005	.005	.005	.005	.005	.005	.003	.000	.000	.000
1.6	.005	.005	.005	.005	.005	.005	.005	.003	.000	.000	.000
1.5	.005	.005	.005	.005	.005	.005	.005	.004	.000	.000	.000
1.4	.005	.005	.005	.005	.005	.005	.005	.005	.000	.000	.000
1.3	.007	.006	.006	.006	.005	.005	.005	.005	.001	.000	.000
1.2	.010	.007	.007	.007	.005	.005	.005	.005	.002	.000	.000
1.1	.012	.009	.009	.009	.005	.005	.005	.005	.004	.000	.000
1.0	.015	.010	.010	.010	.005	.005	.005	.005	.005	.000	.000
0.9	.215	.190	.138	.052	.007	.007	.005	.005	.005	.000	.000
0.8	.415	.371	.267	.094	.010	.010	.005	.005	.005	.000	.000
0.7	.660	.623	.539	.403	.225	.035	.007	.007	.005	.002	.000
0.6	.905	.875	.811	.712	.440	.059	.010	.010	.005	.005	.000
0.5	.722	.774	.801	.808	.719	.487	.198	.015	.010	.005	.000
0.4	.539	.672	.791	.905	.998	.914	.386	.020	.015	.005	.000
0.3	.353	.452	.541	.630	.699	.672	.341	.025	.012	.005	.000
0.2	.168	.232	.292	.356	.400	.430	.297	.030	.010	.005	.000
0.1	.078	.106	.132	.159	.181	.197	.139	.024	.016	.016	.006
0.0	.000	.000	.000	.000	.000	.000	.000	.018	.021	.027	.011
2.0	.005	.005	.005	.005	.005	.005	.005	.001	.000	.000	.000
1.9	.005	.005	.005	.005	.005	.005	.005	.001	.000	.000	.000
1.8	.005	.005	.005	.005	.005	.005	.005	.002	.000	.000	.000
1.7	.005	.005	.005	.005	.005	.005	.005	.003	.000	.000	.000
1.6	.005	.005	.005	.005	.005	.005	.005	.003	.000	.000	.000
1.5	.005	.005	.005	.005	.005	.005	.005	.004	.000	.000	.000
1.4	.005	.005	.005	.005	.005	.005	.005	.005	.000	.000	.000
1.3	.006	.006	.005	.005	.005	.005	.005	.005	.001	.000	.000
1.2	.007	.007	.005	.005	.005	.005	.005	.005	.002	.000	.000
1.1	.008	.008	.005	.005	.005	.005	.005	.005	.003	.000	.000
1.0	.009	.009	.005	.005	.005	.005	.005	.005	.005	.000	.000
0.9	.185	.157	.111	.035	.007	.005	.005	.005	.005	.000	.000
0.8	.360	.304	.217	.065	.009	.005	.005	.005	.005	.000	.000
0.7	.563	.517	.450	.332	.189	.032	.007	.005	.005	.002	.000
0.6	.766	.729	.683	.600	.369	.060	.009	.005	.005	.005	.000
0.5	.609	.648	.676	.678	.602	.441	.201	.009	.007	.005	.000
0.4	.452	.567	.669	.756	.835	.821	.392	.014	.009	.005	.000
0.3	.298	.392	.468	.530	.586	.590	.332	.012	.007	.005	.000
0.2	.143	.217	.268	.304	.337	.360	.272	.009	.005	.005	.000
0.1	.067	.099	.118	.134	.148	.158	.120	.007	.005	.005	.003
0.0	.000	.000	.000	.000	.000	.000	.000	.004	.005	.005	.005

TABLE A-2(CONTINUED)

WAVELENGTH OF UPPER ARRAY = 2.41 MICRONS

WAVELENGTH OF LOWER ARRAY = 2.51 MICRONS

UNITS = .02390 WATTS/SQCM/MICRON/STERADIAN

HORIZONTAL DISTANCE FROM AXIS OF SYMMETRY - MM

HT	0.0	1.0	2.0	3.0	4.0	5.0	6.0	7.0	8.0	9.0	10.0
2.0	.006	.006	.006	.006	.006	.006	.006	.000	.000	.000	.000
1.9	.006	.006	.006	.006	.006	.006	.006	.000	.000	.000	.000
1.8	.006	.006	.006	.006	.006	.006	.006	.000	.000	.000	.000
1.7	.006	.006	.006	.006	.006	.006	.006	.000	.000	.000	.000
1.6	.006	.006	.006	.006	.006	.006	.006	.000	.000	.000	.000
1.5	.006	.006	.006	.006	.006	.006	.006	.000	.000	.000	.000
1.4	.006	.006	.006	.006	.006	.006	.006	.000	.000	.000	.000
1.3	.009	.009	.009	.007	.007	.006	.006	.001	.001	.000	.000
1.2	.011	.011	.011	.009	.009	.006	.006	.003	.003	.000	.000
1.1	.014	.014	.014	.010	.010	.006	.006	.004	.004	.000	.000
1.0	.017	.017	.017	.011	.011	.006	.006	.006	.006	.000	.000
0.9	.218	.189	.143	.057	.017	.006	.006	.006	.006	.000	.000
0.8	.419	.361	.270	.103	.023	.006	.006	.006	.006	.000	.000
0.7	.660	.580	.453	.261	.155	.026	.009	.006	.006	.003	.000
0.6	.901	.798	.637	.419	.287	.046	.011	.006	.006	.006	.000
0.5	.729	.746	.729	.671	.643	.436	.115	.011	.006	.006	.000
0.4	.557	.694	.821	.924	.998	.826	.218	.017	.006	.006	.000
0.3	.370	.465	.551	.628	.691	.631	.298	.046	.009	.006	.000
0.2	.184	.235	.281	.333	.384	.436	.379	.075	.011	.006	.000
0.1	.092	.115	.134	.157	.176	.198	.170	.039	.008	.006	.000
0.0	.001	.000	.000	.000	.000	.000	.000	.003	.005	.006	.000
2.0	.008	.008	.007	.006	.006	.006	.006	.001	.000	.000	.000
1.9	.010	.010	.009	.007	.007	.006	.006	.001	.000	.000	.000
1.8	.013	.013	.010	.008	.008	.006	.006	.002	.000	.000	.000
1.7	.015	.015	.012	.009	.009	.006	.006	.003	.000	.000	.000
1.6	.018	.018	.014	.010	.010	.006	.006	.004	.000	.000	.000
1.5	.020	.020	.015	.010	.010	.006	.006	.005	.000	.000	.000
1.4	.022	.022	.017	.011	.011	.006	.006	.006	.000	.000	.000
1.3	.032	.032	.028	.024	.024	.015	.013	.010	.003	.000	.000
1.2	.042	.042	.039	.037	.037	.025	.020	.014	.006	.000	.000
1.1	.052	.052	.051	.049	.049	.035	.027	.018	.008	.000	.000
1.0	.062	.062	.062	.062	.062	.045	.034	.022	.011	.000	.000
0.9	.256	.236	.191	.115	.051	.028	.022	.014	.008	.000	.000
0.8	.449	.410	.320	.169	.039	.011	.011	.006	.006	.000	.000
0.7	.666	.626	.550	.424	.264	.065	.034	.022	.014	.006	.000
0.6	.882	.843	.781	.680	.489	.118	.056	.039	.022	.011	.000
0.5	.730	.775	.795	.784	.719	.396	.090	.062	.034	.008	.000
0.4	.579	.708	.809	.887	.949	.674	.124	.084	.045	.006	.000
0.3	.418	.506	.579	.635	.685	.562	.242	.107	.062	.022	.006
0.2	.258	.303	.348	.382	.421	.449	.359	.129	.079	.039	.011
0.1	.140	.160	.182	.200	.220	.232	.197	.100	.079	.065	.021
0.0	.022	.016	.016	.018	.019	.015	.034	.072	.079	.090	.030

TABLE A-2(CONTINUED)

WAVELENGTH OF UPPER ARRAY = 2.54 MICRONS
WAVELENGTH OF LOWER ARRAY = 2.62 MICRONS
UNITS = .02230 WATTS/SQCM/MICRON/STERADIAN
HORIZONTAL DISTANCE FROM AXIS OF SYMMETRY - MM

HT	0.0	1.0	2.0	3.0	4.0	5.0	6.0	7.0	8.0	9.0	10.0
2.0	.019	.019	.019	.013	.013	.013	.013	.002	.000	.000	.000
1.9	.020	.020	.019	.014	.014	.014	.014	.005	.000	.000	.000
1.8	.021	.021	.019	.015	.015	.015	.015	.008	.000	.000	.000
1.7	.022	.022	.019	.016	.016	.016	.016	.010	.000	.000	.000
1.6	.023	.023	.019	.017	.017	.017	.017	.013	.000	.000	.000
1.5	.024	.024	.019	.018	.018	.018	.018	.016	.000	.000	.000
1.4	.025	.025	.019	.019	.019	.019	.019	.019	.000	.000	.000
1.3	.041	.037	.033	.033	.031	.030	.027	.023	.005	.000	.000
1.2	.056	.050	.047	.047	.044	.041	.034	.028	.009	.000	.000
1.1	.072	.062	.061	.061	.056	.051	.042	.033	.014	.000	.000
1.0	.087	.075	.075	.075	.069	.062	.050	.037	.019	.000	.000
0.9	.271	.243	.200	.119	.062	.047	.037	.031	.019	.006	.000
0.8	.456	.412	.324	.162	.056	.031	.025	.025	.019	.012	.000
0.7	.680	.640	.568	.446	.309	.122	.062	.056	.037	.016	.000
0.6	.905	.867	.811	.730	.562	.212	.100	.087	.056	.019	.000
0.5	.758	.802	.833	.836	.780	.527	.172	.112	.062	.022	.000
0.4	.612	.736	.855	.942	.998	.842	.243	.137	.069	.025	.000
0.3	.446	.546	.640	.714	.768	.702	.346	.162	.087	.041	.012
0.2	.281	.356	.424	.487	.537	.562	.449	.187	.106	.056	.025
0.1	.153	.189	.222	.253	.278	.292	.244	.138	.103	.085	.029
0.0	.026	.022	.020	.019	.019	.023	.038	.088	.099	.113	.032
2.0	.018	.017	.017	.017	.017	.017	.015	.001	.000	.000	.000
1.9	.020	.018	.018	.018	.018	.018	.014	.002	.000	.000	.000
1.8	.023	.019	.019	.019	.019	.019	.013	.003	.000	.000	.000
1.7	.025	.021	.021	.021	.021	.021	.012	.004	.000	.000	.000
1.6	.027	.022	.022	.022	.022	.022	.010	.006	.000	.000	.000
1.5	.030	.023	.023	.023	.023	.023	.009	.007	.000	.000	.000
1.4	.032	.024	.024	.024	.024	.024	.008	.008	.000	.000	.000
1.3	.038	.032	.032	.032	.032	.030	.016	.014	.004	.000	.000
1.2	.044	.040	.040	.040	.040	.036	.024	.020	.008	.000	.000
1.1	.050	.048	.048	.048	.048	.042	.032	.026	.012	.000	.000
1.0	.056	.056	.056	.056	.056	.048	.040	.032	.016	.000	.000
0.9	.213	.189	.153	.089	.048	.040	.032	.028	.016	.004	.000
0.8	.370	.322	.250	.121	.040	.032	.024	.024	.016	.008	.000
0.7	.543	.495	.423	.310	.181	.072	.044	.036	.028	.012	.004
0.6	.717	.668	.596	.499	.322	.113	.064	.048	.040	.016	.008
0.5	.596	.632	.648	.620	.576	.370	.125	.056	.040	.024	.012
0.4	.475	.596	.700	.741	.829	.628	.185	.064	.040	.032	.016
0.3	.338	.419	.499	.539	.600	.511	.254	.093	.052	.040	.020
0.2	.201	.242	.298	.338	.370	.395	.322	.121	.064	.048	.024
0.1	.110	.127	.152	.169	.183	.193	.162	.075	.051	.044	.020
0.0	.018	.013	.005	.000	.000	.000	.002	.029	.037	.039	.015

TABLE A-2(CONTINUED)

WAVELENGTH OF UPPER ARRAY = 2.74 MICRONS
WAVELENGTH OF LOWER ARRAY = 2.88 MICRONS
UNITS = .02230 WATTS/SQCM/MICRON/STERADIAN
HORIZONTAL DISTANCE FROM AXIS OF SYMMETRY - MM

HT	0.0	1.0	2.0	3.0	4.0	5.0	6.0	7.0	8.0	9.0	10.0
2.0	.047	.047	.040	.040	.031	.030	.021	.003	.000	.000	.000
1.9	.054	.054	.048	.048	.040	.038	.027	.007	.000	.000	.000
1.8	.061	.061	.057	.057	.048	.045	.033	.010	.000	.000	.000
1.7	.069	.069	.065	.065	.057	.052	.039	.014	.000	.000	.000
1.6	.076	.076	.074	.074	.065	.060	.046	.017	.000	.000	.000
1.5	.083	.083	.082	.082	.074	.067	.052	.021	.000	.000	.000
1.4	.091	.091	.091	.091	.082	.074	.058	.025	.000	.000	.000
1.3	.121	.119	.115	.109	.097	.084	.064	.033	.010	.000	.000
1.2	.152	.148	.140	.128	.111	.095	.070	.041	.021	.000	.000
1.1	.183	.177	.165	.146	.125	.105	.076	.049	.031	.000	.000
1.0	.214	.206	.189	.165	.140	.115	.082	.058	.041	.000	.000
0.9	.379	.354	.309	.222	.160	.123	.091	.066	.045	.021	.000
0.8	.543	.502	.428	.280	.181	.132	.099	.074	.049	.041	.000
0.7	.695	.662	.588	.506	.387	.202	.144	.099	.062	.041	.000
0.6	.848	.823	.749	.732	.592	.272	.189	.123	.074	.041	.000
0.5	.769	.802	.806	.835	.794	.592	.354	.193	.119	.045	.012
0.4	.691	.782	.864	.938	.996	.913	.518	.263	.165	.049	.025
0.3	.547	.613	.683	.741	.790	.769	.539	.284	.177	.082	.037
0.2	.403	.444	.502	.543	.584	.625	.560	.304	.189	.115	.049
0.1	.235	.262	.292	.319	.346	.373	.354	.258	.217	.190	.054
0.0	.067	.080	.081	.094	.107	.120	.148	.211	.245	.265	.059
2.0	.033	.033	.032	.027	.014	.014	.013	.002	.000	.000	.000
1.9	.038	.038	.037	.031	.018	.016	.015	.005	.000	.000	.000
1.8	.043	.043	.041	.035	.021	.019	.016	.007	.000	.000	.000
1.7	.049	.049	.045	.039	.025	.021	.018	.010	.000	.000	.000
1.6	.054	.054	.050	.044	.028	.024	.020	.012	.000	.000	.000
1.5	.059	.059	.054	.048	.031	.026	.022	.015	.000	.000	.000
1.4	.064	.064	.058	.052	.035	.029	.023	.017	.000	.000	.000
1.3	.091	.091	.087	.080	.061	.051	.039	.028	.007	.000	.000
1.2	.119	.119	.116	.107	.087	.073	.055	.038	.015	.000	.000
1.1	.147	.147	.145	.135	.113	.094	.071	.048	.022	.000	.000
1.0	.174	.174	.174	.163	.139	.116	.087	.058	.029	.000	.000
0.9	.322	.299	.264	.200	.139	.099	.070	.046	.026	.000	.000
0.8	.470	.424	.354	.238	.139	.081	.052	.035	.023	.000	.000
0.7	.621	.584	.529	.444	.319	.168	.105	.070	.046	.015	.000
0.6	.772	.743	.703	.651	.500	.256	.157	.105	.070	.029	.000
0.5	.685	.726	.749	.755	.700	.555	.340	.163	.102	.055	.017
0.4	.598	.709	.796	.860	.900	.854	.523	.221	.134	.081	.035
0.3	.476	.566	.639	.694	.729	.712	.494	.261	.160	.119	.038
0.2	.354	.424	.482	.529	.558	.569	.465	.302	.186	.157	.041
0.1	.216	.252	.284	.311	.327	.335	.293	.216	.156	.127	.060
0.0	.077	.081	.086	.093	.096	.101	.121	.130	.126	.097	.080

TABLE A-2(CONTINUED)

WAVELENGTH OF UPPER ARRAY = 2.94 MICRONS
WAVELENGTH OF LOWER ARRAY = 3.08 MICRONS
UNITS = .01790 WATTS/SQCM/MICRON/STERADIAN
HORIZONTAL DISTANCE FROM AXIS OF SYMMETRY - MM

HT	0.0	1.0	2.0	3.0	4.0	5.0	6.0	7.0	8.0	9.0	10.0
2.0	.020	.020	.020	.020	.019	.017	.016	.002	.001	.000	.000
1.9	.028	.028	.028	.026	.024	.020	.018	.004	.002	.000	.000
1.8	.035	.035	.035	.032	.029	.023	.020	.006	.003	.000	.000
1.7	.043	.043	.043	.039	.035	.027	.023	.008	.004	.000	.000
1.6	.050	.050	.050	.045	.040	.030	.025	.010	.005	.000	.000
1.5	.058	.058	.058	.051	.045	.033	.027	.012	.006	.000	.000
1.4	.065	.065	.065	.058	.051	.036	.029	.014	.007	.000	.000
1.3	.087	.085	.085	.078	.071	.056	.045	.027	.013	.004	.000
1.2	.108	.105	.105	.098	.090	.076	.061	.040	.018	.007	.000
1.1	.130	.125	.125	.118	.110	.096	.078	.052	.024	.011	.000
1.0	.152	.145	.145	.137	.130	.116	.094	.065	.029	.014	.000
0.9	.318	.289	.246	.177	.123	.101	.080	.058	.036	.018	.000
0.8	.485	.434	.347	.217	.116	.087	.065	.051	.043	.022	.000
0.7	.702	.644	.564	.456	.340	.242	.148	.094	.058	.022	.000
0.6	.919	.854	.781	.694	.564	.398	.231	.137	.072	.022	.000
0.5	.788	.806	.817	.814	.781	.658	.351	.166	.105	.051	.014
0.4	.658	.759	.854	.933	.998	.919	.470	.195	.137	.080	.029
0.3	.510	.590	.665	.734	.792	.763	.470	.253	.170	.105	.043
0.2	.362	.420	.477	.535	.586	.608	.470	.311	.203	.130	.058
0.1	.222	.255	.292	.322	.352	.365	.314	.249	.207	.175	.066
0.0	.082	.091	.108	.108	.117	.123	.158	.188	.211	.221	.074
2.0	.015	.015	.015	.015	.009	.008	.008	.001	.000	.000	.000
1.9	.016	.016	.016	.016	.011	.009	.009	.002	.000	.000	.000
1.8	.018	.018	.018	.018	.013	.010	.010	.003	.000	.000	.000
1.7	.019	.019	.019	.019	.015	.011	.011	.004	.000	.000	.000
1.6	.020	.020	.020	.020	.018	.012	.012	.005	.000	.000	.000
1.5	.021	.021	.021	.021	.020	.013	.013	.006	.000	.000	.000
1.4	.022	.022	.022	.022	.022	.015	.015	.007	.000	.000	.000
1.3	.029	.029	.029	.027	.027	.020	.016	.011	.002	.000	.000
1.2	.036	.036	.036	.033	.033	.025	.018	.015	.004	.000	.000
1.1	.044	.044	.044	.038	.038	.031	.020	.018	.005	.000	.000
1.0	.051	.051	.051	.044	.044	.036	.022	.022	.007	.000	.000
0.9	.203	.181	.134	.073	.051	.044	.029	.025	.011	.000	.000
0.8	.356	.312	.218	.102	.058	.051	.036	.029	.015	.000	.000
0.7	.519	.464	.370	.247	.152	.080	.044	.029	.018	.004	.000
0.6	.682	.617	.523	.392	.247	.109	.051	.029	.022	.007	.000
0.5	.559	.562	.548	.508	.457	.359	.152	.051	.033	.015	.000
0.4	.435	.508	.573	.624	.668	.610	.254	.073	.044	.022	.000
0.3	.345	.403	.450	.490	.523	.501	.269	.091	.058	.036	.015
0.2	.254	.298	.327	.356	.377	.392	.283	.109	.073	.051	.029
0.1	.147	.166	.182	.195	.208	.215	.172	.096	.085	.080	.033
0.0	.040	.034	.038	.034	.039	.037	.060	.084	.097	.109	.037

TABLE A-2(CONTINUED)

WAVELENGTH OF UPPER ARRAY = 3.15 MICRONS

WAVELENGTH OF LOWER ARRAY = 3.36 MICRONS

UNITS = .01160 WATTS/SQCM/MICRON/STERADIAN

HORIZONTAL DISTANCE FROM AXIS OF SYMMETRY - MM

HT	0.0	1.0	2.0	3.0	4.0	5.0	6.0	7.0	8.0	9.0	10.0
2.0	.024	.024	.024	.024	.022	.021	.021	.001	.000	.000	.000
1.9	.025	.025	.025	.025	.022	.019	.019	.003	.000	.000	.000
1.8	.027	.027	.027	.027	.022	.018	.018	.005	.000	.000	.000
1.7	.029	.029	.029	.029	.022	.016	.016	.006	.000	.000	.000
1.6	.030	.030	.030	.030	.022	.015	.015	.008	.000	.000	.000
1.5	.032	.032	.032	.032	.022	.013	.013	.010	.000	.000	.000
1.4	.034	.034	.034	.034	.022	.011	.011	.011	.000	.000	.000
1.3	.037	.037	.037	.037	.025	.017	.014	.014	.003	.000	.000
1.2	.039	.039	.039	.039	.028	.022	.017	.017	.006	.000	.000
1.1	.042	.042	.042	.042	.031	.028	.020	.020	.008	.000	.000
1.0	.045	.045	.045	.045	.034	.034	.022	.022	.011	.000	.000
0.9	.247	.208	.157	.079	.028	.028	.017	.017	.011	.000	.000
0.8	.449	.371	.270	.112	.022	.022	.011	.011	.011	.000	.000
0.7	.685	.623	.534	.399	.275	.230	.034	.022	.017	.011	.000
0.6	.921	.876	.797	.685	.528	.438	.056	.034	.022	.022	.000
0.5	.758	.803	.814	.809	.764	.696	.292	.045	.034	.022	.006
0.4	.595	.730	.831	.932	.*00	.955	.528	.056	.045	.022	.011
0.3	.494	.584	.651	.713	.753	.730	.472	.095	.045	.022	.011
0.2	.393	.438	.472	.494	.505	.505	.416	.135	.045	.022	.011
0.1	.246	.266	.280	.290	.295	.295	.256	.135	.096	.086	.081
0.0	.100	.093	.089	.086	.084	.084	.096	.135	.147	.150	.152
2.0	.011	.011	.011	.011	.011	.011	.011	.001	.000	.000	.000
1.9	.011	.011	.011	.011	.011	.011	.011	.003	.000	.000	.000
1.8	.011	.011	.011	.011	.011	.011	.011	.005	.000	.000	.000
1.7	.011	.011	.011	.011	.011	.011	.011	.006	.000	.000	.000
1.6	.011	.011	.011	.011	.011	.011	.011	.008	.000	.000	.000
1.5	.011	.011	.011	.011	.011	.011	.011	.010	.000	.000	.000
1.4	.011	.011	.011	.011	.011	.011	.011	.011	.000	.000	.000
1.3	.014	.014	.014	.011	.011	.011	.011	.011	.003	.000	.000
1.2	.017	.017	.017	.011	.011	.011	.011	.011	.006	.000	.000
1.1	.020	.020	.020	.011	.011	.011	.011	.011	.009	.000	.000
1.0	.023	.023	.023	.011	.011	.011	.011	.011	.011	.000	.000
0.9	.182	.160	.114	.040	.029	.011	.011	.011	.011	.000	.000
0.8	.342	.297	.205	.068	.046	.011	.011	.011	.011	.000	.000
0.7	.536	.496	.416	.291	.188	.114	.011	.011	.011	.006	.000
0.6	.730	.696	.627	.513	.331	.217	.011	.011	.011	.011	.000
0.5	.582	.633	.662	.667	.627	.547	.268	.011	.011	.011	.000
0.4	.433	.570	.696	.821	.924	.878	.525	.011	.011	.011	.000
0.3	.399	.468	.530	.593	.639	.616	.376	.017	.011	.011	.006
0.2	.365	.365	.365	.365	.354	.354	.228	.023	.011	.011	.011
0.1	.313	.320	.320	.320	.315	.308	.241	.133	.109	.063	.018
0.0	.261	.274	.274	.274	.276	.263	.254	.243	.206	.115	.024

TABLE A-2(CONTINUED)

WAVELENGTH OF UPPER ARRAY = 3.57 MICRONS

WAVELENGTH OF LOWER ARRAY = 3.78 MICRONS

UNITS = .00710 WATTS/SQCM/MICRON/STERADIAN

HORIZONTAL DISTANCE FROM AXIS OF SYMMETRY - MM

HT	0.0	1.0	2.0	3.0	4.0	5.0	6.0	7.0	8.0	9.0	10.0
2.0	.019	.019	.019	.019	.019	.019	.019	.002	.000	.000	.000
1.9	.019	.019	.019	.019	.019	.019	.019	.005	.000	.000	.000
1.8	.019	.019	.019	.019	.019	.019	.019	.008	.000	.000	.000
1.7	.019	.019	.019	.019	.019	.019	.019	.011	.000	.000	.000
1.6	.019	.019	.019	.019	.019	.019	.019	.013	.000	.000	.000
1.5	.019	.019	.019	.019	.019	.019	.019	.016	.000	.000	.000
1.4	.019	.019	.019	.019	.019	.019	.019	.019	.000	.000	.000
1.3	.019	.019	.019	.019	.019	.019	.019	.019	.000	.000	.000
1.2	.019	.019	.019	.019	.019	.019	.019	.019	.000	.000	.000
1.1	.019	.019	.019	.019	.019	.019	.019	.019	.000	.000	.000
1.0	.019	.019	.019	.019	.019	.019	.019	.019	.000	.000	.000
0.9	.228	.200	.152	.057	.019	.019	.019	.019	.010	.000	.000
0.8	.438	.381	.286	.095	.019	.019	.019	.019	.019	.000	.000
0.7	.714	.657	.562	.390	.228	.076	.029	.019	.019	.000	.000
0.6	.990	.933	.838	.685	.438	.133	.038	.019	.019	.000	.000
0.5	.771	.828	.847	.809	.705	.486	.162	.019	.019	.000	.000
0.4	.552	.724	.857	.933	.971	.838	.286	.019	.019	.000	.000
0.3	.419	.514	.590	.647	.685	.638	.286	.029	.019	.010	.000
0.2	.286	.305	.324	.362	.400	.438	.286	.038	.019	.019	.000
0.1	.199	.207	.205	.221	.227	.243	.177	.060	.051	.051	.011
0.0	.113	.110	.086	.080	.054	.048	.069	.081	.084	.084	.022
2.0	.020	.020	.020	.020	.020	.020	.020	.002	.000	.000	.000
1.9	.020	.020	.020	.020	.020	.020	.020	.005	.000	.000	.000
1.8	.020	.020	.020	.020	.020	.020	.020	.008	.000	.000	.000
1.7	.020	.020	.020	.020	.020	.020	.020	.011	.000	.000	.000
1.6	.020	.020	.020	.020	.020	.020	.020	.014	.000	.000	.000
1.5	.020	.020	.020	.020	.020	.020	.020	.017	.000	.000	.000
1.4	.020	.020	.020	.020	.020	.020	.020	.020	.000	.000	.000
1.3	.020	.020	.020	.020	.020	.020	.020	.020	.000	.000	.000
1.2	.020	.020	.020	.020	.020	.020	.020	.020	.000	.000	.000
1.1	.020	.020	.020	.020	.020	.020	.020	.020	.000	.000	.000
1.0	.020	.020	.020	.020	.020	.020	.020	.020	.000	.000	.000
0.9	.205	.166	.127	.059	.020	.020	.020	.020	.010	.000	.000
0.8	.391	.313	.234	.098	.020	.020	.020	.020	.020	.000	.000
0.7	.605	.557	.498	.410	.303	.166	.029	.029	.020	.000	.000
0.6	.820	.801	.762	.723	.586	.313	.039	.039	.020	.000	.000
0.5	.645	.674	.703	.723	.684	.527	.186	.029	.020	.000	.000
0.4	.469	.547	.645	.723	.781	.742	.332	.020	.020	.000	.000
0.3	.322	.391	.469	.527	.566	.557	.293	.039	.020	.010	.000
0.2	.176	.234	.293	.332	.352	.371	.254	.059	.020	.020	.000
0.1	.098	.123	.149	.166	.174	.182	.132	.047	.031	.031	.011
0.0	.020	.012	.004	.000	.000	.000	.010	.036	.042	.042	.022

TABLE A-2(CONTINUED)

WAVELENGTH OF UPPER ARRAY = 3.99 MICRONS — WAVELENGTH OF LOWER ARRAY = 4.19 MICRONS

UNITS = .00780 WATTS/SQCM/MICRON/STERADIAN

HORIZONTAL DISTANCE FROM AXIS OF SYMMETRY - MM

HT	0.0	1.0	2.0	3.0	4.0	5.0	6.0	7.0	8.0	9.0	10.0
2.0	.018	.018	.018	.018	.018	.018	.018	.002	.000	.000	.000
1.9	.018	.018	.018	.018	.018	.018	.018	.005	.000	.000	.000
1.8	.018	.018	.018	.018	.018	.018	.018	.008	.000	.000	.000
1.7	.018	.018	.018	.018	.018	.018	.018	.010	.000	.000	.000
1.6	.018	.018	.018	.018	.018	.018	.018	.013	.000	.000	.000
1.5	.018	.018	.018	.018	.018	.018	.018	.016	.000	.000	.000
1.4	.018	.018	.018	.018	.018	.018	.018	.018	.000	.000	.000
1.3	.023	.018	.018	.018	.018	.018	.018	.018	.000	.000	.000
1.2	.027	.018	.018	.018	.018	.018	.018	.018	.000	.000	.000
1.1	.032	.018	.018	.018	.018	.018	.018	.018	.000	.000	.000
1.0	.037	.018	.018	.018	.018	.018	.018	.018	.000	.000	.000
0.9	.164	.137	.110	.055	.027	.018	.018	.018	.009	.000	.000
0.8	.292	.256	.201	.091	.037	.018	.018	.018	.018	.000	.000
0.7	.466	.448	.411	.347	.247	.073	.018	.018	.018	.009	.000
0.6	.640	.640	.621	.603	.457	.128	.018	.018	.018	.018	.000
0.5	.503	.530	.548	.567	.512	.329	.137	.018	.018	.018	.000
0.4	.366	.420	.475	.530	.567	.530	.256	.018	.018	.018	.000
0.3	.247	.302	.347	.393	.420	.402	.219	.027	.018	.018	.000
0.2	.128	.183	.219	.256	.274	.274	.183	.037	.018	.018	.000
0.1	.086	.110	.126	.142	.139	.139	.100	.037	.029	.029	.010
0.0	.045	.037	.032	.027	.004	.004	.017	.037	.039	.039	.021
2.0	.122	.119	.117	.101	.101	.082	.063	.011	.004	.000	.000
1.9	.133	.128	.123	.109	.109	.090	.071	.025	.010	.000	.000
1.8	.144	.136	.128	.117	.117	.098	.080	.039	.015	.000	.000
1.7	.155	.144	.134	.126	.126	.107	.088	.053	.021	.000	.000
1.6	.166	.153	.139	.134	.134	.115	.096	.066	.027	.000	.000
1.5	.177	.161	.145	.142	.142	.123	.105	.080	.032	.000	.000
1.4	.188	.169	.150	.150	.150	.132	.113	.094	.038	.000	.000
1.3	.221	.202	.188	.183	.174	.155	.132	.108	.056	.005	.000
1.2	.254	.235	.226	.216	.197	.179	.150	.122	.075	.009	.000
1.1	.287	.268	.263	.249	.221	.202	.169	.136	.094	.014	.000
1.0	.320	.301	.301	.282	.244	.226	.188	.150	.113	.019	.000
0.9	.574	.545	.527	.433	.329	.273	.216	.169	.132	.038	.000
0.8	.827	.790	.752	.583	.414	.320	.244	.188	.150	.056	.000
0.7	.912	.884	.818	.677	.508	.357	.273	.216	.169	.094	.019
0.6	.997	.978	.884	.771	.602	.395	.301	.244	.188	.132	.038
0.5	.856	.884	.884	.856	.799	.686	.527	.301	.197	.132	.047
0.4	.715	.790	.884	.940	.997	.978	.752	.357	.207	.132	.056
0.3	.639	.696	.752	.799	.827	.827	.658	.357	.216	.132	.056
0.2	.564	.602	.621	.658	.658	.677	.564	.357	.226	.132	.056
0.1	.340	.367	.386	.412	.423	.442	.393	.315	.268	.238	.099
0.0	.115	.132	.150	.167	.188	.207	.222	.272	.311	.345	.142

TABLE A-2(CONTINUED)

WAVELENGTH OF UPPER ARRAY = 4.23 MICRONS
WAVELENGTH OF LOWER ARRAY = 4.27 MICRONS
UNITS = .01790 WATTS/SQCM/MICRON/STERADIAN
HORIZONTAL DISTANCE FROM AXIS OF SYMMETRY - MM

HT	0.0	1.0	2.0	3.0	4.0	5.0	6.0	7.0	8.0	9.0	10.0
2.0	.165	.155	.145	.126	.115	.104	.092	.030	.004	.000	.000
1.9	.186	.177	.165	.145	.133	.119	.102	.045	.010	.000	.000
1.8	.208	.199	.186	.164	.151	.134	.113	.060	.015	.000	.000
1.7	.230	.220	.206	.183	.168	.149	.124	.075	.021	.000	.000
1.6	.251	.242	.226	.201	.186	.164	.135	.090	.026	.000	.000
1.5	.273	.264	.247	.220	.203	.178	.146	.105	.031	.000	.000
1.4	.295	.285	.267	.239	.221	.193	.157	.120	.037	.000	.000
1.3	.320	.306	.285	.258	.237	.207	.170	.134	.060	.007	.000
1.2	.345	.327	.304	.276	.253	.221	.184	.147	.083	.014	.000
1.1	.371	.348	.322	.295	.269	.235	.198	.161	.106	.021	.000
1.0	.396	.368	.341	.313	.285	.249	.212	.175	.129	.028	.000
0.9	.483	.451	.419	.378	.331	.276	.226	.175	.129	.028	.000
0.8	.571	.534	.497	.442	.378	.304	.239	.175	.129	.028	.000
0.7	.649	.617	.580	.529	.465	.378	.304	.226	.161	.046	.055
0.6	.727	.700	.663	.617	.552	.451	.368	.276	.193	.064	.110
0.5	.677	.686	.672	.654	.622	.548	.437	.322	.239	.138	.124
0.4	.626	.672	.681	.691	.691	.645	.506	.368	.285	.212	.138
0.3	.580	.617	.631	.640	.640	.612	.511	.401	.318	.235	.134
0.2	.534	.562	.580	.589	.589	.580	.516	.433	.350	.258	.129
0.1	.351	.368	.381	.385	.391	.392	.364	.333	.303	.268	.056
0.0	.168	.175	.182	.181	.192	.203	.212	.234	.256	.279	.000
2.0	.189	.189	.187	.169	.163	.142	.134	.017	.000	.000	.000
1.9	.221	.221	.217	.198	.184	.161	.142	.038	.000	.000	.000
1.8	.253	.253	.246	.228	.205	.180	.150	.060	.000	.000	.000
1.7	.285	.285	.275	.257	.227	.198	.158	.081	.000	.000	.000
1.6	.318	.318	.305	.287	.248	.217	.166	.103	.000	.000	.000
1.5	.350	.350	.334	.316	.269	.236	.174	.124	.000	.000	.000
1.4	.382	.382	.364	.345	.291	.254	.182	.145	.000	.000	.000
1.3	.409	.404	.386	.364	.314	.273	.204	.168	.045	.009	.000
1.2	.436	.427	.409	.382	.336	.291	.227	.191	.091	.018	.000
1.1	.463	.450	.432	.400	.359	.309	.250	.214	.136	.027	.000
1.0	.491	.473	.454	.418	.382	.327	.273	.236	.182	.036	.000
0.9	.591	.573	.527	.482	.427	.373	.318	.273	.182	.036	.000
0.8	.691	.673	.600	.545	.473	.418	.364	.309	.182	.036	.000
0.7	.791	.772	.718	.663	.591	.518	.427	.354	.245	.136	.036
0.6	.891	.872	.836	.782	.709	.618	.491	.400	.309	.236	.073
0.5	.872	.872	.863	.845	.800	.736	.618	.500	.373	.264	.109
0.4	.854	.872	.891	.909	.891	.854	.745	.600	.436	.291	.145
0.3	.900	.918	.936	.954	.936	.909	.809	.663	.491	.336	.173
0.2	.945	.963	.982	.*00	.982	.963	.872	.727	.545	.382	.200
0.1	.718	.726	.744	.752	.754	.746	.718	.655	.587	.526	.086
0.0	.491	.488	.506	.504	.527	.530	.563	.582	.628	.671	.000

TABLE A-2(CONTINUED)

WAVELENGTH OF UPPER ARRAY = 4.39 MICRONS
WAVELENGTH OF LOWER ARRAY = 4.47 MICRONS
UNITS = .08620 WATTS/SQCM/MICRON/STERADIAN
HORIZONTAL DISTANCE FROM AXIS OF SYMMETRY - MM

HT	0.0	1.0	2.0	3.0	4.0	5.0	6.0	7.0	8.0	9.0	10.0
2.0	.195	.186	.165	.151	.133	.306	.108	.054	.010	.000	.000
1.9	.221	.211	.190	.174	.155	.293	.123	.069	.022	.000	.000
1.8	.248	.236	.215	.198	.176	.281	.138	.084	.034	.000	.000
1.7	.274	.261	.240	.221	.197	.269	.153	.099	.046	.000	.000
1.6	.300	.286	.265	.244	.219	.257	.169	.115	.059	.000	.000
1.5	.326	.311	.290	.267	.240	.245	.184	.130	.071	.000	.000
1.4	.353	.336	.315	.290	.261	.232	.199	.145	.083	.000	.000
1.3	.408	.388	.362	.332	.297	.259	.222	.166	.103	.019	.000
1.2	.463	.440	.409	.373	.332	.286	.245	.187	.122	.037	.000
1.1	.517	.492	.455	.415	.367	.313	.268	.207	.142	.056	.000
1.0	.572	.543	.502	.456	.402	.340	.290	.228	.162	.075	.000
0.9	.672	.651	.616	.556	.475	.398	.319	.247	.172	.071	.000
0.8	.772	.759	.730	.655	.548	.456	.348	.265	.183	.066	.000
0.7	.796	.790	.772	.726	.653	.581	.481	.382	.270	.124	.000
0.6	.821	.821	.813	.796	.759	.705	.614	.498	.357	.183	.000
0.5	.836	.859	.875	.886	.879	.840	.780	.572	.415	.236	.071
0.4	.850	.896	.938	.975	.*00	.975	.946	.647	.473	.290	.141
0.3	.807	.852	.888	.925	.948	.929	.884	.678	.564	.353	.168
0.2	.763	.809	.838	.875	.896	.884	.821	.709	.655	.415	.195
0.1	.506	.543	.569	.604	.630	.641	.630	.599	.594	.504	.084
0.0	.249	.276	.301	.333	.363	.398	.440	.488	.533	.594	.000
2.0	.161	.148	.147	.141	.131	.109	.080	.028	.003	.000	.000
1.9	.183	.169	.165	.157	.145	.122	.092	.042	.007	.000	.000
1.8	.204	.190	.183	.173	.159	.134	.104	.055	.010	.000	.000
1.7	.226	.211	.202	.190	.173	.147	.116	.069	.014	.000	.000
1.6	.247	.232	.220	.206	.188	.160	.128	.083	.017	.000	.000
1.5	.269	.253	.239	.222	.202	.173	.140	.097	.021	.000	.000
1.4	.290	.274	.257	.239	.216	.185	.152	.111	.025	.000	.000
1.3	.337	.321	.302	.280	.253	.217	.178	.135	.052	.008	.000
1.2	.384	.367	.347	.321	.289	.249	.204	.158	.079	.016	.000
1.1	.431	.414	.392	.362	.326	.281	.230	.182	.107	.025	.000
1.0	.478	.461	.436	.403	.362	.313	.255	.206	.134	.033	.000
0.9	.543	.525	.498	.465	.418	.362	.298	.228	.147	.033	.000
0.8	.609	.589	.560	.527	.473	.412	.342	.251	.161	.033	.000
0.7	.654	.640	.619	.589	.539	.478	.410	.301	.196	.068	.000
0.6	.698	.692	.677	.650	.605	.543	.478	.350	.231	.103	.000
0.5	.679	.687	.689	.680	.659	.615	.543	.428	.301	.175	.049
0.4	.661	.683	.700	.710	.712	.687	.609	.506	.370	.247	.099
0.3	.626	.581	.570	.684	.687	.669	.624	.550	.430	.284	.119
0.2	.591	.480	.440	.659	.663	.650	.638	.593	.490	.321	.140
0.1	.384	.357	.359	.472	.490	.501	.509	.502	.465	.396	.177
0.0	.177	.234	.277	.284	.317	.351	.381	.410	.441	.471	.215

TABLE A-2(CONTINUED)

WAVELENGTH OF UPPER ARRAY = 4.59 MICRONS

WAVELENGTH OF LOWER ARRAY = 4.77 MICRONS

UNITS = .03730 WATTS/SQCM/MICRON/STERADIAN

HORIZONTAL DISTANCE FROM AXIS OF SYMMETRY - MM

HT	0.0	1.0	2.0	3.0	4.0	5.0	6.0	7.0	8.0	9.0	10.0
2.0	.099	.098	.096	.091	.080	.065	.046	.007	.000	.000	.000
1.9	.122	.119	.116	.108	.095	.078	.055	.016	.000	.000	.000
1.8	.146	.140	.135	.126	.110	.090	.065	.025	.000	.000	.000
1.7	.169	.162	.154	.143	.125	.103	.074	.033	.000	.000	.000
1.6	.192	.183	.174	.161	.140	.115	.083	.042	.000	.000	.000
1.5	.215	.204	.193	.178	.155	.128	.093	.051	.000	.000	.000
1.4	.238	.225	.213	.196	.170	.140	.102	.060	.000	.000	.000
1.3	.325	.310	.291	.267	.234	.195	.149	.096	.020	.000	.000
1.2	.412	.395	.370	.338	.298	.249	.196	.132	.040	.000	.000
1.1	.500	.480	.449	.409	.361	.303	.242	.168	.061	.000	.000
1.0	.587	.565	.527	.480	.425	.357	.289	.204	.081	.000	.000
0.9	.672	.646	.608	.563	.506	.434	.357	.257	.117	.000	.000
0.8	.757	.727	.689	.646	.587	.510	.425	.310	.153	.000	.000
0.7	.878	.855	.823	.782	.672	.614	.495	.366	.208	.036	.000
0.6	.999	.982	.957	.918	.757	.719	.565	.421	.264	.072	.000
0.5	.969	.967	.957	.940	.859	.821	.704	.572	.398	.185	.023
0.4	.940	.952	.957	.961	.961	.923	.842	.723	.531	.298	.047
0.3	.823	.863	.893	.914	.929	.921	.867	.772	.585	.364	.087
0.2	.706	.774	.829	.867	.897	.918	.893	.821	.638	.429	.128
0.1	.464	.518	.566	.604	.641	.672	.683	.668	.606	.533	.103
0.0	.223	.262	.302	.341	.385	.426	.473	.516	.575	.637	.079
2.0	.011	.011	.011	.010	.010	.006	.005	.001	.000	.000	.000
1.9	.013	.013	.013	.012	.012	.008	.007	.002	.000	.000	.000
1.8	.016	.016	.016	.014	.014	.010	.008	.004	.000	.000	.000
1.7	.018	.018	.018	.016	.016	.011	.009	.005	.000	.000	.000
1.6	.021	.021	.021	.018	.018	.013	.010	.006	.000	.000	.000
1.5	.023	.023	.023	.019	.019	.015	.012	.007	.000	.000	.000
1.4	.026	.026	.026	.021	.021	.017	.013	.009	.000	.000	.000
1.3	.037	.037	.036	.032	.030	.023	.017	.011	.002	.000	.000
1.2	.049	.049	.047	.043	.038	.030	.021	.013	.004	.000	.000
1.1	.061	.061	.058	.053	.047	.036	.026	.015	.006	.000	.000
1.0	.073	.073	.068	.064	.055	.043	.030	.017	.009	.000	.000
0.9	.102	.100	.092	.081	.068	.053	.038	.023	.011	.000	.000
0.8	.132	.128	.115	.098	.081	.064	.047	.030	.013	.000	.000
0.7	.184	.175	.164	.147	.126	.096	.068	.045	.021	.004	.000
0.6	.235	.222	.213	.196	.171	.128	.090	.060	.030	.009	.000
0.5	.224	.224	.226	.222	.213	.186	.141	.090	.055	.023	.000
0.4	.213	.226	.239	.248	.256	.243	.192	.119	.081	.038	.000
0.3	.218	.226	.235	.241	.248	.239	.203	.149	.111	.062	.013
0.2	.222	.226	.230	.235	.239	.235	.213	.179	.141	.085	.026
0.1	.156	.163	.165	.169	.174	.174	.167	.155	.138	.061	.023
0.0	.091	.100	.100	.104	.108	.113	.121	.131	.136	.037	.021

TABLE A-2(CONTINUED)

WAVELENGTH OF UPPER ARRAY = 4.94 MICRONS
WAVELENGTH OF LOWER ARRAY = 5.10 MICRONS
UNITS = .00450 WATTS/SQCM/MICRON/STERADIAN
HORIZONTAL DISTANCE FROM AXIS OF SYMMETRY - MM

HT	0.0	1.0	2.0	3.0	4.0	5.0	6.0	7.0	8.0	9.0	10.0
2.0	.041	.041	.041	.041	.041	.041	.041	.009	.000	.000	.000
1.9	.046	.046	.046	.046	.046	.046	.046	.019	.000	.000	.000
1.8	.051	.051	.051	.051	.051	.051	.051	.030	.000	.000	.000
1.7	.056	.056	.056	.056	.056	.056	.056	.041	.000	.000	.000
1.6	.062	.062	.062	.062	.062	.062	.062	.051	.000	.000	.000
1.5	.067	.067	.067	.067	.067	.067	.067	.062	.000	.000	.000
1.4	.072	.072	.072	.072	.072	.072	.072	.072	.000	.000	.000
1.3	.091	.091	.091	.091	.082	.082	.082	.072	.009	.000	.000
1.2	.109	.109	.109	.109	.091	.091	.091	.072	.018	.000	.000
1.1	.127	.127	.127	.127	.100	.100	.100	.072	.027	.000	.000
1.0	.145	.145	.145	.145	.109	.109	.109	.072	.036	.000	.000
0.9	.290	.290	.254	.181	.091	.091	.091	.054	.036	.018	.000
0.8	.435	.435	.362	.217	.072	.072	.072	.036	.036	.036	.000
0.7	.670	.634	.562	.435	.290	.199	.127	.072	.054	.054	.000
0.6	.906	.834	.761	.652	.507	.326	.181	.109	.072	.072	.000
0.5	.870	.852	.852	.815	.743	.580	.362	.181	.109	.091	.018
0.4	.834	.870	.942	.978	.978	.834	.544	.254	.145	.109	.036
0.3	.906	.924	.942	.942	.924	.834	.598	.344	.217	.145	.054
0.2	.978	.978	.942	.906	.870	.834	.652	.435	.290	.181	.072
0.1	.690	.711	.716	.721	.726	.731	.652	.579	.516	.490	.093
0.0	.402	.443	.489	.535	.581	.628	.652	.723	.743	.799	.114
2.0	.037	.037	.037	.037	.037	.037	.037	.004	.000	.000	.000
1.9	.037	.037	.037	.037	.037	.037	.037	.010	.000	.000	.000
1.8	.037	.037	.037	.037	.037	.037	.037	.015	.000	.000	.000
1.7	.037	.037	.037	.037	.037	.037	.037	.021	.000	.000	.000
1.6	.037	.037	.037	.037	.037	.037	.037	.026	.000	.000	.000
1.5	.037	.037	.037	.037	.037	.037	.037	.032	.000	.000	.000
1.4	.037	.037	.037	.037	.037	.037	.037	.037	.000	.000	.000
1.3	.056	.056	.046	.046	.037	.037	.037	.037	.009	.000	.000
1.2	.074	.074	.056	.056	.037	.037	.037	.037	.019	.000	.000
1.1	.093	.093	.065	.065	.037	.037	.037	.037	.028	.000	.000
1.0	.111	.111	.074	.074	.037	.037	.037	.037	.037	.000	.000
0.9	.222	.185	.130	.093	.056	.037	.037	.037	.037	.000	.000
0.8	.333	.259	.185	.111	.074	.037	.037	.037	.037	.000	.000
0.7	.500	.426	.370	.296	.204	.111	.056	.056	.037	.019	.000
0.6	.667	.593	.556	.482	.333	.185	.074	.074	.037	.037	.000
0.5	.611	.593	.593	.574	.500	.389	.185	.093	.056	.056	.019
0.4	.556	.593	.630	.667	.667	.593	.296	.111	.074	.074	.037
0.3	.519	.556	.574	.611	.611	.556	.352	.167	.093	.074	.037
0.2	.482	.519	.519	.556	.556	.519	.407	.222	.111	.074	.037
0.1	.334	.371	.392	.408	.429	.413	.365	.285	.237	.200	.037
0.0	.187	.224	.266	.261	.303	.308	.323	.349	.364	.327	.037

TABLE A-2(CONTINUED)

WAVELENGTH OF UPPER ARRAY = 5.25 MICRONS

WAVELENGTH OF LOWER ARRAY = 5.37 MICRONS

UNITS = .00240 WATTS/SQCM/MICRON/STERADIAN

HORIZONTAL DISTANCE FROM AXIS OF SYMMETRY - MM

HT	0.0	1.0	2.0	3.0	4.0	5.0	6.0	7.0	8.0	9.0	10.0
2.0	.079	.079	.079	.079	.079	.079	.071	.008	.000	.000	.000
1.9	.090	.090	.090	.090	.090	.090	.071	.019	.000	.000	.000
1.8	.100	.100	.100	.100	.100	.100	.071	.029	.000	.000	.000
1.7	.110	.110	.110	.110	.110	.110	.071	.040	.000	.000	.000
1.6	.121	.121	.121	.121	.121	.121	.071	.050	.000	.000	.000
1.5	.131	.131	.131	.131	.131	.131	.071	.060	.000	.000	.000
1.4	.142	.142	.142	.142	.142	.142	.071	.071	.000	.000	.000
1.3	.159	.159	.159	.142	.142	.142	.071	.071	.018	.000	.000
1.2	.177	.177	.177	.142	.142	.142	.071	.071	.035	.000	.000
1.1	.195	.195	.195	.142	.142	.142	.071	.071	.053	.000	.000
1.0	.212	.212	.212	.142	.142	.142	.071	.071	.071	.000	.000
0.9	.354	.354	.283	.177	.106	.106	.071	.071	.071	.000	.000
0.8	.496	.496	.354	.212	.071	.071	.071	.071	.071	.000	.000
0.7	.743	.743	.602	.460	.319	.177	.106	.106	.071	.000	.000
0.6	.991	.991	.850	.708	.566	.283	.142	.142	.071	.000	.000
0.5	.885	.921	.921	.850	.779	.602	.319	.142	.071	.035	.000
0.4	.779	.850	.991	.991	.991	.921	.496	.142	.071	.071	.000
0.3	.673	.743	.814	.850	.850	.814	.496	.212	.142	.106	.035
0.2	.566	.637	.637	.708	.708	.708	.496	.283	.212	.142	.071
0.1	.406	.436	.436	.467	.507	.507	.415	.323	.293	.262	.071
0.0	.245	.235	.235	.225	.306	.306	.335	.364	.373	.383	.071
2.0	.017	.017	.017	.017	.017	.017	.008	.008	.000	.000	.000
1.9	.038	.038	.038	.038	.038	.038	.019	.019	.000	.000	.000
1.8	.059	.059	.059	.059	.059	.059	.030	.030	.000	.000	.000
1.7	.080	.080	.080	.080	.080	.080	.040	.040	.000	.000	.000
1.6	.102	.102	.102	.102	.102	.102	.051	.051	.000	.000	.000
1.5	.123	.123	.123	.123	.123	.123	.061	.061	.000	.000	.000
1.4	.144	.144	.144	.144	.144	.144	.072	.072	.000	.000	.000
1.3	.162	.144	.144	.144	.144	.144	.090	.072	.018	.000	.000
1.2	.180	.144	.144	.144	.144	.144	.108	.072	.036	.000	.000
1.1	.198	.144	.144	.144	.144	.144	.126	.072	.054	.000	.000
1.0	.216	.144	.144	.144	.144	.144	.144	.072	.072	.000	.000
0.9	.396	.324	.252	.180	.144	.108	.108	.072	.072	.000	.000
0.8	.576	.504	.360	.216	.144	.072	.072	.072	.072	.000	.000
0.7	.720	.648	.504	.360	.252	.144	.108	.108	.072	.036	.000
0.6	.864	.792	.648	.504	.360	.216	.144	.144	.072	.072	.000
0.5	.756	.756	.720	.648	.612	.504	.360	.180	.108	.072	.000
0.4	.648	.720	.792	.792	.864	.792	.576	.216	.144	.072	.000
0.3	.540	.612	.648	.684	.720	.684	.540	.252	.180	.144	.072
0.2	.432	.504	.504	.576	.576	.576	.504	.288	.216	.216	.144
0.1	.309	.340	.340	.371	.371	.412	.381	.288	.257	.257	.103
0.0	.187	.177	.177	.167	.167	.249	.258	.288	.298	.298	.062

TABLE A-2(CONTINUED)

WAVELENGTH OF UPPER ARRAY = 5.47 MICRONS

WAVELENGTH OF LOWER ARRAY = 5.55 MICRONS

UNITS = .00200 WATTS/SQCM/MICRON/STERADIAN

HORIZONTAL DISTANCE FROM AXIS OF SYMMETRY - MM

HT	0.0	1.0	2.0	3.0	4.0	5.0	6.0	7.0	8.0	9.0	10.0
2.0	.021	.021	.021	.021	.021	.021	.021	.010	.000	.000	.000
1.9	.046	.046	.046	.046	.046	.046	.046	.023	.000	.000	.000
1.8	.072	.072	.072	.072	.072	.072	.072	.036	.000	.000	.000
1.7	.098	.098	.098	.098	.098	.098	.098	.049	.000	.000	.000
1.6	.124	.124	.124	.124	.124	.124	.124	.062	.000	.000	.000
1.5	.149	.149	.149	.149	.149	.149	.149	.075	.000	.000	.000
1.4	.175	.175	.175	.175	.175	.175	.175	.088	.000	.000	.000
1.3	.197	.197	.197	.197	.175	.175	.175	.109	.022	.000	.000
1.2	.219	.219	.219	.219	.175	.175	.175	.131	.044	.000	.000
1.1	.241	.241	.241	.241	.175	.175	.175	.153	.066	.000	.000
1.0	.263	.263	.263	.263	.175	.175	.175	.175	.088	.000	.000
0.9	.394	.350	.350	.306	.175	.175	.175	.175	.088	.000	.000
0.8	.525	.438	.438	.350	.175	.175	.175	.175	.088	.000	.000
0.7	.744	.657	.613	.482	.350	.263	.219	.175	.088	.044	.000
0.6	.963	.875	.788	.613	.525	.350	.263	.175	.088	.088	.000
0.5	.832	.788	.788	.700	.700	.569	.350	.219	.131	.131	.088
0.4	.700	.700	.788	.788	.875	.788	.438	.263	.175	.175	.175
0.3	.569	.613	.657	.700	.744	.700	.482	.306	.219	.175	.175
0.2	.438	.525	.525	.613	.613	.613	.525	.350	.263	.175	.175
0.1	.388	.426	.426	.464	.464	.464	.426	.300	.263	.225	.175
0.0	.338	.326	.326	.314	.314	.314	.326	.251	.263	.275	.175
2.0	.021	.021	.021	.021	.021	.010	.010	.010	.000	.000	.000
1.9	.047	.047	.047	.047	.047	.023	.023	.023	.000	.000	.000
1.8	.073	.073	.073	.073	.073	.036	.036	.036	.000	.000	.000
1.7	.099	.099	.099	.099	.099	.049	.049	.049	.000	.000	.000
1.6	.125	.125	.125	.125	.125	.062	.062	.062	.000	.000	.000
1.5	.151	.151	.151	.151	.151	.075	.075	.075	.000	.000	.000
1.4	.177	.177	.177	.177	.177	.088	.088	.088	.000	.000	.000
1.3	.177	.177	.177	.177	.177	.111	.088	.088	.022	.000	.000
1.2	.177	.177	.177	.177	.177	.133	.088	.088	.044	.000	.000
1.1	.177	.177	.177	.177	.177	.155	.088	.088	.066	.000	.000
1.0	.177	.177	.177	.177	.177	.177	.088	.088	.088	.000	.000
0.9	.310	.265	.221	.177	.177	.133	.088	.088	.088	.000	.000
0.8	.442	.354	.265	.177	.177	.088	.088	.088	.088	.000	.000
0.7	.575	.531	.442	.354	.310	.221	.177	.133	.088	.044	.000
0.6	.707	.707	.619	.531	.442	.354	.265	.177	.088	.088	.000
0.5	.663	.663	.619	.575	.531	.442	.310	.221	.133	.088	.000
0.4	.619	.619	.619	.619	.619	.531	.354	.265	.177	.088	.000
0.3	.486	.486	.531	.531	.531	.486	.398	.265	.177	.133	.088
0.2	.354	.354	.442	.442	.442	.442	.442	.265	.177	.177	.177
0.1	.303	.303	.392	.392	.392	.392	.392	.215	.127	.127	.127
0.0	.253	.253	.342	.342	.342	.342	.342	.165	.076	.076	.076

TABLE A-2(CONTINUED)

WAVELENGTH OF UPPER ARRAY = 5.60 MICRONS
WAVELENGTH OF LOWER ARRAY = 5.61 MICRONS
UNITS = .00130 WATTS/SQCM/MICRON/STERADIAN
HORIZONTAL DISTANCE FROM AXIS OF SYMMETRY - MM

HT	0.0	1.0	2.0	3.0	4.0	5.0	6.0	7.0	8.0	9.0	10.0
2.0	.016	.016	.016	.016	.016	.016	.016	.016	.000	.000	.000
1.9	.036	.036	.036	.036	.036	.036	.036	.036	.000	.000	.000
1.8	.056	.056	.056	.056	.056	.056	.056	.056	.000	.000	.000
1.7	.077	.077	.077	.077	.077	.077	.077	.077	.000	.000	.000
1.6	.097	.097	.097	.097	.097	.097	.097	.097	.000	.000	.000
1.5	.117	.117	.117	.117	.117	.117	.117	.117	.000	.000	.000
1.4	.137	.137	.137	.137	.137	.137	.137	.137	.000	.000	.000
1.3	.171	.171	.171	.171	.171	.137	.137	.137	.034	.000	.000
1.2	.205	.205	.205	.205	.205	.137	.137	.137	.068	.000	.000
1.1	.240	.240	.240	.240	.240	.137	.137	.137	.103	.000	.000
1.0	.274	.274	.274	.274	.274	.137	.137	.137	.137	.000	.000
0.9	.411	.411	.411	.274	.274	.137	.137	.137	.137	.000	.000
0.8	.548	.548	.548	.274	.274	.137	.137	.137	.137	.000	.000
0.7	.753	.753	.685	.479	.411	.205	.205	.137	.137	.068	.000
0.6	.958	.958	.822	.685	.548	.274	.274	.137	.137	.137	.000
0.5	.822	.822	.822	.753	.753	.548	.342	.205	.137	.137	.068
0.4	.685	.685	.822	.822	.958	.822	.411	.274	.137	.137	.137
0.3	.616	.616	.685	.685	.753	.685	.411	.342	.274	.205	.137
0.2	.548	.548	.548	.548	.548	.548	.411	.411	.411	.274	.137
0.1	.470	.470	.470	.470	.470	.470	.333	.333	.333	.196	.137
0.0	.392	.392	.392	.392	.392	.392	.255	.255	.255	.118	.137
2.0	.016	.016	.016	.016	.016	.016	.016	.016	.000	.000	.000
1.9	.036	.036	.036	.036	.036	.036	.036	.036	.000	.000	.000
1.8	.056	.056	.056	.056	.056	.056	.056	.056	.000	.000	.000
1.7	.077	.077	.077	.077	.077	.077	.077	.077	.000	.000	.000
1.6	.097	.097	.097	.097	.097	.097	.097	.097	.000	.000	.000
1.5	.117	.117	.117	.117	.117	.117	.117	.117	.000	.000	.000
1.4	.137	.137	.137	.137	.137	.137	.137	.137	.000	.000	.000
1.3	.171	.171	.171	.171	.137	.137	.137	.137	.034	.000	.000
1.2	.206	.206	.206	.206	.137	.137	.137	.137	.069	.000	.000
1.1	.240	.240	.240	.240	.137	.137	.137	.137	.103	.000	.000
1.0	.274	.274	.274	.274	.137	.137	.137	.137	.137	.000	.000
0.9	.412	.343	.343	.274	.206	.137	.137	.137	.137	.000	.000
0.8	.549	.412	.412	.274	.274	.137	.137	.137	.137	.000	.000
0.7	.617	.549	.549	.480	.412	.274	.206	.206	.137	.069	.000
0.6	.686	.686	.686	.686	.549	.412	.274	.274	.137	.137	.000
0.5	.686	.686	.754	.754	.686	.617	.412	.274	.137	.137	.069
0.4	.686	.686	.823	.823	.823	.823	.549	.274	.137	.137	.137
0.3	.617	.617	.686	.686	.686	.617	.480	.274	.137	.137	.137
0.2	.549	.549	.549	.549	.549	.412	.412	.274	.137	.137	.137
0.1	.471	.471	.471	.471	.471	.334	.334	.196	.137	.137	.137
0.0	.393	.393	.393	.393	.393	.256	.256	.118	.137	.137	.137

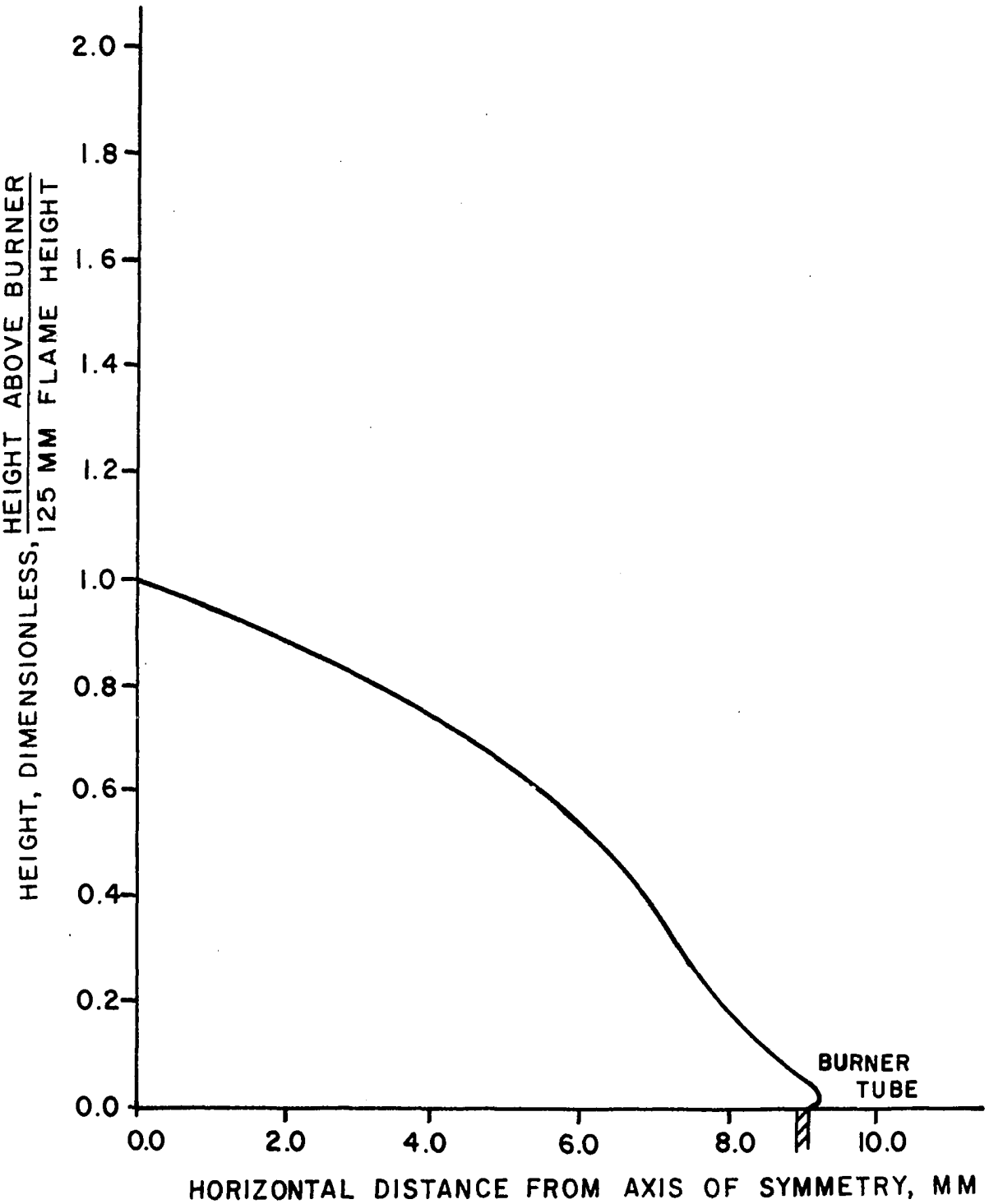

Figure A-3. Outline of Visible Cone for a Laminar Natural Gas Flame.

TABLE A-3

AVERAGE INTENSITY PROFILES FOR A LAMINARE
NATURAL GAS DIFFUSION FLAME

UNITS FACTOR = 0.20 WATTS/CM^2 - MICRON - STERADIAN
HT = DISTANCE ABOVE BURNER/125MM FLAME HEIGHT
ABSOLUTE INTENSITY = (TABLE VALUE) X (UNITS FACTOR)
BAND = 2.54 - 3.15 MICRONS

	HORIZONTAL DISTANCE FROM AXIS OF SYMMETRY - MM										
HT	0.0	1.0	2.0	3.0	4.0	5.0	6.0	7.0	8.0	9.0	10.0
2.0	.033	.033	.032	.031	.028	.024	.013	.003	.000	.000	.000
1.9	.037	.037	.035	.034	.030	.025	.013	.003	.000	.000	.000
1.8	.041	.041	.039	.037	.032	.025	.014	.004	.001	.000	.000
1.7	.046	.045	.043	.041	.034	.026	.015	.004	.001	.000	.000
1.6	.050	.049	.047	.044	.036	.026	.015	.004	.001	.000	.000
1.5	.054	.053	.051	.047	.038	.027	.016	.005	.001	.000	.000
1.4	.058	.057	.055	.050	.040	.027	.017	.005	.001	.000	.000
1.3	.073	.072	.070	.067	.057	.045	.033	.017	.005	.000	.000
1.2	.087	.087	.095	.083	.075	.063	.049	.030	.009	.000	.000
1.1	.101	.101	.101	.099	.092	.080	.065	.042	.014	.000	.000
1.0	.115	.116	.116	.115	.110	.098	.081	.054	.018	.000	.000
0.9	.232	.216	.147	.140	.131	.116	.097	.065	.029	.004	.000
0.8	.349	.316	.177	.165	.152	.135	.113	.077	.039	.008	.000
0.7	.419	.407	.335	.316	.272	.147	.117	.085	.045	.006	.000
0.6	.488	.499	.493	.466	.393	.160	.121	.094	.051	.005	.000
0.5	.405	.419	.420	.407	.366	.238	.200	.144	.061	.004	.000
0.4	.323	.338	.347	.349	.339	.317	.279	.194	.070	.004	.000
0.3	.275	.293	.305	.312	.312	.301	.277	.222	.116	.004	.000
0.2	.227	.248	.263	.276	.286	.286	.276	.250	.162	.003	.000
0.1	.160	.171	.189	.200	.207	.211	.210	.195	.147	.062	.038
0.0	.093	.095	.114	.124	.128	.137	.145	.141	.132	.121	.076

TABLE A-3 (Continued)

UNITS FACTOR = 0.20 WATTS/CM^2 - MICRON - STERADIAN
HT = DISTANCE ABOVE BURNER/125MM FLAME HEIGHT
ABSOLUTE INTENSITY = (TABLE VALUE) X (UNITS FACTOR)
BAND = 4.19 - 4.77

	HORIZONTAL DISTANCE FROM AXIS OF SYMMETRY - MM										
HT	0.0	1.0	2.0	3.0	4.0	5.0	6.0	7.0	8.0	9.0	10.0
2.0	.208	.206	.202	.185	.163	.126	.081	.026	.014	.007	.000
1.9	.249	.248	.242	.223	.198	.158	.105	.043	.026	.013	.000
1.8	.290	.290	.283	.261	.233	.189	.129	.061	.037	.018	.000
1.7	.331	.333	.323	.298	.267	.220	.154	.078	.049	.024	.000
1.6	.371	.374	.364	.336	.302	.252	.178	.096	.060	.030	.000
1.5	.412	.416	.404	.374	.337	.283	.202	.113	.072	.035	.000
1.4	.453	.458	.445	.412	.372	.315	.226	.131	.084	.041	.000
1.3	.498	.499	.485	.453	.413	.356	.271	.176	.102	.038	.000
1.2	.544	.541	.525	.493	.454	.397	.317	.221	.121	.034	.000
1.1	.590	.582	.564	.534	.494	.438	.362	.266	.139	.031	.000
1.0	.636	.624	.604	.575	.535	.479	.408	.310	.157	.027	.000
0.9	.772	.740	.703	.671	.636	.577	.496	.378	.232	.074	.012
0.8	.908	.857	.801	.767	.737	.675	.585	.445	.306	.121	.025
0.7	.896	.849	.800	.764	.724	.654	.556	.437	.298	.136	.021
0.6	.883	.841	.799	.761	.710	.633	.526	.429	.290	.151	.017
0.5	.798	.785	.774	.764	.740	.697	.632	.520	.338	.154	.027
0.4	.714	.730	.750	.766	.770	.761	.738	.612	.386	.157	.037
0.3	.724	.757	.785	.797	.789	.769	.735	.635	.447	.226	.079
0.2	.734	.784	.820	.828	.809	.777	.733	.658	.509	.296	.120
0.1	.510	.549	.580	.594	.596	.591	.578	.544	.459	.326	.172
0.0	.287	.315	.340	.361	.383	.404	.422	.429	.410	.355	.224

TABLE A-3 (Continued)

UNITS FACTOR = 0.20 WATTS/CM^2 - MICRON - STERADIAN
HT = DISTANCE ABOVE BURNER/125MM FLAME HEIGHT
ABSOLUTE INTENSITY = (TABLE VALUE) X (UNITS FACTOR)
BAND = .71 - 2.54, 3.15 - 4.19, 4.77 - 5.60

	HORIZONTAL DISTANCE FROM AXIS OF SYMMETRY - MM										
HT	0.0	1.0	2.0	3.0	4.0	5.0	6.0	7.0	8.0	9.0	10.0
2.0	.007	.008	.008	.008	.006	.003	.002	.001	.000	.000	.000
1.9	.008	.008	.008	.008	.007	.004	.002	.001	.000	.000	.000
1.8	.008	.008	.009	.009	.007	.005	.002	.001	.000	.000	.000
1.7	.008	.009	.009	.009	.008	.005	.003	.001	.000	.000	.000
1.6	.009	.009	.010	.010	.009	.006	.003	.001	.000	.000	.000
1.5	.009	.010	.010	.010	.099	.007	.003	.001	.000	.000	.000
1.4	.009	.010	.011	.011	.010	.007	.003	.001	.000	.000	.000
1.3	.015	.016	.016	.014	.012	.009	.005	.002	.001	.000	.000
1.2	.021	.021	.022	.018	.014	.011	.006	.003	.001	.000	.000
1.1	.026	.027	.027	.022	.017	.012	.007	.004	.001	.000	.000
1.0	.032	.033	.032	.026	.019	.014	.009	.004	.002	.000	.000
0.9	.171	.119	.048	.033	.024	.016	.011	.006	.003	.001	.000
0.8	.309	.205	.063	.041	.030	.019	.013	.007	.004	.001	.000
0.7	.390	.348	.275	.246	.196	.043	.018	.008	.003	.001	.000
0.6	.470	.491	.488	.452	.362	.068	.022	.009	.003	.001	.000
0.5	.345	.363	.367	.349	.296	.130	.072	.020	.004	.001	.000
0.4	.221	.235	.247	.246	.229	.191	.122	.031	.004	.000	.000
0.3	.171	.190	.203	.204	.190	.158	.114	.046	.012	.001	.000
0.2	.122	.145	.159	.163	.152	.125	.107	.061	.019	.001	.000
0.1	.078	.089	.096	.098	.094	.083	.075	.054	.032	.020	.008
0.0	.036	.036	.037	.038	.040	.044	.045	.048	.045	.040	.016

TABLE A-3 (Continued)

UNITS FACTOR = 0.20 WATTS/CM^2 - MICRON - STERADIAN
HT = DISTANCE ABOVE BURNER/125MM FLAME HEIGHT
ABSOLUTE INTENSITY = (TABLE VALUE) X (UNITS FACTOR)
BAND = .71 - 5.60

	HORIZONTAL DISTANCE FROM AXIS OF SYMMETRY - MM										
HT	0.0	1.0	2.0	3.0	4.0	5.0	6.0	7.0	8.0	9.0	10.0
2.0	.041	.041	.040	.038	.033	.025	.015	.005	.002	.001	.000
1.9	.048	.048	.047	.044	.039	.030	.019	.008	.004	.002	.000
1.8	.055	.056	.054	.051	.045	.036	.023	.010	.006	.003	.000
1.7	.062	.063	.061	.057	.051	.041	.027	.013	.008	.004	.000
1.6	.069	.070	.068	.064	.057	.046	.031	.016	.009	.005	.000
1.5	.076	.077	.076	.070	.063	.052	.035	.019	.011	.005	.000
1.4	.083	.084	.083	.077	.069	.057	.039	.022	.013	.006	.000
1.3	.096	.097	.095	.088	.079	.067	.049	.031	.017	.006	.000
1.2	.109	.109	.106	.099	.089	.076	.059	.040	.020	.005	.000
1.1	.122	.121	.118	.110	.099	.086	.069	.048	.024	.005	.000
1.0	.135	.133	.130	.121	.109	.095	.079	.057	.027	.004	.000
0.9	.270	.226	.160	.144	.131	.115	.096	.070	.041	.012	.002
0.8	.406	.319	.190	.167	.153	.134	.113	.083	.054	.030	.004
0.7	.471	.432	.363	.334	.386	.150	.112	.083	.054	.022	.003
0.6	.536	.546	.536	.501	.419	.166	.111	.084	.053	.024	.003
0.5	.422	.435	.436	.420	.372	.230	.173	.112	.062	.025	.004
0.4	.309	.324	.337	.338	.326	.294	.236	.140	.071	.025	.006
0.3	.269	.290	.305	.309	.297	.269	.230	.158	.091	.036	.012
0.2	.229	.255	.273	.279	.269	.245	.224	.176	.112	.046	.018
0.1	.154	.169	.182	.187	.185	.177	.169	.147	.112	.072	.037
0.0	.081	.086	.093	.098	.103	.111	.115	.118	.112	.098	.055

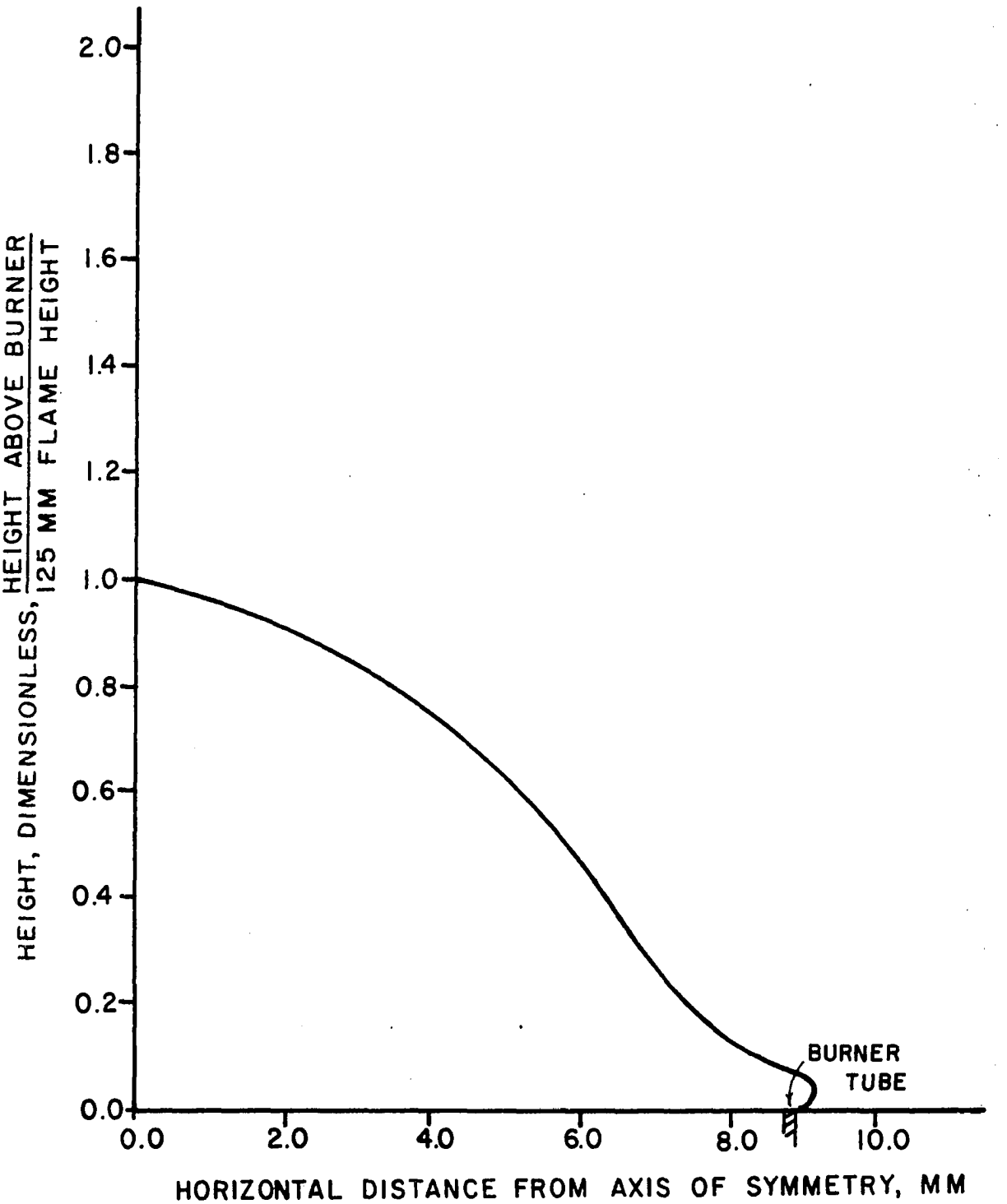

Figure A-4. Outline of Visible Cone for a Laminar Acetone Flame.

TABLE A-4

AVERAGE INTENSITY PROFILES FOR A LAMINAR ACETONE DIFFUSION FLAME

UNITS FACTOR = 0.32 WATTS/CM^2 - MICRON - STERADIAN
HT = DISTANCE ABOVE BURNER/125MM FLAME HEIGHT
ABSOLUTE INTENSITY = (TABLE VALUE) X (UNITS FACTOR)
BAND = 2.54 - 3.15

	HORIZONTAL DISTANCE FROM AXIS OF SYMMETRY - MM										
HT	0.0	1.0	2.0	3.0	4.0	5.0	6.0	7.0	8.0	9.0	10.0
2.0	.018	.018	.016	.015	.012	.011	.010	.001	.000	.000	.000
1.9	.020	.020	.019	.018	.014	.013	.011	.003	.000	.000	.000
1.8	.023	.023	.022	.021	.017	.015	.012	.004	.000	.000	.000
1.7	.026	.026	.025	.024	.020	.017	.014	.005	.000	.000	.000
1.6	.029	.028	.027	.026	.022	.019	.015	.007	.000	.000	.000
1.5	.032	.031	.030	.029	.025	.021	.016	.008	.000	.000	.000
1.4	.035	.034	.033	.031	.027	.023	.017	.010	.000	.000	.000
1.3	.047	.045	.044	.041	.036	.031	.023	.015	.004	.000	.000
1.2	.059	.057	.055	.051	.045	.039	.029	.020	.008	.000	.000
1.1	.071	.069	.066	.061	.055	.046	.035	.024	.012	.000	.000
1.0	.083	.080	.078	.071	.064	.054	.041	.029	.016	.000	.000
0.9	.185	.169	.142	.097	.066	.051	.038	.028	.017	.002	.000
0.8	.287	.257	.207	.123	.067	.048	.035	.027	.018	.004	.000
0.7	.397	.369	.322	.257	.181	.098	.060	.042	.027	.009	.000
0.6	.508	.480	.436	.390	.295	.149	.086	.056	.036	.015	.001
0.5	.438	.457	.463	.461	.432	.328	.168	.078	.049	.023	.007
0.4	.369	.434	.491	.532	.569	.508	.249	.099	.063	.031	.013
0.3	.286	.335	.380	.414	.444	.421	.261	.122	.076	.046	.018
0.2	.203	.235	.269	.297	.319	.334	.274	.145	.089	.061	.024
0.1	.115	.134	.155	.171	.186	.196	.173	.121	.098	.085	.025
0.0	.027	.033	.040	.046	.054	.060	.073	.097	.107	.110	.025

TABLE A-4 (Continued)

UNITS FACTOR = 0.32 WATTS/CM^2 - MICRON - STERADIAN
HT = DISTANCE ABOVE BURNER/125MM FLAME HEIGHT
ABSOLUTE INTENSITY = (TABLE VALUE) X (UNITS FACTOR)
BAND = 4.19 - 4.77

	HORIZONTAL DISTANCE FROM AXIS OF SYMMETRY - MM										
HT	0.0	1.0	2.0	3.0	4.0	5.0	6.0	7.0	8.0	9.0	10.0
2.0	.169	.161	.152	.142	.129	.176	.090	.033	.005	.000	.000
1.9	.195	.185	.175	.163	.147	.181	.103	.047	.010	.000	.000
1.8	.220	.210	.198	.183	.166	.186	.116	.062	.016	.000	.000
1.7	.246	.234	.221	.204	.184	.192	.129	.077	.022	.000	.000
1.6	.271	.259	.244	.225	.202	.197	.142	.091	.028	.000	.000
1.5	.297	.283	.267	.246	.221	.202	.155	.106	.034	.000	.000
1.4	.322	.307	.290	.267	.239	.207	.168	.120	.039	.000	.000
1.3	.385	.368	.345	.318	.284	.244	.199	.147	.065	.010	.000
1.2	.447	.428	.401	.369	.328	.281	.231	.173	.090	.021	.000
1.1	.509	.488	.457	.419	.373	.318	.262	.200	.116	.031	.000
1.0	.571	.548	.513	.470	.418	.354	.293	.226	.141	.041	.000
0.9	.670	.647	.610	.558	.489	.417	.339	.257	.159	.040	.000
0.8	.769	.747	.707	.646	.561	.479	.386	.287	.176	.039	.000
0.7	.848	.831	.800	.752	.667	.589	.486	.368	.239	.088	.004
0.6	.927	.914	.893	.847	.774	.700	.585	.448	.303	.138	.008
0.5	.912	.923	.926	.919	.883	.828	.727	.554	.392	.216	.033
0.4	.897	.931	.959	.982	.993	.957	.870	.660	.481	.295	.059
0.3	.845	.861	.881	.942	.955	.934	.866	.712	.560	.356	.115
0.2	.794	.790	.802	.902	.918	.911	.862	.764	.639	.417	.172
0.1	.531	.550	.574	.636	.662	.677	.673	.645	.606	.506	.130
0.0	.268	.310	.345	.370	.406	.443	.484	.527	.573	.596	.101

TABLE A-4 (Continued)

UNITS FACTOR = 0.32 WATTS/CM^2 - MICRON - STERADIAN
HT = DISTANCE ABOVE BURNER/125MM FLAME HEIGHT
ABSOLUTE INTENSITY = (TABLE VALUE) X (UNITS FACTOR)
BAND = .71 - 2.54, 3.15 - 4.19, 4.77 - 5.60

	HORIZONTAL DISTANCE FROM AXIS OF SYMMETRY - MM										
HT	0.0	1.0	2.0	3.0	4.0	5.0	6.0	7.0	8.0	9.0	10.0
2.0	.007	.007	.007	.007	.007	.007	.006	.001	.000	.000	.000
1.9	.007	.007	.007	.007	.007	.007	.006	.002	.000	.000	.000
1.8	.007	.007	.008	.007	.008	.008	.007	.003	.001	.000	.000
1.7	.008	.008	.008	.008	.008	.008	.007	.004	.001	.000	.000
1.6	.008	.008	.008	.008	.008	.008	.008	.005	.001	.000	.000
1.5	.008	.008	.009	.008	.008	.009	.008	.006	.001	.000	.000
1.4	.009	.009	.009	.009	.009	.009	.008	.007	.002	.000	.000
1.3	.012	.011	.011	.011	.010	.010	.009	.008	.002	.000	.000
1.2	.015	.014	.014	.013	.012	.012	.011	.009	.003	.000	.000
1.1	.018	.017	.017	.016	.014	.014	.012	.010	.004	.000	.000
1.0	.021	.020	.019	.018	.016	.015	.013	.010	.005	.000	.000
0.9	.148	.131	.102	.045	.016	.015	.013	.011	.007	.000	.000
0.8	.276	.241	.186	.071	.017	.014	.013	.012	.910	.001	.000
0.7	.440	.426	.362	.278	.173	.048	.015	.014	.011	.005	.000
0.6	.604	.610	.539	.486	.328	.081	.018	.015	.012	.009	.000
0.5	.496	.548	.554	.562	.511	.367	.150	.018	.014	.010	.001
0.4	.388	.486	.569	.639	.694	.653	.282	.020	.015	.011	.002
0.3	.260	.332	.393	.446	.487	.475	.251	.029	.017	.012	.004
0.2	.131	.178	.216	.253	.280	.298	.221	.038	.019	.014	.005
0.1	.073	.094	.111	.127	.139	.147	.114	.034	.025	.023	.009

TABLE A-4 (Continued)

UNITS FACTOR = 0.32 WATTS/CM^2 - MICRON - STERADIAN
HT = DISTANCE ABOVE BURNER/125MM FLAME HEIGHT
ABSOLUTE INTENSITY = (TABLE VALUE) X (UNITS FACTOR)
BAND = .71 - 5.60

	HORIZONTAL DISTANCE FROM AXIS OF SYMMETRY - MM										
HT	0.0	1.0	2.0	3.0	4.0	5.0	6.0	7.0	8.0	9.0	10.0
2.0	.033	.032	.030	.028	.026	.034	.019	.006	.001	.000	.000
1.9	.038	.036	.034	.032	.030	.035	.022	.009	.002	.000	.000
1.8	.042	.040	.038	.035	.033	.036	.024	.012	.003	.000	.000
1.7	.046	.045	.043	.040	.036	.037	.027	.015	.004	.000	.000
1.6	.051	.049	.047	.044	.040	.038	.029	.019	.005	.000	.000
1.5	.055	.053	.051	.047	.043	.040	.032	.022	.006	.000	.000
1.4	.060	.057	.055	.051	.046	.041	.034	.025	.007	.000	.000
1.3	.073	.070	.067	.062	.056	.049	.040	.030	.012	.002	.000
1.2	.086	.083	.078	.073	.065	.056	.047	.035	.017	.003	.000
1.1	.100	.096	.090	.083	.074	.064	.053	.041	.022	.004	.000
1.0	.113	.108	.102	.094	.083	.072	.059	.046	.027	.006	.000
0.9	.233	.215	.185	.130	.095	.081	.066	.051	.032	.007	.000
0.8	.353	.321	.268	.166	.107	.090	.073	.056	.036	.007	.000
0.7	.497	.481	.424	.348	.250	.137	.093	.071	.048	.018	.001
0.6	.642	.641	.58	.531	.393	.184	.113	.087	.060	.029	.001
0.5	.553	.595	.600	.605	.559	.433	.241	.107	.076	.043	.007
0.4	.464	.548	.619	.678	.724	.682	.368	.128	.092	.057	.012
0.3	.353	.413	.466	.518	.554	.539	.347	.145	.107	.069	.023
0.2	.241	.279	.313	.358	.383	.396	.326	.163	.122	.081	.033
0.1	.149	.169	.187	.211	.225	.234	.207	.139	.123	.105	.029
0.0	.059	.066	.073	.077	.083	.090	.100	.115	.124	.128	.027

APPENDIX B

TABULAR SUMMARY OF MONOCHROMATIC MAXIMUM EMISSION, EXTINCTION, AND VOLUMETRIC EMISSION COEFFICIENTS

TABLE B-1

MONOCHROMATIC MAXIMUM EMISSION COEFFICIENTS FOR
A LAMINAR NATURAL GAS DIFFUSION FLAME

UNITS = WATTS/CM^2 - STERADIAN

WAVELENGTH	HEIGHT = (DISTANCE ABOVE BURNER/FLAME HEIGHT)			
(MICRONS)	0.2	0.4	0.6	0.8
0.71	0.000053	0.000226	0.000334	0.000148
0.72	0.000502	0.001319	0.002545	0.001843
0.73	0.000652	0.002243	0.003591	0.002545
0.75	0.000731	0.003053	0.006853	0.003730
0.78	0.001843	0.005213	0.009577	0.007286
0.83	0.002126	0.007906	0.014750	0.010840
0.88	0.003053	0.011550	0.023390	0.016320
0.94	0.004600	0.017590	0.034140	0.023130
1.01	0.006853	0.025080	0.052270	0.034140
1.10	0.010250	0.036950	0.074900	0.050600
1.19	0.012590	0.049770	0.101700	0.071320
1.30	0.017590	0.067240	0.143100	0.098630
1.36	0.019870	0.073010	0.150000	0.107000
1.42	0.023130	0.086390	0.182500	0.126900
1.55	0.028450	0.114600	0.244400	0.190200
1.69	0.032680	0.131500	0.293800	0.198000
1.84	0.040930	0.158700	0.339900	0.233200
1.87	0.044070	0.159400	0.346200	0.235900
1.95	0.042960	0.150200	0.321200	0.206000
2.00	0.042960	0.153900	0.333600	0.222200
2.07	0.049430	0.190200	0.371900	0.258600
2.17	0.037860	0.147900	0.336800	0.241500
2.36	0.034140	0.123500	0.287800	0.200700
2.43	0.033840	0.116800	0.264400	0.185000
2.54	0.085420	0.202800	0.313400	0.225400
2.64	0.053590	0.120900	0.238900	0.184800
2.74	0.128100	0.215900	0.326600	0.271400
2.78	0.110600	0.185000	0.292800	0.240600
2.88	0.108100	0.195400	0.247400	0.208600
2.94	0.090410	0.159900	0.224900	0.167400
3.15	0.048940	0.065420	0.103800	0.076620
3.35	0.043280	0.040150	0.066330	0.048940
3.57	0.013120	0.023130	0.049770	0.035910
3.78	0.004600	0.015860	0.034870	0.025080
3.99	0.003522	0.011550	0.025750	0.019990
4.13	0.003053	0.009577	0.021860	0.017010
4.19	0.008360	0.015640	0.027360	0.035610
4.23	0.059170	0.063740	0.083130	0.095970
4.27	0.090180	0.080170	0.087970	0.136500

TABLE B-1 (Continued)

UNITS = WATTS/CM^2 - STERADIAN

WAVELENGTH	HEIGHT = (DISTANCE ABOVE BURNER/FLAME HEIGHT)			
(MICRONS)	0.2	0.4	0.6	0.8
4.39	0.780700	0.530700	0.790500	1.452000
4.47	0.822000	0.891700	1.117000	1.211000
4.59	0.360200	0.424100	0.469900	0.400200
4.77	0.037100	0.052270	0.064510	0.046510
4.94	0.012060	0.015300	0.018780	0.012590
5.10	0.005370	0.008360	0.011550	0.007906
5.24	0.003591	0.006179	0.008822	0.006420
5.37	0.003522	0.005058	0.007727	0.006014
5.47	0.003454	0.004600	0.006429	0.005213
5.55	0.002545	0.003185	0.004600	0.003730
5.60	0.001843	0.002423	0.003730	0.002423
5.61	0.001419	0.001079	0.002423	0.001955

TABLE B-2

MONOCHROMATIC EXTINCTION COEFFICIENTS FOR
A LAMINAR NATURAL GAS DIFFUSION FLAME

UNITS = CM^{-1}

WAVELENGTH	HEIGHT = (DISTANCE ABOVE BURNER/FLAME HEIGHT)			
(MICRONS)	0.2	0.4	0.6	0.8
0.71	0.0465	0.0942	0.1558	0.1570
0.72	0.0468	0.0925	0.2033	0.2141
0.73	0.0443	0.1261	0.2139	0.2212
0.75	0.0362	0.1026	0.2481	0.2267
0.78	0.0427	0.1077	0.2317	0.2406
0.83	0.0343	0.1003	0.2092	0.2219
0.88	0.0262	0.0876	0.1886	0.1979
0.94	0.0238	0.0731	0.1591	0.1636
1.01	0.0198	0.0607	0.1430	0.1462
1.10	0.0184	0.0565	0.1246	0.1292
1.19	0.0160	0.0500	0.1136	0.1188
1.30	0.0147	0.0474	0.1098	0.1133
1.36	1.2960	0.0453	0.1024	0.1077
1.42	0.0151	0.0465	0.1051	0.1092
1.55	0.0145	0.0479	0.1103	0.1212
1.69	0.0139	0.0470	0.0907	0.1159
1.84	0.0156	0.0512	0.1190	0.1228
1.87	0.0173	0.0518	0.1198	0.1237
1.95	0.0171	0.0486	0.1128	0.1128
2.00	0.0171	0.0501	0.1149	0.1180
2.07	0.0183	0.0551	0.1193	0.1246
2.17	0.0137	0.0443	0.1074	0.1140
2.36	0.0130	0.0384	0.0937	0.0988
2.43	0.0134	0.0376	0.0897	0.0940
2.54	0.0304	0.0597	0.1012	0.1141
2.64	0.0224	0.0439	0.0891	0.0981
2.74	0.0446	0.0715	0.1196	0.1411
2.78	0.0410	0.0664	0.1131	0.1327
2.88	0.0429	0.0710	0.1087	0.1287
2.94	0.0390	0.0649	0.1044	0.1150
3.15	0.0290	0.0379	0.0671	0.0724
3.35	0.0298	0.0306	0.0557	0.0650
3.57	0.0152	0.0240	0.0534	0.0568
3.78	0.0085	0.0215	0.0498	0.0536
3.99	0.0078	0.0201	0.0476	0.0533
4.13	0.0082	0.0196	0.0475	0.0532
4.19	0.0195	0.0332	0.0617	0.0959
4.23	0.0385	0.0477	0.0710	0.1117
4.27	0.0542	0.0680	0.0829	0.1574

TABLE B-2 (Continued)

UNITS = CM^{-1}

WAVELENGTH	HEIGHT = (DISTANCE ABOVE BURNER/FLAME HEIGHT)			
(MICRONS)	0.2	0.4	0.6	0.8
4.39	0.3160	0.2945	0.4769	1.2230
4.47	0.3674	0.4693	0.7008	1.0270
4.59	0.2019	0.2646	0.3537	0.4504
4.77	0.0877	0.1288	0.1823	0.1989
4.94	0.0456	0.0607	0.0869	0.0847
5.10	0.0296	0.0446	0.0679	0.0689
5.24	0.0257	0.0411	0.0655	0.0698
5.37	0.0270	0.0391	0.0645	0.0725
5.47	0.0285	0.0398	0.0635	0.0711
5.55	0.0259	0.0346	0.0555	0.0599
5.60	0.0214	0.0284	0.0491	0.0474
5.61	0.0187	0.0194	0.0362	0.0413

TABLE B-3

MONOCHROMATIC VOLUMETRIC EMISSION COEFFICIENTS FOR A LAMINAR NATURAL GAS DIFFUSION FLAME

UNITS = WATTS/CM^2 - STERADIAN - MICRON

WAVELENGTH	HEIGHT = (DISTANCE ABOVE BURNER/FLAME HEIGHT)			
(MICRONS)	0.2	0.4	0.6	0.8
0.71	0.0000025	0.0000213	0.0000520	0.0000233
0.72	0.0000235	0.0001219	0.0005175	0.0003946
0.73	0.0000289	0.0002829	0.0007684	0.0005631
0.75	0.0000265	0.0003135	0.0017000	0.0008457
0.78	0.0000787	0.0005619	0.0022190	0.0017530
0.83	0.0000728	0.0007937	0.0030850	0.0024080
0.88	0.0000799	0.0010120	0.0044100	0.0032290
0.94	0.0001094	0.0012860	0.0054330	0.0037850
1.01	0.0001359	0.0015220	0.0074740	0.0049910
1.10	0.0001884	0.0020890	0.0093400	0.0065390
1.19	0.0002013	0.0024890	0.0115600	0.0084730
1.30	0.0002589	0.0031900	0.0157200	0.0111700
1.36	0.0257400	0.0033100	0.0153700	0.0115300
1.42	0.0003502	0.0040150	0.0191800	0.0138700
1.55	0.0004133	0.0054870	0.0269600	0.0230600
1.69	0.0004530	0.0061830	0.0266600	0.0229500
1.84	0.0006395	0.0081220	0.0404600	0.0286400
1.87	0.0007631	0.0082630	0.0415100	0.0291900
1.95	0.0007365	0.0073030	0.0362600	0.0232500
2.00	0.0007359	0.0077100	0.0388400	0.0262100
2.07	0.0009035	0.0104800	0.0444000	0.0322200
2.17	0.0005198	0.0065560	0.0362000	0.0275400
2.36	0.0004430	0.0047410	0.0269800	0.0198200
2.43	0.0004528	0.0043960	0.0237100	0.0173900
2.54	0.0026000	0.0121000	0.0317200	0.0257200
2.64	0.0011980	0.0053080	0.0212900	0.0181200
2.74	0.0057160	0.0154400	0.0390600	0.0382900
2.78	0.0045390	0.0122900	0.0331400	0.0319300
2.88	0.0046370	0.0138700	0.0268700	0.0268600
2.94	0.0035300	0.0103800	0.0234800	0.0192500
3.15	0.0014210	0.0024820	0.0069680	0.0055450
3.35	0.0012890	0.0012280	0.0036930	0.0029630
3.57	0.0001996	0.0005557	0.0026570	0.0020390
3.78	0.0000389	0.0003417	0.0017380	0.0013450
3.99	0.0000274	0.0002326	0.0012260	0.0010650
4.13	0.0000251	0.0001879	0.0010380	0.0009045
4.19	0.0001632	0.0005189	0.0016870	0.0034170
4.23	0.0022770	0.0030430	0.0059000	0.0107200
4.27	0.0048850	0.0048750	0.0072970	0.0214700

TABLE B-3 (Continued)

UNITS = WATTS/CM^2 - STERADIAN - MICRON

WAVELENGTH	HEIGHT = (DISTANCE ABOVE BURNER/FLAME HEIGHT)			
(MICRONS)	0.2	0.4	0.6	0.8
4.39	0.2467000	0.1563000	0.3770000	1.7760000
4.47	0.3020000	0.4185000	0.7831000	1.2440000
4.59	0.0727300	0.1122000	0.1662000	0.1802000
4.77	0.0032540	0.0067410	0.0117600	0.0093100
4.94	0.0005503	0.0009292	0.0016330	0.0010660
5.10	0.0001590	0.0003728	0.0007846	0.0005445
5.24	0.0000923	0.0002537	0.0005782	0.0004488
5.37	0.0000950	0.0001978	0.0004987	0.0004363
5.47	0.0000985	0.0001833	0.0004081	0.0003706
5.55	0.0000660	0.0001101	0.0002555	0.0002234
5.60	0.0000395	0.0000688	0.0001831	0.0001147
5.61	0.0000265	0.0000210	0.0000876	0.0000808

TABLE B-4

MONOCHROMATIC MAXIMUM EMISSION COEFFICIENTS FOR A LAMINAR ACETONE DIFFUSION FLAME

UNITS = WATTS/CM^2 - STERADIAN

WAVELENGTH	HEIGHT = (DISTANCE ABOVE BURNER/FLAME HEIGHT)			
(MICRONS)	0.2	0.4	0.6	0.8
0.71	0.000048	0.000313	0.000278	0.000101
0.72	0.000367	0.002281	0.002233	0.000928
0.73	0.000690	0.004102	0.004458	0.001640
0.75	0.000964	0.006725	0.007860	0.002728
0.78	0.001308	0.010780	0.013300	0.003985
0.83	0.002476	0.016910	0.021920	0.006864
0.88	0.003419	0.025820	0.034700	0.010620
0.94	0.004824	0.039460	0.052970	0.015800
1.01	0.007285	0.056450	0.078140	0.023370
1.10	0.009905	0.079400	0.106000	0.033280
1.19	0.013650	0.110700	0.162800	0.049840
1.30	0.018150	0.146500	0.222900	0.069090
1.34	0.018530	0.141600	0.225400	0.068040
1.42	0.024000	0.186900	0.287600	0.092970
1.55	0.031070	0.248900	0.388500	0.120100
1.69	0.035660	0.286500	0.473300	0.147800
1.84	0.044030	0.332800	0.545000	0.158200
1.92	0.039340	0.290400	0.492500	0.141600
2.00	0.043910	0.333400	0.551700	0.158700
2.07	0.048640	0.351800	0.587200	0.175500
2.17	0.038840	0.314300	0.548400	0.149600
2.36	0.036150	0.262900	0.468500	0.132000
2.43	0.035780	0.253200	0.444900	0.124300
2.49	0.059420	0.275400	0.446500	0.145200
2.54	0.055990	0.225500	0.358900	0.131600
2.60	0.028660	0.148100	0.271200	0.086810
2.74	0.098380	0.284200	0.431300	0.198400
2.84	0.100700	0.296800	0.420500	0.185200
2.94	0.058850	0.189400	0.276900	0.101100
3.15	0.043390	0.096980	0.158400	0.050520
3.35	0.037610	0.061580	0.106500	0.033400
3.57	0.011180	0.043620	0.082340	0.025610
3.78	0.005011	0.030610	0.061160	0.017960
3.99	0.003530	0.022960	0.047260	0.013820
4.15	0.003255	0.020810	0.043620	0.013300
4.19	0.021820	0.072120	0.090470	0.050520
4.23	0.078710	0.153500	0.172300	0.122800
4.29	0.095890	0.241400	0.255400	0.167800

TABLE B-4 (Continued)

UNITS = WATTS/CM^2 - STERADIAN

WAVELENGTH	HEIGHT = (DISTANCE ABOVE BURNER/FLAME HEIGHT)			
(MICRONS)	0.2	0.4	0.6	0.8
4.39	1.278000	2.461000	2.363000	2.049000
4.45	0.892000	1.383000	1.367000	1.164000
4.59	0.370800	0.570900	0.545400	0.435800
4.77	0.057710	0.059560	0.064640	0.033400
4.94	0.026040	0.022030	0.022330	0.008080
5.10	0.007860	0.012520	0.014350	0.004886
5.24	0.003812	0.008301	0.010700	0.004458
5.37	0.002626	0.006046	0.008674	0.004160
5.47	0.001906	0.004701	0.006450	0.002987
5.55	0.001429	0.003093	0.004043	0.002281
5.60	0.001429	0.001816	0.002677	0.001513
5.61	0.001348	0.001513	0.001684	0.001150

TABLE B-5

MONOCHROMATIC EXTINCTION COEFFICIENTS FOR
A LAMINAR ACETONE DIFFUSION FLAME

UNITS = CM^{-1}

WAVELENGTH	HEIGHT = (DISTANCE ABOVE BURNER/FLAME HEIGHT)			
(MICRONS)	0.2	0.4	0.6	0.8
0.71	0.0481	0.1612	0.2232	0.1933
0.72	0.0516	0.2168	0.2970	0.2474
0.73	0.0552	0.2575	0.3849	0.2828
0.75	0.0509	0.2803	0.4414	0.3029
0.78	0.0472	0.2771	0.4426	0.2994
0.83	0.0463	0.2671	0.4287	0.2939
0.88	0.0391	0.2241	0.3860	0.2568
0.94	0.0322	0.1960	0.3337	0.2236
1.01	0.0279	0.1700	0.2892	0.1967
1.10	0.0241	0.1497	0.2511	0.1763
1.19	0.0215	0.1350	0.2415	0.1660
1.30	0.0208	0.1273	0.2286	0.1612
1.34	0.0194	0.1140	0.2105	0.1457
1.42	0.0208	0.1224	0.2214	0.1584
1.55	0.0208	0.1276	0.2334	0.1648
1.69	0.0207	0.1274	0.2415	0.1715
1.84	0.0233	0.1340	0.2528	0.1735
1.92	0.0218	0.1210	0.2328	0.1607
2.00	0.0234	0.1320	0.2513	0.1723
2.07	0.0243	0.1320	0.2522	0.1757
2.17	0.0191	0.1164	0.2293	0.1554
2.36	0.0182	0.1010	0.2016	0.1388
2.43	0.0186	0.0999	0.1961	0.1352
2.49	0.0306	0.1098	0.1991	0.1480
2.54	0.0295	0.0979	0.1753	0.1382
2.60	0.0189	0.0745	0.1465	0.1081
2.74	0.0497	0.1279	0.2178	0.1943
2.84	0.0535	0.1381	0.2250	0.1959
2.94	0.0387	0.1070	0.1773	0.1395
3.15	0.0331	0.0728	0.1330	0.0969
3.35	0.0338	0.0611	0.1186	0.0868
3.57	0.0167	0.0554	0.1151	0.0832
3.78	0.0113	0.0518	0.1120	0.0786
3.99	0.0102	0.0502	0.1108	0.0778
4.15	0.0115	0.0539	0.1183	0.0839
4.19	0.0514	0.1324	0.2140	0.2202
4.23	0.0625	0.1175	0.1675	0.1975
4.29	0.0742	0.1634	0.2178	0.2395

TABLE B-5 (Continued)

UNITS = CM^{-1}

WAVELENGTH	HEIGHT - (DISTANCE ABOVE BURNER/FLAME HEIGHT)			
(MICRONS)	0.2	0.4	0.6	0.8
4.39	0.5869	0.7656	0.9868	1.8470
4.45	0.4607	0.8224	1.0680	1.3370
4.59	0.2594	0.4513	0.5543	0.6679
4.77	0.1585	0.2152	0.2704	0.2441
4.94	0.1008	0.1134	0.1438	0.1062
5.10	0.0497	0.0858	0.1189	0.0893
5.24	0.0345	0.0708	0.1072	0.0935
5.37	0.0291	0.0627	0.1033	0.0961
5.47	0.0256	0.0555	0.0931	0.0867
5.55	0.0217	0.0451	0.0722	0.0735
5.60	0.0224	0.0334	0.0562	0.0607
5.61	0.0216	0.0314	0.0441	0.0534

TABLE B-6

MONOCHROMATIC VOLUMETRIC EMISSION COEFFICIENTS FOR A LAMINAR ACETONE DIFFUSION FLAME

UNITS = WATTS/CM^2 - STERADIAN - MICRON

WAVELENGTH	HEIGHT = (DISTANCE ABOVE BURNER/FLAME HEIGHT)			
(MICRONS)	0.2	0.4	0.6	0.8
0.71	0.0000023	0.0000505	0.0000620	0.0000202
0.72	0.0000189	0.0004943	0.0006631	0.0002297
0.73	0.0000381	0.0010560	0.0017160	0.0004639
0.75	0.0000491	0.0018850	0.0034690	0.0008361
0.78	0.0000617	0.0029870	0.0058850	0.0011930
0.83	0.0001145	0.0045180	0.0093980	0.0020170
0.88	0.0001337	0.0057880	0.0133900	0.0027270
0.94	0.0001552	0.0077350	0.0176700	0.0035320
1.01	0.0002036	0.0095960	0.0226000	0.0045980
1.10	0.0002387	0.0118800	0.0266300	0.0058670
1.19	0.0002940	0.0149600	0.0393300	0.0082750
1.30	0.0003776	0.0186500	0.0509700	0.0111300
1.34	0.0003593	0.0161600	0.0474600	0.0099170
1.42	0.0004987	0.0229000	0.0636900	0.0147200
1.55	0.0006465	0.0317600	0.0906600	0.0198100
1.69	0.0007370	0.0354900	0.1142000	0.0253600
1.84	0.0010250	0.0445900	0.1378000	0.0274600
1.92	0.0008560	0.0351500	0.1146000	0.0227600
2.00	0.0010260	0.0440100	0.1386000	0.0273400
2.07	0.0011810	0.0464400	0.1481000	0.0308300
2.17	0.0007412	0.0366000	0.1258000	0.0232500
2.36	0.0006592	0.0265700	0.0944700	0.0183300
2.43	0.0006674	0.0253000	0.0872500	0.0168100
2.49	0.0018190	0.0302600	0.0888700	0.0214800
2.54	0.0016540	0.0220700	0.0629300	0.0182000
2.60	0.0005413	0.0110400	0.0397300	0.0093920
2.74	0.0048920	0.0363300	0.0939600	0.0385600
2.84	0.0053870	0.0409900	0.0946200	0.0362700
2.94	0.0022790	0.0202800	0.0490900	0.0141000
3.15	0.0014350	0.0070580	0.0210700	0.0048970
3.35	0.0012720	0.0037530	0.0126300	0.0028980
3.57	0.0001870	0.0023630	0.0094840	0.0021290
3.78	0.0000567	0.0015850	0.0068510	0.0014110
3.99	0.0000360	0.0011510	0.0052390	0.0010750
4.15	0.0000374	0.0011220	0.0051610	0.0011160
4.19	0.0011210	0.0095490	0.0193600	0.0111200
4.23	0.0049240	0.0180500	0.0288600	0.0242600
4.29	0.0071150	0.0394300	0.0556300	0.0401800

TABLE B-6 (Continued)

UNITS = WATTS/CM^2 - STERADIAN - MICRON

WAVELENGTH	HEIGHT = (DISTANCE ABOVE BURNER/FLAME HEIGHT)			
(MICRONS)	0.2	0.4	0.6	0.8
4.39	0.7499000	1.8840000	2.3320000	3.7830000
4.45	0.4110000	1.1370000	1.4610000	1.5570000
4.59	0.0961700	0.2576000	0.3023000	0.2911000
4.77	0.0091450	0.0128200	0.0174800	0.0081540
4.94	0.0026250	0.0024980	0.0032110	0.0008581
5.10	0.0003910	0.0010740	0.0017070	0.0004364
5.24	0.0001314	0.0005878	0.0011480	0.0004169
5.37	0.0000764	0.0003791	0.0008964	0.0003996
5.47	0.0000489	0.0002610	0.0006006	0.0002591
5.55	0.0000310	0.0001394	0.0002921	0.0001676
5.60	0.0000321	0.0000606	0.0001504	0.0000919
5.61	0.0000291	0.0000474	0.0000743	0.0000615

APPENDIX C

ERROR ANALYSIS

Many of nature's phenomena can be modeled by equations of the same general form as the transport equation. Thus, this error analysis is not restricted to extinction and maximum emission data and can be applied to a more general class of problems.

An example of an equation of the same general form as the radiative transport equation exists in creep testing. Under conditions of constant stress, total strain can be conviently separated into three components (C-1):

1) Instantaneous elastic
2) "Viscous-type" flow
3) Creep

The creep function describes the component of the total strain versus time relationship by

$$\text{Creep Strain} = C^{\infty}(1 - e^{-\alpha t})$$

where C^{∞} is creep function strain at infinite time

α is time

To complete the analogy, correspondence of the elements of the strain equation with the radiative transport equation are

Strain corresponds to I_λ

C^∞ corresponds to $\frac{J_\lambda}{\beta_\lambda}$

α corresponds to β_λ

t corresponds to X

Also, a large portion of the experimental absorption data is obtained by methods similar to this experiment. Therefore, an estimation of the error contained in these data can be derived from the error analysis.

For this analysis indeterminate errors of measurement of the path lengths and intensities were considered. From the photographs of the flame, the path lengths were measured against a photograph of a scale positioned along the axis of viewing. Determination of the path length to 0.1 millimeter required some estimation. For the error analysis, the value of measurement error of ± 0.05 millimeter was used. Photographs were taken at time exposures of approximately 15 seconds, and even though the flame appears not to fluctuate, movements of flame of the order of 0.05 millimeter or less would be difficult to observe with the eye. Thus it was possible that the measured path lengths were always biased by as much as 0.05 millimeter longer than the true value.

Indeterminate measurement errors for intensities come from three sources; amplifier instability, fuel supply

variations, and environment fluctuations. Fuel supply variations and environment fluctuations both contribute to the flame instability. These instabilities from the instruments and the flame have a long time cycle when compared to the short time cycle noise created by the instruments and small scale flickering of the flame. Since the instrument noise was approximately 0.1% of the recorded signal and the flame flicker noise was not detectable, only the amplifier and flame instability were considered. For the amplifier gains used in this experiment, the monochromator manual (C-2) states the gain stability to be ±0.5%. Stability of ±0.5% tolerance is good considering the gain is approximately 10^6 from the thermocouple output to chart the recording signal. Since the flame size and shape depend on the delicate balance of the flow of fuel up the burner and the flow of air up the annulus, any variation in the fuel supply or surroundings will alter the flame. Considering the difficulty in controlling such variations, an estimate of the long term flame stability was ± 0.5%. Combining instrument and flame instabilities, ±1% was used as the measurement errors in the intensities for the error analysis.

Using intensity measurements with errors of ±1% and path length measurements with errors of 0.05 millimeters, what errors can be expected from the solution of the transport equation for values of β_λ and $\frac{J_\lambda}{\beta_\lambda}$? This question cannot be answered with a standard error analysis, since neither variable can be solved

explicitly. However, the information was obtained by perturbation of each of the path lengths and intensities in the solution of the transport equation. It was assumed there was no computational error in the solution, and all errors were attributed to the perturbations. It can be shown that only the ratio of intensities of two data sets was necessary for solution of β_λ. Path lengths of 1.0 and 2.0 centimeters were used since they represented values close to measured values of the experiment.

The error computations were made by selecting a value of β_λ and computing intensities for each of the path lengths. The plus and minus percent errors in β_λ were computed by holding three of the variables constant and by perturbing the fourth variable. This procedure was repeated for each of four variables and the error was calculated as the sum of the errors for each perturbation. The comparison was made over a wide range of values for β_λ.

Maximum optical path length is a parameter that is related to β_λ and aids in the understanding of reasonable values of β_λ. Maximum optical path length for a flame is defined as the path length at which 99% of maximum intensity is reached. From the transport equation it corresponds to a value of path length that satisfies

$$\exp\left[-\beta_\lambda X_{mop}\right] = .01 \qquad \text{(C-1)}$$

or the equivalent equation

$$X_{mop} = \frac{4.6}{\beta_\lambda}$$

Figure C-1 shows the percentage error in β_λ as the ordinate and β_λ and maximum optical path length as the abscissa. Also the error in $\frac{J_\lambda}{\beta_\lambda}$ is shown as a function of β_λ. It was computed by calculating the error in $(1 - e^{-\beta_\lambda X})$ and adding this error to the error in I_λ since the transport can be rearranged so that

$$\frac{J_\lambda}{\beta_\lambda} = \frac{I_\lambda}{(1 - e^{-\beta_\lambda X})} \qquad (C\text{-}2)$$

From Figure C-1 it can be seen that the error in $\frac{J_\lambda}{\beta_\lambda}$ approaches the error in I_λ, for large values of β_λ, and closely follows the error in β_λ, for small values of β_λ. It is the opinion of the author that the maximum optical path length is greater than 25.0 centimeters for most laminar diffusion flames. As seen from Figure C-1, for maximum optical path lengths greater than 25.0 centimeters errors of plus or minus 10 percent and larger are possible with one percent measurement errors and extremely accurate measurements are required to calculate the transport equation coefficients with any level of confidence.

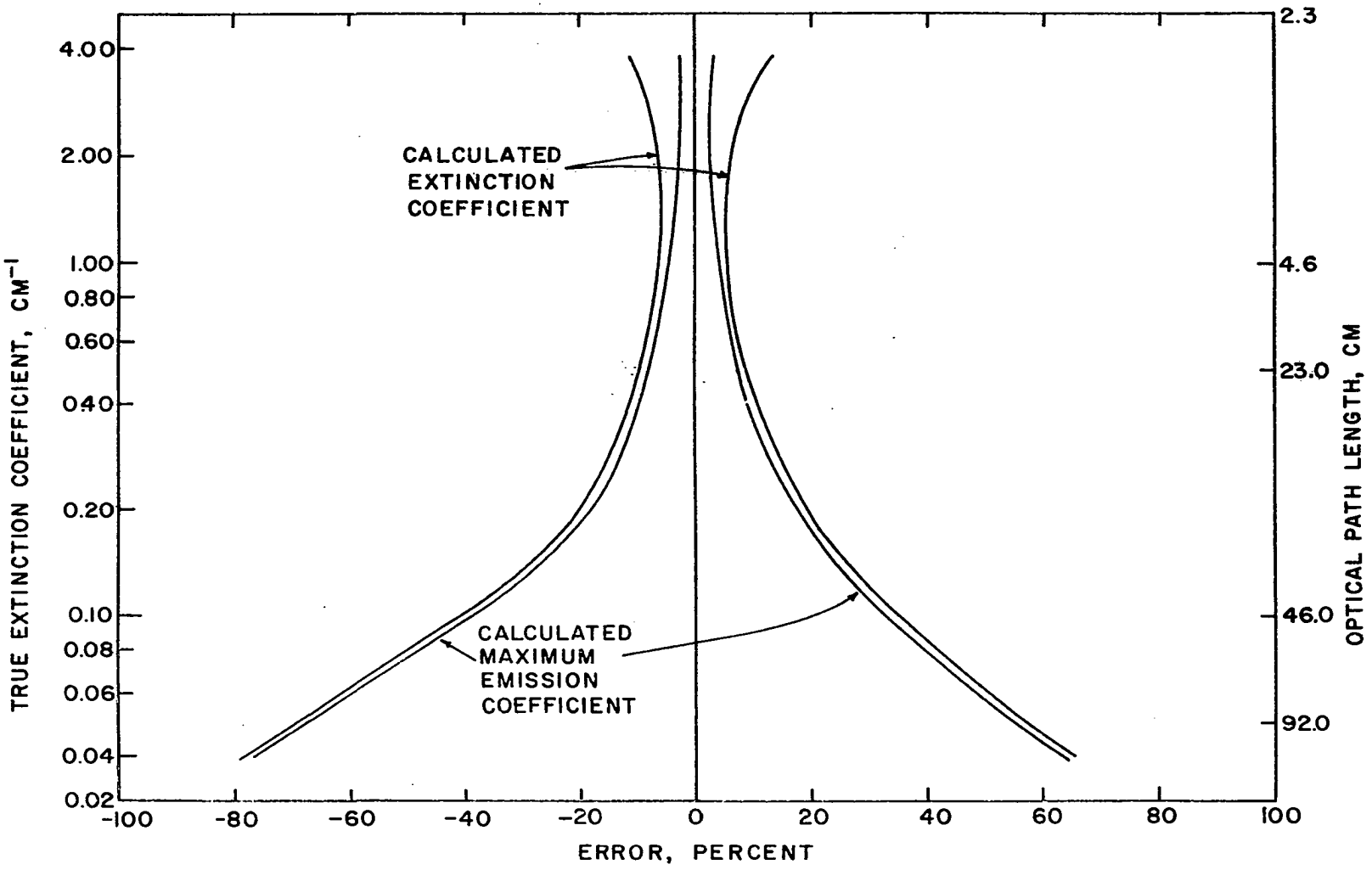

Figure C-1. Extinction and Maximum Emission Coefficient Errors From One Percent Measurement Errors

REFERENCES

C-1 Gross, B., Mathematical Structure of the Theories of Viscoelasticity, Herman et Cia, Paris, (1953) pp. 13-14.

C-2 Instruction Manual for Model 12-C Single Pass Infrared Spectrometer, Perkin-Elmer Corporation, Norwalk, Connecticut, (1956) p. 33.